
GPEN . 2010
University of North Carolina at Chapel Hill

Welcome

Dear GPEN 2010 Participant:

Welcome to the 8th biennial meeting of the Globalization of Pharmaceutics Education Network (GPEN)! More than 250 graduate students, post-doctoral fellows, and faculty members from 50 universities on 5 continents, as well as 30 industry observers, will be participating in this year's meeting. We would like to extend a special welcome to those universities that have been newly invited to participate in GPEN 2010: National Institute of Pharmaceutical Education and Research (NIPER), Seoul National University, Shandong University, and the University of London.

GPEN 2010 will feature 45 oral presentations and 114 poster presentations by attending students and post-doctoral fellows. The program also includes eight short courses that will be taught by experts from academia and the pharmaceutical industry. The GPEN 2010 keynote address will be given by Nobel Laureate Dr. Oliver Smithies, who will speak about the importance of translating basic biomedical research into medicine.

In order to further GPEN's mission of fostering and facilitating international scientific exchange in the pharmaceutical sciences, we have added several new events to the program for GPEN 2010. At the GPEN 2010 conference banquet, Dr. William Charman will be delivering an after-dinner address on his work on diseases in under-developed and developing countries. The meeting will also feature an industry panel discussion, which will include individuals with experience in various segments of the pharmaceutical industry. The discussion will focus on the changes that have occurred in the pharmaceutical industry over the past few years, as well as how students can best prepare themselves to be successful in the industry. Finally, we have made arrangements to hold a "Virtual Poster Session" a few weeks after GPEN 2010, in order to give students and post-doctoral fellows who are unable to be here in person an opportunity to learn about the research that is being done by their colleagues from around the globe.

We are looking forward to a great meeting! Welcome to Chapel Hill!

GPEN 2010 Organizing Committee

UNC Eshelman School of Pharmacy

Keynote Speaker

Wednesday, November 10, 2010

Alumni Hall

4:30-5:30 pm

Oliver Smithies, DPhil, the Excellence Professor of Pathology and Laboratory Medicine at the University of North Carolina at Chapel Hill, will present the keynote lecture at GPEN2010. Smithies was the co-recipient of the 2007 Nobel Prize in Physiology and Medicine for the discovery of the principles of introducing specific gene modifications in mice by the use of embryonic stem cells. His lecture will be titled “Importance of Translating Basic Biomedical Research into Medicine”.

Thursday, November 11, 2010

Carolina Inn

6:30-10:00 pm

Professor William N. Charman is Dean, Faculty of Pharmacy and Pharmaceutical Sciences, Monash University and Director, Monash Institute of Pharmaceutical Sciences in Melbourne, Australia.

He received his BPharm from the Victorian College of Pharmacy in 1981 and his PhD in pharmaceutical chemistry from the University of Kansas in 1985. From 1986-1989 he was a senior research scientist at the Sterling-Winthrop Research Institute in Rennselear, New York. He returned to Australia in 1989 where his research interests include absorption and bioavailability of poorly water soluble drugs, lymphatic drug transport, lead candidate optimisation, and the discovery and development of drugs for neglected diseases.

He received the GlaxoWellcome International Achievement award in Pharmaceutical Sciences from the Royal Pharmaceutical Society of Great Britain in 1999, the Australasian Pharmaceutical Sciences Association Medal in 2005, the Controlled Release Society International Career Achievement in Oral Drug Delivery Award in 2006, and a FIP Pharmaceutical Sciences World Congress Research Achievement Award in 2007. He was a team member of the Drug Discovery Project of the Year selected by the Medicines for Malaria Venture in 2002, 2007 and 2008. He has published over 370 scientific papers and communications and is a member of four international Editorial Boards. He is a fellow of the American Association of Pharmaceutical Scientists, a previous member of two Corporate Boards, Member of the Expert Scientific Advisory Committee for the Medicines for Malaria Venture (Geneva, Switzerland) and Chairman, Seeding Drug Discovery Funding Committee of the Wellcome Trust (London, UK).

Sponsors

We would like to thank the following sponsors for their generous support of GPEN 2010:

Abbott Laboratories
Absorption Systems LP
Allergan
American Association of Pharmaceutical Scientists
American Chemical Society
Amgen (US)
Amylin Pharmaceuticals, Inc.
Analytical Solutions, Inc
Astellas Pharma, Inc (Japan)
Astra Zeneca Pharmaceuticals LP
Biogen Idec
Bristol-Myers Squibb
Center of Global Initiatives, the University of North Carolina at Chapel Hill
Cephalon, Inc
Eisai, Inc
Genentech, Inc
Genzyme
Gilead Sciences, Inc.
GlaxoSmithKline
Human Genome Science, Inc
Johnson & Johnson Pharmaceutical R&D
King Pharmaceuticals
Merck Research Laboratories
Millennium Pharmaceuticals, Inc
North Carolina Biotechnology Center
Novartis Pharmaceuticals Corporation, Inc
Novartis Consumer Health, Inc
Patheon, Inc
Ono Pharmaceutical Company (Japan)
Pfizer, Inc.
Roche Palo Alto, LLC
Sanofi Aventis
Shionogi and Company, Ltd (Japan)
Shire Human Genetic Therapies, Inc
Teikoku Seiyaku Company (Japan)
Warner Chilcott
H. O. West Foundation
Wiley Interscience

Acknowledgements

The planning committee would like to express its gratitude to everyone who contributed to the success of GPEN 2010:

Dr. Oliver Smithies for giving the keynote address

Dr. William Charman for giving the banquet address

Judges of the podium and poster presentations

Industry observers

Staff at Alumni Hall and the William and Ida Friday Center

Staff at the Carolina Inn, Franklin Hotel, Siena Hotel, Courtyard Marriott Hotel, and Hampton Inn

Heavenly Cinnamon Rolls for catering the opening reception and keynote dinner

Twin Pines Imprinting for printing the portfolios, shirts, and conference bags

Horton's Transit Service for providing transportation

General Rental Center for setting up the keynote dinner

Signs Now for making the organizing committee nametags and plaques for award winners

R & R Grill for hosting the Friday night happy hour

Sarah Krantz and Rabiah Choudhary for their assistance in compiling the GPEN 2010 program

Julian Wooten for his assistance with the Career Center

Dr. Peter Koval for his assistance with the Virtual Poster Session

Dave Maldonado and ITSOP for technical assistance

John Zhu for designing the GPEN 2010 logo and for assistance with the GPEN 2010 website

Bernard Van Eerdenbrugh and the GPEN 2008 planning committee for their helpful advice

Meeting at a Glance

	Tuesday, November 9 Genetic Medicine Building	Wednesday, November 10 Alumni Hall, George Watts Hill Alumni Center	Thursday, November 11 William and Ida Friday Center		Friday, November 12 Alumni Hall, George Watts Hill Alumni Center	Saturday, November 13
8:00 AM		**Welcome & Opening Remarks** 8-8:15 AM			**Podium Presentations:** Morning Session 8-12 PM	**Optional Social Activity** 8 AM-5 PM
9:00 AM		**Podium Presentations:** Morning Sessions 8:15-12 PM	**Short Courses:** Morning Sessions 8:30-12 PM	**Career Center** 8:30-12 PM		
10: 00 AM						
11:00 AM						
12:00 PM		**Lunch and Poster Sessions** 12-2 PM	**Lunch and Industry Panel Discussion** 12-1:30 PM		**Lunch and Poster Sessions** 12-2 PM	
1:00 PM			**Short Courses:** Afternoon Sessions 1:30-5 PM	**Career Center** 1:30-5 PM		
2:00 PM		**Podium Presentations:** Afternoon Sessions 2-4:30 PM			**Podium Presentations:** Afternoon Session 2-4:30 PM	
3:00 PM						
4:00 PM		**Keynote Lecture:** Oliver Smithies, D. Phil 4:30-5:30 PM			**Awards and Closing Remarks** 4:30-5 PM	
5:00 PM						
6:00 PM	**Welcome Reception** 6-8 PM	**Dinner** UNC Eshelman School of Pharmacy & FedEx Global Education Building 6-9 PM	**Conference Banquet and Invited Lecture:** William N. Charman, Ph. D. Carolina Inn 6:30-10 PM			
7:00 PM						
8:00 PM						
9:00 PM						
10:00 PM						

Agenda

Tuesday, November 9

Time	Location	Event
6-8 PM	Genetic Medicine Building	**Welcome Reception**

Agenda

Wednesday, November 10

Time	Location	Event
8 AM	Alumni Hall, George Watts Hill Alumni Center	**Welcome and Opening Remarks**
8:15 AM -12 PM	Alumni Hall, George Watts Hill Alumni Center	**Podium Presentations:** Morning Session
12 PM-2 PM	Alumni Hall, George Watts Hill Alumni Center	**Lunch and Poster Sessions**
2-4:30 PM	Alumni Hall, George Watts Hill Alumni Center	**Podium Presentations:** Afternoon Session
4:30-5:30 PM	Alumni Hall, George Watts Hill Alumni Center	**Keynote Lecture:** Oliver Smithies, D. Phil
6-9 PM	UNC Eshelman School of Pharmacy and FedEx Global Education Building	**Dinner**

Agenda

Thursday, November 9

Time	Location	Event
8:30 AM-12 PM	William and Ida Friday Center	**Short Courses: Morning Session**** • Drug-Induced Toxicity: A Major Factor in the Clinical Failure of Drug Candidates • Drug Discovery in Academic Institutions: New Opportunities • Nanomedicines and Gene Therapy Delivery: Challenges and Opportunities • Transporters: Implications in the Design, Delivery, and Safety of Medicines
12 PM-1:30 PM	William and Ida Friday Center	**Lunch and Industry Panel Discussion**
1:30-5 PM	William and Ida Friday Center	**Short Courses: Afternoon Session**** • Emerging Role of Pharmacogenomics in Drug Development and Human Therapeutics • De-Risking Drug Candidates: Optimizing Solubility, Permeability, and DM-PK Stability of Proteins and Peptides in Solid Phase Formulations • Computer-Aided Drug Design
6:30-10 PM	Carolina Inn	**Conference Banquet and Invited Lecture:** William N Charman, Ph.D.

Agenda

Friday, November 12

Time	Location	Event
8 AM-12 PM	Alumni Hall, George Watts Hill Alumni Center	**Podium Presentations:** Morning Session
12 PM-2 PM	Alumni Hall, George Watts Hill Alumni Center	**Lunch and Poster Sessions**
2-4:30 PM	Alumni Hall, George Watts Hill Alumni Center	**Podium Presentations:** Afternoon Session
4:30-5 PM	Alumni Hall, George Watts Hill Alumni Center	**Awards and Closing Remarks**

Agenda

Saturday, November 13

Time	Location	Event
8 AM- 5 PM	Off Campus	**Optional Social Activity**

Podia Session Schedule

Date: Wednesday, November 10

Location: Alumni Hall, George Watts Hill Alumni Center

Podia Session: Morning

Time	Presenter	Title
8:00 AM		**Opening Remarks**
8:20 AM	Matthias Wacker	Photosensitizer loaded HSA nanoparticles – Preparation process and cellular uptake
8:40 AM	Tyson Smyth	Cell Type Dependence on Extent of Exosome Internalization
9:00 AM	Tugba Gulsun	Enhancement of Solubility of Nimesulide by Preparing Nanocrystal Formulation
9:20 AM	Dhaval Patel	Maintenance of Supersaturation: Indomethacin Crystal Growth Kinetics in Aqueous Suspensions and Inhibitory Effects of Excipients
9:40 AM	Jan Bevernage	Impact of drug supersaturation on absorption and vice-versa
10:00 AM		**Coffee Break**
10:30 AM	Marcus Kehrel	A novel approach for increasing sensitivity in Lateral-Flow-Assays
10:50 AM	Vasco Filipe	Monitoring the aggregation state of therapeutic IgG aggregates in human serum and plasma
11:10 AM	Kashappa-Goud Desai	Active Self-healing Microencapsulation of Vaccine Antigens in PLGA Microspheres with High Encapsulation Efficiency
11:30 AM	Daryn Goodwin	Lipid and Carbohydrate Based Systems to Enhance the Bioavailability, Immunogenicity and Targeting of Therapeutic Peptides
11:50 AM	Amolnat Tunsirikongkon	In vivo evaluation of $Al(OH)_3$ and chitosan conjugated plga microparticles as nasal Japanese Encephalitis vaccine carrier
12:10 PM		**Lunch**

Podia Session Schedule

Date: Wednesday, November 10

Location: Alumni Hall, George Watts Hill Alumni Center

Podia Session: Afternoon

Time	Presenter	Title
2:00 PM	Ngoc On	Rapid and reversible enhancement of blood-brain barrier (BBB) permeability using lysophosphatidic acid (LPA)
2:20 PM	Fransisca Leonard	In Vitro Model of Inflammatory Bowel Disease for Screening of Drug Formulations
2:40 PM	Abeer Mohamed Ahmed	New formulation of amphotericin B for the treatment of leishmaniasis
3:00 PM	Jee Heon Jeong	Bioadhesive 6 arm-PEG-catechol Grafted Islet Transplantation for Treatment of Type 1 Diabetes
3:20 PM	Katherine Theken	High-Fat Diet Alters Hepatic and Renal Cytochrome P450-Mediated Eicosanoid Metabolism in Mice
3:40 PM	Li Pan	Delineating Potential Effects of Bisphenol A on Placental Fatty Acid Homeostasis
4:00 PM	Emmy Dolman	Proximal tubular cell-targeted kinase inhibitor-lysozyme conjugates for the intervention in renal fibrosis
4:20 PM	Ryan Funk	Cationic Amphiphilic Drugs can Induce an Increase in Apparent Lysosomal Volume: Implications towards a Novel Intracellular Drug-Drug Interaction Pathway
4:40 PM		**End of Session**

Photosensitizer loaded HSA nanoparticles – Preparation process and cellular uptake

M. Wacker, A. Preuss, K. Chen, B. Röder, K. Langer

Purpose: HSA nanoparticles were established as a drug carrier system for the new generation photosensitizer mTHPC. In the first step the lipophilic molecule was adsorbed to the polymer after complexation of the drug. To overcome the disadvantage of desorption, a second formulation of mTHPC was based on the covalent modification of the particle surface. The behaviour of adsorptively loaded HSA nanoparticles was investigated in a cellular environment and revealed fast release of the photosensitizer under *in vitro* conditions.

Methods: HSA nanoparticles were prepared by ethanolic desolvation and stabilized by chemical cross linking with glutaraldehyde. The adsorptive loading of the nanoparticles with mTHPC was performed in a hydroethanolic solution of the photosensitizer in the presence of dissolved HSA. For covalent modification of the colloid a carbodiimid cross linker was utilized. The drug loading was quantified photometrically after degradation of the particle system and hydrolysis of introduced bindings. The intracellular release was investigated via CLSM with a FLIM extension.

Results: The photosensitizers were bound to HSA nanoparticles by two different strategies. After formation of a complex between photosensitizer and dissolved albumin the adsorption of the drug to the colloid could be performed in a hydrophilic medium. A stable particle system showing the disadvantage of a weak drug binding was achieved. To enhance drug binding capabilities of the carrier system a second formulation was based on the covalent modification of the nanoparticle surface. Drug loading rates of about 25 µg/mg mTHPC for adsorptively loaded HSA nanoparticles and 20 µg/mg for covalently modified HSA nanoparticles were reached. A drug release within 24 h could be shown for adsorptively mTHPC loaded nanoparticles (see Fig. 1).

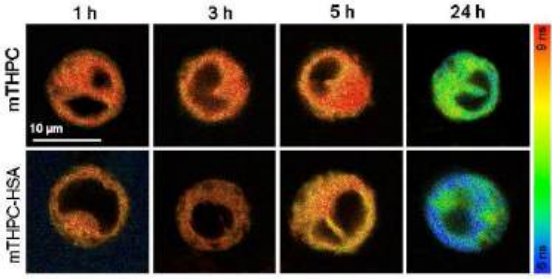

Conclusion: HSA nanoparticles are an efficient carrier system to transport photosensitizers into the lysosomes. While adsorptively loaded nanoparticles show a burst release of the drug in cellular environment, covalently modified HSA nanoparticles can be assumed to release the drug only after degradation of the particle system.

Cell Type Dependence on Extent of Exosome Internalization

T. Smyth[1], T.J. Anchordoquy[1]

[1] School of Pharmacy, University of Colorado, Aurora, CO

Purpose: Exosomes are membrane vesicles of 30-90 nm in size formed by the budding off of lipid membranes within endosomes inside cells. The subsequent fusion of the endosome with the cell membrane releases the exosomes into the extracellular environment. To date, the biological role of exosomes is not well defined, but the fact that exosome levels in patient blood increase at successive stages of disease suggests a potential role in cancer progression and metastasis. It has been suggested that exosomes are involved in intercellular communication among tumor cells. We hypothesize that exosomes released by cancer cells will preferentially target and fuse with cancer cells from the same parent cell line over cells of varying origin.

Methods: *In vitro* cell culture experiments will be used to characterize the ability of exosomes to fuse with specific cells. To date we have successfully fluorescently labeled exosomes derived from breast cancer cells with the hydrophobic fluorochrome DiD, and used confocal microscopy to visualize their ability to fuse with parent breast cancer cells (MCF7). Forth coming experiments are designed to compare the ability of MCF7-derived exosomes to be internalized by lung, skin, colon and liver cancers cell lines, macrophages and a normal lung cell line. The extent of fusion will be quantified with FACS.

Results: We have extensively characterized the exosome preparations to ensure that our purified fractions are free of cellular debris (e.g., apoptotic bodies). Results on uptake are forthcoming, and we expect MCF7 exosome internalization to be greatest when incubated in the presence of MCF7 cells. Additionally, we may find that other cancer cell lines take up more MCF7 exosomes than non-cancerous cells lines. Macrophages are known to phagocytose exosomes, and will serve as a control for cellular uptake.

Conclusion: The ability to exploit exosomes for drug delivery has yet to be investigated. These vesicles from an endogenous tumor communication network may prove to have enhanced stability in the circulation and specificity for tumor targets that is not possible with liposomal delivery systems. The known role of exosomes in transferring biomolecules among tumor cells suggests that this communication network can be hijacked as a novel mode of targeted anti-cancer drug delivery.

Enhancement of Solubility of Nimesulide by Preparing Nanocrystal Formulation

C.Budak, T. Gulsun, I. Vural, S. Sahin, L. Oner

Hacettepe University, Faculty of Pharmacy, Department of Pharmaceutical Technology, 06100, Ankara, Turkey

Purpose: Nimesulide is an acidic non steroidal drug which can be classified as a Class II drug (low solubility and high permeability) according to the Biopharmaceutical Classification System. The purpose of this study was to reduce particle size of nimesulide by preparing nanocrystal and hence to enhance its aqueous solubility.

Methods: A suspension of nimesulide (3%, w/v) and pluronic F127 1:0.5 (w/w) was prepared in distilled water. The suspension was mixed by using 16 pieces of 20 mm, 11 pieces of 10 mm and 3 pieces of 50 mm agate balls for 15 minutes, and then the dispersion medium was removed by lyophilization. The physicochemical characteristics of nimesulide, pluronic F127 and nanocrystal formulation were determined by Fourier Transform Infrared Spectroscopy (FT-IR), Differential Scanning Calorimetry (DSC) and X-ray diffractometry. Particle size of nanocrystal formulation was determined before and after the lyophilization. Solubilities of nimesulide, physical mixture (nimesulide: pluronic F127, 1:0.5) and nanocrystal formulation were determined at $37^{O}C$ as a function of pH (1.2, 4.6, 6.8 and 7.4). Apical-to-basolateral permeabilities of nimesulide, physical mixture (nimesulide: pluronic F127, 1:0.5), nanocrystal formulation were determined across Caco-2 monolayers 21 days after seeding.

Results: Conservation of crystalline structure of nimesulide in nanocrystal formulation was demonstrated by X-ray diffraction analysis. FT-IR spectra showed that chemical structure of nimesulide was protected in the nanocrystal formulation. DSC analyses confirmed the interaction between nimesulide and pluronic F127 in nanocrystal formulation. The particle size of nimesulide powder (5021±433.5 nm) was decreased by 87% in nanocrystal formulation. The solubility of nimesulide in powder, physical mixture and nanocrystal formulation increased as a function of pH. For a given pH condition (e.g. 6.8), the highest solubility was obtained with the nanocrystal formulation (520.21 µg/mL), then physical mixture (268.15 µg/mL) and the lowest with the powder nimesulide (82.51 µg/mL). Nimesulide was a highly permeable compound either in powder form or in physical mixture and nanocrystal formulation (Papp> $12x10^{-6}$ cm/sec for all).

Conclusion: All these results clearly indicated that solubility of nimesulide was significantly enhanced by preparing nanocrystal formulation.

Maintenance of Supersaturation: Indomethacin Crystal Growth Kinetics in Aqueous Suspensions and Inhibitory Effects of Excipients

Dhaval Patel[1], Vijay Joguparthi[2], Zeren Wang[2], and Bradley Anderson[1]

[1]Dept. of Pharmaceutical Sciences, University of Kentucky, Lexington, KY
[2]Pharmaceutical R&D, Boehringer-Ingelheim Pharmaceuticals Inc., Ridgefield, CT

Purpose: The aims of this study were: (i) to develop techniques and models to study the crystal growth kinetics of indomethacin (IND), a poorly water soluble drug, in aqueous suspension, and (ii) to apply the quantitative methodology to explore mechanisms of crystal growth inhibition by two model excipients.

Methods: An online second derivative UV spectroscopic method was developed to study the crystal growth kinetics of IND. Crystal growth rates with and without excipients (e.g., 2-hydroxypropyl-β-cyclodextrin (HP-β-CD) and PVP) at 25ºC were determined from IND loss over time in aqueous supersaturated suspensions (pH 2.15). IND seed crystals (~11 μ) were characterized before and after growth for size, number, morphology, and physical form using a Coulter counter, SEM, and PXRD. IND powder dissolution kinetics were also determined.

Results: The apparent solubility of IND after crystal growth (C_{app}=5.2±0.6(95% CI)×10^{-6}M) was ~55% higher than the intrinsic solubility (C_s) (3.4±0.2×10^{-6} M), suggesting that the newly grown layer was a higher energy form. The crystal growth at a high degree of supersaturation (S≈6) was modeled using a first-order diffusion-reaction model and C_{app}. The mass transfer coefficient for dissolution (4.9±1.8×10^{-3}cm/sec) was similar to that obtained for crystal growth (4.9±0.8×10^{-3} cm/sec) consistent with aqueous diffusion controlled processes. At high S (≈5), values for the IND crystal growth inhibition factor (R), defined as the ratio of crystal growth rate coefficients with and without excipients, were 0.83, 0.63, and 0.50 for 0.25, 0.5, and 1% w/w HP-β-CD, and 0.04 for 0.2% PVP, respectively. The inhibitory effect of HP-β-CD (S≈6) could be accounted for by complexation in the diffusion layer. At lower S (≈2), R for HP-β-CD (1%) was 0.09.

Conclusions: C_{app} for IND after growth was higher than C_s. IND crystal growth kinetics at higher S were aqueous diffusion controlled. At higher S, PVP was a better crystal growth inhibitor than HP-β-CD, and the effect of HP-β-CD could be explained by reversible complexation in the diffusion layer. At lower S, HP-β-CD (1%) was ~6× more effective as a crystal growth inhibitor suggesting a change in inhibition mechanism.

Impact of drug supersaturation on absorption and vice-versa

Jan Bevernage, J. Brouwers, P. Annaert, P. Augustijns

Laboratory for Pharmacotechnology and Biopharmacy, K.U. Leuven, Belgium

Purpose: Traditional supersaturation screening is typically performed by adding a concentrated drug stock solution to aqueous solution in the presence or absence of precipitation inhibitors. This approach ignores transepithelial permeation as an alternative for precipitation in the intraluminal environment. In the present study, supersaturation was explored in the apical compartment of the Caco-2 system along with its beneficial effect on transepithelial transport.

Methods: Supersaturation of the anti HIV agent loviride was investigated in FaSSIF in the absence or presence of HPMC-AS (0.05%) using the traditional screening setup as well as in the apical compartment of a Caco-2 system. The solvent shift method using a DMSO stock solution was used to generate an initial degree of supersaturation (DS) of 5 and 20.

Results: In the traditional supersaturation screening setup, loviride precipitation was observed and the kinetics appeared to be dependent on the initial DS (DS20 >> DS5); inclusion of HPMC-AS inhibited precipitation over 60min upon induction of supersaturation. Application of a supersaturated solution in the apical compartment of the Caco-2 model demonstrated that the initial DS was translated in transport enhancement: loviride transport after 60min was increased with a factor around 5 and 20 when supersaturated solutions with an initial DS of 5 and 20 were employed apically. Furthermore, inclusion of HPMC-AS in FaSSIF, resulting in complete precipitation-inhibition in the traditional setup, was not reflected in any further transport enhancement compared to the plane FaSSIF condition. The recovery of loviride from the Caco-2 system was 100% after 60min with or without HPMC-AS indicating that for any condition, no precipitation occurred in the apical compartment.

Conclusions: The precipitation/permeation approach illustrates that beneficial effects of supersaturation may be underestimated looking at the precipitation profiles obtained in the traditional setup whereas beneficial effects of precipitation inhibitors on the other hand might be overestimated from the precipitation profiles alone.

A novel approach for increasing sensitivity in Lateral-Flow-Assays

M. Kehrel[1], S. Merkl[1], N. Dassinger[1], D. Vornicescu[1], M. Keusgen[1]

[1] Institut für Pharmazeutische Chemie, Philipps-Universität Marburg, Marburg, Germany

Purpose: Lateral-Flow-Assays (*e.g.*, pregnancy tests) are frequently used, fast and easy-to-handle immunoassays. Nevertheless, they are often lacking sensitivity. In order to detect even small amounts of analyte in big volumes, our idea is to integrate some kind of amplifier module in the test system.

Methods: Based on previous research and experience in the working group of Prof. Keusgen [1], the assembly of the amplifier module shall look as follows: the polysaccharide mannan is preferentially covalently attached to a solid support (porous sintered body). In the next step a multifunctional "linker-protein" is captured by its polysaccharide binding domain (lectin). This hybrid-protein shall be expressed recombinant from *E. coli*. Using its streptavidin unit, a biotinylated analyte-specific antibody can be bound to the surface. After capturing and therefore concentrating the analyte, it can be transferred in direction of the detection unit by specifically loosening the sugar-lectin-bond.

Results: For the "proof of principle" of this Lateral-Flow-Assay we are currently using planar gold surfaces as solid support and a Surface Plasmon Resonance (SPR)-based biosensor and planar glass supports plus a Reflectometric Interference Spectroscopy (RIfS)-based biosensor respectively. First measurements showed success regarding the assembly of a functional surface and the immobilization as well as specific removal of essential components of the planned amplifier module.

Conclusion: With the drafted approach it could be possible to establish a highly specific, sensitivity-increasing amplifier module for the detection of various biomolecules as analytes and a specific procedure for the detection without affecting the analyte.

[1] Vornholt W, Hartmann M, Keusgen M: SPR studies of carbohydrate-lectin interactions as useful tool for screening on lectin sources. *Biosens. Biolectron.*, 22 (2007), 2983-2988

Acknowledgements: This work is supported by the "Arbeitsgemeinschaft industrieller Forschungsvereinigungen (AiF)" with financial means from the BMWi.

.

Monitoring the aggregation state of therapeutic IgG aggregates in human serum and plasma

V. Filipe[1,2], R. Poole[1], Kevin Braeckmans[3], O. Oyetayo[1], W. Jiskoot[1]

[1] Division of Drug Delivery Technology, LACDR, Leiden University, The Netherlands
[2] Department of Pharmaceutics, Utrecht Institute for Pharmaceutical Sciences (UIPS), Utrecht University, The Netherlands
[3] Laboratory of General Biochemistry and Physical Pharmacy, Faculty of Pharmacy, Ghent University, Belgium

Purpose: The purpose of this work was to monitor whether the aggregation state of stressed therapeutic monoclonal IgG changes once brought into contact with human serum or plasma.

Methods: A therapeutic human IgG was covalently labeled with Alexa Fluor 488 dye. Aggregates of unlabeled and labeled IgG were obtained by pH shift and heat stress. The effect of the label on the aggregation state of the IgG was tested by size exclusion chromatography (SEC). Unstressed and stressed labeled IgG formulations were diluted in formulation buffer, in human serum and in human plasma. The aggregates were analyzed with fluorescent activated cell sorting (FACS), confocal microscopy and single particle tracking (SPT) analysis.

Results: SEC indicated that the Alexa 488 dye does not affect the aggregation state of the IgG formulations. FACS and confocal microscopy showed that the unstressed IgG does not aggregate in serum and plasma, and that the aggregates of both stressed formulations are still present after dilution in serum or plasma. SPT showed that the nanometer sized heat-induced aggregates do not change their average size once in contact with serum or plasma, but the pH shift-induced aggregates become smaller once in contact with either of these biological fluids.

Conclusion: Depending on the type of IgG aggregates, IgG aggregates can drastically change their characteristics once in contact with human serum and plasma.

Active Self-healing Microencapsulation of Vaccine Antigens in PLGA Microspheres with High Encapsulation Efficiency

Kashappa Goud H. Desai and Steven P. Schwendeman

Department of Pharmaceutical Sciences, University of Michigan, 428 Church St., Ann Arbor, USA.

Purpose: The purpose of this study was to develop active self-microencapsulating (active SM) poly(DL-lactic-co-glycolic acid) (PLGA) microspheres for the encapsulation and delivery of vaccine antigens with minimal manufacturing instability stresses on the antigen (i.e., no exposure to organic solvents, excessive shear, or elevated temperature).

Methods: Porous active SM microspheres, which contained $Al(OH)_3$ to absorb antigen in the PLGA pores, lyoprotectant to stabilize $Al(OH)_3$ during freeze-drying, and + or – 5 wt% diethyl phthalate (DEP) to change the glass transition temperature (T_g) of PLGA, were prepared by an emulsion-solvent evaporation method. Active self-microencapsulation of the model antigen, ovalbumin (OVA), was achieved by incubating blank active SM PLGA microspheres with an aqueous OVA solution (0.5 - 1 mg/mL) under mild agitation at 10, 25 and 37 ºC. Determination of $Al(OH)_3$ loading was performed by ICP-OES. Assay of OVA was performed by Coomassie Plus (Pierce) and SEC-HPLC. Monitoring goodness of encapsulation was examined by laser confocal scanning microscopy (LCSM) and extent of OVA release in 190 mM citrate buffer, which dissolves $Al(OH)_3$. Controlled release kinetics of OVA from self-encapsulated PLGA microspheres was conducted in PBS (pH 7.4) at 37 ºC.

Results: $Al(OH)_3$ was encapsulated in PLGA microspheres with 87-98% encapsulation efficiency. Active loading of OVA was a) found to increase proportionally with an increasing loading of $Al(OH)_3$ (0.9-3.2 wt%) and trehalose (2-5 wt%), b) found to decrease when the inner water phase volume was > 200 µL/mL PLGA/methylene chloride oil phase, and c) did not change significantly with varying polymer concentration and initial incubation (loading) temperature. The fraction of $Al(OH)_3$ accessible for OVA sorption in microsphere formulations studied ranged from 28-55%. Nearly all OVA was incorporated into the $Al(OH)_3$-containing PLGA pores when OVA in the loading solution was reduced to ~200 µg/20 mg PLGA (~0.5 mg/mL OVA). The distribution of OVA in PLGA microspheres after active self-healing microencapsulation was nearly homogeneous as examined by LCSM. Slow release of OVA from active self-microencapsulated microspheres in citrate buffer and PBS compared to rapid release from non-encapsulated $Al(OH)_3$ indicated an effective active self-encapsulation in $Al(OH)_3$/PLGA microspheres and slow and continuous release of antigen for > 28 days. Percent OVA monomer in self-encapsulated protein was 98 ± 1. Active self-encapsulated PLGA microspheres exhibited 17, 49, and 68 % OVA monomer release respectively after 1, 14, and 28 days with a total (released + remaining OVA monomer) recovery of 88 ± 3 % after 28 days (mean ± SE, n = 3).

Conclusion: Active self-healing microencapsulation of OVA in PLGA microspheres was achieved in the absence of encapsulation stresses. The new microencapsulation paradigm provided excellent OVA loading (1 wt%), >96% encapsulation efficiency, and long-term release. It is now possible to microencapsulate biomacromolecules in PLGA with high efficiency by simple mixing of preformed polymer and low aqueous concentrations of biomacromolecules.

Lipid and Carbohydrate Based Systems to Enhance the Bioavailability, Immunogenicity and Targeting of Therapeutic Peptides

D. Goodwin[1,2], P. Simerska[1], S. Mureev[2], K. Alexandrov[2], I. Toth[1].

[1] The University of Queensland, School of Chemistry and Molecular Biosciences, St. Lucia, QLD, Australia

[2] The University of Queensland, Institute for Molecular Bioscience, St. Lucia, QLD, Australia

Purpose: Develop liposaccharide-based delivery systems for a variety of synthetic peptide therapeutics. A luteinizing hormone-releasing hormone (LHRH)-based delivery and vaccination system has been utilized with the potential to treat prostatic cancer and for use in anti-fertility applications. Additionally, the Leu-enkephalin (Leu-Enk) peptide is currently being optimized to achieve superior delivery to opioid receptors, and ovalbumin (OVA) has been employed as a model antigen for a vaccine system with an anticipated targeted delivery to dendritic cells.

Methods: All peptides were prepared by solid-phase peptide synthesis. LHRH was conjugated at its N-terminus with C12 (2-amino-dodecanoic) or C8 (2-amino-octanoic) lipoamino acids (LAAs) in monomeric and dimeric additions. Leu-Enk was conjugated at its C-terminus with one C16 LAA residue. Four copies of LHRH or $OVA_{257-264}$/$OVA_{323-339}$ were incorporated into a dendritic arrangement utilising a poly-lysine core. This system was then altered with two and three C16/C12 LAA residues conjugated to the C-terminus, resulting in a Lipid Core Peptide (LCP) vaccine system. Glycosyl/glycosylamine derivatives were prepared for conjugation to the N-termini of each peptide/peptide vaccine candidate. An expression vector was developed to produce a poly-LHRH peptide/antigen for incorporation into the LCP system. Peptides were purified using high-performance liquid chromatography (HPLC).

Results: The parent peptides, four lipid-LHRH conjugates (one and two additions of C12 or C8 LAAs), Leu-Enk-C16 conjugate, and two LHRH LCPs (two and three C16 LAA residues) were successfully synthesized and characterized by HPLC, MS. A number of glycosyl succinate linkers were prepared using literature methods for their inclusion in each of these peptide-based drug candidates.

Conclusions: It has previously been shown that conjugation with lipidic amino acids increases the half life of peptides dramatically in Caco-2 cell homogenates during incubation. Due to increased stability and permeability through epithelial cells, there is a potential for these conjugates to be administered orally. Carbohydrate conjugations have the potential to increase the solubility of these conjugates, with the additional benefit of increased targeting and transport via certain cells and their receptors. Through lipidation of a multivalent peptide carrier system, resulting in an LCP, a high titre antibody response should be induced without the need for any additional adjuvant.

GPEN. 2010
University of North Carolina at Chapel Hill

IN VIVO EVALUATION OF $Al(OH)_3$ AND CHITOSAN CONJUGATED PLGA MICROPARTICLES AS NASAL JAPANESE ENCEPHALITIS VACCINE CARRIER

A. Tunsirikongkon, G.C. Ritthidej

Department of Pharmaceutics and Industrial Pharmacy, Faculty of Pharmaceutical Sciences, Chulalongkorn University, Bangkok, 10330, Thailand

Purpose: To study the effect of variable parameters on enhancing the intranasal immune response of JE vaccine in Balb/c mice ; dose of JE vaccine, size of PLGA particles, surface charge of PLGA particles conjugated with mucoadhesive substances, CS (1C) and $Al(OH)_3$ (1A), respectively.

Methods: Balb/c mice were either subcutaneously or intranasally administered 10, 40 and 80μg doses of JE antigen at day 0, 7 and 28. To study the effect of particle size, Balb/c mice were intranasally immunized with 1, 5 and 15μm of JE encapsulated PLGA particles (JEP) with appropriate dose at day 0, 7 and 28. $Al(OH)_3$ conjugated JEP and CS conjugated JEP were given to Balb/c mice intranasally received at day 0 and 7 with an appropriate particle size and dose. The systemic and mucosal immune responses shown as titer from blood sample were evaluated by ELISA.

Results: Mice immunized intranasally with JE significantly elicited lower IgG ($p<0.05$) for all doses than mice immunized with 10μg JE subcutaneously. Their IgG titers were comparable and tended to increase except from the 80μg dose that decreased at week 6. The IgA antibodies were fairly low for both administration routes. Particles could enhance the level of immunological titer compared to soluble vaccine alone and 1μm increased the IgG titer by a statistically significant amount ($p<0.05$) compared to 5μm, 15μm. All sizes stimulated the low IgA and the booster dose at day 28 was still necessary. After conjugation with CS and $Al(OH)_3$, the titer persisted for a longer period of time. The CS formulations raised slightly higher antibody response than the $Al(OH)_3$ formulation The booster dose was not require for conjugated formulation.

Conclusions: There was a dose dependent effect of JE vaccine administered intranasally within 10μg to 40μg. The effect of size was obviously observed for 1, 5, and 15μm particles that particles of smaller than 5μm could induce a high titer. The delivery of CS and $Al(OH)_3$ conjugated particles seemed to help the particles overcome the mucosal barrier and enhanced the level of immune response.

Rapid and reversible enhancement of blood-brain barrier (BBB) permeability using lysophosphatidic acid (LPA)

N. On, M. Hinton, D.W. Miller

Department Pharmacology and Therapeutics, Faculty of Medicine, University of Manitoba, Winnipeg, MB, Canada

Purpose: The present study examined modulation of blood-brain barrier (BBB) permeability with the phospholipid, lysophosphatidic acid (LPA). The objectives were to characterize both the time course and magnitude of BBB opening that could be achieved with LPA and to evaluate the potential of this approach for enhancing drug delivery to the brain.

Methods: Changes in human brain microvessel endothelial cell (HBMEC) permeability following LPA (0.1-10 μM) exposure was assessed using fluorescein labeled dextran (FDX; MW3000). The profile of LPA receptor expression in brain microvessel endothelial cells was determined using RT-PCR. Effects of LPA on BBB permeability were also examined in adult Balb/c mice following bolus i.v. injection of LPA (1 mg/kg), or vehicle using magnetic resonance imaging (MRI) and near infrared fluorescent imaging techniques with small molecule gadolinium (Gd) contrast agent and large molecule polyethylene glycol IRdye (IRDye 800cw PEG), respectively.

Results: Primary cultured HBMEC express LPA1, LPA2 and LPA3 receptors. Activation of these receptors with exogenous LPA produced concentration-dependent increases in FDX permeability in HBMEC monolayers. Permeability increases in HBMEC monolayers occurred within 30 minutes of LPA exposure. The MRI of BBB integrity following systemic administration of LPA indicated significantly greater (as much as 20-fold enhancement) accumulation of gadolinium contrast agent in the mouse brain compared to control mice. Increases in BBB permeability were observed within 6 minutes of LPA administration and appeared to return to normal within 21 minutes of LPA administration. Qualitatively similar responses were observed for the brain penetration of the IRDye 800cw PEG imaging agent.

Conclusions: LPA produced a rapid and reversible increase in brain microvessel endothelial cell permeability. These studies indicate that administration of LPA, or LPA analogs in combination with therapeutic agents may be an effective strategy to increase drug delivery to the brain.

In Vitro Model of Inflammatory Bowel Disease for Screening of Drug Formulations

Fransisca Leonard[1], Eva-Maria Collnot[1,2], Bart J. Crielaard[3], Twan Lammers[3], Gert Storm[3], Claus-Michael Lehr[1,2]

[1]Department of Biopharmaceutics and Pharmaceutical Technology,
[2]Department of Drug Delivery (DDEL), Helmholtz Institute for Pharmaceutical Research Saarland (HIPS), Helmholtz Centre for Infectious Research (HZI), Saarland University, Saarbruecken, 66123 Germany
[3] Department of Pharmaceutics, Utrecht Institute for Pharmaceutical Sciences, University of Utrecht, Utrecht, The Netherlands

Purpose: Drugs and formulation screening for treatment of inflammatory bowel disease (IBD) so far has been mostly conducted with DSS or TNBS animal models. However, the latter represent more an acute injury-caused inflammation instead of a chronic condition. To replace these scientifically and ethically questionable models, an in vitro model is needed that reflects the pathophysiological changes in the inflamed intestine and allows high-throughput screening of anti-inflammatory drugs and formulations.

Methods: An in vitro co-culture model of IBD was developed and established in our laboratory, consisting of Caco-2 intestinal epithelial cells and human blood-derived macrophages and dendritic cells. Inflammation is triggered by addition of pro-inflammatory cytokine interleukin 1-β. Upon stimulation of inflammation, increased release of pro-inflammatory marker interleukin-8, rearrangement of tight junctional proteins accompanied by reduction of barrier function and increased mucus production were observed. Various budesonide formulations (free budesonide solution, budesonide-loaded PLGA nanoparticles, or budesonide-loaded liposomes) were applied to the inflamed model and IL-8 release was measured for inflammation monitoring. Transepithelial electrical resistance was monitored to observe recovery in epithelial barrier function. Furthermore particle deposition was observed using confocal laser scanning microscopy.

Results: Free budesonide solution and PLGA budesonide nanoparticles were effective in vitro: a decrease of IL-8 protein release and recovery of epithelial barrier function within 24 hours after treatment was observed, indicating reduced inflammation. However, free budesonide treated cells showed a rebound of IL-8 release after 48 h while PLGA-budesonide treated cells maintained their effect. The model also provides mechanistic insight, as an accumulation of PLGA nanoparticles intercellularly between epithelial cells was observed, hinting at enhanced permeability and retention effect. In contrast, liposomes accumulated in basolateral side of the model, co-localized with macrophages and dendritic cells.

Conclusion: The proposed in vitro model of the inflamed intestinal mucosa is an adequate tool for the screening of novel IBD drugs and formulations, combining the convenience of in vitro studies with the complexity of pathophysiological changes of inflamed mucosal tissue. In our study, PLGA nanoparticles were the most effective formulation to treat IBD.

New formulation of amphotericin B for the treatment of leishmaniasis

A Mohamed Ahmed[1,2], V Yardley[2], K Seifert[2], S L Croft[2], S Brocchini[1]

[1]Department of Pharmaceutics, The School of Pharmacy, 29-39 Brunswick Square, London WC1N 1AX, UK.
[2]Department of Infectious and Tropical Diseases, London School of Hygiene and Tropical Medicine, Keppel Street, WC1E 7HT, UK.

Purpose: To develop a cost effective and stable water soluble non covalent complex between amphotericin B (AmB) and poly(α-glutamic acid) (PGA) which is non toxic to mammalian cells and active against *Leishmania in vitro* and *in vivo*

Methods: The AmB–PGA complex was prepared by dissolving PGA (50-70 kDa) in dry DMSO. AmB was dissolved separately in dry DMSO for 1 h. PGA solution was added dropwise to AmB solution. The mixture was stirred for 1 h, and then sodium hydroxide (2 equivalents, 1N) was added dropwise followed by addition of water. The reaction mixture was left to stir at room temperature for 1 h then purified by dialysis and freeze dried. The AmB loading was determined by UV spectroscopy at 409 nm in methanol (50%).

Results: Water soluble non-covalent AmB-PGA complexes were prepared with loadings in the range of 20.0-50.0%. The size of the complex was in the range of 125-130 nm with a negative surface charge (-54.97±6.00 mV). AmB-PGA complexes were non-toxic to human RBCs and KB cells at AmB concentrations of 50 µg/ml and 200 µg/ml respectively. These complexes were stable and non-haemolytic with retention of antileishmanial activity against intracellular *L.donovani* amastigotes in differentiated THP-1 cells *in vitro* (EC_{50} 0.27±0.03–0.35±0.04 µg/ml; EC_{50} of Fungizone® 0.22±0.04 µg/ml) after storage at 37°C for 7 days as an aqueous solution. The associated concentration of AmB-PGA complex (50.0 % AmB loading) with differentiated THP-1 cells at an extracellular AmB concentration of 10 µg/ml after 4 h incubation at 37ºC was 1.42±0.06 AmB nmole/mg protein. In comparison Fungizone® displayed 2.37±0.06 AmB nmole/ mg protein. AmB-PGA complex with AmB loading of 50.0% displayed potent activity against *L.donovani* infection in BALB/c mice. The parasite burden was inhibited by 84.44±3.2% and 94.4±1.5 % at AmB dose of 1.25 mg/kg and 2.5 mg/kg (given as single iv injection in three alternate days) respectively. This *in vivo* antileishmanial activity was similar to AmBisome® (95.52±0.4 % inhibition at AmB dose of 1.0 mg/kg at same dose regimen).

Conclusion: We have prepared non-toxic AmB-PGA complexes in a range of AmB loadings from ~20.0-50.0% that are active against *L.donovani* amastigotes *in vitro* and *in vivo*.

Bioadhesive 6 arm-PEG-catechol Grafted Islet Transplantation for Treatment of Type 1 Diabetes

J. Jeong[1], S. Hong[2], S. Yook[1], Y. Jung[1], C. Khue[1], S. Hong[1], B. Im[1], J. Park[1], H. Lee[3], C. Ahn[4], D. Lee[5], and Y. Byun[6]

[1] College of Pharmacy, Seoul National University, Seoul 151-742, South Korea
[2] Department of Chemistry, College of Natural Science, Advanced Institute of Science and Technology, Taejeon, 305-701, South Korea
[3] Graduate School Nanoscience and Technology, College of Natural Science, Advanced Institute of Science and Technology, Taejeon, 305-701, South Korea
[4] Research Institute of Advanced Materials (RIAM), Department of Materials Science and Engineering, Seoul National University, Seoul 151-742, South Korea
[5] Department of Bioengineering, College of Engineering, Hanyang University, Seoul 133-791, South Korea
[6] Departments of Molecular Medicine and Biopharmaceutical Sciences, College of Pharmacy, Seoul National University, Seoul, South Korea

Purpose: Immunoprotection is the most concerned challenge facing islet transplantation for the treatment of type I diabetes mellitus. As a result it is important to find a highly efficient islet cell protection method against host immune reaction after islet transplantation. The purpose of this study is to evaluate the effect of islet surface modification using multi-arm PEG derivatives, in combination with low dose of tacrolimus (FK506) in the rat to mice xenograft.

Methods: Pancreatic islets were isolated from pancreas of outbred male Sprague-Dawley (SD) rats by collagenase digestion. Isolated islets were suspended and incubated in serum-free HBSS containing 1% of 6 arm-PEG-catechol (MW 16,000 Da) for 1 hr. Functionality, viability and surface density of 6 arm-PEG-catechol grafted islets were evaluated. Then, 6 arm-PEG-Catechol grafted islets were transplanted into the kidney of C57Bl/6 mice and 0.2 mg/kg of FK506 were daily injected into the intraperitoneal cavity.

Results: 6 arm-PEG-catechol was incorporated on the islet surface without apparent damage to islet morphology. No significant difference in insulin release was examined between unmodified islets and 6 arm-PEG-catechol grafted islets. The blood glucose level returned to normal after transplantation of islets. The median survival time (MST) of 6 arme-PEG-catechol grafted islet transplanted group and control islet transplanted group were 12 ± 1.32 days and 10.5 ± 1.32 days, respectively. However, very interestingly combinational effect could be observed in the recipients transplanted with 6 arm-PEG-catechol grafted islets in addition to the injection of low dose of FK506, where the MST was significantly increased to 21 ± 1.91 days (Control+FK506: 10 ± 2.89 day).

Conclusion: Immunoprotective therapy using 6 arm-PEG-catechol and low dose of FK506 is a very promising strategy for protecting transplanted islets against host immune reaction.

High-Fat Diet Alters Hepatic and Renal Cytochrome P450-Mediated Eicosanoid Metabolism in Mice

Katherine N. Theken[1], Yangmei Deng[1], Robert N. Schuck[1], M. Alison Kannon[1], Tricia M. Miller[2], Samuel M. Poloyac[2], and Craig R. Lee[1]

1. Division of Pharmacotherapy and Experimental Therapeutics, Eshelman School of Pharmacy, University of North Carolina, Chapel Hill, NC
2. Department of Pharmaceutical Sciences, School of Pharmacy, University of Pittsburgh, Pittsburgh, PA

Purpose: Cytochrome P450 (CYP)-mediated eicosanoid metabolism regulates inflammation and may be involved in the pathophysiology of metabolic syndrome. CYP2C-derived epoxyeicosatrienoic and dihydroxyeicosatrienoic acids (EET+DHETs) are anti-inflammatory, while CYP4A-derived 20-hydroxyeicosatetraenoic acid (20-HETE) is pro-inflammatory. We sought to evaluate the effect of high-fat diet (HFD)-induced metabolic changes on hepatic and renal CYP eicosanoid metabolism.

Methods: Male *ApoE*$^{-/-}$ and C57BL/6 (WT) mice received HFD (21% fat, 0.21% cholesterol) or standard diet (Std) for 4 (N=8) or 8 weeks (N=4). CYP epoxygenase (EET+DHET formation) and ω-hydroxylase (20-HETE formation) metabolic activity was assessed by incubating liver and kidney microsomes with arachidonic acid and expressed relative to the WT/Std group as mean±SEM %control formation rate. Data were analyzed by ANOVA with post-hoc Dunnett's test.

Results: HFD induced metabolic dysfunction, resulting in higher plasma total cholesterol and insulin compared to WT/Std. Total cholesterol was significantly higher in *ApoE*$^{-/-}$/HFD compared to WT/HFD, but no differences in insulin were observed between the HFD-fed groups. Relative to WT/Std, HFD significantly suppressed hepatic EET+DHET formation at 4 (*ApoE*$^{-/-}$: 49.9±5.6%, WT: 53.3±3.1%, P<0.01) and 8 weeks (*ApoE*$^{-/-}$: 43.0±4.3%, WT: 57.3±6.2%, P<0.01). At 4 weeks, hepatic 20-HETE formation was significantly lower in HFD-fed mice (*ApoE*$^{-/-}$: 79.8±4.8%, WT: 80.0±4.5%, P<0.01), relative to WT/Std. However, no differences were observed at 8 weeks (*ApoE*$^{-/-}$: 92.7±9.2%, WT: 99.5±5.0%). The hepatic 20-HETE:EET+DHET formation rate ratio was significantly greater in HFD-fed mice at both 4 (*ApoE*$^{-/-}$: 1.64±0.13, WT: 1.48±0.06, P<0.01) and 8 weeks (*ApoE*$^{-/-}$: 2.13±0.16, WT: 1.73±0.10, P<0.01), compared to WT/Std (1.01±0.06). No significant differences in renal EET+DHET formation were observed. Renal 20-HETE formation was significantly greater in HFD-fed mice at both 4 (*ApoE*$^{-/-}$: 192.7±22.6%, WT: 378.0±39.9%, P<0.01) and 8 weeks (*ApoE*$^{-/-}$: 239.4±46.6%, WT: 357.8±36.5%, P<0.01). The renal 20-HETE:EET+DHET formation rate ratio was significantly greater in HFD-fed mice at 4 (*ApoE*$^{-/-}$: 4.25±0.49, WT: 7.67±0.72, P<0.01) and 8 weeks (*ApoE*$^{-/-}$: 5.49±1.11, WT: 7.62±0.31, P<0.01), compared to WT/Std (1.86±0.23).

Conclusions: HFD significantly suppressed hepatic CYP epoxygenase and induced renal CYP ω-hydroxylase metabolic activity, shifting the functional balance between these pathways in favor of the pro-inflammatory CYP ω-hydroxylase pathway. Studies elucidating the underlying mechanism and biological implications of these effects remain necessary.

Delineating Potential Effects of Bisphenol A on Placental Fatty Acid Homeostasis

L. F. Pan, G. Knipp

Purdue University, Department of Industrial and Physical Pharmacy, College of Pharmacy, 575 Stadium Mall Dr., West Lafayette, IN 47907

Purpose: Essential fatty acids (EFAs) play a critical role in guiding proper fetal development and influencing pregnancy outcomes. The transfer of EFAs from the maternal to fetal compartments across the placenta is a highly regulated, directional fetoprotective process that can be altered by xenobiotics. Previous results from our laboratory have demonstrated that rat exposure to Di-(2-ethylhexyl)-phthalate (DEHP) and its metabolites dramatically alters the expression of EFA homeostasis maintaining isoforms in the rat placenta and can subsequently lead to a significant change in the fetal brain lipid metabolome. The purpose of this study is to determine the effects of another widely used plastic derived chemical, Bisphenol A (BPA), on the EFA homeostasis maintaining isoforms utilizing the *in vitro* rat HRP-1 trophoblastic model.

Methods: The HRP-1 trophoblastic cells were cultured in RPMI-1640 media and seeded at 5×10^4 cells/cm^2 in T-25 cm^2 flasks. To investigate the time-dependent effects of BPA, confluent HRP-1 cells were treated with 50uM BPA and harvested at 2, 4, 12, and 24 hr. Total RNA and protein lysates were extracted at each of those time points, and relative mRNA and protein expression determination of the target genes was performed by quantitative PCR and Western blot analysis, respectively. Uptake and transport studies were performed with arachidonic acid and docosahexanoic acid to characterize the functional effects of BPA exposure on placental EFA transfer.

Results: BPA differentially regulates the mRNA and protein expression patterns of several genes involved in the regulation of EFA transfer and metabolism in a time-dependent manner. Characterization of the uptake and transport of fatty acids such as arachidonic acid and docosahexanoic acid indicate differences in the functional activity of EFA transport conferring proteins after exposure to BPA.

Conclusions: These results suggest that BPA may differentially regulate the mRNA expression level changes of crucial genes that are required for maintaining the EFA homeostasis across the placenta, thereby increasing the risk of aberrant pregnancy and/or fetal outcomes. Results from these studies may provide insight into the mechanisms of BPA in altering placental EFA homeostasis and its contributions to the pathogenesis of adverse pregnancy and/or fetal outcomes.

Proximal tubular cell-targeted kinase inhibitor-lysozyme conjugates for the intervention in renal fibrosis

M.E.M. Dolman[1], K.M.A. van Dorenmalen[1], S. Harmsen[1], E. Pieters[1], D.M. van der Giezen[2], M. Lacombe[3], G. Storm[1], W.E. Hennink[1] and R.J. Kok[1]

[1]Dept of Pharmaceutics, Utrecht Institute for Pharmaceutical Sciences, Utrecht, Netherlands; [2]Dept of Pathology, University Medical Center Utrecht, Utrecht, Netherlands and [3]Kreatech Biotechnology, Amsterdam, Netherlands

Purpose: The aim of the present study is to inhibit the profibrotic signaling pathways in proximal tubular cells, by means of cellular targeted kinase inhibitor-lysozyme conjugates. Growth factor activated signaling pathways in proximal tubular cells play an important role in the pathogenesis of renal fibrosis. But the high doses needed and the potential side effects of kinase inhibitors limit their use in the treatment of diseases like renal fibrosis. We therefore investigate the delivery of kinase inhibitors to the kidney, as a novel targeted strategy to interfere in renal fibrosis.

Methods: The PDGF receptor kinase inhibitor imatinib was conjugated to the low molecular weight protein lysozyme (LZM) via the platinum-based linker ULS^{TM}. Imatinib-ULS-LZM was characterized by protein content and HPLC analysis. The in vivo biodistribution of intravenously and intraperitoneally administered imatinib-ULS-LZM was studied in mice. The in vivo efficacy was evaluated in the unilateral ureteral obstruction (UUO) model for renal fibrosis. The inhibitory effects on profibrotic gene expression and the production of profibrotic markers were analyzed by quantitative PCR and immunohistochemical staining.

Results: Imatinib was successfully coupled at a 1:1 molar ratio to LZM via a coordination chemistry based linker. Both after intravenous administration and after intraperitoneal injection, imatinib-ULS-LZM accumulated rapidly in the kidneys. Extensive accumulation of drug-LZM conjugates in the targeted cell type, i.e. proximal tubular cells of the kidney, was detected by immunofluorescence microscopy (anti-LZM staining). Analysis of renal drug levels showed that imatinib-ULS-LZM remained in the kidneys for at least 24 hours and slowly released the drug. In the UUO model of renal fibrosis, promising results have been achieved with a TGF-β kinase inhibitor-LZM conjugate in rats and we are investigating whether a beneficial outcome can be achieved by delivering imatinib to the kidney.

Conclusions: Kinase inhibitor-LZM conjugates have been developed which accumulate in the kidneys and can be administered intravenously and intraperitoneally. Targeting of kinase inhibitor-LZM conjugates to the proximal tubular cells is a promising approach to interfere in renal fibrotic disorders.

GPEN . 2010
University of North Carolina at Chapel Hill

Cationic Amphiphilic Drugs can Induce an Increase in Apparent Lysosomal Volume: Implications towards a Novel Intracellular Drug-Drug Interaction Pathway

Ryan S. Funk and Jeffrey P. Krise

University of Kansas, Department of Pharmaceutical Chemistry, Lawrence, KS 66049 USA

Purpose: Various mechanisms have been described in which the administration of one drug influences the pharmacokinetic parameters of a second. The ability of such drug-drug interactions to impact drug therapy has resulted in research into understanding the mechanisms by which drugs can interact within biological systems. This work illustrates a novel intracellular drug-drug interaction pathway resulting from drug-induced expansion of the apparent lysosomal volume of cells, which results in a significant increase in the cellular uptake of subsequently administered drugs that have a propensity to accumulate within the lysosomal compartment (i.e. lysosomotropic amines).

Methods: Lysosomotropic amine retention following cationic amphiphilic drug (CAD) treatment in MDA-1986 cells was measured using the amine probe, Lysotracker Red. Fluorescence microscopy was used to evaluate CAD-induced changes in probe accumulation and distribution in human fibroblasts. Kinetic studies of probe uptake and release following CAD treatment were conducted to identify the source of enhanced probe retention. Studies on lysosomal pH dependent probe retention in MDA-1986 cells were used to gauge the extent of change in apparent lysosomal volume following CAD treatment. Treatments known to inhibit endo-lysosomal accumulation of cholesterol were tested for their ability to inhibit CAD-induced expansion of the apparent lysosomal volume.

Results: Exposure to CADs results in an increase in the cellular retention of the amine-containing probe, Lysotracker Red. Fluorescence imaging indicates enhanced vesicular probe staining following CAD treatment, indicative of increased lysosomal retention. Kinetic studies of cellular probe retention following CAD treatment reveal that enhanced probe retention results from increased probe uptake rather than a decrease in its release. Measurements of apparent lysosomal volume show a 3-fold increase following CAD treatment. Treatments known to inhibit the endo-lysosomal cholesterol accumulation caused by CADs also prevent increased probe retention.

Conclusion: A newly identified intracellular drug-drug interaction pathway is described in which CADs cause an increase in the apparent lysosomal volume of cells resulting in the enhanced cellular uptake of subsequently administered lysosomotropic amines. Current work into understanding the molecular basis of this interaction indicates the role of CAD-induced alterations in the normal egress of cholesterol and possibly other lipids from the endo-lysosomal pathway as important.

Podia Session Schedule

Date: Friday, November 12

Location: Alumni Hall, George Watts Hill Alumni Center

Podia Session: Morning

Time	Presenter	Title
8:00 AM	Hardeep Oberoi	Cross-linked Polymer Micelles for Delivery of Anticancer Drug Cisplatin
8:20 AM	Deborah Goldberg	G3.5 PAMAM Dendrimer-SN38 Conjugates Enhance Transepithelial Transport of the Drug while minimizing Gastrointestinal Toxicity
8:40 AM	Kohta Mohri	Structural and immunological properties of polypod-like structure forming nucleic acids
9:00 AM	Elizabeth Giger	Delivery of plasmid DNA by calcium phosphate nanoparticles stabilized with bisphosphonate derivatives
9:20 AM	Fabiana Vicentini	Evaluation of in vivo efficacy of a nanodispersion as a topical carrier of siRNA
9:40 AM	Tsz Chung Lai	pH-Sensitive Multi-PEGylated Block Copolymer as a Bioresponsive pDNA Delivery Vector
10:00 AM		**Coffee Break**
10:20 AM	Liang Jin	Transport of colistin across the healthy and inflamed mouse blood-brain barrier
10:40 AM	Anna Vildhede	Specific and general inhibitors of the three hepatic organic anion transporters OATP1B1 (SLCO1B1), OATP1B3 (SLCO1B3) and OATP2B1 (SLCO2B1).
11:00 AM	Ting Zhao	Site-specific chemical modification with polyethylene glycol of human serum albumin prolongs half-life and improves intravascular retention in mice
11:20 AM	Benjamin Weber	Bioequivalence of Inhaled Corticosteroids - A Population Pharmacokinetic Approach
11:40 AM	Jing Wang	The Use of Phenanthrene Tetraol as a Pharmacokinetic Biomarker for Benzo[a]pyrene Activation in Humans
12:00 PM	Yoshiaki Suwa	Thermodynamic analysis of the interactions between organochlorine compounds and their recognition protein using Biacore T100 technology-The cases of polychlorinated biphenyl congeners and the monoclonal antibody PCB4
12:20 PM		**Lunch**

Podia Session Schedule

Date: Friday, November 12

Location: Alumni Hall, George Watts Hill Alumni Center

Podia Session: Afternoon

Time	Presenter	Title
2:10 PM	Tarang Nema	Use of silica based monolith as SPE cartridge for extracting catecholamine and metaheprine from urine
2:30 PM	Nicky Thomas	In vitro digestion of lipid-based formulations: Effect of lipid chain length and drug load
2:50 PM	Ryusuke Takano	Strategy for improving oral absorption of poorly water-soluble drugs based on model and simulation
3:10 PM	Xiaoming Xu	A Quality by Design (QbD) Approach to Understand Liposomal Formulations Containing a Hydrophilic Compound
3:30 PM	Surekha Ravji Pimple	Synthesis and Biological Evaluation of Quinazoline and Quinoline Derivatives as Positron Emission Tomography (PET) Tracers for Imaging of Growth Factor Receptors
3:50 PM	Pyry Valitalo	Population pharmacokinetics of naproxen in children In-vivo assessment of novel self nano-emulsifying drug delivery system
4:10 PM	Anna Elgart	(SNEDDS) indicates improved oral bioavailability of amiodarone by improved solubilization, reduced efflux and pre-systemic metabolism
4:30 PM	Yoshiyuki Shirasaka	Differential Interaction of Grapefruit Juice with Intestinal Absorption of HMG-CoA Reductase Inhibitors Pravastatin and Pitavastatin
4:50 PM		**Closing Remarks**

Cross-linked Polymer Micelles for Delivery of Anticancer Drug Cisplatin

H. S. Oberoi[1], F. C. Laquer[3], N. V. Nukolova[1], L. L. Arnold[2], S.M. Cohen[2] and T. K. Bronich[1]

[1]Department of Pharmaceutical Sciences and Center for Drug Delivery and Nanomedicine, College of Pharmacy,
[2]Department of Pathology and Microbiology, University of Nebraska Medical Center, Omaha, Nebraska;
[3]Department of Chemistry, University of Nebraska at Omaha, Omaha, Nebraska

Purpose: Benefits of the frequently prescribed platinum (Pt) chemotherapeutic drug cisplatin are compromised by undesirable side effects, poor pharmacokinetics and development of drug resistance. In this study, polymer micelles with cross-linked ionic cores, were prepared and utilized as carriers for cisplatin, an approach with the potential to overcome such limitations.

Methods: Poly(ethylene oxide)-poly(methacrylic acid) block copolymer (PEO-b-PMA) based cross-linked micelles were synthesized via condensation of PEO-b-PMA by Ca^{2+} into spherical micelles, core cross-linking, and removal of Ca^{2+} by extensive dialysis. Cisplatin was incorporated into the ionic core by reversible polymer-metal complex formation. The altered biodistribution (BD) and pharmacokinetics (PK) of cisplatin upon entrapment into micelles (cisplatin/M) were evaluated in tumor-bearing mice. Blood and representative organs were analyzed for Pt content using ICP-MS at various time intervals. The PK parameters were evaluated using noncompartmental analysis with WinNonlin software. The antitumor activity and toxicity were evaluted after 4 i.v. doses, each at 4-day intervals.

Results: Stable core cross-linked polymer micelles with efficient (up-to 40%) and reversible cisplatin loading were obtained. Slow and sustained release of the drug from cisplatin/M was observed without loss of drug activity. The cisplatin/M demonstrated prolonged blood circulation and increased tumor accumulation with significantly higher maximum observed plasma platinum concentration (Cmax), plasma area under the curve (AUC), tumor Cmax and tumor AUC compared to the free cisplatin treatment. Kidney, the primary target organ of cisplatin toxicity, had about threefold lower Pt Cmax than cisplatin-treated mice. Organs responsible for removing micelles from the bloodstream, the liver and spleen, had elevated Pt levels. The cisplatin/M treatment group had significantly reduced tumor burden compared to free drug treatment. Despite higher liver and spleen accumulation cisplatin/M treatment group had significantly lower general toxicity as evaluated by reduced body weight loss compared to free drug treatment group and normal levels of blood markers of toxicity.

Conclusions: Core cross-linked micelles with efficient, reversible, sustained drug release behavior, prolonged circulation, increased tumor accumulation and lower renal accumulation were developed. Such complexes have significantly improved antitumor activity and reduced general toxicity.

G3.5 PAMAM Dendrimer-SN38 Conjugates Enhance Transepithelial Transport of the Drug while minimizing Gastrointestinal Toxicity

D. Goldberg[1,2], V. Nirmalkumar[3], P. Swaan[1,2] H. Ghandehari[1,3]

[1] Fischell Department of Bioengineering, University of Maryland, College Park, MD
[2] Department of Pharmaceutical Sciences, Center for Nanomedicine and Cellular Delivery, University of Maryland, Baltimore, MD
[3] Departments of Pharmaceutics and Pharmaceutical Chemistry & Bioengineering, Center for Nanomedicine, Nano Institute of Utah, University of Utah, Salt Lake City, UT

Purpose: Poly (amido amine) (PAMAM) dendrimers have shown promise in oral drug delivery. Conjugation of SN38 to PAMAM dendrimers has the potential to improve its oral absorption while minimizing gastrointestinal toxicity. In this work we examined the in vitro toxicity, transepithelial transport and stability of G3.5-SN38 conjugates in a simulated gastrointestinal environment.

Methods: Cytotoxicity of G3.5-Glycine-SN38, G3.5-bAlanine-SN-38 and free SN38 was evaluated in Caco-2 cells by the WST-1 cell viability assay. Transepithelial transport of the conjugates was determined at 10 mM and 100 mM across Caco-2 monolayers and compared to transport of the free drug. Stability of the conjugates in simulated gastric fluid (SGF) and simulated intestinal fluid (SIF) was monitored for up to 6 and 24 hours, respectively, by quantifying release of SN38 by HPLC.

Results: Treatment of Caco-2 cells with G3.5-SN38 conjugates at concentrations up to 100 mM did not cause a reduction in cell viability. Comparable concentrations of SN38 reduced cell viability by 50%, suggesting that conjugation to dendrimers may reduce the gastrointestinal toxicity of the drug. Both conjugates showed a statistically significant increase in overall SN38 transepithelial transport compared to the free drug. Transport of G3.5-Glycine-SN38 was highly concentration dependent whereas transport of G3.5-bAlanine-SN38 was concentration independent. This suggests a saturable transport mechanism for G3.5-bAlanine-SN38 and highlights the importance of spacer chemistry on transport. G3.5-bAlanine-SN38 showed the highest stability with only 1% SN38 released in SGF and 3% released in SIF. G3.5-Glycine-SN38 showed slightly lower stability with up to 10% release in SGF and 20% release in SIF.

Conclusion: Conjugation of SN38 to anionic G3.5 PAMAM dendrimers minimizes its toxicity and release in the gastrointestinal environment while enhancing transepithelial transport of the drug. Together these results show that PAMAM dendrimers have the potential to improve the oral bioavailability of potent anti-cancer drugs.

Acknowledgement: Financial Support was provided by the Fischell Fellowship in Bioengineering to D. Goldberg, and NIH R01EB07470.

Structural and immunological properties of polypod-like structure forming nucleic acids

K. Mohri, M. Nishikawa, N. Matsuoka, N. Takahashi, Y. Takahashi, Y. Takakura

Department of Biopharmaceutics and Drug Metabolism, Graduate School of Pharmaceutical Sciences, Kyoto University, Kyoto, Japan

Purpose: Recent studies have shown that DNA can be immunostimulatory when outside the nucleus. Unmethylated CpG dinucleotides, or CpG motifs, has been proved to be one of the most potent immunostimulatory DNA molecules. Because DNA-mediated immunostimulation can be used in a variety of therapeutic applications, we examined whether the activity of CpG DNA is increased by building it up into polypod-like structures.

Methods: A series of polypod-like structure-forming nucleic acids, or polypodna, were designed and constructed using 3 to 6 oligodeoxynucleotides (ODNs) with the halves of each ODN being partially complementary to a half of other ODNs. The formation of polypodna was evaluated by polyacrylamide gel electrophoresis (PAGE), and the thermal stability was evaluated by measuring the melting temperature (Tm). The immunostimulatory activity of polypodna was examined in murine macrophage-like RAW264.7 cells by measuring the release of tumor necrosis factor (TNF)-α. Uptake by RAW264.7 cells was examined using polypodna prepared with Alexa Fluor 488-labeled ODN. Each polypodna was incubated in 20% mouse serum, and the degradation was evaluated by PAGE analysis.

Results: All preparations of polypodna had a major single band on PAGE, indicating that polypodna with 3 to 6 pods, i.e., tripodna to hexapodna, were successfully prepared. The Tm of polypodna decreased with increasing the pod number, even though ODNs with the identical base numbers were used. This pod number-dependent reduction in Tm could be explained by the assumed structural properties of polypodna; the bent angle at the center of ODN becomes smaller with an increase in the pod number. The TNF-α level released from cells was the highest with hexapodna, followed by penta-, tetra- and tripodna. Increasing pod numbers increased the cellular uptake of polypodna, but reduced the stability in mouse serum.

Conclusion: These results indicate that polypodna, especially hexapodna, containing CpG motifs can be a novel biodegradable adjuvant useful for a variety of immunotherapy.

Delivery of plasmid DNA by calcium phosphate nanoparticles stabilized with bisphosphonate derivatives

E.V. Giger, B. Castagner, J.-C. Leroux

Institute of Pharmaceutical Sciences, Department of Chemistry and Applied Biosciences, Swiss Federal Institute of Technology (ETH) Zurich, Switzerland

Purpose: Gene therapy offers a tremendous potential but its successful use has been hampered by the lack of sustained gene expression and major delivery problems. Calcium phosphate-DNA co-precipitate has been used for more than 35 years for the *in vitro* delivery of nucleic acids. A drawback of this procedure is the instability of the particles, which creates reproducibility problems and prevents *in vivo* administration. We present here a new system of delivering nucleic acids using DNA-loaded calcium phosphate nanoparticles stabilized with PEG-bisphosphonate.
Bisphosphonates are used in the clinic to treat osteoporosis due to their affinity for bone hydroxyapatite.

Methods: Green fluorescent protein DNA (6.6 µg/mL) and calcium chloride (250 mM) were added to HEPES buffer containing 1.5 mM phosphate. PEG-bisphosphonate was added immediately afterwards (Figure 1). Particle size was measured over time by dynamic light scattering. HeLa cells were used for transfection. Transfection efficiency was determined by flow cytometry.

Results: The size of DNA-loaded calcium phosphate nanoparticles coated with PEG-bisphosphonate was around 220 nm. Nanoparticles stabilized by 25 µM PEG-bisphosphonate remained stable 48 h after preparation while the ones decorated with 10 µM PEG-bisphosphonate increased in size by ~100 nm. The nanoparticles could transfect 60% of HeLa cells. Calcium phosphate co-precipitate transfected around 40% of the cells when added to the cells directly after preparation. When nanoparticles were first incubated for 48 h at room temperature, transfection efficiency of calcium phosphate-DNA co-precipitate decreased to less than 5% while the one of the stabilized nanoparticles remained constant at around 60%.

Conclusion: We showed that calcium phosphate nanoparticles could be stabilized by a PEG-bisphosphonate coating. The nanoparticles were stable for at least 48 h and as effective as freshly prepared calcium phosphate co-precipitate to transfect cells.
These nanoparticles are bioresorbable, biocompatible and could eventually be used *in vivo.* The addition of a targeting ligand will be investigated in the future.

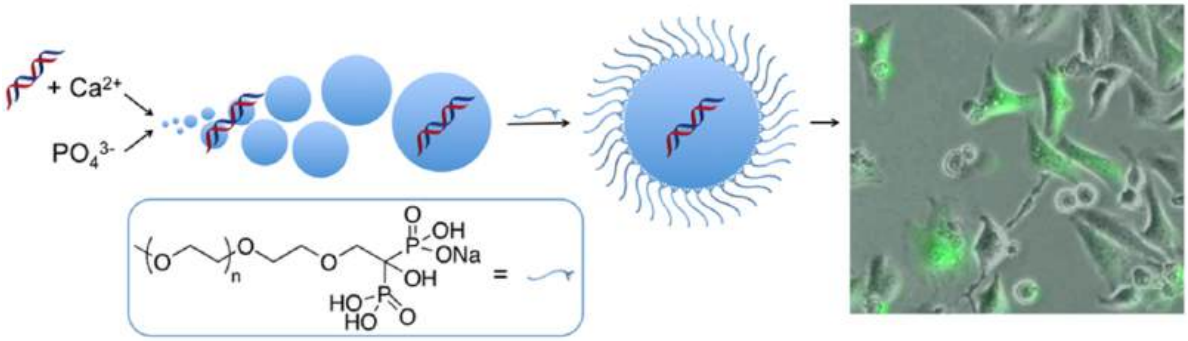

Figure 1: Preparation of stabilized calcium phosphate nanoparticles and subsequent transfection of HeLa cells.

Evaluation of *in vivo* efficacy of a nanodispersion as a topical carrier of siRNA

F. T. M. C. Vicentini, A. C. M. Polizello, M. V. L. B. Bentley

Faculdade de Ciências Farmacêuticas de Ribeirão Preto, Universidade de São Paulo, Brazil

Purpose: The ability of small-interfering RNA (siRNA) to potently, but reversibly, silence genes *in vivo*, has made them particularly well suited as a new class of drugs that interfere with disease-causing or disease-promoting genes, however, the largest remaining hurdle for widespread use of this technology in skin is an effective delivery system. Therefore, the present study was aimed to evaluate the potential functionality and the skin irritation of a nanodispersion of monoolein (MO) and oleic acid (OA) containing the cationic polymer polyethylenimine (PEI) as carrier systems for the delivery of siRNA into the skin.

Methods: The nanodispersion was obtained by mixing MO/OA/ PEI/ Tris-HCl 0.1 M, pH 6.5 containing 1.5% (w/ w) of poloxamer at 8:2:5:85 (w/w/w/w) and the GAPDH siRNA was incorporated at 10 µM. This system (100 µL) was administered on the dorsal skin of hairless mice and at 24 and 48 h post-application, the animals were killed with an overdose of carbon dioxide and the skin sections evaluated according to the established endpoints of irritation: infiltration of inflammatory cells and epidermis thickening. The ability of the nanodispersion to effectively deliver siRNA was investigated by evaluation of GAPDH protein knockdown by Western blot analysis.

Results: The skin irritation test showed no significant difference in the epidermis thickness after the treatment with the nanodispersions when compared to saline-treated animals. Furthermore, it was not observed infiltration of inflammatory cells. The *in vivo* efficacy study demonstrated an evident GAPDH protein reduction with the use of the studied nanodispersion containing GAPDH siRNA.

Conclusion: The present study demonstrates the safety and efficacy of the proposed nanodispersion as a delivery system for topical application of siRNA.

Acknowledgments: This work was supported by CNPq and FAPESP, Brazil.

pH-Sensitive Multi-PEGylated Block Copolymer as a Bioresponsive pDNA Delivery Vector

T.C. Lai[1], Y. Bae[2], K.Kataoka[3], and G. S. Kwon[1]

[1] Division of Pharmaceutical Sciences, School of Pharmacy, University of Wisconsin – Madison, 777 Highland Avenue, Madison, WI 53705-2222, USA
[2] Division of Pharmaceutical Sciences, College of Pharmacy, University of Kentucky, 725 Rose Street, Lexington, KY 40536-0082, USA
[3] Department of Materials Engineering, Graduate School of Engineering, The University of Tokyo, 7-3-1 Hongo, Bunkyo-ku, Tokyo, 113-8656, Japan

Purpose: To achieve higher gene delivery ability, non-viral vectors should be designed to respond to the rapidly changing environments inside human body in a sophisticated way. PEGylation is a very common method employed to increase the extracellular stability and the systemic circulation time of polyplex systems; however, PEGylated polyplexes always show lower transfection compared to their non-PEGylated counterparts, which is known as the "PEG dilemma". To deal with this, detachable PEGylated systems, such as carriers PEGylated through disulfide linkage, hydrazone linkage, have been investigated by various researchers. A reversibly-PEGylated diblock copolymer, poly[aspartate-hydrazide-poly(ethylene glycol)]-*block*-poly(aspartate-diaminoethane) (p[Asp(Hyd-PEG)]-*b*-p[Asp(DET)]) was reported here for enhanced gene transfection and colloidal stability. The diblock copolymer possessed a unique architecture based on a poly(aspartamide) backbone. The first block, p[Asp(Hyd)], was used for multi-PEG conjugations through hydrazone linkage, and the second block, p[Asp(DET)], was used for DNA condensation and facilitated endosomal escape.

Methods: p[Asp(Hyd-PEG)]-*b*-p[Asp(DET)] was synthesized and characterized by ^{1}H-NMR. Polyplexes were formed by mixing the synthesized polymers and pDNA at different N/P ratios. The polyplex size, ζ-potential, and *in vitro* transfection efficiency was determined by dynamic light scattering, ζ-potential measurements, and luciferase assays, respectively. Toxicity of the polyplexes or free polymers was evaluated based on cellular metabolism and membrane toxicity.

Results: The polyplexes were determined to be 70–90 nm in size, and the surface charge was effectively shielded by a PEG layer. The transfection efficiency of the reversibly-PEGylated polyplexes was confirmed to be comparable to that of the non-PEGylated counterparts and 1000 times higher than that of the irreversibly-PEGylated polyplexes under the conditions tested. PEG release from the reversibly-PEGylated polymers was demonstrated to be pH-sensitive. Toxicity of the DET-based polymers was shown to be minimal compared to branched PEI control.

Conclusions: The pH-sensitive nature of the PEG conjugation on p[Asp(Hyd-PEG)]-*b*-p[Asp(DET)] allows temporary PEGylation of the polyplexes. The physical characteristics and *in vitro* transfection efficiency evaluated using the reversibly-PEGylated polyplexes suggest that reversibly-PEGylated polyplexes can maintain satisfactory polyplex stability without compromising transfection efficiency.

Transport of colistin across the healthy and inflamed mouse blood-brain barrier

L. Jin[1], J. Li[1], R. Nation[1], J. Nicolazzo[1]

[1] Drug Delivery, Disposition and Dynamics, Monash Institute of Pharmaceutical Sciences, Monash University, Parkville, Victoria, Australia

Purpose: To investigate the blood-brain barrier (BBB) transport of colistin under physiological conditions and to assess the impact of systemic inflammation on the transport of this antibiotic across the BBB.

Methods: Brain exposure of colistin was assessed in Swiss Outbred mice using both in vivo and in situ techniques. Colistin (40 mg/kg) was administered subcutaneously (as a single dose or multiple doses) to determine whether brain uptake altered with increasing plasma concentrations. To assess the effect of P-glycoprotein (P-gp) and breast cancer resistance protein (BCRP) on BBB transport, colistin (5 mg/kg) was concomitantly administered intravenously with PSC833 or GF120918 (10 mg/kg). Brain and plasma concentrations were measured 5 min post-dose. To assess the impact of systemic inflammation on brain uptake, three intraperitoneal injections of lipopolysaccharide (LPS, 3 mg/kg) or saline were administered, and colistin brain uptake was measured either following subcutaneous administration (40 mg/kg) or by in situ perfusion (40 µg/mL colistin perfused into the left ventricle at 2 mL/min for 4 min). Colistin concentrations in brain, plasma and perfusate were determined by HPLC.

Results: Concentrations of colistin in brain homogenate following single or multiple subcutaneous administration were low at all post-dose time points, with brain-to-plasma (B:P) ratios ranging between 0.02 and 0.04. Co-administration of the P-gp and BCRP inhibitors did not significantly increase the B:P ratios of colistin ($p>0.05$). While LPS pre-treatment did not affect plasma concentrations of colistin, the brain concentrations were significantly increased ($p<0.05$), resulting in B:P ratios ranging between 0.08-0.14. Moreover, using the in situ perfusion technique, a significant ($p<0.01$) difference in brain-to-perfusate ratio was observed between LPS- and saline-treated mice (0.019 ± 0.001 and 0.014 ± 0.001, respectively).

Conclusion: Under healthy conditions, the brain uptake of colistin was minimal regardless of the plasma concentrations present, whereas higher BBB penetration was observed in the LPS inflammation model, which more closely resembles scenarios encountered in infected patients. This study provides insight into the potential for colistin to exhibit central neurotoxicity when used to treat systemic infections.

Specific and general inhibitors of the three hepatic organic anion transporters OATP1B1 (*SLCO1B1*), OATP1B3 (*SLCO1B3*) and OATP2B1 (*SLCO2B1*).

M. Karlgren, G. Ahlin, A. Vildhede, P. Artursson

Department of Pharmacy, Uppsala University, Uppsala, Sweden

Purpose: Knowledge about specific and general inhibitors of drug transporters is important for studying transport processes in complex *in vitro* systems, like primary human hepatocytes, but also for drug interaction screening assays in e.g. drug development. The aim of this study was to screen for drug interactions with OATP1B1, OATP1B3 and OATP2B1 and to study and compare the inhibition patterns of these uptake transporters that all are expressed in the human liver.

Methods: A structurally diverse data set of 130 compounds was studied in HEK293 cells stably transfected with human OATP1B1*1a, OATP1B3*2 or OATP2B1*1. Compounds inhibiting the uptake of the model substrates to 50% or more at 20 uM were defined as inhibitors, and comparisons for all compounds tested were made between the three transporters.

Results: Approximately one third of the tested compounds were classified as inhibitor for two or three of the OATP transporters, whereas 10-15% of all compounds were specific inhibitors for one of the OATP transporters when using the 50% cut off classification.

Conclusions: In conclusion, this study show that the three OATP transporters, OATP1B1, OATP1B3 and OATP2B1, show a broad overlap with regard to interacting compounds, but also that some compounds are specific inhibitors for only one of the transporters. These inhibitors will be valuable for understanding hepatic drug transport mechanisms and can also serve as a starting point for development of computational models for prediction of specific and multi-specific OATP inhibitors.

Site-specific chemical modification with polyethylene glycol of human serum albumin prolongs half-life and improves intravascular retention in mice

T. Zhao[1], Y. Cheng[3], H. Tan[2], J.Liu[1], G. Pang[4] and F. Wang[1, 2]

[1] Institute of Biochemical and Biotechnological Drugs, School of Pharmaceutical Sciences, Shandong University, Jinan, China
[2] National Glycoengineering Research Center, Shandong University, Jinan, China
[3] Department of Pharmacology, School of Pharmaceutical Sciences, Shandong University, Jinan, China
[4] Shandong Taibang Biologic Products Co.,Ltd, Taian,China

Purpose: Human serum albumin (HSA), the most abundant protein in plasma, contributes to 80% of the normal plasma colloid osmotic pressure (COP). It is used as an important plasma volume expander in clinical practice. However, the use of HSA in treating the critically illness related to the marked increase in capillary permeability remains contentious, because the infused HSA may extravasate into the interstitial space and induce peripheral edema. Such poor intravascular retention not only leads to interstitial edema but also demands a frequent administration of HSA. In addition, human plasma, from which HSA is prepared, is also in limited supply. Aimed at the two problems mentioned above, we hypothesize that increasing the molecular weight of HSA by PEGylation may be a potential approach to decrease capillary permeability and extravasation of HSA, and further prevent the interstitial edema and reduce the infusion frequency.

Methods: HSA was PEGylated in a site-specific manner by taking the advantage of the only one free cystein residue (Cys34) in HSA molecule. Homogeneous PEGylated HSA was isolated by DEAE Sepharose FF chromatography and ultrafiltration. The purity, PEGylated site and secondary structure of the modified protein were characterized by sodium dodecyl sulfate polyacrylamide gel electropheresis (SDS-PAGE), thiol group blockage method and circular dichroism (CD) measurement respectively. In addition, the pharmacokinetics in normal mice was investigated and vascular permeability of the PEGylated HSA was evaluated in lipopolysaccharide (LPS)-induced lung injury mouse model.

Results: The PEGylated HSA was heterogeneous when examined by SDS-PAGE,and PEG-Mal was specifically attached to the unique thiol group of HSA, Cys34. CD measurements indicated PEGylation didn't induce significant alteration of the secondary protein structure. The *in vivo* experiment showed that the biological half-life of the modified HSA was approximately 2.2 times that of the native HSA, and PEG-HSA had a lower vascular permeability than HSA, which suggests that the PEGylation of HSA could reduce the extravasation into interstitial space.

GPEN . 2010
University of North Carolina at Chapel Hill

Bioequivalence of Inhaled Corticosteroids - A Population Pharmacokinetic Approach

B. Weber, B. Kandala, G. Hochhaus

Department of Pharmaceutics, College of Pharmacy, University of Florida, Gainesville, FL

Purpose: The methodology to assess bioequivalence (BE) of inhaled corticosteroid (ICS) is still under discussion. The purpose of this project was to assess the suitability of pharmacokinetic (PK) metrics (AUC, C_{max}, T_{max}) as BE criteria for ICS.

Methods: A clinical trial simulation (CTS) approach was developed to systematically evaluate the sensitivity of PK metrics to differentiate between hypothetical test (T) and reference (R) products. The simulations were based on a population PK model (*Figure a*) that incorporated physiological aspects of inhalation therapy (central to peripheral (C/P) lung deposition, mucociliary clearance) as well as associated variability terms (inter- and intra-individual variability). Fluticasone propionate (FP) was selected as a representative ICS. Different scenarios were systematically simulated and the performance of the PK metrics evaluated. A scenario consisted of a hypothetical T product which either differed (not bioequivalent) from the R product in at least one PK parameter (pulmonary dose, C/P lung deposition ratio, pulmonary absorption rate constant) or was identical (bioequivalent) to the R product. In addition, all scenarios were repeated for different number of subjects. For each scenario, 200 independent BE trials were generated. For each trial, BE assessment was performed by applying standard criteria (AUC, C_{max}) or potentially appropriate alternative criteria (T_{max}) to the simulated PK data.

Results: A fraction of the results is presented in the figure. The figure shows the % of 200 independent BE trials that passed the respective BE criteria (AUC (*b*) and C_{max} (*c*) shown) for different scenarios (pulmonary dose and C/P ratio varied, pulmonary absorption rate constant fixed). More results will be presented at the meeting.

Conclusion: For slowly dissolving ICS with negligible oral bioavailability as FP, PK metrics (AUC, C_{max}) are very sensitive to differences in pulmonary dose and pulmonary absorption rate constant. Their sensitivity to differences in C/P lung deposition ratio depends on the impact of mucociliary clearance mechanisms. T_{max} is not suitable regardless of the statistical analysis method. Actual PK BE studies need to be conducted in healthy subjects and/or asthmatic patients to support the results and gain a better understanding of the effect of mucociliary clearance mechanisms.

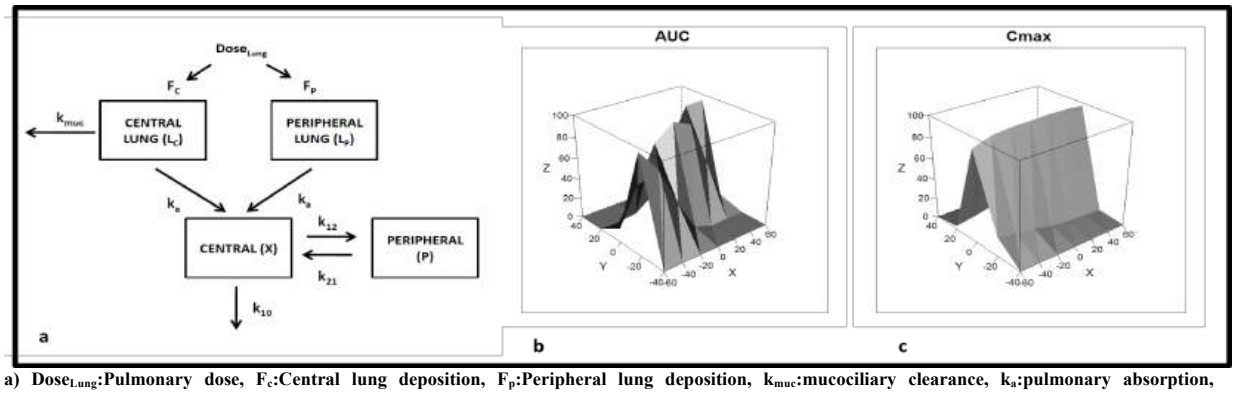

a) $Dose_{Lung}$:Pulmonary dose, F_C:Central lung deposition, F_P:Peripheral lung deposition, k_{muc}:mucociliary clearance, k_a:pulmonary absorption, k_{10}:elimination, k_{12} and k_{21}:distribution, all rate constants (k) follow first-order kinetics; b) and c) X:Difference in C/P ratio between T and R product, Y: Difference in pulmonary dose between T and R product, Z: % of trials which met respective BE criterion

The Use of Phenanthrene Tetraol as a Pharmacokinetic Biomarker for Benzo[*a*]pyrene Activation in Humans

J. Wang[1], Y. Zhong[2], S. G. Carmella[2], P. Upadhyaya[2], S. S. Hecht[2], and C. L. Zimmerman[1]

[1]Department of Pharmaceutics, University of Minnesota, Minneapolis MN
[2]Masonic Cancer Center, University of Minnesota, Minneapolis MN

Purpose: *r*-1,*t*-2,3,c-4-Tetrahydroxy-1,2,3,4-tetrahydrophenanthrene (phenanthrene tetraol, PheT) is a metabolite of phenanthrene (Phe), and its biotransformation from Phe parallels the metabolic activation of benzo[*a*]pyrene (BaP) to its diol epoxides (BPDE). BPDE can bind to DNA, resulting in mutations that can initiate carcinogenesis. Although Phe and BaP are present in cigarette smoke, Phe is not considered to be carcinogenic, and can be administered to humans. The hypothesis is that the balance between metabolic activation and detoxification of Phe (and BaP) is one determinant of an individual's cancer risk. As part of a broader validation of PheT as a biomarker for cancer risk, the relative exposure to deuterated PheT ([D_{10}]PheT) after the administration of [D_{10}]Phe via oral dosing and smoking was determined.

Methods: [D_{10}]Phe was administered to 10 subjects in a crossover design, either by oral administration or by smoking cigarettes. [D_{10}]Phe was used in order to avoid interference from environmental Phe. A dose of 10 µg [D_{10}]Phe was administered either as an oral solution or by smoking cigarettes doped with [D_{10}]Phe. Serial blood samples were collected over 24 hr after [D_{10}]Phe administration. Urine was collected over 48 hr after [D_{10}]Phe administration. Blood and urine samples were analyzed by GC-MS/MS. Two pharmacokinetic (PK) methods were used to determine the relative exposure to [D_{10}]PheT by the two routes of administration.

Results: In the smoking arm of the study [D_{10}]PheT was already present at high levels in the plasma at the first sampling time, suggesting that there was a significant pulmonary "first-pass" formation of [D_{10}]PheT. The relative exposure to [D_{10}]PheT from oral dosing over smoking was 0.92 ± 0.24 and 0.83 ± 0.28, based on the ratio of plasma AUCs and the ratio of the amount of PheT excreted in the urine, respectively. There was no statistically significant difference in the relative exposure determined from the two methods.

Conclusions: For large-scale risk assessment studies, the simpler the study design, the easier it will be to recruit subjects. Based on the preliminary results reported here, it appears that oral dosing of [D_{10}]Phe with subsequent urine collections will adequately reflect systemic exposure to [D_{10}]PheT.

Acknowledgements: Financial support for this work was from NCI grant CA-92

Thermodynamic analysis of the interactions between organochlorine compounds and their recognition protein using Biacore T100 technology
- The cases of polychlorinated biphenyl congeners and the monoclonal antibody PCB4 -

Y. Suwa[1,2], T. Saotome[2], M. Uchida[1,2], Y. Taniguchi[3], T. Kawaguchi[3], C. Kataoka[4], K. Sawadaishi[4], H. Morioka[1,2]

[1]Faculty of Life Sciences, [2]Graduate School of Pharmaceutical Sciences, [3]School of Pharmacy, Kumamoto University, Kumamoto, Japan, [4]Carbuncle Bio Scien Tech LLC., Kyoto, Japan

Purpose: Polychlorinated biphenyls (PCBs) comprise one of the largest classes of hazardous, persistent environmental pollutants. Of the 209 PCB congeners, four non-*ortho* (no chlorine atom in the 2,2',6,6' positions) and eight mono-*ortho* (chlorine atom in only one of the same four positions) congeners are currently designated by the WHO as "dioxin-like" in their toxic effects. The toxicity of the non-*ortho* coplanar PCBs (Co-PCBs) is thought to correlate with their ability to bind to the aryl hydrocarbon receptor, estrogen receptors and other proteins, however, the toxic mechanisms of Co-PCBs remain unclear. The pattern of chlorine atom positions on biphenyl ring provides a structural basis for different toxicological modes of action. Therefore, in order to clarify the molecular details of these interactions and understand how proteins recognize such organochlorine compounds, we focused on the interactions between Co-PCBs and their specific antibody PCB4.

Methods: We have created a single-chain Fv (scFv) protein from PCB4 antibody that binds specifically to four non-*ortho* Co-PCBs (PCB-77, PCB-81, PCB-126. PCB-169). ScFv is composed of the heavy-chain variable domain (VH) and the light-chain variable domain (VL) connected by a short polypeptide linker, and has several advantages as compared with intact antibody. PCB4scFv protein was produced as insoluble inclusion bodies in *Escherichia coli*. We therefore employed an *in vitro* refolding system and purified PCB4scFv to apparent homogeneity by several column chromatography procedures. The secondary structure of PCB4scFv was evaluated by CD spectra, and the binding of Co-PCBs to PCB4scFv was measured by Surface Plasmon Resonance (SPR) analysis using Biacore T100.

Results: We confirmed that PCB4scFv maintained proper protein folding and had specific antigen-binding activities. The kinetic and thermodynamic parameters of PCB4scFv to four non-*ortho* Co-PCBs indicated that the position and number of chlorine atoms on the biphenyl ring was important for favorable antigen binding. Thermodynamic analyses suggested that PCB4scFv mainly bound to Co-PCBs by van der Waals interactions and hydrogen bonding.

Conclusion: We elucidated molecular details of interactions between Co-PCBs and their specific antibody PCB4. These results contribute importantly to understandings of interactions between organochlorine compounds and their recognition protein.

Use of silica based monolith as SPE cartridge for extracting catecholamine and metanephrine from urine

T. Nema[1], E.C.Y. Chan[1], P.C. Ho[1],

[1] Department of Pharmacy, National University of Singapore, Singapore

Purpose: The silica monolith with ionizable silanol groups and large surface area was utilized as an offline cation exchange solid phase-extraction (SPE) cartridge for extracting polar catecholamine and metanephrine in urine.

Methods: The prepared cartridge was housed in a 2-mL syringe fixed over a SPE vacuum manifold. The unique property of this silica monolithic cartridge was demonstrated by extracting biogenic amines including epinephrine, normetanephrine and metanephrine from urine samples. These analytes were chosen as model compounds for testing because of their high hydrophilicity, and being candidates monitored for clinical diagnosis. The extracted analytes, after concentration and re-constitution were then quantitated by high-performance liquid-chromatography coupled to mass spectrometer (HPLC/ESI/MS).

Results: Multiple reactions monitoring was carried out with transitions: 184→107, 184→134 and 198→148 for analyzing epinephrine, normetanephrine and metanephrine, respectively. The limit of detection was 3ng/mL for metanephrine and 5ng/mL for normetanephrine and epinephrine. The relative standard deviations of measurements ranged from 2-10%. The sorbent offered good linearity with correlation coefficients > 0.99, over a concentration range of 20-200ng/mL. The relative recoveries ranged from 60-67%, 55-59% and 99-105% for epinephrine, normetanephrine and metanephrine, respectively.

Conclusion: This preliminary study based on silica monolith had shown potential and was found more robust in extracting polar analytes repeatedly without any significant loss in efficiency.

***In vitro* digestion of lipid-based formulations: Effect of lipid chain length and drug load**

N. Thomas, T. Rades, A.Graf

School of Pharmacy, University of Otago, Dunedin, New Zealand

Purpose: To investigate the performance of two oral lipid-based formulations (LBF) upon *in vitro* digestion. Formulations varied in the chain length of the lipid component and in drug loads.

Methods: Two LBF were designed as self-nanoemulsifying drug delivery systems (SNEDDS) with a constant lipid-to-surfactant ratio but with different chain length of the lipid component. Formulations were prepared by mixing 55% oil phase (either medium-chain (MC) or long-chain (LC) lipids), 35% surfactant (Cremophor RH40) and 10% cosolvent (ethanol). Equilibrium drug solubilities of simvastatin (100% drug load) in formulations were determined by HPLC. Dispersions (1:250) of drug- free and drug loaded SNEDDS were investigated by PCS and cryo-SEM. Thereafter, 1 g of each formulation was subjected to *in vitro* lipolysis for 60 minutes at 25%, 50% and 100% of the corresponding drug loads. Samples were withdrawn at designated time points. After ultracentrifugation the resulting precipitates and micellar supernatants were analysed for their drug content by HPLC. Lipolysis experiments without lipase were carried out as controls. All experiments were done in triplicates.

Results: MC and LC-SNEDDS showed high drug solubilities (112.9 mg/g and 84.3 mg/g, respectively), rapid dispersion (< 1min) and droplet sizes of 33 nm (MC-SNEDDS) and 43 nm (LC-SNEDDS). Compared to drug-free formulations the droplet sizes of dispersed formulations did not change significantly up to 50% drug load. Although digestion of MC-SNEDDS occurred faster compared to LC-SNEDDS they were able to maintain the drug in solution throughout the experiment and independent of drug loads. Elevating the drug load from 25% to 50% and 100% in LC-SNEDDS initially resulted in increased precipitation of simvastatin (from 21% to 33%). However, after 60 minutes 95% of the drug was solubilised in the colloidal digestion products.

Conclusion: The ability of LC-SNEDDS to keep the coadministered drug in solution was affected by drug load and progress of digestion. MC-SNEDDS performed independently of digestion and drug load, maintaining the drug in solution despite rapid digestion of the formulation *in vitro*. The results obtained from *in vitro* digestion suggest the potential benefit for SNEDDS based on MC for the delivery of poorly water-soluble drugs like simvastatin.

Strategy for improving oral absorption of poorly water-soluble drugs based on model and simulation

R. Takano[1,2], S. Yamashita[1]

[1] Faculty of Pharmaceutical Sciences, Setsunan University, Osaka, Japan
[2] Discovery Platform Technology Department, Chugai Pharmaceutical Co., Ltd., Shizuoka, Japan

Purpose: Low solubility often causes poor and variable oral absorption because the dissolution rate or solubility is insufficient to be absorbed completely from the GI tract. Therefore, it is critical to predict oral absorption of poorly soluble compounds at the early stage of drug development. The purposes of this study are (1) to develop a model to describe the oral absorption process, (2) to elucidate the rate-limiting process and (3) to establish the strategy for improving oral absorption of poorly soluble compounds.

Methods: Structurally diverse 12 BCS class II drugs were used as model compounds. Intrinsic parameter of dissolution rate (*Z*) was derived from the *in vitro* miniscale dissolution test and used for the simulation of *in vivo* dissolution profile. Oral absorption of each drug was simulated by a physiology-based kinetic model using solubility, dissolution rate and permeability. Intraluminal drug concentration was also simulated to elucidate the rate-limiting step of oral absorption. Finally, to clarify the effect of supersaturation that can improve the absorption of poorly soluble drugs, *in vivo* intraluminal concentration of a novel farnesyltransferase inhibitor (FTI-2600) after oral administration of crystalline free base or HCl salt was estimated.

Results: (1) The *in vitro* dissolution profile in a biorelevant medium with bile and lecithin gave better estimations of oral absorption for all model drugs than that in a conventional buffer. The predicted fraction of dose absorbed of BCS class II drugs correlated well with clinical data. (2) By comparing the maximum solubility and the intraluminal concentration *in vivo*, rate limiting step of each drug, dissolution-rate-limited and solubility-limited, was clearly demonstrated (3) In the oral administration study in dog, HCl salt of FTI-2600 resulted in the 4-fold increase in the plasma concentration than the free base. From the kinetic analysis, it was revealed that HCl salt caused supersaturation in the intestinal tract that increased intraluminal concentration of the drug. These results provide clear evidence that the supersaturation phenomenon improved the solubility-limited absorption.

Conclusion: The present model contributes to the improvement of oral absorption and will aid in the success of BCS class II drug development.

GPEN. 2010
University of North Carolina at Chapel Hill

A Quality by Design (QbD) Approach to Understand Liposomal Formulations Containing a Hydrophilic Compound

X. Xu[1], M. A. Khan[2], D. J. Burgess[1]

[1] School of Pharmacy, University of Connecticut, Storrs, CT 06269
[2] FDA/CDER/DPQR, Silver Spring, MD 20993

Purpose: The encapsulation of hydrophilic drugs into liposomes presents unique challenges. Specifically, the high water solubility of these molecules makes it difficult to achieve a high degree of entrapment. In addition, it is unknown how different process and product variables impact product quality and performance. Therefore, an investigation of the application of QbD concepts to liposomes containing a hydrophilic compound was performed to obtain valuable information on critical formulation and process variables.

Methods: The anti-viral drug tenofovir was selected as a model compound and liposome formulations were successfully prepared and characterized. To apply QbD principles, a complete risk analysis (Ishikawa diagram) was performed to identify high risk factors. This was followed by screening (Plackett-Burman) and optimization (Response Surface Method) studies. Key parameters were varied and mapped against each other to determine the design space within which the critical quality attributes are maintained.

Results: Eight high-risk variables were identified, and these were used in the Plackett-Burman screening study. It was discovered that except for lipid concentration and drug concentration, the other six parameters did not have any significant effect on the drug encapsulation efficiency. Lowering the drug concentration as well as increasing the lipid concentration contributed to a higher degree of drug encapsulation. The subsequent response surface method study fully elucidated the relationship between lipid concentration, drug concentration and encapsulation efficiency. The accuracy and robustness of the model were confirmed on comparison of the model generated response surface with additional data points used for verification. Accordingly, the design space for tenofovir liposomes for the prediction of drug encapsulation efficiency has been successfully established. The liposomes were stable (9 months, study ongoing) and retained the entrapped drug until disruption by an external force.

Conclusion: The feasibility and the advantages of applying QbD concepts to liposomes containing small molecule hydrophilic drugs has been demonstrated using tenofovir. The design space was established for tenofovir liposomes to predict drug encapsulation efficiency.

Acknowledgement: FDA critical path funding (REQ1044477).

Disclaimer: The views expressed are those of authors and do not necessarily represent the official position of the Agency.

Synthesis and Biological Evaluation of Quinazoline and Quinoline Derivatives as Positron Emission Tomography (PET) Tracers for Imaging of Growth Factor Receptors

S. R. Pimple[1,2], L. Scapozza[1] and Y. Seimbille[2]
[1]School of Pharmaceutical Sciences, University of Geneva & University of Lausanne, 30 Quai Ernest Ansermet, 1211 Geneva, Switzerland.
[2]HUG Division of Nuclear Medicine, Cyclotron and Radiopharmaceutical Chemistry Unit, Rue Gabrielle-Perret-Gentil 4, 1211 Geneva, Switzerland.

Purpose: Our research focuses on synthesis and biological evaluation of ^{18}F-labeled and unlabeled reversible (5-substituted-anilinoquinazoline) and irreversible (6,7-disubstituted-4-anilinoquinoline-3-carbonitrile) inhibitors of epidermal growth factor receptor (EGFR) and HER-2 tyrosine kinases, which will be finally used as PET tracers.

Methods: The first series of compounds was synthesized by introducing the N-methyl-piperidinyl moiety at position 5 with subsequent conversion of the quinazolones into 4-chloro- or 4-thiomethyl-quinazolines and final amination with aniline or substituted benzyloxyaniline moiety. The compounds of the second series were prepared either by acylation of 6-amino-4-(arylamino)-quinoline-3-carbonitriles with unsaturated acid chlorides or by amination of 4-chloro-6-(crotonamido)-quinoline-3-carbonitriles with monocyclic or bicyclic anilines. The precursors for the hot chemistry, which will be labeled with ^{18}Fluorine by nucleophilic substitution reaction, have been synthesized by modified synthetic routes starting from 2-chloro-4-nitroaniline and N,N-dimethylbenzaldehyde.

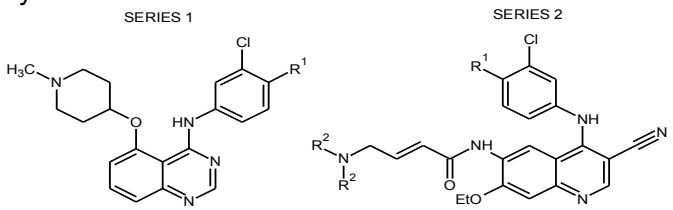

Results: The synthesized cold compounds as well as the precursors for the hot chemistry were chemically characterized by high resolution mass spectrometry and NMR techniques. Also, the elemental analysis results lie within limits indicating high purity. They are under evaluation by *in vitro* methods such as tyrosine kinase assay, cell based autophosphorylation assay (A-431 and HTB-20) and cell proliferation assay on HTB-16, A-431 and HTB-20 cancer cell lines. Some of the compounds have exhibited IC_{50} values in nanomolar concentration range. Experiments quantifying absorption of the labeled analogs in viable cancer cells using γ-counter are ongoing and data will be presented.

Conclusion: New potent EGFR and HER-2 inhibitors were successfully synthesized by multistep synthetic pathways. The *in vitro* assay protocols were well developed and implemented to achieve reliable results. In view of PET analysis, the precursors have been synthesized and characterized. The excellent inhibition potency of some of the compounds suggests that they have the potential to be developed as PET imaging probes for noninvasive assessment of the growth factor receptor status in malignant tumors for the better understanding of biological and clinical criteria for patient selection and monitoring of EGFR targeted therapies.

Population pharmacokinetics of naproxen in children

P. Välitalo[1], E. Kumpulainen[1], M. Manner [1], M. Kokki[2], M. Lehtonen[1], A. Hooker[3], V-P. Ranta[1], H. Kokki[2]

[1] Faculty of Health Sciences, University of Eastern Finland, Kuopio, Finland
[2] Department of Anesthesiology and Intensive Care, Kuopio University Hospital, Kuopio, Finland
[3] Department of Pharmaceutical Biosciences, University of Uppsala, Uppsala, Sweden

Purpose: To our knowledge, there are no published data available about the pharmacokinetics of naproxen in children younger than 5 years of age. The purpose of this study was to investigate the pharmacokinetics of naproxen in children aged 3 months to 13 years and to evaluate the permeation of naproxen into cerebrospinal fluid in children using population pharmacokinetic modelling.

Methods: 53 children were enrolled in the study. The children received a single dose (10 mg/kg) of oral naproxen suspension. The concentration-time data included 270 total plasma concentrations, 52 unbound plasma concentrations and 52 CSF concentrations. The pharmacokinetics data were modelled using nonlinear mixed-effects models with NONMEM VI 2.0 software.

Results: The plasma data were best described with a 2-compartmental model with first-order absorption. Bodyweight predicted plasma clearance of naproxen linearly, and age did not seem to affect the clearance after weight had been included as a covariate. When scaled to 70kg, the apparent clearance of naproxen was 0.6 l/h and the apparent volumes of distribution were 7.4 l and 4.4 l for central and peripheral volumes, respectively.
The fraction of unbound naproxen in plasma was 0.14%. The concentrations of naproxen in CSF were about four times higher than the concentration of unbound naproxen in plasma.

Conclusion: Estimating the pharmacokinetic parameters would not have been possible from these sparse data when using individual pharmacokinetic modeling methods. When scaled by weight, the pharmacokinetic parameters of naproxen in children aged 3 months to 13 years were found to be similar to previously reported values for children older than 5 years of age.

GPEN. 2010
University of North Carolina at Chapel Hill

In-vivo assessment of novel self nano-emulsifying drug delivery system (SNEDDS) indicates improved oral bioavailability of amiodarone by improved solubilization, reduced efflux and pre-systemic metabolism

A. Elgart, I. Cherniakov, Y. Aldouby, A. J. Domb and A. Hoffman

Institute for Drug Research, School of Pharmacy, the Hebrew University of Jerusalem

Purpose: Numerous BCS Class 2 compounds exhibit low and erratic absorption. Improved bioavailability by incorporation into SNEDDS is attributed mainly to solubilization. This study aims to elucidate additional mechanisms involved in the superior bioavailability of this delivery system.

Methods: SNEDDS of amiodarone (AM) was developed and optimized. PK parameters and tissue distribution were assessed *in-vivo*. Permeability was evaluated *in-vitro* (Caco-2) and *ex-vivo* (Ussing chamber). Solubilization was assessed by dynamic lipolysis model. The effect on intraenterocyte metabolism was evaluated in CYP3A4 microsomes. P-gp efflux inhibition was determined using talinolol as substrate. LDH assay was used for cytotoxicity evaluation. Mannitol permeability and TEER served as markers for tissue integrity and para-cellular transport.

Results*: In-vivo,* AM-SNEDDS and AM co-administrated with blank SNEDDS showed significantly higher AUC vs. AM (9.23±0.83 and 10.65±4.38 vs. 6.28±3.0 hr*μg/ml) and C_{max} following PO administration. AM-SNEDDS exhibited more consistent absorption and higher tissue exposure. *Ex-vivo*, AM-SNEDDS permeability coefficient (Papp) was significantly higher than AM. *In-vitro*, no significant difference was found. In contrast, talinolol *in-vitro* studies resulted in significantly higher Papp of talinolol-SNEDDS. Higher solubilized AM concentration was found following AM-SNEDDS lipolysis vs. AM (90.5±1.33% vs. 59.1±9.45% respectively). Significantly higher AM concentrations remained intact following incubation of AM-SNEDDS vs. AM with CYP3A4 (102.4±5.61% vs. 68.57±1.17%). Adding blank SNEDDS to testosterone also resulted in significantly reduced testosterone metabolism. SNEDDS toxicity to the enterocytes is negligible. No affect on AUC was found when AM was administered 2h subsequently to blank SNEDDS. No differences in mannitol Papp and TEER values was found in Caco-2 in the presence or absence of SNEDDS.

Conclusions: Our SNEDDS not only improves solubilization, but also reduces intra-enterocyte metabolism and P-gp activity. Thus, SNEDDS increases bioavailability of Class 2 compounds and reduces their typical high variability in bioavailability by multi-processes mechanism. The fact that AM bioavailability increased both upon incorporation into SNEDDS and following co-administration with blank SNEDDS highlights the unique activity of our delivery system. SNEDDS effect is reversible and doesn't cause tissue or cell damage. These notable findings contribute to our understanding of the investigated phenomenon of the *in-vivo* impact of SNEDDS on oral bioavailability.

GPEN . 2010
University of North Carolina at Chapel Hill

Differential Interaction of Grapefruit Juice with Intestinal Absorption of HMG-CoA Reductase Inhibitors Pravastatin and Pitavastatin

Y. Shirasaka, K. Suzuki, T. Nakanishi, I. Tamai

Faculty of Pharmacy, Institute of Medical, Pharmaceutical and Health Sciences, Kanazawa University, Kakuma-machi, Kanazawa 920-1192, Japan

Purpose: We have reported that OATP/Oatp-mediated transport may contribute to intestinal absorption of nonmetabolic statins pravastatin and pitavastatin. Recently, several investigations have indicated that OATP/Oatp- and MDR1/Mdr1-mediated absorption of drugs is a putative site of grapefruit juice (GFJ) and drug interactions. In the present study, we aimed to investigate the effect of GFJ on transporter-mediated absorption of pravastatin and pitavastatin in rats.

Methods: Oatp1a5-mediated uptake of drugs was evaluated with *Xenopus* oocytes. Mdr1a-mediated drug transport was evaluated in LLC-PK1/Mdr1a cells. Rat intestinal permeability of drugs was measured by the *in situ* closed loop method. *In vivo* drug absorption was kinetically assessed by measuring plasma concentration after oral administration in rats. The concentration of drugs in all samples was measured by LC/MS/MS analysis.

Results: The plasma concentration of pravastatin after oral administration was significantly decreased by coadministration of GFJ, while that of pitavastatin was significantly increased. Similar results were obtained in *in situ* absorption studies. Uptakes of pravastatin and pitavastatin by Oatp1a5 cRNA-injected oocytes were significantly increased compared with those by water-injected oocytes, suggesting that both pravastatin and pitavastatin are substrates of Oatp1a5. Naringin, the main constituent flavonoid of GFJ, inhibited the Oatp1a5-mediated uptakes of pravastatin and pitavastatin. Therefore, a decrease of pravastatin absorption in the presence of GFJ may be due to the inhibition of Oatp-mediated transport by naringin. On the other hand, in LLC-PK1/Mdr1a cells, the permeability of pitavastatin in the BL to AP direction was markedly greater than that in the AP to BL direction, indicating that pitavastatin is a substrate of Mdr1a. Since naringin was found to inhibit Mdr1a-mediated transport of pitavastatin, it was considered that an apparent increase of pitavastatin absorption by GFJ was caused by an inhibitory effect of naringin on both Oatp and Mdr1.

Conclusion: The present study indicates that the intestinal absorption of pravastatin and pitavastatin can be explained by the involvement of Oatp for both statins and Mdr1 for only pitavastatin. Therefore, differential effect of GFJ on intestinal absorption between them may be due to the effect of naringin on the transport of those drugs mediated by Oatp- and Mdr1.

Poster Session, Wednesday, November 10th

Location: Alumni Hall, George Watts Hill Alumni Center

Display: 8:00 AM – 5:00 PM

Authors Present: 12:00 – 2:00 PM

ADME		
POSTER ID	**PRESENTER**	**TITLE**
PS-W-1	CHRISTIAN WAGNER	FORECASTING PLASMA PROFILES OF A POORLY SOLUBLE DRUG, NIFEDIPINE, BY COUPLING BIORELEVANT DISSOLUTION TESTS WITH A PBPK COMPUTER MODEL
PS-W-2	JOHANNA RAIKKONEN	ZOLEDRONIC ACID INDUCES FORMATION OF A PRO-APOPTOTIC ATP ANALOG AND ISOPENTENYL PYROPHOSPHATE IN VIVO AND IN VITRO
PS-W-3	MATTHEW DUFEK	P-GLYCOPROTEIN (P-GP) ENHANCES THE PORTAL BIOAVAILABILITY OF LOPERAMIDE IN MOUSE BY REDUCING FIRST-PASS INTESTINAL METABOLISM
PS-W-4	MAYUKO YOSHIFUJI	URIC ACID TRANSPORTER-MEDIATED URICOSURIC EFFECT OF RDEA594, A METABOLITE OF ANTIVIRAL AGENT RDEA806
PS-W-5	MELINA MALINEN	GENERATION OF FUNCTIONAL THREE-DIMENSIONAL LIVER CELL CULTURE MODEL FOR DRUG DEVELOPMENT
PS-W-6	TATIANA CLARO DA SILVA	TRANSMEMBRANE DOMAIN I OF THE BILE ACID TRANSPORTER SLC10A2 CONTRIBUTES TO SUBSTRATE TRANSLOCATION EVENTS AND PROTEIN STABILITY
PS-W-7	WUJIAN JU	PEDIATRIC METABOLISM OF MEROPENEM IN INFANTS <91 DAYS OF AGE WITH COMPLICATED INTRA-ABDOMINAL INFECTIONS
PS-W-8	YUKI TERASHIMA	ESTABLISHMENT OF HUMAN-CYP3A4 EXPRESSED MDCK II CELL MONOLAYER TO INVESTIGATE INTESTINAL FIRST-PASS METABOLISM

CLINICAL/ TRANSLATIONAL RESEARCH		
POSTER ID	**PRESENTER**	**TITLE**
PS-W-9	CRISTINA SANTOS	A SURVEY OF NEUROBIOCHEMICAL LEVELS IN A PANEL OF GENETICALLY DIVERSE MOUSE INBRED STRAINS TO IDENTIFY A BIOMARKER FOR ANXIETY AND MOOD DISORDER
PS-W-10	DUAN WANG	THE DIFFERENT ROLES OF CAR IN THE INDUCTION OF DME BY CYCLOPHOSPHAMIDE AND IFOSFAMIDE
PS-W-11	NATHAN PFEIFER	EFFECT OF STEADY-STATE AND SINGLE-DOSE RITONAVIR ON THE HEPATOBILIARY DISPOSITION OF ^{99M}TC-MEBROFENIN (^{99M}TC-MEB) IN HEALTHY VOLUNTEERS
PS-W-12	SUMITO ITO	INVESTIGATION OF THE DRUG-DRUG INTERACTION BETWEEN METFORMIN AND A POTENT MATE INHIBITOR, PYRIMETHAMINE ON THE DISPOSITION OF METFORMIN

DRUG DESIGN		
POSTER ID	**PRESENTER**	**TITLE**
PS-W-13	CLAUDIA HENN	ESSENTIAL STEP TO THE IN VIVO PROOF OF CONCEPT: DESIGN AND SYNTHESIS OF 17B-HSD1 INHIBITORS FOR THE TREATMENT OF

		ESTROGEN-DEPENDENT DISEASES IN CALLITHRIX JACCHUS.
PS-W-14	JAKOB SHIMSHONI	SYNTHESIS, ABSOLUTE CONFIGURATION AND ENANTIOSELECTIVE BIOLOGICAL ACTIVITIES OF 4-OH-RETINOIC ACID ENANTIOMERS
PS-W-15	JULIANNE YOST	DEVELOPMENT OF SMALL MOLECULE PROTEIN LYSINE METHYLTRANSFERASE G9A INHIBITORS
PS-W-16	KAVYA RAMKUMAR	DESIGN OF GRP78 INHIBITORS AS NOVEL THERAPEUTICS FOR BREAST CANCER
PS-W-17	MARTIN HEROLD	CHEMICAL BIOLOGY OF CHROMATIN REGULATION: THE FIRST SMALL MOLECULE ANTAGONISTS OF MBT DOMAINS
PS-W-18	MAN LUO	DATA VALIDATION FOR PUBCHEM HTS ASSAY OF 5-HT1A LIGANDS USING CLASSIFICATION QSAR METHOD
PS-W-19	MINGYAN YU	DESIGN, SYNTHESIS AND BIOLOGICAL EVALUATION OF 2-PHENYLAMINOCARBONYLMETHYL SUBSTITUTED DIHYDRO-ALKYLTHIO-BENZYL-OXOPYRIMIDINES (DABOS) AS HIV-1 NNRTIS
PS-W-20	QINGZHONG HU	POTENT CYP17 INHIBITORS FOR THE TREATMENT OF PROSTATE CANCER: EVOLUTION OF BIPHENYL METHYLENE HETEROCYCLES FROM IMIDAZOLES TO PYRIDINES
PS-W-21	RIMA HAJJO	COMPUTATIONAL IDENTIFICATION AND EXPERIMENTAL VALIDATION OF SELECTIVE ESTROGEN RECEPTOR MODULATORS AS LIGANDS OF 5-HYDROXYTRYPTAMINE-6 RECEPTORS AND POTENTIAL ANTI-ALZHEIMER'S AGENTS

FORMULATION		
POSTER ID	**PRESENTER**	**TITLE**
PS-W-22	ANNE LARSEN	DEVELOPMENT OF SMEDDS WITH WELL DEFINED EXCIPIENTS FOR ORAL DELIVERY OF CINNARIZINE, A POORLY WATER SOLUBLE DRUG COMPOUND
PS-W-23	GE GAO	IDENTIFICATION OF TRANSPORT MECHANISMS FOR TWO SIMULTANEOUSLY OCCURRING MYCOTOXINS - OCHRATOXIN A AND CITRININ - INTO THE HUMAN LIVER
PS-W-24	KOSUKE KUSAMORI	ACCELERATION OF WOUND HEALING BY INCREASING SURVIVAL OF TRANSPLANTED CELLS USING ADHSAMINE, A SYNTHETIC CELL ADHESION MOLECULE
PS-W-25	LEI DIAO	IN VITRO CHARACTERIZATION OF DRUG-L-CARNITINE CONJUGATE AS POTENTIAL PRODRUG TARGETING ORGANIC CATION/CARNITINE TRANSPORTER (OCTN2)
PS-W-26	LEI HU	CHARACTERIZATION OF EBOLA AND MARBURG VIRUS-LIKE PARTICLES
PS-W-27	LOKESH KUMAR	EFFECT OF COUNTERION ON THE GLASS TRANSITION TEMPERATURE ON LYOPHILIZATION OF GANCICLOVIR SALT FORMS
PS-W-28	MICHIEL VAN SPEYBROECK	ENHANCED ABSORPTION OF THE POORLY SOLUBLE DRUG FENOFIBRATE BY TUNING ITS RELEASE RATE FROM ORDERED MESOPOROUS SILICA
PS-W-29	MIKOLAJ MILEWSKI	INFLUENCE OF DONOR SOLUTION VISCOSITY ON THE MICRONEEDLE-ENHANCED NALTREXONE HYDROCHLORIDE SKIN TRANSPORT
PS-W-30	OZGE CEVIK	DESIGN AND CHARACTERIZATION OF TUMOR SPECIFIC LYP-1 PEPTIDE-CONTAINING SMEDDS FOR THE LYMPHATIC TARGETING OF SOLID TUMORS IN CANCER THERAPY
PS-W-31	PERRINE PIVETTE	INCORPORATION OF WATER-SOLUBLE API IN LIPID-BASED MICROSPHERES OBTAINED BY PRILLING: FROM THE PROCESS TO THE CONTROLLED RELEASE MECHANISMS
PS-W-32	TANYA CLAPP	ENHANCING THE FREEZE-THAW STABILITY OF AN ALUMINUM-

		CONTAINING ADJUVANT

GENE/ PROTEIN DELIVERY		
POSTER ID	**PRESENTER**	**TITLE**
PS-W-33	AHMED BADAWI	DEVELOPMENT OF PEPTIDES TO TARGET ANTIGEN PRESENTING CELLS FOR CONTROLLING THE IMMUNE RESPONSE IN EXPERIMENTAL AUTOIMMUNE ENCEPHALOMYELITIS
PS-W-34	KOEN VAN DER MAADEN	DEVELOPMENT OF SMALL PDNA-CONTAINING LIPOSOMES FOR DNA VACCINATION
PS-W-35	MIKA REINISALO	REVERSE TRANSFECTION: A VERSATILE TOOL FOR CELL BIOLOGY AND PHARMACEUTICAL RESEARCH
PS-W-36	SANG KYOON KIM	INTRACELLULAR PEPTIDE DELIVERY FOR CANCER THERAPY

MOLECULAR IMAGING		
POSTER ID	**PRESENTER**	**TITLE**
PS-W-37	PAOLA LUCIANI	QUANTITATIVE IMAGING OF LYMPHATIC FUNCTION WITH LIPOSOMAL INDOCYANINE GREEN

NANOMEDICINE		
POSTER ID	**PRESENTER**	**TITLE**
PS-W-38	AIKATERINI LALATSA	NANOMEDICINES WHICH DELIVER NEUROPEPTIDES TO THE BRAIN VIA THE ORAL ROUTE
PS-W-39	AMIT JAIN	ENGINEERED PLGA NANOPARTICLES FOR ORAL INSULIN DELIVERY
PS-W-40	CHRISTIAN RUGE	INTERACTIONS OF SURFACE MODIFIED MAGNETIC NANOPARTICLES WITH LUNG SURFACTANT PROTEIN A
PS-W-41	EFRAT HAREL	TARGETING TRANSFERRIN RECEPTOR WITH PEGYLATED NANO-IMMUNOLIPOSOMES: A POTENTIAL METHOD FOR THE LOCAL TREATMENT OF IBD VIA THE LUMINAL ROUTE
PS-W-42	LEI PENG	DESIGN AND TESTING OF ACOUSTICALLY-ACTIVE MICROBUBBLE-NANOPARTICLE HYBRID FOR ULTRASOUND-TARGETED CHEMOTHERAPY
PS-W-43	PING MA	TARGETED BEHENOYL-PACLITAXEL CONJUGATE NANOPARTICLES FOR THE TREATMENT OF RESISTANT AND METASTATIC BREAST CANCER
PS-W-44	SHUANG CAI	LYMPHATIC DELIVERY OF CISPLATIN FOR THE TREATMENT OF METASTATIC HEAD AND NECK SQUAMOUS CELL CANCER
PS-W-45	STEFANIE WOLFART	THERAPEUTIC EFFICACY OF DOXORUBICIN-LOADED PLGA NANOPARTICLES AGAINST RAT GLIOBLASTOMA 101/8
PS-W-46	TANMOY SADHUKHA	MAGNETIC HYPERTHERMIA FOR LUNG CANCER
PS-W-47	VINITH YATHINDRANATH	CHARACTERIZATION AND BIO-COMPATIBILITY OF IRON OXIDE NANOPARTICLES SYNTHESIZED USING A NOVEL ONE STEP, LOW TEMPERATURE HYDROLYSIS/REDUCTION METHOD

PHARMACEUTICAL ANALYSIS		
POSTER ID	**PRESENTER**	**TITLE**
PS-W-48	FIRAT YERLIKAYA	LC-UV DETERMINATION OF CLOZAPINE IN ORALLY DISINTEGRATING TABLETS
PS-W-49	JESSICA CREAMER	DEVELOPMENT OF MICROFLUIDIC BASED DEVICES TO EVALUATE THE INTEGRITY OF PROTEIN BASED PHARMACEUTICALS IN DEVELOPING COUNTRIES

PS-W-50	REGINA HUTCHINGS	CHARACTERIZATION OF INTERACTIONS BETWEEN ANTIMICROBIAL PRESERVATIVES AND PROTEINS

PKPD		
POSTER ID	**PRESENTER**	**TITLE**
PS-W-51	ANNE SOPHIE GRANDVUINET	INTERACTIONS BETWEEN STEROIDAL COMPOUNDS ON TRANSPORTERS IN CACO-2 CELLS
PS-W-52	CHESTER COSTALES	APICALLY LOCALIZED MOUSE INTESTINAL CATION-SELECTIVE TRANSPORTERS PLAY A ROLE IN THE ORAL ABSORPTION AND PHARMACOLOGY OF METFORMIN
PS-W-53	CHRISTINA WON	A MODIFIED GRAPEFRUIT JUICE ELIMINATES FURANOCOUMARINS AND POLYMETHOXYFLAVONES AS CANDIDATE MEDIATORS OF THE FEXOFENADINE-GRAPEFRUIT JUICE INTERACTION IN HEALTHY VOLUNTEERS
PS-W-54	DIOGO RIVELLI	ENZYMATIC HYDROLYSIS OF HYDROETHANOLIC EXTRACT OF ILEX PARAGUARIENSIS: BIOAVAILABILITY, SKIN DISTRIBUTION AND ANTIOXIDANT ACTIVITY EVALUATION
PS-W-55	MICHAEL COHEN-WOLKWIEZ	SAFETY AND PHARMACOKINETICS (PK) OF MULTIPLE-DOSE ANIDULAFUNGIN IN NEONATES

SAFETY		
POSTER ID	**PRESENTER**	**TITLE**
PS-W-56	ANNA ASTASHKINA	THREE-DIMENSIONAL PRIMARY ORGANOID CULTURE MODEL IS MORE PREDICTIVE THAN 2D SECONDARY CELL LINES FOR DRUG NEPHROTOXICITY ASSESSMENT
PS-W-57	ETHAN GEIER	ROLE OF THE COPPER TRANSPORTER, CTR1, IN PLATINUM-INDUCED OTOTOXICITY

PS-W-1

Forecasting Plasma Profiles of a Poorly Soluble Drug, Nifedipine, by Coupling Biorelevant Dissolution Tests with a PBPK Computer Model

C. Wagner[1], E. S. Kostewicz[1], A. Müllertz[2], J. B. Dressman[1]

[1] Institute of Pharmaceutical Technology, Goethe University Frankfurt/Main, Germany
[2] Faculty of Pharmaceutical Sciences, University of Copenhagen, Copenhagen, Denmark

Purpose: The purpose of this work was to assess the *in vitro* dissolution behavior of several commercially available nifedipine immediate release (IR) formulations in biorelevant media. Using the results from the biorelevant dissolution tests, nifedipine plasma profiles were predicted using the STELLA® software for Adalat® under both fasting and fed conditions.

Methods: Dissolution studies of three commercially available immediate release nifedipine formulations, Adalat® 10mg soft gelatin capsule, Nifedipin ratiopharm® drops, and Aprical® 10mg hard gelatin capsule, as well as dissolution of the pure drug substance, were performed using biorelevant media simulating both fasting and fed conditions along the gastrointestinal tract. Fasted State Simulated Gastric Fluid *p*H 1.6 (FaSSGF) and Fed State Simulated Gastric Fluid *p*H 5.0 (FeSSGF) were used to simulate the stomach. An update media composition was used to simulate the intestine under both fasting and fed conditions which included both Fasted State Simulated Intestinal Fluid *p*H 6.5 (FaSSIF v2) and Fed State Simulated Intestinal Fluid *p*H 5.8 (FeSSIF v2).
Most dissolution studies were performed using USP apparatus 2 with a paddle rotation speed of 75 rpm in 500mL dissolution media. In FaSSGF, the dissolution studies were conducted in just 250mL of medium using the mini paddle assembly.
Pharmacokinetic (PK) assessment of nifedipine plasma profiles after intravenous application was performed using WinNonlin 4.1 (Pharsight Corp., USA). Nifedipine plasma profiles were simulated using the STELLA® 9.1.3 software (Isee Systems Inc., USA).

Results: The results of this study indicate that the dissolution behavior of the different nifedipine IR formulations examined was superior to the profile of the pure drug substance alone. For all formulations, complete dissolution was observed in FaSSIF v2, FeSSIF v2 and FeSSGF. In contrast, the rate and extent of dissolution of the pure drug substance was much slower.
Using the Stella® software, the plasma profiles for Adalat® could be simulated quantitatively in both the fasted and fed state.

Conclusions: Results from dissolution studies conducted in biorelevant media provide useful information to qualitatively predict food effects. By coupling biorelevant dissolution tests with PBPK models, e.g. the STELLA® software, food effects and plasma profiles of nifedipine can be simulated quantitatively.

PS-W-2

Zoledronic acid induces formation of a pro-apoptotic ATP analog and isopentenyl pyrophosphate *in vivo* and *in vitro*

J. Räikkönen[1,2], J.C. Crockett[3], M.J. Rogers[3], H. Mönkkönen[1,2], S. Auriola[1,2], J. Mönkkönen[1,2]

[1]School of Pharmacy, Faculty of Health Sciences, University of Eastern Finland, Kuopio, Finland
[2]Biocenter Kuopio, Kuopio, Finland
[2]Institute of Medical Sciences, University of Aberdeen, Aberdeen, UK

Purpose: Bisphosphonates (BPs) are highly effective inhibitors of bone resorption. Recently we discovered a new mechanism of action for nitrogen-containing bisphosphonates (N-BPs). N-BPs, such as

zoledronic acid (ZOL), induce the formation of a novel ATP analog (1-adenosin-5'-yl ester 3-(3-methylbut-3-enyl) ester triphosphoric acid; ApppI), as a result of the inhibition of farnesyl pyrophosphate synthase in the mevalonate pathway and consequent accumulation of intracellular isopentenyl pyrophosphate (IPP). ApppI is able to induce direct apoptosis through blockade of mitochondrial adenine nucleotide translocase. In order to further evaluate a pharmacological role for ApppI, we obtained more detailed data on IPP/ApppI formation *in vivo* and *in vitro*.

Methods: After giving ZOL *in vivo* to rabbits, IPP/ApppI formation and accumulation was assessed in isolated osteoclasts (purified using immunomagnetic bead separation). The formation of IPP/ApppI *in vitro* was studied in MCF-7 breast cancer cells, after pulse and continuous treatment with ZOL. Identification and quantitation of IPP/ApppI in cell extracts after ZOL treatment was determined using HPLC negative ion electrospray ionization mass spectrometry.

Results: We discovered that IPP/ApppI were formed in osteoclasts *in vivo*, after a single, clinically relevant dose of ZOL. Moreover, the IPP/ApppI formation profile *in vivo* resembled the *in vitro* pulse profile, both demonstrating that IPP/ApppI levels decreased significantly after 24 hours post-treatment. In contrast, continuous ZOL treatment induced gradual and time-dependent formation of IPP/ApppI in MCF-7 cells during the 48 h exposure.

Conclusion: In summary, both *in vivo* and *in vitro* results confirmed that ApppI formation results from accumulation of IPP as a result of FPP synthase inhibition following ZOL treatment. Importantly, this study provided the first conclusive evidence that pro-apoptotic ApppI is a biologically significant molecule, and demonstrated that IPP/ApppI analysis is a sensitive tool for investigating pathways involved in BP action.

PS-W-3

P-glycoprotein (P-gp) Enhances the Portal Bioavailability of Loperamide in Mouse by Reducing First-pass Intestinal Metabolism

M. B. Dufek[1], L. Zhao[1], A. S. Bridges[2], D. R. Thakker[1]

[1] Eshelman School of Pharmacy and [2] Department of Pathology and Laboratory Medicine, School of Medicine, University of North Carolina at Chapel Hill, Chapel Hill, NC

Purpose: Recent *in vitro* studies in our lab have shown that the rate of CYP3A-mediated metabolism of the dual-P-gp/CYP3A substrate, loperamide, decreases in the presence of Pgp efflux and that this decrease is concentration dependent, with the maximum effect occurring near the apparent K_m for metabolism. In this study, we examined the effect P-gp on intestinal first-pass metabolism and portal bioavailability ($F_{Gut,0\text{-}4hr.}$) of loperamide, at different doses/concentrations relative to the apparent K_m for metabolism, using wild type and P-gp knockout mice.

Methods: The portal and jugular veins of wild type and P-gp knockout mice were catheterized, and loperamide was administered in 300 µl of saline by oral gavage at doses expected to produce intestinal concentrations near or exceeding the apparent K_m for metabolism. Serial blood samples were taken over four hours. Portal bioavailability (F_{Gut}) was determined by quantification of the total mass of loperamide absorbed from the intestine, derived from portal and systemic $AUC_{0\text{-}4\ hrs}$.

Results: The loperamide dose of 0.23 mg/kg, producing gastric concentration of ~50 µM, which is near the apparent metabolic K_m, the portal bioavailability of loperamide was 7-times greater in wild type than P-gp knockout mice. For the loperamide dose of 0.47 mg/kg, producing gastric concentration of ~100 µM, which is significantly higher than the K_m for metabolism, the portal bioavailability in wild type and P-gp

knockout mice was equivalent. The portal bioavailability did not change with dose in wild type mice. However, it increased by 3-fold when the dose was increased from 0.23 to 0.47 mg/kg in knockout mice.
Conclusion: Increased portal bioavailabiliy in the P-gp knockout mice suggests that the higher intracellular concentration of loperamide that occurs in the absence of P-gp is sufficient to, at least, partially saturate the metabolic enzyme at the higher dose. For doses of loperamide that produce gastric concentrations near the apparent K_m for metabolism, P-gp increases the portal bioavailability of loperamide, suggesting that the effect of P-gp on decreasing intestinal first-pass metabolism of loperamide outweighs the reduced loperamide absorption caused by P-gp efflux alone. However, at a higher dose, the two opposing effects balanced out with no change in portal bioavailability.

PS-W-4

Uric Acid Transporter-Mediated Uricosuric Effect of RDEA594, A Metabolite of Antiviral Agent RDEA806

M. Yoshifuji[1], M. Sato[1] , L.T. Yeh[2], K. Ohya[1], Y. Shirasaka[1], T. Nakanishi[1], and I.Tamai[1]

[1]Faculty of Pharmacy, Institute of Medical, Pharmaceutical and Health Sciences, Kanazawa University, Japan
[2]Ardea Biosciences Inc., San Diego, CA, USA

Purpose: RDEA806, an antiviral agent, demonstrated a serum uric acid lowering effect in clinical trials. Although RDEA806 exhibited an inhibitory effect on uric acid reabsorptive transporter, URAT1, RDEA806 showed little excretion into urine. The purpose of the present study is to clarify the mechanism of the serum uric acid-lowering effect of RDEA806 by focusing on its major metabolite RDEA594, which is under development as a uricosuric agent.

Methods: Transport and inhibitory effects of RDEA594 on renal transporters URAT1, URATv1, OAT1, and OAT3 were evaluated using *in vitro* cell systems expressing respective transporters. *Cis*-effect of RDEA594 was evaluated by adding simultaneously with [^{14}C]uric acid into cell suspension. *Trans*-effect of RDEA594 was evaluated by pre-loading RDEA594 into oocytes by microinjection and subsequent incubation with [^{14}C]uric acid .

Results: RDEA594 exhibited *cis*-inhibitory effect on URAT1-mediated uptake of uric acid with IC_{50} value of 52.5 mM. Renal clearance of RDEA594 was higher than f_b*GFR, suggesting that RDEA594 was actively secreted. Urinary concentration of RDEA594 was higher than IC_{50} value of RDEA594 on URAT1. Therefore, it was conceivable that RDEA594 inhibits URAT1-mediated reabsorption of uric acid after tubular secretion into proximal lumen. On the other hand, RDEA594 also exhibited *trans*-inhibitory effect on URAT1-mediated uptake of uric acid. Further analysis of inhibition kinetics suggested a noncompetitive inhibition of RDEA594 on URAT1. RDEA594 was accumulated in kidney compared with plasma. Therefore, it was considered that RDEA594 *trans*-inhibited URAT1-mediated reabsorption of uric acid at clinically relevant concentration. Since RDEA594 was found to be a substrate of OAT1 and OAT3, accumulation in kidney and excretion into tubular lumen can be explained by OAT1- and OAT3-mediated transport.

Conclusions: RDEA594 at clinical dose may exhibit both of *cis*- and *trans*-inhibitory effects on URAT1-mediated reabsorption of uric acid. Moreover, OAT1 and OAT3 were involved in renal accumulation and subsequent tubular secretion of RDEA594, leading to a higher concentration of RDEA594 in tubular cells and lumen. These findings suggested that serum uric acid lowering effect is attributed to the effective inhibition of URAT1-mediated uric acid reabsorption by RDEA594.

PS-W-5

Generation of functional three-dimensional liver cell culture model for drug development

M. Malinen[1,2], Y-R. Lou[2], M. Bhattacharya[2], M. Yliperttula[2], A. Urtti[1]

[1] Centre for Drug Research, University of Helsinki, Helsinki, Finland
[2] Division of Biopharmaceutics and Pharmacokinetics, University of Helsinki, Helsinki, Finland

Purpose: To be able to mimic the liver function in vitro, the shift from the conventional monolayer culture towards upregulated system is needed. Since it is known that extracellular matrix (ECM) has important role for the phenotype of hepatocytes in liver, our aim was to compare various ECM-like biomaterials with hepatic cell lines and set up a three-dimensional hepatic cell culture for metabolism and transport of drugs studies.

Methods: HepG2, HepaRG, hESC-derived hepatic progenitor cells were cultured with commercial and newly synthesized biomaterials. The viability and growth of cells were analyzed, and the cells were characterized with qRT-PCR and immunocytochemistry. In addition, the function of hepato-biliary efflux transporters and formation of bile canaliculi was analyzed with fluorescent probes and real-time confocal microscopy.

Results: The three-dimensional spheroid formation, elongated bile canaliculi structures, expression profiles and vectorial efflux transport resemble the morphology and functionality of hepatocytes in vivo.

Conclusions: This study reveals the influence of various biomaterials on morphology and functions of hepatic cells. Our results suggest that studying metabolism and transport of drugs and other chemicals with three-dimensional culture system may be more likely to reflect physiological responses than conventional monolayer system.

PS-W-6

Transmembrane Domain I of the Bile Acid Transporter SLC10A2 Contributes to Substrate Translocation Events and Protein Stability

T. Claro da Silva, N. Hussainzada, C.M. Khantwal, and P.W. Swaan

Department of Pharmaceutical Sciences, University of Maryland, Baltimore, MD, 21201

Purpose: The human apical sodium-dependent bile acid transporter (hASBT, SLC10A2) is the chief bile acid transporter in the intestine and plays a critical role in the enterohepatic circulation of bile acid, various drugs as well as in cholesterol homeostasis. ASBT reclaims bile acid from the distal ileum via active sodium co-transport. In the present study, we probed ASBT structure-function requirements, especially the role of its highly conserved, relatively amphipatic transmembrane domain 1 (TM1; Asn^{29}-Gly^{50}).

Methods: We employed a combination of mutagenesis, thiol modification (SCAM), kinetics and proteomics approaches, to study TM1 amino acids, as well as amino acids close to its aqueous-membrane boundary (Asn^{27} and Asn^{28}), which could potentially interact with TM1 residues during the transport cycle.

Results: Site-directed Cys replacement delineated the importance of TM1 on ASBT function, with about 60% of the protein affected by mutation. Likewise, impaired transport of N27C suggested a critical role for

Asn[27] on ASBT function, whereas N28 remained unaffected. Residues clustered along the TM1 exofacial half clearly showed solvent accessibility, when probed with MTSET during Substituted Cysteine Accessibility Method (SCAM) experiments. Involvement of Leu[34] in bile acid interactions, and Leu[38] and Met[46] in sodium transport was corroborated by bile acid and cation protection experiments, as well as kinetic analysis. Mutant G50C was not expressed at the membrane, but its cell surface expression was rescued upon inhibition of G50C proteasomal degradation with MG132, as well as lactacystin. Incubation with the chemical chaperones DMSO, 4-PBA and glycerol did not rescue ASBT levels. These results indicate that, rather than causing protein folding defects, mutation at Gly[50] may have affected proteasomal degradation. Thus, Gly[50] appears to play a critical role in ASBT degradation by the proteasome.

Conclusions: Overall, our observations indicate a pivotal role for TM1 on ASBT function and stability. Collectively with previous findings, the present work contributes to the design of a mechanistic model for ASBT transport, which may serve as a paradigm for other proteins in the SLC super family, and help in the rational design of ASBT-targeted therapeutic agents. Supported by NIH RO1 DK61425.

PS-W-7

Pediatric Metabolism of Meropenem in Infants <91 Days of Age with Complicated Intra-abdominal Infections

W. Ju[1], M. Cohen-Wolkowiez[1,2], D. K. Benjamin Jr.[2], and D. R. Thakker[1]

[1]UNC Eshelman School of Pharmacy, The University of North Carolina at Chapel Hill, Chapel Hill, NC, and [2]Division of Quantitative Sciences, Duke University, Durham, NC

Purpose: Meropenem is a third generation β-lactam antibiotic used for treating serious microbial infections in adults and children, including newborns. Meropenem is predominantly cleared by renal elimination of intact drug and dehydropeptidase-1 (DHP-1)-mediated metabolism in the kidney. The purpose of this study was to determine if metabolic clearance of meropenem increases in children to compensate for less developed kidney function compared to adults.

Methods: Frozen human tissues obtained from the Cooperative Human Tissue Network were categorized by organs and donor's age. Metabolic assays were conducted by incubating meropenem at desired concentrations with tissue homogenate in 25 mM Tris-HCl (pH 8.0) at 37ºC for 30 min and quenched by cold acetonitrile. Rates of metabolite formation were determined by measuring the concentration of the hydrolytic metabolite of meropenem as a function of time using HPLC-UV analysis. The apparent K_m and V_{max} for hydrolysis of meropenem by intestinal tissue homogenates were determined and *in vivo* metabolic clearance by each tissue was calculated from the experimentally determined *in vitro* intrinsic clearances. The contribution of metabolism by each tissue to the total clearance was determined. DHP-1-mediated hydrolytic metabolism of meropenem by tissue homogenates was evaluated in the presence of the specific inhibitor, cilastatin, at various concentrations.

Results: The rates of meropenem metabolism by adult and pediatric tissues, determined under linear conditions of protein and time were: 0.39±0.10 nmol/min/mg (adult intestine), 0.40±0.12 nmol/min/mg (pediatric intestine), 1.66±0.52 nmol/min/mg (adult kidney), 3.24±0.94 nmol/min/mg (pediatric kidney), 0.28±0.04 nmol/min/mg (adult liver), and 0.25±0.14 nmol/min/mg (pediatric liver). Cilastatin inhibited metabolism of meropenem by renal tissue in a concentration-dependent manner. However, it exhibited minimal inhibition of meropenem metabolism by intestinal tissue, indicating that only DHP-1 in the kidney plays a significant role in the metabolic clearance of meropenem.

Conclusion: These results show that intestinal and hepatic metabolism contribute to only a small percentage of total meropenem clearance, whereas renal metabolism plays a significant role, with DHP-1

contributing to most of the metabolic activity. Interestingly, the pediatric kidney has greater metabolic activity toward meropenem than the adult kidney, while there are no differences between adults and children with respect to meropenem metabolism by the intestine or liver.

PS-W-8

Establishment of Human-CYP3A4 Expressed MDCK II Cell Monolayer to Investigate Intestinal First-Pass Metabolism

Y. Terashima[1], Y. Masaoka[1], M. Kataoka[1], S. Sakuma[1], K. Nagata[2], T. Yokoi[3], S. Yamashita[1]

[1] Setsunan University
[2] Tohoku Pharmaceutical University
[3] Kanazawa University

Purpose: In the human small intestine, CYP3A4 dominates the intestinal first pass metabolism of orally administered drugs. The purpose of this study is to establish an *in vitro* system to assess quantitatively the intestinal metabolism of CYP3A4 substrate drugs.

Methods: Madin-Darby canine kidney type II (MDCK II) cells were transduced with a novel adenoviral vector (AdV) expressing CYP3A4 (AdCYP3A4) or green fluorescent protein (AdGFP).
MDCK II cells were seeded onto semipermeable membrane, and on day 2, cells were transduced with various MOIs (multiplicity of infection; 0-200) of AdV. On day 5, cell monolayers were used for drug transport study. The expression of GFP and CYP3A4 in MDCK II cells was determined by fluorescent microscopy and Western blotting, respectively. The drug transport study was performed with midazolam (MDZ, CYP3A4 substrate). Several non-CYP3A4 substrate drugs were used to check the integrity of monolayers.

Results: After transduced with AdGFP, GFP expression level in MDCK II cells increased with time and reached a plateau on day 3. Also, the expression level increased linearly with increasing MOIs. AdGFP showed no effect on the permeability of non-CYP3A4 substrates across cell monolayers. After transduced with AdCYP3A4, high expression of CYP3A4 was confirmed by Western blotting analysis. CYP3A4-mediated metabolism of MDZ during the membrane permeation process was investigated by adding MDZ (100μM) to the apical medium. Major metabolites of MDZ, 1'-hydoroxy midazolam (1'-OH-MDZ) and 4'-hydoroxy midazolam (4'-OH-MDZ), were detected in both apical and basal compartments, while the permeability of MDZ was not affected. The ratio of total amount of metabolites to the permeated amount of MDZ was calculated in each monolayer transduced with various MOIs of AdGFP. The ratio of metabolite was 0.07-0.18% and increased linearly with increasing MOI (in the range of 25 to 200 of MOIs).

Conclusion: In this report, although metabolic activity in CYP3A4-expressed MDCK II cell monolayer was low compared to that in human intestine, expression of CYP3A4 was controllable with AdV transduction. By improving the expression level of CYP3A4, it is possible to establish a useful *in vitro* system to assess the intestinal first pass metabolism of oral drugs.

PS-W-9

A Survey of Neurobiochemical Levels in a Panel of Genetically Diverse Mouse Inbred Strains to Identify a Biomarker for Anxiety and Mood Disorder

C. Santos[1], A. Su[2], L. Tarantino[3], and T. Wiltshire[1]

[1]University of North Carolina at Chapel Hill, Division of Pharmacotherapy and Experimental Therapeutics
[2]Genomics Institute of Novartis Research Foundation La Jolla, California
[3]University of North Carolina at Chapel Hill, Department of Psychiatry

Purpose: Identification of a biomarker that can establish diagnosis, prognosis or treatment response is critical to the advancement of research and clinical management of patients with mood and anxiety disorders. Since tissue collection in humans is limited to serum and post-mortem brain samples, neurobiochemical abnormalities observed on both cellular and biochemical levels are difficult to distinguish as causal or as consequence of disease or treatment. Therefore, in order to understand how biochemical changes correlate with behavior, measurement of putative neurobiochemical analytes must be obtained in brain and serum under various conditions. In this study, we measured thirty-six neurobiochemical analytes proposed to have some influence on mood disorder in brain and serum under treatment-naïve, control, and fluoxetine-treated conditions across a panel of genetically diverse mouse inbred strains.

Methods: Levels of thirty-six analytes were measured simultaneously using Zeptosens reverse protein array system. Briefly, brain lysates were spotted on ZEPTOchips in duplicates at four serial dilutions ranging from 0.05 to 0.2 mg/mL of total protein. Samples were incubated with 36 antibodies at concentrations optimized to obtain maximum signal detection and minimal cross reactivity. Array was read using planar waveguide technology, which confined excitation to a depth of ~200 nm leading to significant antibody-antigen signal to noise ratio. Relative fluorescence intensities of each analyte were used to compare inter-strain biochemical differences. Genomic regions significantly associated with gene expression, depressive behavior, and biological changes were identified using haplotype-association mapping (HAM) and efficient mixed-model association (EMMA) analyses.

Results: We used factor analysis to identify the underlying factors that can account for the common variance shared between biochemical markers. Using a stepwise regression model, we identified a factor that can explain significant variation in baseline depressive behavior. This factor was primarily influenced by levels of norepinephrine transporter, which suggests that norepinephrine transporter levels can be a useful biomarker for identifying patients at risk of developing depression.

Conclusions: Anxiety and depression are clinically and genetically heterogeneous disorders. A biomarker that can be used for diagnosis or therapeutic management can significantly improve patient care and aid in the identification of more effective drug targets and critical pathways involved in mood disorders and brain pathophysiology.

PS-W-10

The different roles of CAR in the induction of DME by Cyclophosphamide and Ifosfamide

D.Wang and H.Wang

Department of Pharmaceutical Sciences, School of Pharmacy, University of Maryland at Baltimore, Baltimore, MD

Purpose: Cyclophosphamide (CPA) and Ifosfamide (IFO) are anti-cancer prodrugs that require hepatic activation by CYP450s. Constitutive androstane receptor (CAR) is an important regulator of drug

metabolizing enzymes (DMEs). Our research is to study the role of CAR in the regulation of relevant Drug Metabolising Enzymes (DME) by CPA and IFO, thus to expand our knowledge of drug-drug interaction involving these drugs.

Methods:
Translocation assay:Hepatocytes were isolated from human liver specimens and infected with 2 µl Ad/EYFP-hCAR for 12 hrs. After 24 hrs treatment, cells were fixed and stained. Confocal laser scanning microscopy imaging was performed.
Luciferase assay:Human primary hepatocytes in 24-well Biocoat plates were transfected 12 hrs.Briefly, the transfection mixes contained 200ng of CYP2B6 reporter construct (CYP2B6-2.2kb) and 25ng of internal control plasmid (pRL-TK Renilla luciferase). Transfected cells were treated with solvent (0.1% DMSO) or test compounds for 24 hrs. Subsequently, luciferase activities were measured with hepatocyte lysates using the Dual Luciferase Reporter reagents.
Real time-PCR and Western blot.

Results: The expressions of CYP2B6 and CYP3A4 mRNA as well as protein were induced in human primary hepatocytes by both CPA and IFO in a dose related manner. Both CPA and IFO were able to induce the mRNA expression of UGT1A1 but not CYP1A2 in human primary hepatocytes. Part of the CPA induction was proved to be attributed to CAR in hepatocyte-based induction and reporter assays, and CPA was proved to act as an indirect activator of CAR. IFO induction of CYP450s may be attributed to a combination of pregnane X receptor (PXR) and other factors as proved by reporter assay on HepG2 cells transfected with PXR. CPA but not IFO induced translocation of CAR from cytoplasm to nucleus in human primary hepatocytes, a process indicating the activation of CAR.

Conclusion: Our study has provided a novel insight into the different roles of CAR in the regulation of CPA and IFO induced DME expressions and potential drug-drug interactions.

PS-W-11

Effect of steady-state and single-dose ritonavir on the hepatobiliary disposition of ^{99m}Tc-mebrofenin (^{99m}Tc-MEB) in healthy volunteers

Nathan D. Pfeifer[1], Sandy L. Goss[1], Ryan M. Criste[1], Brandon Swift[1], William D. Heizer[2], Lisa M. Gangarosa[2], Kim L.R. Brouwer[1]

[1]Eshelman School of Pharmacy, University of North Carolina, Chapel Hill, NC
[2]School of Medicine, University of North Carolina, Chapel Hill, NC

Purpose: ^{99m}Tc-MEB is a hepatobiliary imaging agent that is taken up rapidly by hepatocytes and extensively excreted into bile unchanged. This study investigated the effect of ritonavir, an inhibitor of multiple transport proteins, on ^{99m}Tc-MEB hepatobiliary disposition in healthy volunteers.

Methods: Healthy volunteers were administered 2.5 mCi ^{99m}Tc-MEB by IV bolus either (a) alone (control; n=7), (b) 2 hr after a single, 200 mg oral ritonavir dose (n=6), or (c) following 300 mg oral ritonavir doses administered at 14 and 2 hr prior to ^{99m}Tc-MEB (2x300 mg; n=3). Blood samples were collected at designated time points, urine was collected at baseline and 180 min, and scintigraphic images of the liver were acquired at 1-min intervals over 180 min; duodenal aspirates were collected continuously for 180 min via an oroenteric tube and pooled over designated intervals. At 120 min, cholecystokinin-8 was infused intravenously (0.02 mg/kg over 30 min) to stimulate gallbladder contraction. Biliary recovery of ^{99m}Tc-MEB was corrected for gallbladder ejection fraction. All other pharmacokinetic parameters were determined by noncompartmental analysis of ^{99m}Tc-MEB activity vs. time curves in blood and liver.

Results: Ritonavir concentrations in blood and bile during the study period were greater following pre-treatment with a 2x300 mg dose regimen compared to a single, 200 mg dose. The 2x300 mg ritonavir regimen significantly increased systemic exposure ($AUC_{0-\infty}$) of ^{99m}Tc-MEB compared to control (4464 ±1850 vs. 1960 ±334 nCi*min/mL; Dunnett's test p=0.014 following ANOVA on ranks p=0.044). Ritonavir decreased the biliary clearance of ^{99m}Tc-MEB in a concentration-dependent manner and increased the hepatic exposure of ^{99m}Tc-MEB, but differences failed to reach statistical significance (ANOVA on ranks p=0.051).

Conclusions: Ritonavir decreased the biliary clearance of ^{99m}Tc-MEB, resulting in increased systemic and hepatic exposure of this probe substrate. Impaired biliary excretion of a drug may redirect the route of hepatic excretion, and/or predispose individuals to greater hepatic exposure, depending on the transport characteristics of the compound and individual hepatobiliary transport function. These data demonstrate for the first time in humans the potential for clinically-relevant drug-drug interactions mediated by ritonavir at the level of biliary transport.

PS-W-12

Investigation Of The Drug-Drug Interaction Between Metformin And A Potent MATE Inhibitor, Pyrimethamine On The Disposition Of Metformin

S Ito[1], H. Kusuhara[1], Y. Kumagai[2], T. Shiroshita[3], Y. Moriyama[4], Y. Sugiyama[1]

[1]Laboratory of Molecular Pharmacokinetics, Graduate School of Pharmaceutical Sciences, The University of Tokyo, Tokyo, Japan
[2]Clinical Trial Center, Kitasato University East Hospital, Kanagawa, Japan
[3]ADME Tox. Research Institute, Sekisui Medical Co.,Ltd. Ibaraki, Japan
[4]Department of Membrane Biochemistry, Okayama University Graduate School of Medicine, Dentistry and Pharmaceutical Sciences, Okayama, Japan

Purpose: Multidrug and toxin extrusion 1 (MATE1) and its homolog MATE2-K are expressed in the apical membrane of the kidney. They are considered to mediate the efflux of cationic drugs into the lumen driven by inward gradient of H^+ across the plasma membrane. Recently, we found that pyrimethamine (PYR), a potent MATE inhibitor, significantly reduced the efflux of metformin into the urine and PYR completely inhibit the uptake of metformin by the blush border membrane vesicles prepared from human kidney in the presence of outward H^+ gradient. Clinical dose of PYR may be able to inhibit MATE proteins without affecting the uptake transporter OCT1 and OCT2. The present study examined the effect of PYR on the renal elimination of a typical MATE substrate, metformin in healthy volunteers.

Methods: Healthy male volunteers were given a microdose of metformin (100 μg) orally with or without preadministration of PYR (50 mg, po) in a crossover fashion. Plasma concentrations and amount of metformin excreted into the urine were measured by LC/MS/MS.

Results: PYR treatment caused a slight delay in the elimination of metformin from the systemic circulation. The AUC (ng▪hr/ml) and fraction excreted into the urine (%) were 2.1 and 78, and 2.3 and 65 in control and PYR-treated groups, respectively. The renal clearance, and intrinsic clearance for tubular secretion of metformin, calculated based on dispersion model, were reduced by 23 and 35% in PYR-treated group, respectively.

Conclusion: PYR could inhibit the MATE-mediated tubular secretion of metformin, suggesting its usefulness to assess the contribution of MATE proteins to the disposition of cationic drugs in human. However, comparison of the renal clearance with regard to plasma concentrations may underestimate the significance of MATE proteins since the renal elimination of metformin seems to be uptake-limited. For

further studies, it is necessary to measure the tissue concentration of metformin by positron emission tomography.

Acknowledgment: This study is a part of the Research Project for the "Establishment of Evolutional Drug Development with the Use of Microdose Clinical Trial" sponsored by the New Energy and Industrial Technology Development Organization (NEDO).

PS-W-13

Essential step to the *in vivo* proof of concept: Design and synthesis of 17β-HSD1 inhibitors for the treatment of estrogen-dependent diseases in *callithrix jacchus*.

C. Henn[1,2], T. Klein[1,2], A. Oster[2], R. Werth[2], S. Marchais-Oberwinkler[2], M. Frotscher[2] and R.W. Hartmann[1,2]

[1] Department Drug Design and Optimization, Helmholtz-Institute for Pharmaceutical Research Saarland (HIPS), Helmholtz Center for Infectious Research (HZI), Saarbrücken/Germany
[2] Pharmaceutical and Medicinal Chemistry, Saarland University, Saarbrücken/Germany

Purpose: Estradiol (E2) is the most important estrogen in humans. The last step of E2-biosynthesis (reduction of the weakly active estrone (E1) to the potent E2) is catalyzed by 17β-hydroxysteroid dehydrogenase type 1 (17β-HSD1). E2 is responsible for the development and differentiation of estrogen-sensitive tissues. But besides its physiological effects it is involved in the initiation and progression of estrogen-dependent diseases (EDD) like breast cancer[1] and endometriosis.[2] 17β-HSD1 acts via an intracrine mechanism and its mRNA was found to be highly expressed e.g. in breast cancer tissue and endometrial lesions. Therefore 17β-HSD1 is a promising target for a new therapy concept of estrogen-dependent diseases. We focus on non-steroidal inhibitors mimicking E2, which show selectivity toward 17β-HSD2 (catalyzes the oxidation of E2 to E1) and have already identified three classes of potent inhibitors.[3-5] Aim of the present work is to identify new compounds in the class of hydroxyphenylnaphthalenesulfonamides which show also high inhibitory activity on 17β-HSD1 of *callithrix jacchus*. *Callithrix jacchus* is a new world monkey with 80% and 85 % sequence identity and homology of 17β-HSD1 compared to the human one. Focussing on an endometriosis model[6] in this species we want to provide the *in vivo* proof of concept for our compounds.

Methods: A new parallel synthesis approach in the class of hydroxyphenyl-naphthalenesulfonamides using benzyloxy as protecting groups was established as well as a noncellular assay with 17β-HSD1 and 17β-HSD2 of *callithrix jacchus* to evaluate the compounds. The inhibitors were also tested on human cytosolic placental preparations for inhibitory activity on 17β-HSD1 and microsomal placental preparations[7] for selectivity toward 17β-HSD2.

Results: We have synthesized and evaluated inhibitors in the class of hydroxyphenyl-naphthalenesulfonamides which show selectivity and inhibitory activity in the low nanomolar range of 17β-HSD1 in human and *callithrix jacchus.*

Conclusion: Due to their strong inhibitory activity in *callithrix jacchus* we have identified a series of compounds which are appropriate candidates for the *in vivo* proof of concept.

References:

[1] Jansson et al., *J. Steroid. Biochem. Mol. Biol.* **2009**, *114,* 64-67.
[2] Blomquist et al., *J. Steroid. Biochem. Mol. Biol.* **2002**, *81,* 343-351.
[3] Oster et al., *Bioorg. Med. Chem.* **2010**, *18,* 3494-3505.
[4] Frotscher et al., *J. Med. Chem.* **2008**, *51,* 2158-2169.
[5] Bey et al., *Bioorg. Med. Chem.* **2008**, *16,* 6423-6435.
[6] Einspanier et al., *Mol. Hum. Reprod.* **2006**, *12,* 291-299.
[7] Kruchten et al., *Mol. Cell. Endocrinol.* **2009**, *301,* 154-157.

PS-W-14

Synthesis, Absolute Configuration and Enantioselective Biological Activities of 4-OH-Retinoic Acid Enantiomers

Jakob Avi Shimshoni[1], Michele Scian[2], Wendel L. Nelson[2], Nina Isoherranen[1]

[1]Department of Pharmaceutics, School of Pharmacy, University of Washington, Seattle, WA, USA;
[2]Department of Medicinal Chemistry, School of Pharmacy, University of Washington, Seattle, WA, USA

Purpose: All-trans retinoic acid (RA) is the major active metabolite of vitamin A and its levels in-vivo are tightly regulated by its synthesis and clearance. CYP26A1 is the main enzyme responsible for RA clearance. Previous studies showed that 4-OH-RA, a major RA metabolite formed by CYP26A1, exerts some biological activities by binding to retinoic acid receptors (RAR) and modulating the transcription of a subset of genes. As 4-OH-RA possesses a chiral center at the C-4 position, the aim of this study was to synthesize 4-OH-RA enantiomers and investigate the enantioselective formation and elimination of the 4-OH-RA enantiomers, and to determine their possible enantioselective effects on RAR activation.

Methods: (S) and (R)-4-OH-RA enantiomers were synthesized in a four-step sequence: protection of the carboxylic group as methyl ester, followed by allylic oxidation with MnO2 providing 4-Oxo-RA. 4-Oxo-RA was enantioselectively reduced using the (S) and (R)- Corey-Bakshi-Shibata (CBS)-oxazaborolidine catalysts, yielding (R)- and (S)-4-OH-RA, respectively. Their absolute configuration was determined by circular dichroism (CD) exciton chirality spectra. The enantioselective formation of (S)-and (R)-4-OH-RA was determined with CYP26A1, 3A4, 3A5, 3A7 and 2C8 using a chiral HPLC method. HepG2 cells were treated with (S)- and (R)-enantiomers and the mRNA of CYP26A1 and RAR was measured by quantitative rtPCR.

Results: The (S)- and (R)- enantiomers were obtained in 95% ee (97.5:2.5) and 91% ee (95.5:4.5), respectively. CYP2C8, 26A1 and 3A7 metabolized RA stereoselectively to (S)-4-OH-RA, while, CYP3A5 formed preferentially the (R)-4-OH-RA. However, incubation of RA with CYP3A4, yielded the enantiomers in equal amounts. (S)-4-OH-RA was depleted twice as fast as (R)-OH-RA by CYP26A1. A homology model of CYP26A1 was further optimized to accommodate the observed stereoselectivity in RA hydroxylation and RA was docked intp CYP2C8 active site to explain the enantioselectivity.

Conclusion: This study reports for the first time the synthesis and absolute configuration determination of 4-OH-RA enantiomers. CYP26A1, 2C8 and 3A7 showed enantioselective formation of the (S)-enantiomer, which was cleared faster by CYP26A1, while the (R)-enantiomer was preferentially formed by CYP3A5. Racemic 4-OH-RA was reported by to bind to RAR and induce differentiation of various cell lines, including neurons and stem cells. Our study shows that pharmacological studies should be conducted with single (S)-4-OH-RA enantiomer instead of the racemate.

PS-W-15

Development of Small Molecule Protein Lysine Methyltransferase G9a Inhibitors

Feng Liu,[1] Xin Chen,[1] Julianne Yost,[1] Dalia Barsyte,[2] Abdellah Allali-Hassani,[2] Tim Wigle,[1] Amy Quinn,[3] Gregory Wasney,[2] Aiping Dong,[2] Ivona Kozieradzki,[2] Guillermo Senisterra,[2] Irene Chau,[2] Alena Siarheyeva,[2] Dmitri Kireev,[1] Ajit Jadhav,[3] J. Martin Herold,[1] William Janzen,[1] Anton Simeonov,[3] Masoud Vedadi,[2] Peter Brown,[2] Stephen Frye,[1] Cheryl Arrowsmith,[2] and Jian Jin[1]

[1] Center for Integrative Chemical Biology and Drug Discovery, Eshelman School of Pharmacy, University of North Carolina at Chapel Hill, Chapel Hill, NC, USA
[2] Structural Genomics Consortium, University of Toronto, Toronto, Ontario, Canada
[3] NIH Chemical Genomics Center, National Human Genome Research Institute, National Institutes of Health, Bethesda, MD, USA

Purpose: Protein lysine methyltransferase (PKMT) G9a, a H3K9 methyltransferase, is over expressed in human cancers and knockdown of G9a inhibits cancer cell growth. Despite evidence that PKMTs play an important role in the development of various human diseases, only a handful of PKMT inhibitors have been reported. Thus, high quality small molecule PKMT inhibitors are needed to serve as research tools for studying the biological function of PKMTs.

Methods: For hit to probe optimization, we took a systematic approach by carrying out iterative structure-based design, parallel synthesis, and *in vitro* profiling using ThioGlo and AlphaScreen to rapidly assess potency, selectivity, and cellular activity.

Results: SAR exploration of the 2,4-diamino-6,7-dimethoxyquinazoline template led to the discovery of UNC0224 as a potent and selective inhibitor of G9a. The first cocrystal structure of G9a with a small molecule inhibitor (UNC0224) was obtained, enabling structure-based design of novel PKMT inhibitors. Structural insights led to the optimization of the 7-dimethylaminopropoxy side chain, resulting in the discovery of the most potent G9a inhibitor so far, UNC0321.

Conclusions: The SAR exploration leading to the discovery of UNC0321 and other potent PKMT inhibitors will be presented.

PS-W-16

Design of GRP78 inhibitors as novel therapeutics for breast cancer

K. Ramkumar, B. Debnath, N. Neamati

Department of Pharmacology and Pharmaceutical Sciences, School of Pharmacy,
University of Southern California, Los Angeles, CA 90007

Purpose: GRP78 (78 kDa glucose regulated protein), an endoplasmic reticulum chaperone, is a key nodal point for the transduction of stress signals and for the activation of the unfolded protein response pathway. It has been found to be overexpressed in several cancers and has also been shown to confer a growth advantage on tumor cells, promoting cancer cell proliferation, survival and drug resistance. There are no selective GRP78 inhibitors currently under development even though there is ample evidence of its critical role in cancer cell survival and drug resistance. Therefore, we are developing novel small-molecule GRP78 inhibitors, which target its ATPase activity, as an innovative strategy to overcome drug resistance and improve treatment outcomes in breast cancer.

Methods: We have designed several structure and ligand based pharmacophores using the docking conformation of the known GRP78 inhibitor, EGCG, and performed virtual screening of our in-house database with over 3 million compounds. To assess the effect of selected hits on recombinant human GRP78's ATPase activity, we have developed four different screening assays and have optimized two of them in high-throughput formats. We then determined the binding affinities of active compounds using a fluorescence polarization assay. We also performed cell proliferation and clonogenic assays to assess the i*n vitro* anticancer effects of promising GRP78 inhibitors.

Results: Based on the docking scores, pharmacophore fitness values and structural diversity, we have identified 200 novel compounds with favorable ADMET properties and tested them in our *in vitro* screening assays. Among them, several compounds showed promising GRP78 inhibitory activity. One of our lead compounds, G101, showed a 63% inhibition of GRP78 ATPase activity, which is comparable to EGCG (52% inhibition at 25 μM).

Conclusions: We have identified novel compounds that can be further optimized as selective GRP78 inhibitors. Our lead compounds show promising GRP78 inhibitory activity and we will characterize their

anticancer effects in combination with doxorubicin and paclitaxel in *in vitro* cell-based and *in vivo* xenograft models of breast cancer.

PS-W-17

Chemical Biology of Chromatin Regulation: The First Small Molecule Antagonists of MBT Domains

J. Martin Herold[1], Tim J. Wigle[1], Cen Gao[1], Jacqueline L. Norris[1], Dmitri B. Kireev[1], William P. Janzen[1], Stephen V. Frye[1]

[1] Center for Integrative Chemical Biology and Drug Discovery (CICBDD), Eshelman School of Pharmacy, University of North Carolina at Chapel Hill, 120 Mason Farm Road, Chapel Hill, NC 27599, Martin.Herold@unc.edu

Purpose: The state of chromatin, and therefore access to the genetic code, is largely regulated by specific chemical modifications to histone proteins and DNA, and the recognition of these marks by other proteins and protein complexes. The recognition of histone lysine-methylation is one critical event in epigenetic regulation that has been shown to be involved in both active and repressed states of transcription. The malignant brain tumor (MBT) repeat is a structural domain which recognizes mono- and dimethyl-lysine modifications of histones. While small molecule antagonists to the enzymes involved in "writing" and "erasing" of the methylation marks on histone lysine-residues are under active investigation, synthetic ligands interacting with the "readers" are currently unprecedented.
The goal of our research is the development of potent and selective small molecule probes disrupting the interaction between MBT domains and methylated lysine-residues in histone tails and the subsequent investigation of the phenotypic consequences of this antagonism.

Methods: To explore potential antagonists of MBT domains, a combination of structure-based drug design using the published crystal structure of L3MBTL1, virtual screening methods and a high-throughput screen of a 100,000 compound diversity library were used.
The initial screening is based on the AlphaScreen platform which is suited for low-affinity interactions. The hits are then confirmed using isothermal titration calorimetry (ITC).
In addition, atomic-level energetics and dynamics of small molecules interacting with a MBT domains have been studied to elucidate the binding of methylated histone tails to the readers of the histone code.

Results: Low µM antagonists were developed and characterized for their thermodynamic binding signature using ITC. We were able to confirm the binding pocket for these small molecules using a mutant L3MBTL1 protein.

Conclusion: Starting with a high µM interaction of MBT domains with their respective histone peptides, we were able to develop small molecule antagonists showing 25-fold increase in binding affinities compared to the native peptides.

PS-W-18

Data Validation for PubChem HTS Assay of 5-HT1A Ligands Using Classification QSAR Method

Man Luo[1], Xiang S. Wang[1], Alexander Golbraikh[1], Alexander Tropsha[1]

[1] Laboratory for Molecular Modeling, Division of Medicinal Chemistry and Natural Products, Eshelman School of Pharmacy, University of North Carolina at Chapel Hill, USA

Purpose: The Molecular Libraries Program (MLP), an NIH Roadmap Initiative. aims to enhance chemical biology through High Throughput Screening (HTS) to obtain ***chemical probes*** effective at modulating specific biological processes or disease states. PubChem is an open-access data repository system, acting as the portal site for MLP. To evaluate the quality of some biological activities deposited in PubChem, we have conducted *in silico* modeling studies on 5-Hydroxytryptamine Receptor Subtype 1A (5-HT1A) ligands (PubChem Assay id (AID) 613, 718, 755).

Methods: The dataset of 105 binders/61 non-binders were retrieved from the NIMH Psychoactive Drug Screening Program (PDSP) Ki database. Three methods of Quantitative Structure Activity Relationships (QSAR) modeling, *k*-Nearest Neighbor, Random Forest and Support Vector Machines, were employed for model building with five-fold cross validation. Models were build using Dragon descriptors and were further validated by predicting 69 additional 5-HT1A ligands from the WOMBAT database to confirm their robustness and predictive accuracy. Then 46 5-HT1A agonists/antagonists available from PubChem were predicted by consensus models, some of these predictions were experimentally tested by Dr. Bryan Roth's lab at UNC.

Results: QSAR models built with five-fold cross validation achieved high predictive accuracy for all three methods, and achieved the Correct Classification Rate of 94% when predicting external 69 5-HT1A ligands from WOMBAT database. However, 25 out of the 46 agonists/antagonists in PubChem bioassays were predicted to be non-binders with high confidence. Ten of them were confimed as non-binders experimentally , indicating that they are false positives in PubChem Bioassay.

Conclusion: PubChem HTS assay results may not be used as a golden standard, and their quality should be further evaluated. We propose that rigorously developed QSAR models could be used to identify both false positives and false negatives reported in PubChem.

PS-W-19

Design, Synthesis and Biological Evaluation of 2-phenylaminocarbonylmethyl substituted Dihydro-alkylthio-benzyl-oxopyrimidines (DABOs) as HIV-1 NNRTIs

Mingyan Yu[1], Xinyong Liu[1], Christophe Pannecouque[2] and Erik De Clercq[2]

[1] Department of Medicinal Chemistry, School of Pharmaceutical Sciences, Shandong University, 44, West Culture Road, 250012, Jinan, Shandong, P.R.China
[2] Rega Institute for Medical Research, Katholieke Universiteit Leuven, Minderbroedersstraat 10, B-3000 Leuven, Belgium

Purpose: HIV-1 NNRTIs bind to an allosteric site on reverse transcriptase (RT) and represent an important therapeutic class of inhibitors used in the treatment of HIV-1 infection. But the problem of resistance has limited NNRTIs' clinical use. Thus, there is an urgent need for the design and development of new and safer NNRTIs, specifically active against mutant viral strains.

Methods: Among NNRTIs, dihydroalkyloxybenzyl- oxopyrimidines (DABOs) are an interesting class of compounds active at nanomolar concentrations. Based on the method of computer-aided drug design, a new series of *S*-DABOs was prepared, by the insertion of a phenylaminocarbonylmethylthio chain at *C*-2, a 2-chloro-6-fluoro-, 1-naphthylmethyl, or 2,6-difluorobenzyl group at *C*-6, and methyl or ethyl substituent at *C*-5. All of the new compounds were evaluated for their anti-HIV activities in MT-4 cells.

Results: Most of these new congeners exhibited moderate to good activities against wild-type virus with an EC_{50} value ranging from 1.40-0.19 μM. Among them, 2-[(4-cyanophenylamino)carbonylmethylthio]-6-(2-chloro-6-fluoro- benzyl)-5-ethyl-pyrimidin-4(3*H*)-one was one of the compounds endowed with the highest broad spectrum HIV-1 inhibitory activity, with EC_{50} = 0.19 ± 0.005 μM against the wild-type virus,

EC_{50} = 1.05±0.24 μM (fold resistance = 2) against the E138K strain and EC_{50} =2.38±0.13 μM (fold resistance = 4.5) against the Y181C strain.

Conclusion: The 2-phenylaminocarbonylmethyl-*S*-DABOs can be promising novel DABO candidates for further synthesis, and biological studies aimed to evaluate their effectiveness as anti-AIDS agents that are active against both wt and mutated strains of HIV-1.

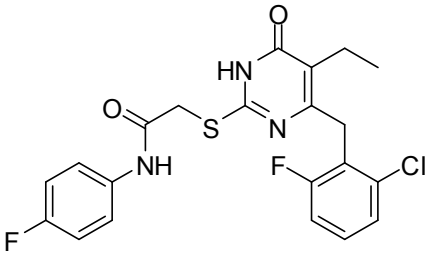

2-[(4-cyanophenylamino)carbonylmethylthio]-6-(2-chloro-6-fluoro-benzyl)-5-ethyl-pyrimidin-4(3*H*)-one

PS-W-20

Potent CYP17 Inhibitors for the Treatment of Prostate Cancer: Evolution of Biphenyl Methylene Heterocycles from Imidazoles to Pyridines

Qingzhong Hu, Carsten Jagusch, Rolf W. Hartmann

Pharmaceutical and Medicinal Chemistry, Saarland University, Campus C23,
& Helmholtz Institute for Pharmaceutical Research Saarland (HIPS), D-66123 Saarbrücken, Germany

Purpose: It is well known that the growth of up to 80% of prostate carcinoma depends on androgen stimulation. Therefore, segregation of tumour cells from androgen will effectively prevent cancer cell proliferation. However, current standard therapy “combined androgen blockade” (CAB) often leads to resistance which can be associated with androgen receptor mutations. The mutated androgen receptor recognizes antagonists or glucocorticoids as agonists leading to the collapse of CAB therapy. Therefore, inhibition of CYP17, which is the crucial enzyme in androgen biosyntheses, was proposed as a promising therapy because it totally blocks androgen formation in testes and adrenals, as well as inside cancer cells. The recent success in phase II and III clinical trials of steroidal CYP17 inhibitor Abiraterone demonstrates the benefits of CYP17 inhibition as therapy for castration-resistant prostate cancer. However, due to possible side effects associated with steroidal scaffolds, non-steroidal CYP17 inhibitors were designed and synthesized.

Methods: By mimicking the natural substrates, several series of biphenyl methylene heterocycles were designed as CYP17 inhibitors. Although potent inhibitors have been identified in imidazoles showing favorable pharmacokinetic properties, they were not sufficiently selective. After replacing imidazolyl by 4-pyridyl, improvements of activity and selectivity were observed. Inspired by the imidazole SARs that substituents on the A-ring and the methylene bridge showed profound influence on the activity, thorough investigation was performed on the pyridyl scaffold. It has been found that H-bond forming groups furnishing on the A-ring largely elevated the activity. As for the methylene bridge, flexible alkyl groups reduced potency, whereas conformation rigidifying i-propylidene groups significantly improved activity and selectivity.

Results: These efforts resulted in compounds more potent than or comparable to the drug candidate Abiraterone (IC_{50} = 72 nM). Most of these potent compounds also exhibited better selectivity profiles toward CYP11B1, CYP11B2, CYP19 and hepatic CYP3A4 than Abiraterone.

Conclusion: Successful optimization of biphenyl methylene heterocycles was achieved resulting in the evolution from imidazoles to pyridines. The compounds obtained are promising drug candidates after further validation in vivo.

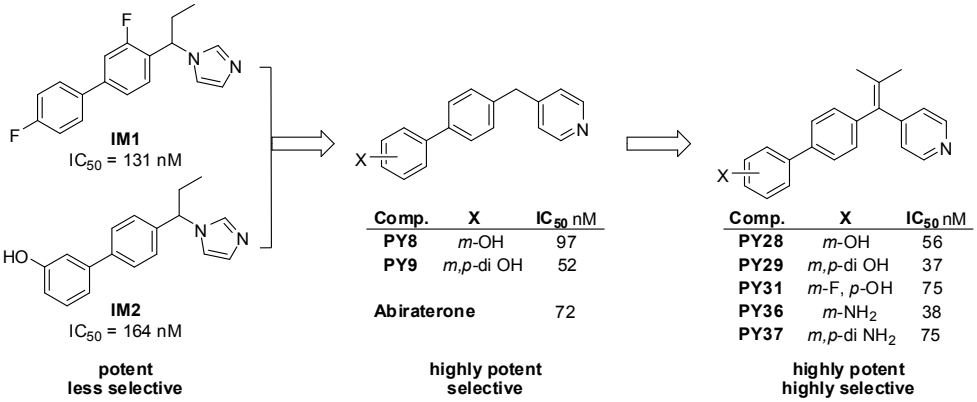

Comp.	X	IC_{50} nM
PY8	*m*-OH	97
PY9	*m,p*-di OH	52
Abiraterone		72

Comp.	X	IC_{50} nM
PY28	*m*-OH	56
PY29	*m,p*-di OH	37
PY31	*m*-F, *p*-OH	75
PY36	*m*-NH_2	38
PY37	*m,p*-di NH_2	75

PS-W-21

Computational Identification and Experimental Validation of Selective Estrogen Receptor Modulators as Ligands of 5-Hydroxytryptamine-6 Receptors and Potential Anti-Alzheimer's Agents.

R. Hajjo[1], B. L. Roth[2], and A. Tropsha[1]

[1]Laboratory for Molecular Modeling and Carolina Exploratory Center for Cheminformatics Research, Division of Medicinal Chemistry and Natural Products, School of Pharmacy, University of North Carolina at Chapel Hill, Chapel Hill, North Carolina 27599
[2]National Institute of Mental Health Psychoactive Drug Screening Program and Department of Biochemistry, School of Medicine, University of North Carolina at Chapel Hill, Chapel Hill, North Carolina 27599.

Purpose: We have devised an integrative chemocentric informatics methodology for the discovery of new drug candidates and finding new uses for existing drugs by fusing structural hypotheses generated from different approaches to knowledge discovery in chemical databases. As a proof of concept, we focused on Alzheimer's disease (AD), which is one of the most complex debilitating neurodegenerative diseases.

Methods: An integrative chemocentric informatics approach, combining QSAR modeling, model-based virtual screening (VS), and mining of both biological literature and online databases of gene signatures and biological profiles, has been devised and employed. Gene signatures for Alzheimer's disease were used to query the Connectivity Map (CMap: http://www.broad.mit.edu/cmap/) database to formulate testable hypotheses about potential treatments. Concurrently, QSAR models have been developed for the serotonin (5-HT) receptor family where, e.g., 5-HT_6 is involved in cognition enhancement. Externally validated models were used for VS of the World Drug Index (WDI) database to identify putative ligands. Common chemical hits from QSAR/VS studies and the CMap were subjected to radioligand binding assays against 5-HT receptors.

Results: Our chemocentric informatics approach identified 34 chemicals as possible therapeutics for AD, out of 59000 chemicals included in the WDI. Nine compounds out of a total of 12 common hits submitted for experimental testing were found to be nanomolar binders of 5-HT_6 receptor, a promising novel target for cognition enhancement. Evidence extracted from the biomedical literature indicated that at least one of these compounds can prevent the development of AD. This compound is undergoing comprehensive receptorome-wide experimental screening.

Conclusions: We have devised a novel integrative chemocentric informatics approach combining quantitative cheminformatics with text and database mining. This approach was shown to be useful in predicting novel experimentally confirmed ligands for 5-HT_6 receptors that may be viewed as putative cognitive enhancers. The approach could be extended towards many similar receptor systems serving as a cost-effective *in silico* tool to rationally select chemicals and screening assays in an effort to identify novel clinically relevant drugs and their targets.

PS-W-22

Development of SMEDDS with Well Defined Excipients for Oral Delivery of Cinnarizine, a Poorly Water Soluble Drug Compound

Anne Larsen[1], Ragheb A. Rmaileh[2], Jesper Østergaard[1], and Anette Müllertz[1].

[1]University of Copenhagen, Department of Pharmaceutics and Analytical Chemistry, Copenhagen, Denmark. E-mail: al@farma.ku.dk
[2]AstraZeneca, Pharmaceutical Development, Macclesfield, United Kingdom

Purpose: To design oral self-micro-emulsifying drug delivery systems (SMEDDSs) that will enable a mechanistic understanding of drug release; SMEDDSs were prepared from well defined excipients allowing lipolysis of formulations to be mimicked without lipases.

Methods: Excipients were selected based either of two criteria: 1) excipients not lipolysed in the gastro-intestinal tract or 2) structurally defined excipients, forming well-defined lipolysis products. The following non-lipolysed excipients were selected: Cremophor RH40, Brij97, oleic acid, PEG400, and ethanol. As a well defined excipient sesame oil was selected, lipolysed mixtures can be created by mixing fatty acids and monoglycerides.
SMEDDSs compositions were defined based on the selected excipients, using a pseudo-ternary phase diagram approach and the following criteria: ability to form homogeneous pre-concentrates and formation of clear-opalescent microemulsions upon dilution (1+99 water %w/w). Cinnarizine solubility in SMEDDSs was determined by HPLC. Dispersion times were evaluated in simulated fasted state gastric fluid (1g to 250ml, pH 1.6). The particle sizes of intact, and mimicked lipolysed microemulsions were determined by dynamic light scattering after dispersion in media containing 15mM taurocholic acid and 3.75mM phospholipids (pH 6.5).

Results: From the preparation of 174 excipients mixtures, 39 mixtures were homogeneous, out of these 4 were found to form microemulsions in water. Compositions of the 4 SMEDDSs, the solubility of cinnarizine, and the particle sizes are shown in Table I. The solubility decreased when the amount of sesame oil and oleic acid was lowered. Dispersion times were 9.7±1.5, 10.3±2.0, 1.7±0.6, and 1.8±0.4min for SMEDDS I, II, III, and IV respectively. When I and II are lipolysed smaller particles are formed, for III and IV no change are observed. In III and IV little is likely to happen due to small amounts of lipolyseable excipient. The visible particles in IV 100% lipolysed is most likely precipitated cinnarizine.

Conclusion: It is possible to design SMEDDSs that can be prepared as their lipolysed counterparts without incubation with lipases and thus can be used to achieve a fundamental mechanistic understanding of drug behaviour and release from SMEDDSs.

Table I. Composition of formulations (w/w %), solubility of cinnarizine, and particle sizes.

Excipient	SMEDDS I	SMEDDS II	SMEDDS III	SMEDDS IV
Sesame oil	27	20.6	10.3	5.1
Oleic acid	18	15.4	7.7	3.9
Cremophor RH 40	45	45	45	54
Brij 97		9	18	18
PEG 400			9	9
Ethanol	10	10	10	10
Cinnarizine solubility[1] (mg/g, n = 3)	67.4±0.9	58.8±0.5	36.4±0.7	28.3±0.8
Particle sizes (radius, nm)				
Intact SMEDDSs	32	19	11	9
50 % lipolysed SMEDDSs	13	9	8	8
100 % lipolysed SMEDDSs	12	10	8	visible particles

PS-W-23

Identification of transport mechanisms for two simultaneously occurring mycotoxins - ochratoxin A and citrinin - into the human liver

G. Gao[1], K. Artursson[2], P. Artursson[1]

[1] Department of Pharmacy, Uppsala University, Sweden
[2] National Veterinary Institute, Uppsala, Sweden

Purpose: The liver is one of the most important organs for accumulation and elimination of mycotoxins. However, the hepatic uptake clearance mechanisms for the two simultaneously occurring mycotoxins ochratoxin A and citrinin have not been fully investigated. The aim of this study was to investigate the uptake mechanisms for these two toxins by relevant *SLC*-transporters in the human liver.

Methods: The transport of ochratoxin A or citrinin by HEK 293 cells stably transfected with human OATP1B1 (*SLCO1B1*), OATP1B3 (*SLCO1B3*), OATP2B1 (*SLCO2B1*), NTCP (*SLC10A1*) and OCT1 (*SLC22A1*). Kinetic parameters were derived and passive permeability was determined using mock-transfected cells.

Results: Ochratoxin was actively transported by the anion transporters but not by OCT1. In addition, ochratoxin A inhibited all anion transporters. In contrast, citrinin was passively transported into the cells and only inhibited OATP1B1. Simultaneous administration of the two toxins resulted in synergistic effects on the transport of endogenous transporter substrates at low nanomolar concentrations.

Conclusions: Ochratoxin A is transported into human hepatocytes by several active mechanisms while citrinin transport is mainly passive. Together, the two toxins show synergistic effects on transport mechanisms at very low concentrations, but whether these effects are of significance *in vivo* remains to be seen.

PS-W-24

Acceleration of wound healing by increasing survival of transplanted cells using adhsamine, a synthetic cell adhesion molecule

K. Kusamori[1], M. Nishikawa[1], T. Suehara[1], Y. Takahashi[1], S. Yamazoe[2], M. Uesugi[2], Y. Takakura[1]

[1] Department of Biopharmaceutics and Drug Metabolism, Graduate School of Pharmaceutical Sciences, Kyoto University, Kyoto, Japan.

[2]Institute for Integrated Cell-Material Sciences, Kyoto University, Kyoto, Japan

Purpose: Rapid progress in the technology for cell culture and differentiation has made it a general laboratory technique to prepare specific types of cells from embryonic stem cells or induced pluripotent stem cells, and tissue-specific stem cells. However, the efficacy of cell-based therapy is not satisfactory because of rapid clearance and undesirable distribution of administered cells. Adhesamine, a diaryldispirotripiperazine derivative, which promotes cell adhesion and cell growth in culture condition, could be used to increase the adhesion and survival of cells administered. In this study, the effects of adhesamine on wound healing by cell transplantation were examined in mice.

Methods: Full thickness skin wounds were made on the dorsal skin of normal ICR or diabetic model *db/db* mice. Mouse NIH3T3 fibroblasts or bone marrow-derived cells (BMCs) were preincubated with adhesamine, collagen or fibronectin and administered to the wound by instillation, subcutaneous injection, or intradermal injection. NIH3T3/Luc cells, a line stably expressing firefly luciferase, were used to trace the survival of administered cells. Separately, the changes in mRNA level of TGF-β and FGF, both of which were reported to be important for wound healing, in the wound area were measured by RT-PCR.

Results: Adhesamine significantly increased the survival of NIH3T3/Luc cells and the effect was greater than that of collagen or fibronectin, representative natural molecules involved in cell adhesion and survival. Wounds in normal mice healed over 4 weeks, and NIH3T3/Luc pre-incubated with adhesamine, but not adhesamine or NIH3T3/Luc, accelerated the healing. Irrespective of the route of administration, adhesamine significantly increased the survival of NIH3T3/Luc cells. Furthermore, this accelerated healing was associated with increased mRNA expression of TGF-β. BMCs were effective in healing the wound after intradermal injection to both normal and diabetic mice, and those pre-incubation with adhesamine showed better effects.

Conclusion: This study demonstrates that adhesamine increases the potency of cell transplantation for wound healing by improving the adhesion and survival of cells administered. These results indicate that adhesamine, a synthetic cell adhesion molecule, is beneficial for cell-mediated wound healing.

PS-W-25

***In vitro* characterization of drug-L-carnitine conjugate as potential prodrug targeting Organic cation/carnitine transporter (OCTN2)**

Lei Diao, James Polli

University of Maryland School of Pharmacy

Purpose: A drug conjugate of the native OCTN2 substrate L-carnitine was hypothesized to be potential prodrug targeting OCTN2. Model drugs were conjugated to L-carnitine with/without linker and characterized for their uptake by OCTN2, inhibition of L-carnitine uptake by OCTN2, , and chemical/metabolic stabilities *in vitro*.

Methods: Naproxen, ketoprofen and valproic acid were used as model drugs. Ketoprofen-glycolic acid-L-carnitine and ketoprofen-glycine-L-carnitine were also synthesized to evaluate the influence of the linker on the prodrug stability.

Results: Only certain portions of carnitine's structure were found to be necessary for carnitine recognition by OCTN2 and 3' hydroxyl position was used in this study to conjugate drug to L-carnitine.

Naproxen-L-carnitine, ketoprofen-L-carnitine and valporic acid-L-carnitine were substrates for OCTN2, where uptake for each was concentration-dependent (K_t = 257±56 μM for naproxen-L-carnitine, 74.1±3.9 μM for ketoprofen-L-carnitine and 130±3.9 μM for valproic acid-L-carnitine), sodium-dependent, and inhibited by L-carnitine. Naproxen-L-carnitine, ketoprofen-L-carnitine and valproic acid-L-carnitine also inhibited L-carnitine uptake (K_i is 5.97±0.81 μM, 82.2±5.3 μM, and 155±19 μM, respectively). Both naproxen-L-carnitine and ketoprofen-L-carnitine were able to release parent drugs in 0.2 M KOH solution in methanol. However, they remained stable in various metabolic matrixes including rat, mouse and human plasma, rat kidney homogenate, mouse liver microsome and S9 fraction. Although degraded to release parent drug ketoprofen in various metabolic matrixes including mouse plasma, rat plasma and rat kidney homogenate, ketoprofen-glycolic acid-L-carnitine were too unstable *in vitro* for uptake studies (ketoprofen-glycolic acid-L-carntine degrades to 50% in HBSS within 2.5 h). On the contrary, ketoprofen-glycine-L-carnitine demonstrated better chemical stability *in vitro* than ketoprofen-glycolic acid-L-carnitine and was an inhibitor as well as a substrate for OCTN2 (K_i = 14.4±1.4 μM; K_t = 58.2±8.7 μM). Furthermore, ketoprofen-glycine-L-carnitine was degraded to some extent in various metabolic matrixes including mouse plasma, mouse liver S9 fraction, and rat kidney homogenate.

Conclusion: OCTN2 is abundantly expressed, with the important physiological function to transport L-carnitine into several tissues such as kidney and brain. Hence, the drug conjugate of L-carnitine has the potential to serve as prodrug targeting kidney and/or brain. Glycine linker seems to have a balance for acceptable chemical stability and releasing parent drug in metabolic matrixes.

PS-W-26

Characterization of Ebola and Marburg Virus-like Particles

Lei Hu[1], Jared M. Trefethen[1], Vu L. Truong[2], Yuhong Zeng[1], Sangeeta B.Joshi[1], C. Russell Middaugh[1]

[1]Department of Pharmaceutical Chemistry, School of Pharmacy, University of Kansas
Lawrence, KS.
[2] Aridis Pharmaceuticals, LLC. San Jose, CA.

Purpose: This work focuses on the characterization of Virus-like particles from Ebola (eVLP) and Marburg (mVLP) viruses with the long term goal of development of stable vaccines. The filoviruses, Ebola and Marburg, cause severe hemorrhagic fever with 70-80 % human mortality. EVLP and mVLP are attractive vaccine candidates. Expression of glycoprotein (GP), nucleoprotein (NP) and the VP40 of viruses leads to self–assembly of the viral proteins into filamentous virus-like particles. Development of effective vaccines against filoviruses is crucial to protect against natural outbreaks.

Methods: The physical stability of the VLPs was investigated by various spectroscopic techniques as a function of temperature and pH. Intrinsic fluorescence, extrinsic fluorescence using laurdan, and circular dichroism (CD) spectroscopies were monitored over the pH range of 3 to 8 from 10 to 87.5 ºC. Temperature-induced aggregation of the VLPs at various pH values was monitored by static and dynamic light scattering. Empirical phase diagrams of Ebola and Marburg were constructed using the data generated from these techniques. Empirical phase diagrams (EPD) are used to summarize large volumes of data and can be used to describe physical changes in macromolecules. Apparent phase change can be visualized as a function of temperature and pH in an EPD.

Results: Far UV CD studies suggest that eVLP and mVLP contain proteins that predominantly consist of alpha-helical (possibly some beta) secondary structure. Both VLPs are more structured and thermally stable at higher pH. Intrinsic tryptophan fluorescence analysis also suggests that the most stable environment for eVLP and mVLP is within the pH range of 7-8. The laurdan extrinsic fluorescence study shows that the VLPs have broad thermal transitions at each pH. Each VLP shows significant thermal and pH sensitivity in static light scattering measurements. Dynamic light scattering studies show that the diameters of the VLPs at lower pH are much larger (> 1000 nm) due to aggregation.

Conclusion: Our results show that eVLP and mVLP are maximally stable at pH 7-8. Both VLPs are much less stable at pH 3-4 due to aggregation. Preformulation studies of the VLPs in solution provide key information for optimal vaccine development.

PS-W-27

lyophilization of ganciclovir salt forms

Lokesh Kumar[1], Ankit Baheti[2] and Arvind K. Bansal[1]

[1]Department of Pharmaceutics, National Institute of Pharmaceutical Education and Research, Sector - 67, S.A.S. Nagar, Punjab, India - 160062.
[2] Department of Pharmaceutical Technology (Formulations), National Institute of Pharmaceutical Education and Research, Sector - 67, S.A.S. Nagar, Punjab, India - 160062

Purpose: Salt formation is used for solubility modulation of limited water solubility drugs, to enable development of an aqueous lyophilization process. Selection of the counterion, apart from affecting solubility, however, also affects the critical process parameter during lyophilization. Effect of counterion on the intra and inter-molecular interactions governs the critical process temperature during lyophilization. Designing of an efficient lyophilization cycle hence, demands selection of an optimal salt form, with the highest possible critical process temperature for lyophilization.

Methods: Salts of ganciclovir, viz., sodium, potassium, rubidium and cesium were prepared by *in-situ* salt formation, and analyzed using an optimized modulated differential scanning calorimetry (modulation amplitude ±0.2° every 60 seconds, underlying heating rate 1°C/min). Also, the critical process parameter for ganciclovir free base was determined by a modified MDSC protocol, employing supersaturation of the free base. Role of intramolecular interaction between the drug and the counterion and the associated intermolecular interactions shall be discussed.

Results: All the salt forms, as well as the free base showed a glass transition in the reversible heat flow signal, depicting their amorphous nature. T_g' of the free base, sodium, potassium, rubidium and cesium was found to be -39.59, -39.94, -48.18, -51.19 and -56.72 °C respectively. Difference in the glass transition temperature is attributed to different levels of ionic interactions between the drug and the counterion, with sodium having the highest level of intra-molecular interaction and cesium the least. Additionally, the bulk (or molecular weight) of the counterion also plays a role; contributing to the increase in glass transition temperature from sodium to cesium.

Conclusion: The type of counterion affects the glass transition temperature T_g' for lyophilization, which should be determined to select an optimal salt form for lyophilization.

PS-W-28

Enhanced Absorption of the Poorly Soluble Drug Fenofibrate by Tuning its Release Rate from Ordered Mesoporous Silica

Michiel Van Speybroeck[1], Randy Mellaerts[2], Thao Do Thi[1], May Issa[2], Johan Martens[2], Jan Van Humbeeck[3], Pieter Annaert[1], Guy Van den Mooter[1] and Patrick Augustijns[1]

[1]Laboratory for Pharmacotechnology and Biopharmacy, KU Leuven, Belgium
[2]Centre for Surface Chemistry and Catalysis, KU Leuven, Belgium
[3]Department of Metallurgy and Materials Engineering, KU Leuven, Belgium

Purpose: To evaluate the effect of release rate from ordered mesoporous silica materials on the rate and extent of absorption of the poorly soluble drug fenofibrate.

Methods: Three ordered mesoporous silica materials with different pore diameter (7.3 nm, 4.4 nm and 2.7 nm) were synthesized and loaded with fenofibrate via impregnation. Release experiments were conducted under sink conditions and under supersaturating conditions in biorelevant media simulating the fasted and the fed state. Subsequently, all silica-based formulations were evaluated in vivo (rats, *n*=3).

Results: The release experiments under sink conditions indicated a clear increase in release rate with increasing pore size. However, under supersaturating conditions, the pharmaceutical performance (in terms of both the degree and duration of supersaturation) increased with decreasing pore size. The same trend was observed in vivo: the area under the plasma concentration-time profile amounted to 102±34 µM.h, 86±19 µM.h and 20±13 µM.h for the materials with pore diameter of 2.7 nm, 4.4 nm and 7.3 nm, respectively.

Conclusions: The results of this study demonstrate that a decrease in drug release rate – and thus, a decrease of the rate at which supersaturation is created – is beneficial to the absorption of fenofibrate.

Plasma concentration-time profiles following oral dosing of fenofibrate formulations

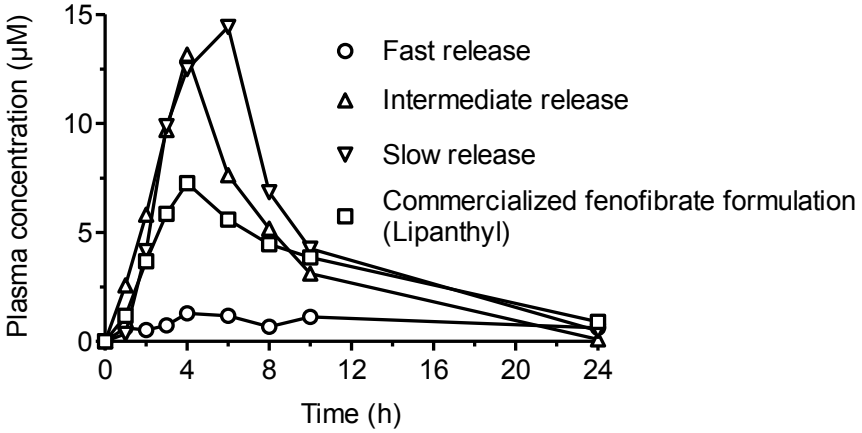

PS-W-29

Influence of donor solution viscosity on the microneedle-enhanced naltrexone hydrochloride skin transport

Mikolaj Milewski, Audra L. Stinchcomb

College of Pharmacy, University of Kentucky, Lexington, KY 40536-0082

Purpose: The aim of this study was to investigate the importance of donor solution viscosity on the rate of naltrexone hydrochloride (NTX HCl) skin transport *in vitro* with the usage of microneedles (MN).

Methods: A flow-through diffusion cell apparatus was used for the assessment of transdermal fluxes of NTX HCl. Full-thickness Yucatan pig skin was used intact or pretreated with 100 MN insertions. Donor solutions consisted of NTX HCl (110 mg/ml) in binary mixtures of propylene glycol (PG) and water, and receiver solution consisted of HEPES-buffered Hanks' balanced salt solution. Seven different composition PG-water donor solutions were tested and the corresponding transdermal fluxes measured by HPLC.

Results: The first set of experiments evaluated the permeation of NTX HCl through MN-enhanced skin. The fluxes varied greatly depending on the donor solution composition. The lowest flux, 2.1 ± 0.9 nmol/cm^2/h, was obtained from a pure PG solution (51.7 cP) while the highest, 81.6 ± 11.6 nmol/cm^2/h, was obtained from a pure aqueous solution (1.05 cP). The increase in the NTX HCl transdermal flux correlated very well with the drug diffusivity change calculated from donor solution viscosity measurements. Additionally, the same set of experiments was repeated with the intact, non-MN-treated skin. The results revealed that for all donor solutions tested the fluxes were much lower ranging from 0.8 ± 0.1 to 9.0 ± 2.6 nmol/cm^2/h. Moreover, they didn't follow the viscosity-related relationship recognized for MN-enhanced transport but rather were in qualitative agreement with different NTX HCl saturation levels in donor solutions.

Conclusions: A considerable, approximately 40-fold, difference in the NTX HCl transport rate was observed between pure PG and pure water donor solutions. This difference can be explained in terms of varying donor solution viscosity and the use of the Stokes-Einstein equation to calculate the change in the drug diffusivity. As expected, this approach can not be used to account for percutaneous flux changes when carrying out experiments with intact skin. These findings are in good agreement with the fact that, after MN-treatment, the stratum corneum is no longer the rate-limiting step in the enhanced transdermal transport.

Funding: NIHR01DA13425

PS-W-30

Design and Characterization of Tumor Specific Lyp-1 Peptide-Containing SMEDDS for the Lymphatic Targeting of Solid Tumors in Cancer Therapy

O. Cevik[1], R. N. Gürsoy[1]

[1]Department of Pharmaceutical Technology, Faculty of Pharmacy, Hacettepe University, Ankara, TURKEY

Purpose: Recent studies on tumor homing peptides have shown that the LyP-1 peptide (CGNKRTRGC) is specific to tumor lymphatics. Knowing that the lymphatic system is an important pathway of tumor metastasis, the purpose of the present work was to design SMEDDS (Self-Microemulsifiying Drug Delivery System) formulations for the lymphatic delivery of a LyP-1 peptide-lipid reversible conjugate targeted to solid tumors.

Methods: Preformulation studies were carried out to determine the optimum formulation components of the SMEDDS. Ternary phase diagrams were constructed containing different oils, surfactants and cosolvents. Characterization studies were conducted using polarized light microscopy (Leica, Germany) and a nanosizer (Malvern Zetasizer Nanoseries, UK).

Results: Optimum SMEDDS formulations were obtained using Peceol as the oil phase, Labrasol:Gelucire (4:1 and 1:2 ratios) mixture as the surfactant system, and PEG 300 as the cosolvent. The oil (5 – 10%), surfactant (50 – 85%), and cosolvent (5 – 45%) were mixed homogenously on a 40°C water bath until a clear mixture was obtained. This mixture was then diluted with pH 7,4 phosphate buffer at a ratio of 1:10. The formulations were clear, isotropic systems with Newtonian type flow properties. These SMEDDS formulations were physically stable with no phase separation following a two week stability study at 25±1°C. The pH of the formulations varied between 7,05 – 7,20. The formulations were evaluated using polarized light microscopy for the possibility of liquid crystal structures that give specific anisotropic image under polarized light. None of the SMEDDS formulations appeared to have liquid crystal structures. Since non-ionic surfactants were used in the formulations, the zeta potential values were close to zero. The droplet size was 28,25±5,52 nm (PDI:0,19) and 18,04±1,84 nm (PDI:0,19) for the SMEDDS formulations containing Labrasol:Gelucire at a ratio of 4:1 and 1:2, respectively.

Conclusions: Suitable SMEDDS formulations were designed and characterized for the targeted lymphatic delivery of the anticancer peptide LyP-1.

Acknowledgment: This project is supported by TUBITAK, The Scientific and Technological Research Council of Turkey, SBAG 1001 – 109S341.

PS-W-31

Incorporation of water-soluble API in lipid-based microspheres obtained by prilling: from the process to the controlled release mechanisms

P. Pivette[1], V. Faivre[1], G. Daste[2], M. Ollivon[1], S. Lesieur[1]

[1]Université Paris-Sud XI, UMR CNRS 8612, 5 rue J.B. Clément, 92290 Châtenay-Malabry, France
[2] Sanofi-Aventis, 20 avenue Raymond Aron, 92165 Antony, France

Purpose: The aim of this work is to prepare and characterize lipid microspheres loaded with water-soluble API of industrial interest in order to control its release kinetics. The purpose here focuses on the correlation between the process and the release properties.

Methods: Sustained release microspheres for oral route were obtained by melting excipients and API. By extrusion through vibrating nozzles, molten solutions were dispersed into calibrated droplets which solidify during their fall in a temperature-regulated air column[1]. Microspheres were essentially characterized using XRD, DSC and SEM.

Results: Model equations were established to predict the solidification time required to crystallize the molten mixture as a function of its thermal characteristics and optimize prilling operating parameters. It results from these calculations that droplet cooling rates are very fast, in the range of thousands of K/min. Taking advantage of the process and this rapid cooling rate, it is possible to generate perfectly spherical microspheres in which the crystalline domains are very thin and drug finely dispersed. In such kind of inert lipid-based microspheres, and considering the important water-solubility of the API, the release kinetics is governed i) by the water diffusion through the drug-filled channels and ii) by the API molecular diffusion in the pores created after drug dissolution.

In practice, microspheres were prepared, characterized and dissolution analysis attested a prolonged release dissolution profile. Shape studies have shown that the matrix remains globally intact during dissolution.
To get further insight onto the drug release mechanisms, XRD and HPLC analysis were made simultaneously to quantify the solubilized-drug fraction within the particles and the effective released fraction respectively. The XRD analysis also confirmed the stability of the lipid matrix structure at a supramolecular level, allowing the use of model equations based on dissolution-diffusion mechanisms to fit the data.

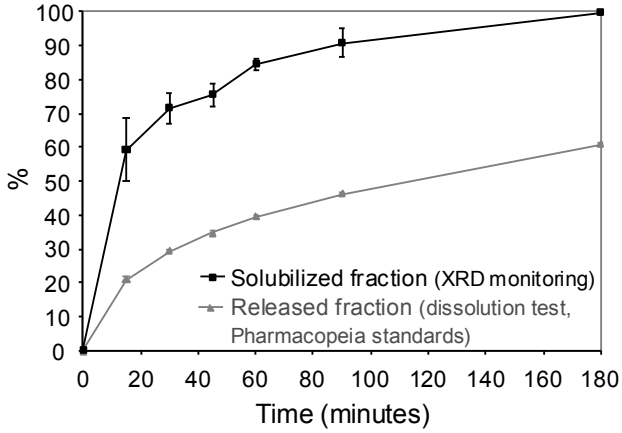

Conclusion: In agreement with the theoretical prediction, we prepared by prilling process lipid microspheres able to control the release of a water-soluble drug. Monitoring the crystallized-API disappearance within the matrix complements classical dissolution methods which measure the drug fraction released in the dissolution media.

[1] Pivette et al., *JTAC*, **98**, 47-55, 2009

PS-W-32

Enhancing the Freeze-Thaw Stability of an Aluminum-Containing Adjuvant
T. Clapp and L. Jones Braun

Department of Pharmaceutical Sciences, School of Pharmacy, University of Colorado Denver, Aurora, CO

Purpose: The majority of FDA-licensed childhood vaccines have poor thermal stability. Exposure to freeze-thaw stresses causes vaccines with aluminum-containing adjuvants to agglomerate. This agglomeration has been implicated in reduced vaccine efficacy. Because of limitations with formulation strategies, the lab purposes that an engineered approach via surface modification has potential to enhance the thermal stability of aluminum-containing adjuvants, while retaining formulation integrity and immunogenic adjuvant properties.

Methods: The effect of adjuvant concentration and presence of select buffer ions on the freeze-thaw agglomeration of Alhydrogel, a commercially available aluminum-containing adjuvant, was determined. The effect of differences in the adsorptive capacities of two commercially available aluminum hydroxide adjuvants and freeze-thaw agglomeration was also determined. These results were used to select experimental conditions for the remaining studies. Preliminary adjuvant modification studies used commercially available compounds. Adjuvant modification was verified using size-exclusion HPLC to

detect unbound modifiers. The particle size distributions of the modified and control adjuvants were determined using a Micro-Flow Imaging (MFI) Dynamic Particle Analyzer DPA 4100A (Brightwell Technologies Inc. Ottawa, Canada). This same technique was used to assess freeze-thaw induced agglomeration of control and modified adjuvants. The effect of modification on the antigen binding properties of the adjuvant was accessed via UV-Vis spectroscopy.

Results: The initial studies characterizing the commercially available adjuvants suggested that formulating the adjuvant in water for injection (WFI) and subjecting it to three to four freeze-thaw cycles should produce sufficient damage (agglomeration) to permit evaluation of the protective effects of adjuvant modification. In a well-characterized system, surface modification of the adjuvant was successfully achieved and validated via UV-Vis spectroscopy and SE-HPLC. With sufficient amounts of modifier, agglomeration of the adjuvant following freeze-thaw stress was inhibited.

Conclusion: Our strategy for altering the surfaces of aluminum-containing adjuvants appears to be feasible. Modification may improve the freeze-thaw stability of aluminum-containing adjuvants. The ability of the modifier to protect the adjuvant against F/T-induced agglomeration may be dependent on the properties of the modifier. It remains to be determined how the protective modifications affect the immune-enhancing qualities of the adjuvant.

PS-W-33

Development of Peptides to Target Antigen Presenting Cells for Controlling the Immune Response in Experimental Autoimmune Encephalomyelitis

A. H. Badawi and T. J. Siahaan

Department of Pharmaceutical Chemistry, University of Kansas, Lawrence, KS 66047

Purpose: The myelin sheath is composed of various proteins including myelin proteolipid protein (PLP) and myelin oligodendrocyte glycoprotein (MOG). Patients suffering from multiple sclerosis (MS) develop an immunogenic response towards these proteins. Our lab has developed a group of peptides known as bifunctional peptide inhibitors (BPI), which have been shown to induce immunotolerance in EAE, an animal model for MS. The BPI molecules were designed to bind to MHC-II and cell adhesion receptors (i.e., ICAM-1) on the surface of APC and control the activation of T cells to induce immunotolerance. We propose that the induction of immunotolerance takes place due to the activation of regulatory (T_{reg}) and suppressive responses (T_H2) of the immune system. In this study, we evaluated the effectiveness of different BPI molecules in a "vaccine-like" treatment for suppressing EAE. The BBB leakiness-prevention and the mechanism of the BPI molecules will also be elucidated.

Methods: Peptides were injected 11 to 5 days prior to disease induction. EAE is induced by the injection of the antigen and complete Freund's adjuvant, followed by two injections of pertussis toxin. Disease severity is monitored by using a standard clinical scoring protocol and observing the change in body weight. Gadolinium enhanced magnetic resonance imaging (MRI) was used to look at the BBB leakiness. Cytokine analyses will be performed by collecting blood samples from the mice on different days and ELISA will be used to determine the cytokine population.

Results: Mice treated with BPI molecules showed normal increase in body weight, and no or very little EAE was seen. In contrast mice treated with control peptides or PBS showed a decrease in body weight and a high disease score. Using MRI, we have shown sick mice have a leaky BBB as seen by the increased enhancement by gadolinium.

Conclusion: BPI molecules showed significant suppression of EAE as compared to the control peptides. Current studies are being undertaken to look at the effect of the BPI molecules on BBB leakiness. In addition, using cytokine analysis studies that are in progress we can determine what type of immune response is being activated which will help us better understand the mechanism of the BPI molecules.

PS-W-34

Development of small pDNA-containing liposomes for DNA vaccination

Koen van der Maaden, Myrra Carstens, Joke Bouwstra, Wim Jiskoot

Drug Delivery Technology, Leiden/Amsterdam Center for Drug Research (LACDR), Leiden University

Purpose: DNA vaccination is based upon the administration of antigen-encoding plasmid DNA (pDNA), and subsequent production of the antigen, to which an immune response is elicited. DNA vaccines can induce both humoral and cellular immune responses and have several benefits over the current vaccines like the possibility of using multiple antigens in one vector, higher stability, better safety and their potential capability of offering protection against intracellular infectious agents like HIV, malaria and tuberculosis. One of the main disadvantages of DNA vaccination is the low potency in humans, which may be related to poor delivery of pDNA to the appropriate cells and/or degradation of pDNA by endonucleases. This can be overcome by using particulate delivery systems, such as liposomes, to formulate the pDNA. The purpose of this research was to develop small pDNA-containing liposomes for DNA vaccination.

Methods: Liposomes composed of egg L-α-phosphatidylcholine (EPC), 1,2-dioleoyl-*sn*-glycero-3-phosphoethanolamine (DOPE) and 1,2-dioleoyl-3-trimethylammonium-propane (DOTAP) were prepared by the dehydration-rehydration method and were sized by extrusion. Liposomes were analyzed by DLS and electron microscopy, DNA content and integrity by a PicoGreen assay, UV spectroscopy, and gel electrophoresis, respectively. The encapsulation efficiency was determined by separating non-encapsulated pDNA from the liposomes with a membrane filter, followed by a PicoGreen assay.

Results: Sizing by extrusion (2x400 + 4x200 nm) of large pDNA-containing liposomes (diameter ~460 nm) resulted in liposomes with an average particle size of 145±7 nm (mean ± sd), a narrow size distribution (as reflected by a polydispersity index of 0.15±0.02), and a zeta potential of 54±2 mV. Electron microscopy showed that liposomes were unilamellar after extrusion. DNA recovery after extrusion was 48±8% of the initial DNA content, of which most was encapsulated inside the liposome (91.1±0.3%). The pDNA was intact after sizing by extrusion and protected against DNase degradation. Reduction of the liposome size could also be achieved by sonication and extrusion through 100 nm filters, but this resulted in a low DNA content and/or pDNA damage.

Conclusion: The dehydration-rehydration method, followed by an extrusion cycle of 2x400 + 4x200 nm enabled us to create well-defined small pDNA-containing liposomes that can be used for DNA vaccination.

PS-W-35

Reverse transfection: a versatile tool for cell biology and pharmaceutical research

M. Reinisalo[1], E. Voutilainen[1], M. Courtney[2] and P. Honkakoski[1]

[1] School of Pharmacy and Biocenter Kuopio, University of Eastern Finland, Kuopio, Finland
[2] A.I.Virtanen Institute and Biocenter Kuopio, University of Eastern Finland, Kuopio, Finland
Email: mika.reinisalo@uef.fi

Purpose: In pharmaceutical and natural sciences there is a need for gene delivery methods which are efficient and also of low toxicity. In addition, features such as simplicity of production and long-term stability of the DNA complexes are desirable. Our purpose was to test different factors affecting the long-term stability of freeze-dried reverse transfection plates and capability to utilize this method in different applications.

Methods: For reverse transfection, different formulations of DNA/polyethylenimine 25 kDa (PEI25) complexes were prepared on cell culture plates, freeze-dried and stored until use. Role of formulation, influence of storage time and temperature was studied. Furthermore, gene silencing by using siRNA delivery and the efficiency to analyze weak promoters in retinal primary cultures was also studied. Moreover, reverse transfection method was applied to live-cell imaging.

Results: Prepared reverse transfection plates retain biological activity over long-term storage even at higher temperatures (+37^{o}C). In addition, transfection efficiency was related to lyoprotectant used in formulation. Importantly, reverse transfection method turned out to be a versatile method enabling the siRNA delivery and live-cell imaging as well as with hard-to-transfect retinal primary cultures.

Conclusions: Reverse transfection is a straightforward and reproducible gene delivery method where DNA/carrier complex can promote cell adhesion with concurrent complex uptake. In reverse transfection, plates can be prepared in advance and stored for long periods still retaining the biological activity of the complexes. Noteworthy, this method can be utilized in different applications in the field of natural and pharmaceutical sciences.

PS-W-36

Intracellular peptide delivery for cancer therapy

Sang Kyoon Kim, Leaf Huang

Division of Molecular Pharmaceutics, Eshelman School of Pharmacy, University of North Carolina, Chapel Hill, NC

Purpose: EGFR (epidermal growth factor receptor) is highly expressed in several types of cancers and activated by the stimulation of growth factors, resulting in enhanced cell proliferation and survival. In this study, we investigated a peptide-based therapy aimed at blocking intracellular protein-protein interactions, which play crucial roles in cellular function, during EGFR signaling and evaluated a targetable lipid carrier system that can deliver peptides to intracellular targets in human cancer cells.

Methods: EEEEpYFELV (EV), a nonapeptide mimicking the Y845 site of EGFR which is responsible for STAT5b phosphorylation, was designed to block EGFR downstream signaling, including mainly to STAT5b, which signals to multiple effector pathways. EV was loaded onto LPH nanoparticles that are comprised of a membrane/core nanoparticle formulation including a surface-grafted polyethylene glycol (PEG) used to evade the reticuloendothelial system (RES). In these nanoparticles the PEG chain is tethered to anisamide (AA) in order to target tumor cells expressing the sigma receptor.

Results: EV formulated with PEGylated and targeted LPH (LPH-PEG-AA) was taken up by human lung tumor cells and trafficked to the cytoplasm with high efficiency, such that the estimated intracellular concentration approached the extracellular concentration. Using this approach, EV acted as a dominant negative inhibitor of STAT5b phosphorylation that also arrested cell proliferation and induced massive apoptosis. Intravenous administration of EV loaded in LPH-PEG-AA, but not free peptide, led to the efficient delivery of EV to tumor sites in a xenograft mouse model of lung cancer and multiple injections inhibited tumor growth in a dose-dependent manner.

Conclusion: Our findings offer proof-of-concept for an intracellular peptide-mediated cancer therapy that is delivered by an effectively targeted nanoparticle-based approach.

PS-W-37

Quantitative Imaging of Lymphatic Function with Liposomal Indocyanine Green

Paola Luciani, Steven T. Proulx, Stefanie Derzsi, Matthias Rinderknecht, Viviane Mumprecht, Jean-Christophe Leroux, and Michael Detmar

Institute of Pharmaceutical Sciences, Department of Chemistry and Applied Biosciences, ETH Zurich, 8093 Zurich, Switzerland

Purpose: Near infrared fluorescence (NIRF) imaging methods have recently shown great promise for imaging lymphatic vascular system. Recent studies have demonstrated the potential of indocyanine green (ICG) to image lymphatics in animal models and in humans. However, this NIRF dye is unstable in solution and may rapidly enter venous capillaries after local injection. In this study, we designed a liposomal formulation of ICG (LP-ICG) that possesses ideal attributes for lymphatic function imaging.

Methods: The formulation of the liposomal contrast agent was optimized taking into account the physico-chemical features of the dye and the physiology of the target tissue. LP-ICG was compared to ICG after intradermal injection into the paws of normal mice, mutant mice with lymphatic dysfunction or tumor-bearing mice. A time sequence of *in vivo* NIRF images was recorded using an IVIS Spectrum imaging system. Regions of interest were placed over the popliteal and medial iliac lymph nodes, and the liver. Normalized data were fit to an exponential decay model.

Results: The LP-ICG formulation exhibited several advantages over ICG, including a red-shifted 4-fold increase in fluorescence intensity and improved stability in solution. When injected intradermally into normal mice, LP-ICG rapidly showed enhancement of draining lymph nodes, and demonstrated a more specific uptake by the lymphatics than ICG alone. No retention of LP-ICG in the lymph nodes or other organs was observed. An improved visualization of deep lymph nodes allowed the dynamics of lymphatic flow to be quantified. Quantitative imaging of lymphatic function with LP-ICG was validated in a genetic model of lymphatic dysfunction and in a melanoma tumor model of lymphatic metastasis. In mutant mice lacking dermal lymphatics, slower clearance from the injection site and no enhancement of draining lymph nodes was observed. Lymphatic flow through tumor draining lymph nodes was increased in comparison to normal nodes. In tumor-bearing mice, the flow pattern through lymph nodes was negatively correlated to the extent of metastatic burden.

Conclusion: LP-ICG showed substantially enhanced dye stability and enabled specific uptake into the lymphatic system. The improved visualization of deeper lymph nodes *in vivo* allowed quantifying tumor-associated lymph flow, making the developed model attractive for early diagnostics and future preclinical studies.

PS-W-38

Nanomedicines which deliver neuropeptides to the brain via the oral route

A. Lalatsa [1], A.G. Schätzlein [1], I.F. Uchegbu [1]

[1] The Nanomedicines Research Centre, Department of Pharmaceutics, The School of Pharmacy, University of London, 29-39, Brunswick Square, U.K., WC1N 1AX

Purpose: The current project is aimed at enhancing the bioavailability of water soluble peptides, e.g. Leucine^5-Enkephalin (LENK) by lipidisation and/or encapsulation in a carbohydrate bioavailability enhancer, Quaternary Ammonium Palmitoyl Glycol Chitosan (GCPQ). LENK is an endogenous opioid neuropentapeptide with a blood half-life of 3 minutes in man. A lipophilic prodrug, palmitoylated Leucine Enkephalin (TPLENK), comprising a cleavable ester bond susceptible to blood esterases was synthesised and characterised.

Methods: Standard solid-phase peptide synthesis of LENK was carried out and the free hydroxyl group of LENK was esterified. ESI-MS, NMR, & analytical/preparative HPLC were utilised for peptide characterisation and purification. Bioconversion of TPLENK was assessed utilising rat plasma and liver homogenates. Gut stability studies were conducted in the presence of SGF and rat intestinal wash. A radioimmunoassay was used for peptide quantification in plasma and brain. The tail flick bioassay was performed to assess the pharmacodynamic response after intravenous and oral administration.

Results: The lipophilic prodrug was converted into the parent drug by plasma and liver esterases with apparent half-lives for the disappearance of the pro-drug of ~73 and ~44 minutes in plasma and liver homogenates respectively. GCPQ-peptide formulations were more stable in SGF and rat intestinal wash. GCPQ increased the plasma half life of LENK on oral administration (Figure 1a) and doubled the AUC of LENK in the brain (Figure 1b). TPLENK was converted to LENK in vivo and the use of GCPQ – TPLENK increased the half life of LENK in the plasma and doubled the AUC of LENK when compared to the administration of LENK alone (Figure 1b). The oral administration of GCPQ – LENK and GCPQ – TPLENK resulted in a significant increase in LENK central analgesic activity (Figure 1c,d)

Conclusion: The present study is the first study to demonstrate the oral delivery of the labile small hydrophilic linear peptide LENK to the CNS via both pharmacokinetics as well as pharmacodynamics data. We hypothesise that the increase in brain bioavailability following the strategy adopted is due to: (i) an inhibition of peptide degradation in the gastrointestinal tract and in plasma leading to an increase in brain levels of LENK and (ii) a plausible increased transport of the prodrug across the lipid membranes of the gastrointestinal epithelium and the blood brain barrier.

pharmacokinetic data after the oral administration of the equivalent of 70 mg kg^{-1} LENK. % of LENK dose recovered after the oral administration of LENK (square), GCPQ - LENK (circle) and GCPQ - TPLENK (triangle) formulations to CD-1 Mice (n=4).

Figure 2: Central analgesic effects as demonstrated using the Tail Flick Bioassay after the oral administration of 7 LENK, a) Water (square), LENK (up triangle), GCP triangle), % antinocicepti Mice (n = 10). * = p < 0.05 versus LENK. #, = p LENK. b) black bars = % maximum possible respon removal of tail from noxious stimuli was truncated at 10sec), grey bar = % of animals which achieved a lag time for removal of tail from a noxious stimuli that was at least twice their

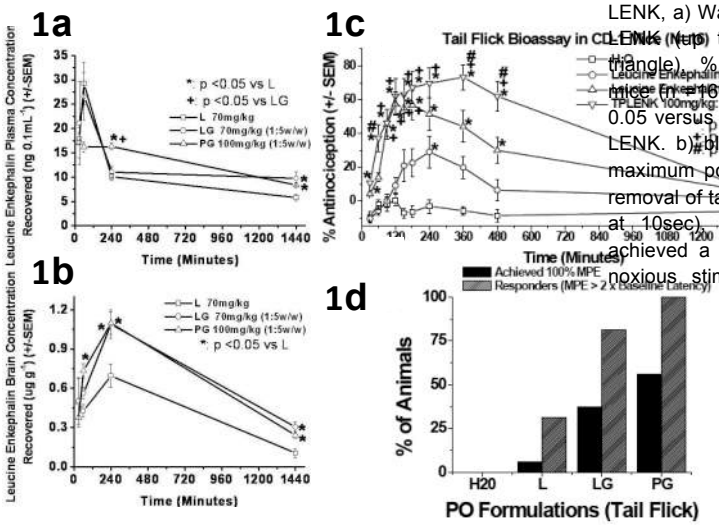

PS-W-39

Engineered PLGA Nanoparticles for Oral Insulin Delivery

Vishal Rathi, Amit K. Jain, Nitin K. Swarnakar, Chandraiah Godugu, Sanyog Jain

Centre for Pharmaceutical Nanotechnology, Department of Pharmaceutics,
National Institute of Pharmaceutical Education and Research
S. A. S Nagar, Punjab (160062) India

Purpose: Oral insulin delivery is still a dream because of its enzymatic degradation in gastrointestinal tract and poor intestinal permeability. Aim of the present study was to investigate the potential of folic acid-poly ethylene glycol-poly(lactic-co-glycolic acid) nanoparticles (FA-PEG-PLGA NPs) as oral insulin delivery system.

Methods: Insulin loaded PLGA, PEG-PLGA and FA-PEG-PLGA NPs were prepared by double emulsion solvent evaporation method and freeze dried. In process stability studies involved chemical stability, confirmed by RP-HPLC and native PAGE, whereas conformational stability was assessed by circular dichroism. Stability of freeze dried formulation was evaluated upon storage at 4ºC and room temperature for three months. Protection of insulin in different nanoparticulate formulations was carried out in simulated gastric fluid (SGF, pH 1.2) and simulated intestinal fluid (SIF, pH 6.8). *In vitro* release studies of nanoparticulate formulations were carried out at different pH. Finally, *in vivo* pharmacodynamic and pharmacokinetic studies were carried out in streptozotocin induced diabetic rat model.

Results: All 3 nanoparticulate formulations of uniform size (below 260 nm) with 7 % of drug loading at encapsulation efficiency of 87.0 ± 3 % were obtained. Negligible impact on different in process stability *viz.* chemical and conformational stability of insulin was observed. Freeze dried formulations were found stable upon storage. Encapsulation into NPs was found to render protection to the drug against SGF and SIF. *In vitro* release studies revealed initial burst release (40.0 ± 2.46 %) in 30 min followed by controlled release (56.0 ± 3.17 %) in 24 h. Upon oral administration, insulin solution (50 IU/kg) was totally inactive while insulin loaded nanoparticulate formulations (50 IU/kg) resulted in significant hypoglycemic response in controlled manner for at least 24 h. Subcutaneous (SC) insulin showed a transient hypoglycemia for 6 h. Amongst of all formulations, FA-PEG-PLGA NPs demonstrated highest oral efficacy with cumulative hypoglycemia approximately 2 times higher than SC insulin.

Conclusion: The results clearly indicate that FA-PEG-PLGA NPs can be designed as a potential carrier for oral delivery of insulin.

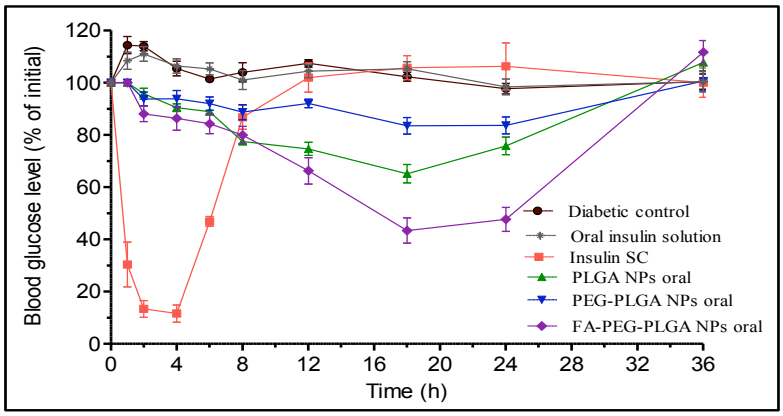

Figure: Plasma glucose level versus time profile of diabetic rats after oral administration of insulin loaded PLGA, PEG-PLGA, FA-PEG-PLGA NPs (50 IU/Kg). Control: untreated diabetic animals, free insulin solution SC (5 IU/Kg and oral (50 IU/Kg). Data represents mean±SEM (n=6)

PS-W-40

Interactions of surface modified magnetic nanoparticles with lung surfactant protein A

Christian A. Ruge[1], Jennifer Herrmann[2], Ulrich F. Schäfer[1] and Claus-Michael Lehr[3]

[1]Department of Biopharmaceutics and Pharmaceutical Technology, Saarland University, D-66123 Saarbrucken, Germany
[2]Department of Pharmaceutical Biotechnology, Saarland University, D-66123 Saarbrucken
[3]Department of Drug Delivery, Helmholtz-Institute for Pharmaceutical Research Saarland (HIPS), D-66123 Saarland University, Saarbrucken, Germany

Purpose: To study the influence of surface properties on the adsorption of the immunologically relevant pulmonary surfactant protein A (SP-A, 26-38 kD) on surface modified magnetic nanoparticles.

Methods: Magnetic nanoparticles (mNPs; Chemicell, Germany) with different pharmaceutical relevant polymer surface modifications (Chitosan [CH], Poly-Maleic-Oleic acid [PMO], Starch [ST], Phosphatidylcholine [PL] or Carboxymethyldextran [CMX]) were incubated for 20 min in a porcine native surfactant preparation (pn-Surf), mNP to protein ratio was 1:2 [w/w]. After incubation, particles were separated magnetically. Three sample fractions were analyzed by SDS-PAGE: *unbound* (non-adsorbed proteins), *bound* (adsorbed proteins) and *particles* (after desorption of bound proteins). Identity of adsorbed SP-A was investigated using Western Blot and MALDI ToF MS. Quantification of adsorbed SP-A was performed after Coomassie-staining by densitometric estimation of SP-A band intensity. Dynamic Light Scattering (DLS) was used for characterization of the tested mNP in terms of hydrodynamic diameter (Z-ave) and surface charge (Zeta-Potential) using a Zetasizer NanoZS (Malvern Instruments, UK).

Results: Particle size measurements by DLS resulted in a Z-ave between 140 (CH) and 190 nm (CMX). Zeta-Potential measurements revealed negative values for ST, CMX, PMO and PL (-2.3±0.2, -17.9±1.4, -21.4±0.2 and -31.6±1.4 mV, respectively), and a slight positive value for CH (13.8±0.4 mV). Identity of the 36 kD protein band in the *bound* fraction on SDS-PAGE gels could be confirmed as adsorbed porcine SP-A by means of Western Blot and MALDI ToF MS. Quantification by densitometric estimation of SP-A

bands revealed high amounts of adsorbed SP-A for mNP modified with PL and PMO (0.602 and 0.568 µg/cm^2, respectively), moderate adsorption for CH-mNPs (0.409 µg/cm^2) and a rather low amounts of adsorbed SP-A for ST- and CMX-mNPs (0.246 and 0.236 µg/cm^2, respectively).

Conclusion: The different binding behavior of SP-A with the tested mNPs implies that the adsorption of SP-A seems to be strongly dependant on surface properties (e.g. Zeta-Potential) of the respective nanoparticles. Possible biological effects of SP-A adsorption e.g. on particle clearance by alveolar macrophages are now under investigation.

PS-W-41

Targeting Transferrin Receptor with PEGylated Nano-Immunoliposomes: A Potential Method for the Local Treatment of IBD via the Luminal Route

Efrat Harel[1], Abraham Rubinstein[1], Aviram Nissan[2] and Boaz Tirosh[1]

The Hebrew University of Jerusalem, Faculty of Medicine; [1]The School of Pharmacy Research Institute for Drug Research, P.O.Box 12065, Jerusalem 91120, Israel; [2]Department of Surgery, Hadassah - Hebrew University Medical Center, Mount Scopus

Purpose: To explore a novel approach for the local, luminal drug treatment of IBD, employing transferrin receptor (TfR) as a target and PEGylated nanosized immunoliposomes as a specific vehicle.

Methods: TfR expression in the colonic mucosa of either IBD patients or DNBS-induced rat model was evaluated by immunofluorescent staining. To assess the effect of induced inflammation on TfR levels on the surface of colon epithelial cells, Caco-2 cell line was analyzed by flow cytometry after incubation with a variety of proinflammatory cytokines. Fluorescently-tagged, nano sized, negatively charged, immunoliposomes were prepared by conjugating negatively charged liposomes with anti-TfR antibody. Their specific binding and cellular uptake was measured in Caco-2 cells, in the presence or absence of proinflammatory cytokines, by fluorescence microscopy. Ex vivo uptake of the immunoliposomes was carried out on everted sacs preparations from DNBS-induced colitis rats.

Results: The colonic mucosa of both IBD patients and DNBS induced rats expressed elevated levels of TfR, in the apical membrane. The major cytokine which promoted TfR expression on the surface of the Caco-2 cells was TNFα. We found that anti-TfR fluorescently-tagged nano-immunoliposomes was accumulated in the Caco-2 cells, better then naked liposomes, in a concentration dependent manner. This trait was also observed in the everted sacs from DNBS-induced colitis rats.

Conclusion: Apical cell surface TfR is upregulated in IBD, This observation could be exploited for targeting drugs to the inflamed gut mucosa via the luminal route. Because nano size, negatively charged, αTfR immunoliposomes were attracted to the inflamed mucosa they could serve as specific carriers to deliver a variety of antiinflammatory agents to the apical inflamed mucosa of IBD patients.

PS-W-42

Design and Testing of Acoustically-Active Microbubble-Nanoparticle Hybrid for Ultrasound-Targeted Chemotherapy

Lei Peng[1], Lee Mullin[2], Saurabh Wadhwa[1], Ping Ma[1], Russell Mumper[1,3], Paul Dayton[1,2]

[1] Division of Molecular Pharmaceutics, Center for Nanotechnology in Drug Delivery, UNC Eshelman School of Pharmacy, University of North Carolina at Chapel Hill
[2] Joint Department of Biomedical Engineering, UNC-Chapel Hill and NCSU, NC, USA

[3] UNC Lineberger Comprehensive Cancer Center, University of North Carolina at Chapel Hill

Purpose: Ultrasound has the ability to spatially concentrate acoustically-active particles in-vivo as well as locally enhance vascular permeability. Our goal was to develop a microbubble-nanoparticle hybrid delivery vehicle which combines the acoustic activity of gas-core microbubbles with the high payload and extravasation ability of nanoparticles for improved spatial specificity in cancer chemotherapy.

Methods: The hybrid vehicle is generated through binding of streptavidin-BTM nanoparticles with biotinylated microbubbles. BTM nanoparticles were prepared using **B**rij 78, D-alpha-tocopheryl polyethylene glycol 1000 succinate (**T**PGS) and **M**iglyol 812. DGS-NTA-Ni was incorporated to bind his-GFP and his-streptavidin. Microbubbles were composed of DSPC, DSPE-PEG2000, and DSPE-PEG2000-Biotin for the shell and perfluorbutane as the gas core. After incubation and wash, hybrid vehicles were visualized under fluorescence microscope. For *in vitro* studies, R3230 cells were exposed to the hybrid delivery vehicle and sonicated with the focused transducer for three minutes. Nanoparticle delivery to the cell monolayer was compared with and without ultrasound using fluorescence microscopy.

Results: When observed under fluorescence microscope, microbubbles (5 micron) with fluorescent "dots" (200 nanometer nanoparticles) on the surface were seen, indicating that nanoparticles successfully bound to microbubbles. For *in vitro* study, a 10-fold increase of nanoparticle fluorescence was observed in the focus of ultrasound transducer compared to that outside the focus, indicating that ultrasound successfully concentrated delivery of these vehicles.

Conclusion: Optical microscopy confirmed successful formulation of hybrid vehicles consisting of 200 nanometer particles conjugated to 5 micron gas-core bubbles. Acoustic experiments demonstrated these vehicles could be concentrated by ultrasound, and nanoparticles could be released at a target site. Future cellular uptake studies will be performed with microbubbles bound to paclitaxel-loaded nanoparticles.

PS-W-43

Targeted Behenoyl-Paclitaxel Conjugate Nanoparticles for the Treatment of Resistant and Metastatic Breast Cancer

Ping Ma[1], S. Rahima Benhabbour[1], Russell J. Mumper[1,2]

[1] Division of Molecular Pharmaceutics, Center for Nanotechnology in Drug Delivery, UNC Eshelman School of Pharmacy, University of North Carolina at Chapel Hill, Chapel Hill, NC 27599, USA
[2] UNC Lineberger Comprehensive Cancer Center, University of North Carolina at Chapel Hill, NC 27599, USA

Purpose: The main objective of the present work was to develop a novel targeted behenoyl-paclitaxel conjugate nanoparticle (NP) formulation for the treatment of resistant and metastatic breast cancer.

Methods: To increase the lipophilicity of paclitaxel and facilitate its retention within the core of our lipid-based nanoparticles (NPs), behenoyl-paclitaxel conjugate was synthesized using behenoyl chloride and paclitaxel via a one-step esterification reaction. The synthesized behenoyl-paclitaxel conjugate was characterized by TLC, NMR, and HPLC analyses. The behenoyl-paclitaxel conjugate NP formulations were engineered from warm microemulsion precursors which consisted of Miglyol 812 as the oil phase, and Brij 78 and Vitamin TPGS as the surfactants. To selectively target breast cancer cells, Brij 700-NTA-Ni conjugate was synthesized and incorporated into the NPs using either the pre- or post-insertion methods to optimize the incorporation of Nickel (Ni) into the NPs. This strategy allows us to target the Ni-NPs by binding his-tagged breast cancer targeting ligands such as EGFR binding ligand and SFRP2 antibody.

Results: Characterization of the behenoyl-paclitaxel conjugate by TLC showed that the R_f of paclitaxel and behenoyl-paclitaxel were 0.34 and 0.74, respectively. ^{1}H and ^{13}C NMR analysis confirmed that behenoyl carbon chain (C22) was successfully coupled to paclitaxel at the C-2' hydroxyl position. The behenoyl-paclitaxel conjugate NPs were successfully prepared with a mono-size distribution of about 200 nm. The entrapment efficiency of behenoyl-paclitaxel conjugate within the NPs showed a significant increase compared to the incorporation of paclitaxel using Sepharose CL-4B GPC column. Brij 700-NTA-Ni conjugate was characterized by ^{1}H and ^{13}C NMR and the mole% of Ni was estimated by ICP-MS analysis. Results showed that about 50% of Ni could be incorporated into the NPs via either pre- or post-insertion of Brij 700-NTA-Ni conjugate.

Conclusion: The Ni-loaded behenoyl-paclitaxel NPs can be used to bind various his-tagged tumor targeting ligands, which may provide a potential platform to improve the survival for the treatment of resistant and metastatic breast cancer.

Acknowledgment: This research was supported by NIH-NCI R01 CA115197.

PS-W-44

Lymphatic Delivery of Cisplatin for the Treatment of Metastatic Head and Neck Squamous Cell Cancer

S. Cai[1], Y. Xie[1], S. Thati[1], T. R. Bagby[1], M. S. Cohen[2], M. L. Forrest[1]

[1] Department of Pharmaceutical Chemistry, School of Pharmacy, University of Kansas, Lawrence, KS
[2] Department of Surgery, University of Kansas Medical Center, Kansas City, KS

Purpose: To develop an intralymphatically-targeted chemotherapy treating metastatic head and neck squamous cell cancer, which may significantly reduce side effects and increase the effectivity of cisplatin based chemotherapy.

Methods: Cisplatin was conjugated to hyaluronan (HA), which is a highly biocompatible and nonimmunogenic polymer. Cell viability of cisplatin was evaluated in human HNSCC cell line, MDA-1986. In vitro release of cisplatin from the polymer was examined using atomic absorption spectrometry (AAS). Sprague-Dawley rats were employed for pharmacokinetics and biodistribution studies. In addition, a lymphatic metastasis model was established for head and neck cancer by orthotopic implantation of MDA-1986 in nude mice. Three doses of subcutaneous Hyaluronan-cisplatin (HA-Pt) or intravenous cisplatin (CDDP) were administered three weeks after tumor cell inoculation.

Results: Cisplatin was conjugated to HA with a conjugation degree of 20-30 w/w%. HA-Pt conjugates demonstrate antiproliferative efficacy similar to standard cisplatin formulations in HNSCC cells in vitro (CDDP IC_{50}=2 μg/mL; HA-Pt IC_{50}=2 μg/mL). HA-Pt conjugates demonstrated sustained release of cisplatin ($t_{1/2}$ =10 hours at pH 7.4) from the HA carriers. The area-under-the-curve of CDDP in the axially lymph nodes after injection with HA-Pt increased 74% compared to normal CDDP. The intralymphatic delivery model also exhibits sustained release kinetics, allowing higher plasma AUC and lower C_{max} levels, which could translate into lower organ toxicities. Pathology studies demonstrated that animals with HA-Pt treatment showed milder degenerative changes in livers and less congestion and necrosis in kidneys. Head and neck cancers (1/wk × 3 wks) were completely cured for 60% of the animals. Partial response was observed for the remaining animals.

Conclusions: This study demonstrates that intralymphatic delivery of platinum chemotherapeutics may greatly increase the local concentration in drain lymph node basin, compared to conventional intravenous cisplatin. Subcutaneous delivery of the hyaluronan-cisplatin conjugates may be a promising treatment regimen to deliver chemotherapeutics to the primary malignancy, locoregional lymphatics and

metastases, with greatly improved *in vivo* efficacy and survival compared with conventional cisplatin chemotherapy.

PS-W-45

Therapeutic efficacy of Doxorubicin-loaded PLGA nanoparticles against rat glioblastoma 101/8

Stefanie Wohlfart[1], Christian Bernreuther[2], Alexander S. Khalansky[3], Svetlana Gelperina[4], Olga Maksimenko[3], Markus Glatzel[2], Jörg Kreuter[1]

[1]Institute of Pharmaceutical Technology, Goethe University, Frankfurt, Germany
[2]Institute of Neuropathology, University Medical Centre Hamburg-Eppendorf, Hamburg, Germany
[3]Institute of Human Morphology, Moscow, Russia
[4]Nanosystem Ltd., Moscow, Russia

Purpose: Our earlier study showed that poly (lactic-co-glycolic acid) (PLGA) nanoparticles coated with poloxamer 188 (Pluronic® F68) hold great promise as drug-carriers for brain delivery. The purpose of the present work was to investigate the anti-tumour efficacy of the surfactant-coated doxorubicin-loaded PLGA nanoparticles (Dox-PLGA) against rat glioblastoma using histological and immunochemical methods.

Methods: Dox-PLGA particles were prepared by a high-pressure solvent evaporation technique using 1% PVA (Dox-PLGA/PVA) or 1% HSA (Dox-PLGA/HSA) as stabilizers. Additionally, Dox-PLGA/HSA containing lecithin were prepared (Dox-Lecithin-PLGA/HSA). The resulting particles were freeze-dried in presence of 5% mannitol and characterized for size and drug loading.

For animal experiments, male Wistar rats, bearing intracranially implanted 101/8 glioblastoma, were randomly divided into 4 groups (n=6) and treated with Dox formulations (3 x 2.5mg/kg) coated with 1% poloxamer 188 on days 2, 5 and 8 after tumour inoculation. The following formulations were tested: Dox solution as control, Dox-PLGA/PVA, Dox-PLGA/HSA or Dox-Lecithin-PLGA/HSA, respectively. On day 18 after tumour implantation, the rats were sacrificed. Subsequently, the brains were removed and processed for histological and immunohistochemical evaluation.

The efficacy of the chemotherapy was determined by measurement of tumour size and extent of necrotic areas in brain sections stained with haematoxylin-eosin. Staining with antibodies against Ki67 was performed for proliferation analysis. To determine the neovascularization index, staining with Isolectin B4 was performed. In addition, GFAP and VEGF expression was investigated.

Results: Histological evaluation of all groups revealed an advantage of the nanoparticulate formulations in comparison with the Dox solution. Especially a decrease in tumour size and a reduction of a number of proliferating cells were detectable. In addition, the treatment with nanoparticles led to lower necrosis and vessel density as well as to a diminished expression of GFAP. The overall best results were observed for the group of animals treated with Dox-Lecithin-PLGA/HSA. It is possible that, being a plasticizing agent for PLGA, lecithin increases the release rate of doxorubicin thus enhancing the antitumour effect of this formulation.

Conclusion: These results demonstrate that poloxamer 188-coated PLGA nanoparticles are useful carriers for brain delivery. Doxorubicin formulations based on these particles represent a very promising preparation for intravenous therapy of glioblastomas.

PS-W-46

Magnetic Hyperthermia for Lung Cancer

T. Sadhukha[1], T. S. Wiedmann[1], J. Panyam[1]

[1]Department of Pharmaceutics, University of Minnesota, Twin Cities, MN

Purpose: To determine the tumor cell kill effectiveness of magnetic hyperthermia induced using superparamagnetic iron oxide (SPIO) nanoparticles.

Methods: SPIO nanoparticles were synthesized by alkaline precipitation of ferrous and ferric chlorides. Successive coatings of myristic acid and pluronic F127 were applied to prevent oxidation and to facilitate aqueous dispersibility, respectively. Nanoparticle size was determined by transmission electron microscopy. Magnetic heating was performed using an induction heating system; suspension of SPIO nanoparticles was placed at the center of a multiturn copper coil that generated alternating magnetic field (field strength of 6 kA/m and frequency of 386 kHz). Effect of nanoparticle concentration on heating rate was determined by dispersing different amounts of SPIO nanoparticles in liquid medium (F12K cell culture medium) and gel (2.5% agarose gel). To determine the tumor cell kill effectiveness of magnetic hyperthermia, A549 cells (non-small cell lung cancer cells) were treated with 2.5 mg/ml SPIO nanoparticles and exposed to an alternating magnetic field for different durations of time after the temperature reached 43°C. Percent cell death was determined based on the amount of lactate dehydrogenase released by the dead cells in the medium.

Results: SPIO nanoparticles were found to have an average size of 12 ± 3 nm. The heating rate was strongly dependent on SPIO concentration and was similar in both liquid and solid medium. The minimum concentration of SPIO nanoparticles needed to induce hyperthermic cell death was determined to be 2.5 mg/ml. Increased cell death was observed with increasing duration of exposure of the cells to the alternating magnetic field. Additionally, incubation of cells with SPIO nanoparticles in the absence of external magnetic field did not have a significant effect on cell viability compared to untreated cells indicating lack of toxicity of the SPIO nanoparticles.

Conclusion: SPIO nanoparticles developed can heat liquid as well as solid medium and the heating rate depends on the concentration of the SPIO nanoparticles. Magnetic hyperthermia induced by SPIO nanoparticles is effective in killing lung cancer cells.

PS-W-47

Characterization and bio-compatibility of iron oxide nanoparticles synthesized using a novel one step, low temperature hydrolysis/reduction method

V. Yathindranath[1], T. Hegmann[1], J. van Lierop[2], D. W. Miller[3]

[1] Department of Chemistry, University of Manitoba, Winnipeg (MB)
[2] Departmentof Physics & Astronomy, University of Manitoba, Winnipeg (MB)
[3] Department of Pharmacology and Therapeutics, University of Manitoba

Purpose: Iron oxide nanoparticles (IONPs) have a number of emerging applications in clinical medicine. The aim of this work is to assess the cytotoxicity of IONPs synthesized by hydrolysis/reduction method and to understand the effects of surface coating and applied magnetic fields on cell permeability *in vitro*.

Methods: The IONPs were synthesized from iron(III)acetyl acetonate following a new hydrolysis/reduction method, at room temperature. Using this method, we have made naked, poly(ethylene glycol) and oleic acid coated IONPs. Physicochemical characterization of the resulting

IONPs were performed using powder x-ray diffraction, transmission electron microscopy (TEM), Fourier transform infrared spectroscopy and Mössbauer spectroscopy. To determine bio-compatibility of the IONPs, cell viability assays were performed in Caco2 and HepG2 cell lines using MTT cytotoxicity assay. Cells cultured in Dulbecco's Modified Eagle's Medium (DMEM) were treated with various concentrations (0.01, 0.032, 0.1, 0.32 and 1 mg/ml) of IONPs. After 24 hour exposure to the IONPs, cells were washed once, replenished with 200 µL of fresh media, and incubated for an additional 48 h. Cell viability was determined colormetrically using MTT reagent. Permeability of hydrophobic oleic acid coated IONPs were carried out on confluent monolayers of human brain micro endothelial cells (HBMEC) and Caco2 grown on Transwell membrane inserts. For these studies, IONPs (333 ug/mL) dispersed in 1.5 mL of Dulbecco's Modified Eagle's Medium (DMEM) containing 10 µM fluoresceine labeled dextran (MW 3000) were added to the donor compartment of the Transwell insert. The cell inserts were then incubated for 24 hours in a 5 % CO_2 incubator. Rare earth magnets were placed below some of the inserts to study the effect of an applied magnetic field on the permeability. After 24 hours, the amount of IONPs in the receiver compartment was determined by adding 1 mL of Pearl's reagent and absorbance was measured at a wavelength of λ = 500 nm using a plate reader (Synergy HT, Biotek).

Results: The average particle size determined using TEM for the IONPs synthesized at room temperature were around 5 nm. Based on the performed MTT assays, the uncoated IONPs synthesized by the new hydrolysis/reduction method showed little toxicity (less than 10% loss in cell viability over 48 hours). In the permeability studies, IONPs were found in all cases in the receiver compartment after 24 hours as determined by the Prussian blue absorbance with respect to the control (which didn't receive any IONPs). Oleic acid coated IONPs exhibited poor dispersibility in DMEM, but still permeated the cell membrane in all cases. Applied magnetic field clearly produced an enhancement in the permeability of hydrophobic IONPs over 24 hours. According to our initial results, HBMEC showed higher permeability as compared to Caco2 monolayers and magnetic field produced greater permeability with HBMEC.

Conclusions: A simple, one-step reduction reaction was used to create IONPs of various compositions. The resulting IONPs were bio-compatible, producing little toxicity in cell culture models. Although modest, passage of IONPs was observed across both intestinal epithelial and brain endothelial monolayers. Alterations in surface coating and the application of magnetic fields may be used to enhance IONP permeability.

PS-W-48

LC-UV Determination of Clozapine in Orally Disintegrating Tablets

SS. Olmez[1], F. Yerlikaya[1], I. Vural[1], S. Sahin[1], A. Ertugrul[2], Y. Capan[1]

[1] Department of Pharmaceutical Technology, Faculty of Pharmacy, Hacettepe University, Ankara, Turkey
[2] Department of Psychiatry, Faculty of Medicine, Hacettepe University, Ankara, Turkey

Purpose: Although there are compendial methods for determination of clozapine by HPLC in current versions of United States Pharmacopeia (USP) and European Pharmacopoeia (EP) these methods have some disadvantages. A C_8 column is used in USP, which is not a very commonly used HPLC column. In EP, a relatively complex mobile phase is used although C_{18} is preferred as HPLC column. The purpose of this study is to develop and validate a HPLC method for quantitative determination of clozapine in orally disintegrating tablets by HPLC using the mobile phase of USP and a C_{18} column.

Methods: An Agilent 1200 Series HPLC System (Agilent, USA) equipped with a Develosil ODS-UG-5, 250x4.6 mm (Nomura Chemical, Japan) column was used. The mobile phase was consisted of methanol:water:triethylamine (80:20:0.75) as indicated in USP. The flow rate of the mobile phase was 1 ml/min with isocratic elution. The injection volume was 20 µl, the UV detector wavelength was set at 257 nm, and column thermostat temperature was maintained at 25 °C. Specificity, linearity, range, accuracy, precision, detection and quantitation limits of the method have been evaluated for validation. Standard solutions of clozapine were prepared by dissolving clozapine in methanol. Clozapine orally disintegrating tablets including superdisintegrants (Crospovidone B or Acdisol or Explotab), Avicel PH102, Sugartab, Pearlitol SD200, Pruv® and aspartame as excipients were prepared by direct compression method. Before analysis, tablets were grinded; powders were dissolved in methanol, and filtered through 0.20 µm filters prior to injection.

Results: The method was linear (R^2 = 0.9999) over the concentration range of 1.00–40.00 µg/ml. The *RSD*% of intra- and inter-day precision studies was less than 2% while the recovery% values were between 100 and 102%. The detection and quantitation limits were 5 and 13 ng/ml, respectively. The method was found to be specific, accurate, precise and sensitive for the determination of clozapine in orally disintegrating tablets.

Conclusion: Since the existing methodology described in major Pharmacopeias for the quantitative determination of clozapine in tablets is relatively complex for routine analysis, this method may be useful for quality control laboratories of pharmaceutical industry.

PS-W-49

Development of Microfluidic Based Devices to Evaluate the Integrity of Protein Based Pharmaceuticals in Developing Countries

Jessica S. Creamer, Dr. Susan M. Lunte

Department of Pharmaceutical Chemistry, School of Pharmacy, University of Kansas, Lawrence, KS

Purpose: The overall goal of this project is to determine the stability and integrity of biopharmaceuticals in locations where traditional quality control testing is unavailable. Lab-on-a-chip devices are a promising technology for resource-poor settings because they have the potential to be cheap, portable, and easy to use. Deamidation represents a significant degradation pathway for many protein based drugs and is a particularly useful indicator of thermal degradation. Since deamidation alters the charge of the resulting peptide, the degradation process can be studied by electrophoretic methods. The model pharmaceutical chosen for this project is insulin.

Figure 1: Electropherogram of a CE separation and LIF detection of the major peaks from a 10μM tryptic digest of bovine insulin. The length of the capillary was 50cm and the separation voltage was 25kV. The background electrolyte was 25mM sodium phosphate.

Methods: Conventional capillary electrophoresis (CE) with laser induced fluorescence detection (LIF) is being used to develop an assay for insulin and its degradation products. Insulin is digested with trypsin and the resulting fragments are derivatized with a fluorescent derivatization reagent prior to analysis. The results from the capillary electrophoresis studies will be used to develop a microchip based devices for monitoring insulin integrity. Several different microchip substrates will be evaluated for the separation of tryptic digests of insulin and its degradation products using fluorescence detection. These include glass, polydimethylsiloxane (PDMS), polyester toner (PT) and paper-based materials.

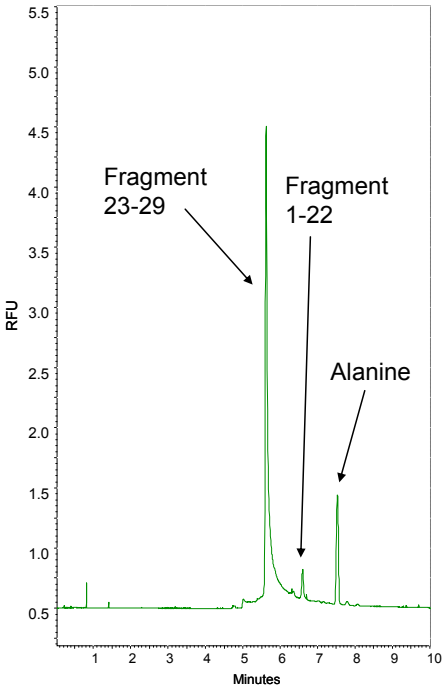

Results: Optimization of both the separation conditions and the derivatization chemistry has been achieved. Several derivatization reagents were evaluated but it was found that naphthalene-2,3-dicarboxaldelyde gave the best response. The major peaks associated with a tryptic digest of native B-chain bovine insulin have been separated and identified based on their derivatization reaction rate, charge to size ratios, and relative migration time (Figure 1). Some preliminary results on PDMS chips have been obtained.

Conclusions: Work from this project will further the understanding of electrophoretic separations of proteins and peptides with several different microfluidic substrates. This is advantageous because the use of these substrates will aid in the development of an inexpensive portable-system that can be used for on-site analysis of pharmaceutical in developing countries.

PS-W-50

Characterization of Interactions between Antimicrobial Preservatives and Proteins

Regina L. Hutchings, Surinder M. Singh, Krishna M.G. Mallela

Department of Pharmaceutical Sciences, University of Colorado Denver School of Pharmacy, 12700 E 19th Ave, C238-P15, Aurora, CO 80045.
(Email: Regina.Hutchings@ucdenver.edu)

Purpose: Proteins are dynamic structures that continuously unfold and refold even in their thermodynamically stable native states. Proteins exhibit a wide variation in their thermodynamic stabilities as a function of the addition of small molecules such as antimicrobial preservatives (APs). APs have been particularly shown to interact with pharmaceutical proteins and cause unfolding as well as aggregation. The purpose of this investigation is to characterize the interactions between pharmaceutically relevant APs and proteins using a model protein, cytochrome *c* (cyt c).

Methods: Using temperature denaturation studies, the stability of cyt c in the presence of different APs at varying AP concentration was assessed. The apparent temperature of aggregation in each case was deduced by monitoring changes in absorbance. FT-IR and fluorescence was utilized to determine structural changes in cyt c as a function of antimicrobial agent and its concentration.

Results: With increasing concentration of preservative, the apparent aggregation temperature of cyt c decreased linearly with the slope dependent on the nature of the preservative. However, the antimicrobial agents did not significantly perturb the secondary and tertiary structure of cyt c, but instead caused unfolding of a local protein region.

Conclusions: The preservatives used in this study interacted with the protein to the extent of decreasing the apparent aggregation temperature without causing shifts in global secondary and tertiary structures. In future work, we plan to identify the molecular nature of these interactions between APs and proteins.

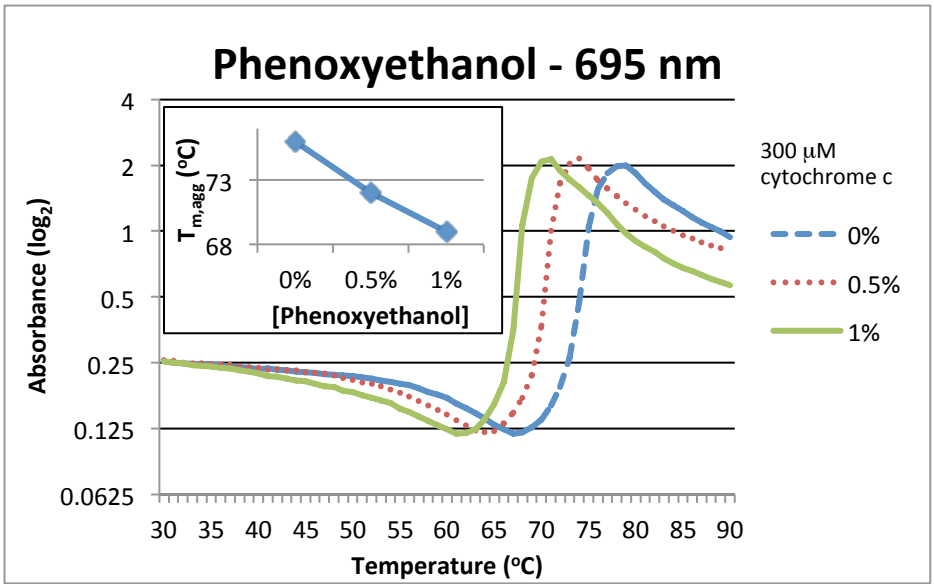

PS-W-51

Interactions between steroidal compounds on transporters in caco-2 cells
A. Grandvuinet, H. Al-amood, B. Steffansen

Faculty of Pharmaceutical Sciences, University of Copenhagen

Purpose: To investigate possible interactions between the endogenic steroidal compounds taurocholate (TCA), estrone-3-sulphate (E_1S) and taurolithocholate (TLC) on membrane transporters in caco-2 cells, a cell model for the intestinal wall.

Methods: Caco-2 cells were grown to 80% confluence and seeded on filter supports at a density of $9*10^4$ cells/cm^2 24-29 days prior to all experiments with media being replaced every other day. Initial linear uptake permeabilites for [^{3}H]-TCA (4,6 Ci/mmol; 100 nM) or [^{3}H]-E_1S (54,26 Ci/ mmol; 9 nM) across Caco-2 cells were studied in the presence of increasing concentrations of TLC (0- 1000 µM). Uptake permeability was studied at both the apical and basolateral membrane. Intracellular accumulation of [^{3}H]-TCA or [^{3}H]-E_1S was determined by liquid scintillation counting.

Results: [^{3}H]-TCA showed highest uptake at the apical membrane whereas [^{3}H]-E_1S uptake was highest at the basolateral membrane. TLC showed strong concentration-dependent inhibitory properties on apical uptake of [^{3}H]-TCA but did not have any effect on basolateral uptake of [^{3}H]-TCA in the employed concentration range of TLC. In the contrary, TLC did not inhibit apical uptake of [^{3}H]-E_1S whereas basolateral uptake of [^{3}H]-E_1S was inhibited by TLC in a concentration-dependent manner.

Conclusion: The differences in TLC inhibition of [^{3}H]-TCA and [^{3}H]-E_1S in these experiments indicate that these two steroids may be transported by different transporters in both the apical and basolateral membrane. Alternatively, TCA and E_1S have different affinities for the same transporters in both the apical and basolateral membrane, i.e. TCA has respectively higher and lower affinities than E_1S to apical and basolateral transporters. More studies are required to investigate if different transporters dominate in the intestinal transport of TCA and E_1S.

PS-W-52

Apically Localized Mouse Intestinal Cation-selective Transporters Play a Role in the Oral Absorption and Pharmacology of Metformin
C.L. Costales, W.R. Proctor, M.B. Dufek, and D.R. Thakker

UNC Eshelman School of Pharmacy, University of North Carolina, Chapel Hill, NC

Purpose: The purpose of the present study was to evaluate if cation-selective transporters (e.g., organic cation transporter 1 (OCT1), plasma membrane monoamine transporter (PMAT)) play a role in both the oral absorption and pharmacology of metformin in mouse.

Methods: Mouse jejunal tissue segments were placed in an Ussing-type diffusion chamber to evaluate the apical uptake of [^{14}C]metformin in the presence/absence of a pan inhibitor of cation-selective transporters, quinidine. Apical and basolateral efflux of [^{14}C]metformin from pre-loaded intestinal tissue were measured in the presence/absence of quinidine by determining metformin concentration as a function of time in each chamber of the diffusion apparatus. An *in vivo* diabetic db/db mouse model was then implemented to measure intestinal absorption of metformin in the presence/absence of quinidine. This was achieved by administration of [^{14}C]metformin by oral gavage and sampling the drug in the portal circulation over four hours via a surgically implanted portal vein catheter. Finally, because the portal concentration can serve as a surrogate measure for hepatic exposure (the primary site of metformin

action), pharmacologic effect of metformin, i.e., lowering of systemic blood glucose levels, in db/db mouse was related to the exposure of the drug in the portal circulation upon its oral absorption in the presence/absence of quinidine.

Results: The results showed that apically localized cation-selective transporters do play a role in metformin accumulation in mouse intestine as evidenced by a significant reduction in apical uptake when treated with quinidine in the Ussing chamber experiments. Additionally, the mouse intestinal tissue exhibited high apical compared to basolateral efflux. The apical efflux, but not the basolateral efflux, was decreased significantly by quinidine. Further, quinidine caused a significant decrease in metformin intestinal absorption as evidenced by lower portal $AUC_{0 \text{ to } 4 \text{ hr}}$ when the animals were treated with the pan inhibitor of cation-selective transporters. Lastly, quinidine attenuated metformin-mediated lowering of the systemic blood glucose levels.

Conclusion: These data suggest that cation-selective transporters, localized in the apical membrane of the intestinal epithelium, play a role in the oral absorption and subsequent pharmacologic effects of metformin in db/db mice.

PS-W-53

A Modified Grapefruit Juice Eliminates Furanocoumarins and Polymethoxyflavones as Candidate Mediators of the Fexofenadine-Grapefruit Juice Interaction in Healthy Volunteers

C. S. Won[1], Y. V. Scarlett[1], W. W. Widmer[2], M. F. Paine[1]

[1]University of North Carolina at Chapel Hill
[2]US Department of Agriculture/Agricultural Research Service

Purpose: Grapefruit juice (GFJ) reduces the systemic exposure of the antihistamine fexofenadine. Due to potential attenuation in efficacy, the labeling of fexofenadine contains statements cautioning concomitant intake with GFJ. The mechanism underlying this interaction has been postulated to involve inhibition by GFJ of fexofenadine active uptake in the intestine
mediated by organic anion transporting polypeptides (OATPs). Flavonoids, furanocoumarins, and polymethoxyflavones have been identified as enteric OATP inhibitors *in vitro*. Only the flavonoid naringin has been shown to contribute to the interaction *in vivo*. Accordingly, the effects of a GFJ removed of furanocoumarins (>98%) and polymethoxyflavones (>97%)
were compared to those of the original GFJ on the pharmacokinetics of fexofenadine.

Methods: Healthy volunteers (n=18) were randomized to receive fexofenadine (120 mg) with 240 mL of water, GFJ, or modified GFJ. Blood (7 mL) was collected over 72 hours. Plasma was analyzed for fexofenadine by LC/MS/MS. Each phase was separated by ≥2 weeks. Fexofenadine pharmacokinetics were evaluated by noncompartmental methods.

Results: The geometric mean concentration-time profiles of fexofenadine following administration of GFJ and modified GFJ were nearly superimposable. Relative to water, both juices significantly decreased the geometric mean (range) AUC, from 4.2 (1.7-8.4) to ~3.2 (1.9-6.0) μM*h, and Cmax, from 0.6 (0.2-1.2) to ~0.4 (0.2-1.1) μM ($p<0.01$). Both juices increased Cl/F, from 52 (27-129) to ~70 (36-120) L/h ($p<0.01$). Neither juice altered the geometric mean λz and median tmax ($p\geq0.09$).

Conclusion: The 25% decrease in fexofenadine systemic exposure with no change in terminal t½ by GFJ and modified GFJ is consistent with inhibition of uptake in the intestine. The similar effects between juices on fexofenadine pharmacokinetics eliminate furanocoumarins and polymethoxyflavones as mediators of the fexofenadine-GFJ interaction. Retainment of flavonoids in modified GFJ supports flavonoids as candidate enteric OATP inhibitors. Further elucidation of specific causative ingredients is

warranted to evaluate potential interaction liability of GFJ with other substrates of enteric OATPs, including some fluoroquinolones, beta-blockers, and antidiabetic agents. *Supported in part by NIH (UL1RR025747).*

PS-W-54

Enzymatic hydrolysis of hydroethanolic extract of *Ilex paraguariensis*: bioavailability, skin distribution and antioxidant activity evaluation

D. P. Rivelli, R. L. Almeida, C. D. Ropke, S. B. M. Barros

Department of Clinical and Toxicological Analyses, School of Pharmaceutical Sciences, University of São Paulo, Brasil.

Purpose: Evaluate if enzymatic hydrolysis of hydroethanolic extract of *Ilex paraguariensis* improves its *in vivo* and *in vitro* antioxidant activity, the bioavailability of caffeic acid and the skin distribution.

Methods: Extract hydrolysis was achieved by incubation with clorogenate esterase (Kikkoman, Noda, Japan). ORAC and DPPH methods were used to evaluate the antioxidant activity (AA). Chlorogenic and caffeic acid and caffeine, were quantified by HPLC methods. For *in vivo* assays, animals received by gavage 200 mg caffeic acid equivalents/kg of hydrolyzed (HE) and non-hydrolyzed (NHE) hydroalcoholic extract of *Ilex paraguariensis* (single-SD or multiple doses-MD for 30 days). Plasma and skin concentration of chlorogenic acid, caffeic acid and caffeine, as well as, plasma AA (by ORAC method) were measured.

Results: Concentration of chlorogenic acid was 7,93% in NHE yielding 18,02% of caffeic acid after hydrolysis. Caffeine levels were 1,48% in both extracts. The results of *in vitro* AA were 4221 ± 319 μmol eq.Trolox/g (TE) (NHE) and 4287 ± 456 TE (HE) by ORAC method and 1492 ± 83 TE (NHE) and 2161± 133 TE (HE) by DPPH method. Total phenolic compounds values were 1157 ± 69 μmol eq. caffeic acid/g (NHE) and 1120 ± 64 μmol eq. caffeic acid/g (HE). The *in vivo* assay showed the presence of caffeic acid in plasma of both HE treated experimental groups and a 70% increase of plasma AA for SD-HE. No caffeic acid was detected in plasma and no change in AA was detected in plasma of other groups. Skin AA was not altered after SD and MD administration of HE and NHE. Caffeic acid nor caffeine could be detected in the skin. Plasma concentration of caffeine was in the same range in all treated groups.

Conclusions: These results demonstrate that the extract of *Ilex paraguariensis* has good *in vitro* AA and phenolic content. Enzymatic hydrolysis of the extract can improve the bioavailability of caffeic acid and in consequence plasma AA.

PS-W-55

Safety and Pharmacokinetics (PK) of Multiple-Dose Anidulafungin in Neonates

[1]M Cohen-Wolkowiez, [1]DK Benjamin Jr., [1]L Piper, [1]C Moran, [2]P Liu, [2]J Aram, [3]A Kashuba, [4]E Capparelli, [5]TJ Walsh, [6]WW Hope, [1]PB Smith

[1]Duke University, Durham, NC; [2]Pfizer Inc., New London, CT; [3]University of North Carolina, Chapel Hill, NC; [4]UCSD San Diego, San Diego, CA; [5]NCI, Bethesda, MD; [6]Univ of Manchester, Manchester UK.

Purpose Disseminated candidiasis and hematogenous *Candida* meningoencephalitis (HCME) cause substantial morbidity and mortality in neonates. Anidulafungin, an echinocandin antifungal agent, is attractive for neonates given its favorable safety and metabolic profile. Experimental models of HCME suggest that high weight-based echinocandin dosages are required for successful therapy. However, the

PK of anidulafungin in neonates is uncharacterized. This open-label study determined the PK of multidose intravenous anidulafungin in neonates <30 days of age.

Methods Subjects received a 3 mg/kg loading dose followed by 1.5 mg/kg every 24 hours for up to 5 days. A total of 3-5 plasma samples were obtained from each subject around doses 3-5. Concentrations were analyzed by validated LC/MS/MS methods with an LLQ=50 ng/mL. PK parameters were estimated using NCA analysis in WinNonLin v5.

Results 8 subjects with a median birth weight of 1.1 kg (0.7-3.7) were enrolled with 3-5 samples collected per subject; 37 samples total.

Subject	AUCss (h*µg/mL)	C24 (h*µg/mL)	Gestational Age (wks)	Postnatal Days
1	56.2	1.3	39	2
2	55.5	1.3	26	9
3	78.3	2.6	26	9
4	71.8	2.9	27	10
5	85.6	2.6	27	12
6	116.6	3.8	27	17
7	30.5	0.8	36	24
8	89.2	2.6	38	28
Median	75.1	2.6	27	11
Range	30.5-116.6	0.8-3.8	26-39	2-28

AUCss: area under the curve at steady state; C24: trough predicted concentration.

No drug related adverse events were seen during therapy; 1 death occurred upon discontinuation of extracorporeal membrane oxygenation per standard of care.

Conclusions Anidulafungin was well tolerated in these neonates. The total exposure (AUC_{ss}) at this dosage was ~25% lower than that observed in older children given the same weight-based dosage and adults receiving 100 mg/day. Optimal dosing for *Candida* meningoencephalitis in neonates remains to be determined.

PS-W-56

Three-dimensional primary organoid culture model is more predictive than 2D secondary cell lines for drug nephrotoxicity assessment

Anna Astashkina[1], Brenda Mann[2], Glenn Prestwich[3] , David Grainger [1,2]

[1] Pharmaceutics and Pharmaceutical Chemistry, University of Utah
[2] Bioengineering, University of Utah
[3] Medicinal Chemistry, University of Utah

Purpose: To validate a novel *in vitro* drug nephrotoxicity assay to improve rapid and clinically relevant drug toxicity data acquisition. The technology exploits encapsulation of freshly isolated kidney proximal tubules (PTs) in a commercial hyaluronic acid (HA)-derived hydrogel that is a semi-synthetic substitute for extracellular matrix (ECM). The PT is a hollow tubular portion of the kidney's filtration system and primary site of drug-induced nephrotoxicity in humans. Encapsulated culture of whole PTs avoids unpredictable cell-polymer interactions, while preserving native three-dimensional (3D) cellular environments and cell-cell physiological communications that better ensure culture longevity and *in vivo*-like responses to drug testing. The toxicity data obtained from the primary 3D organoid culture is compared to traditional two-dimensional (2D) secondary cell line methods.

Methods: Murine PTs were isolated from surgically harvested from C56/BL mice kidneys using enzymatic digestion and mechanical size-based sieving. Tubules were resuspended in commercial (Sentrx) thiol-modified carboxymethylated HA (CMHA-S) and cross-linked using poly(ethylene glycol) diacrylate (PEGDA) bifunctional electrophile (4:1 CMHA-S:PEGDA) into 3-D constructs. Secondary kidney cell lines, HEK293 and LLCK1, were maintained in 10% FBS-DMEM cell media. Tubule and secondary cell line responses to drug toxicity of known chemotherapeutic drugs, cisplatin, doxorubicin, colchicine, and nephrotoxic metabolite 4-aminophenol (PAP) were assessed using IC_{50} assays, shedding of intracellular and brush border enzymes, N-acetyl-ß-D-glucosaminidase (NAG) and γ-glutamyl-transferase into culture media, and expression of nephrotoxic genes heme oxygenase I (H.O), KIM-1, clusterin (Clu), and vimentin (VIM).

Results: Toxicity data reflects a 2-100 fold difference in cell IC_{50} values between the secondary cell lines and primary 3D organoid PT cultures. We also observed statistically significant shedding of the intracellular enzyme NAG upon exposure to nephrotoxic drugs in 3D culture but not in 2D culture. These enzyme and viability data were further corroborated using reverse polymerase chain reaction (RT-PCR) evaluation for marker genes representing kidney toxictiy. Our results indicate that mRNA message upregulation upon IC_{50} drug exposure in 3D PT cells and lack of analogous upregulation in secondary cell cultures.

Conclusions: An organoid 3D primary cell culture of PTs is more sensitive to drug exposure than the traditional 2D culture of secondary cells. The method is suitable for high-throughput drug nephrotoxicity testing applications and will be applied to elucidate mechanisms of drug nephrotoxicity.

Acknowledgements: The project was funded by the Technology Commercialization Office Microgrant and SEED grant, University of Utah

PS-W-57

Role of the copper transporter, CTR1, in platinum-induced ototoxicity

Swati S. More[1], Omar Akil[2], Alexandra G. Ianculescu[1], Ethan G. Geier[1], Lawrence R. Lustig[2], Kathleen M. Giacomini[1]

Safety

[1]Department of Bioengineering and Therapeutic Sciences and [2]Department of Otolaryngology–Head and Neck Surgery, University of California, San Francisco, San Francisco, California 94143-0449.

Purpose: Cisplatin is among the most widely used anti-cancer drugs. Although highly effective, cisplatin treatment is also associated with severe dose limiting ototoxicity. In particular, about 30% of individuals on cisplatin experience some degree of irreversible hearing loss. The goal of this study was to test the hypothesis that the copper influx transporter, CTR1, plays a key role in cisplatin-induced ototoxicity.

Methods: RT-PCR, quantitative RT-PCR, western blot and immunohistochemistry were used to determine the cellular localization of mouse CTR1 (Ctr1) in the mouse cochlea. *In vitro* studies used the mouse organ of corti cell line, HEI-OC1, and human embryonic kidney cells transfected with CTR1 (HEK-CTR1) to measure cisplatin cytotoxicity, cellular platinum accumulation, and platinum-DNA adduct formation in the presence and absence of a CTR1 inhibitor. Finally, *in vivo* studies used auditory brain stem response (ABR) measurements conducted in C57BL/6 mice to determine the effect of intratympanic copper sulfate administration on cisplatin-induced ototoxicity.

Results: Ctr1 was highly localized to the sites of cisplatin toxicity in the inner ear; outer hair cells, inner hair cells, stria vascularis, spiral ganglia and surrounding nerves in the mouse cochlea. Treatment of HEI-OC1 and HEK-CTR1 with copper sulfate decreased cellular accumulation and cytotoxicity of cisplatin. This same treatment also reduced the formation of platinum DNA adducts in HEK-CTR1 cells. Similarly, siRNA-mediated knockdown of Ctr1 in HEI-OC1 cells attenuated cellular platinum accumulation. In mice, intratympanic administration of copper sulfate 30 min before intraperitoneal administration of cisplatin was found to prevent hearing loss at click and 8, 16 and 32 kHz frequencies.

Conclusions: Our results suggest that cisplatin-induced ototoxicity involves uptake of cisplatin into the cochlea via Ctr1. Furthermore, our *in vivo* experiments establish a novel otoprotective strategy to prevent hearing loss in individuals on cisplatin therapy.

Poster Session, Friday, November 12th

Location: Alumni Hall, George Watts Hill Alumni Center

Display: 8:00 AM – 5:00 PM

Authors Present: 12:00 – 2:00 PM

ADME		
POSTER ID	**PRESENTER**	**TITLE**
PS-F-1	ANNE JENSEN	IN VITRO MODELS FOR INVESTIGATING PROTON-COUPLED AMINO ACID TRANSPORTER 1 (PAT1, SLC36A19) FUNCTION
PS-F-2	DANIEL PREISIG	ABSORPTION OF POORLY WATER SOLUBLE DRUGS FROM SELF-EMULSIFYING FORMULATIONS IN THE CACO-2 CELL MODEL USING BIORELEVANT MEDIA
PS-F-3	HIDENORI SUZUKI	KINETIC ANALYSIS OF NONLINEAR ORAL ABSORPTION OF THREE CA-ANTAGONISTS IN THE CLINICAL STUDY WITH MICRODOSE AND THERAPEUTIC DOSE
PS-F-4	KEVIN HAN	SPECIFIC CLAUDIN FAMILY OF PROTEINS MODULATE TRANSPORT OF SMALL ORGANIC CATIONS OR ANIONS ACROSS TIGHT JUNCTIONS OF EPITHELIAL CELL MONOLAYERS.
PS-F-5	MARY KLEPPE	PREDICTING THE RANGE OF ABSORPTION FOR COMPOUNDS THAT PRECIPITATE IN THE GI TRACT USING A NOVEL BIOPHARMACEUTICAL MODEL
PS-F-6	MASAYA SUITA	OLIGOARGININE-LINKED POLYMERS AS A NEW CLASS OF PENETRATION ENHANCERS
PS-F-7	STEPHANIE MOWERY	MEMBRANE EXPRESSION, LOCALIZATION, AND FUNCTIONAL ANALYSIS OF HUMAN PEPTIDE/HISTIDINE TRANSPORTER 1 IN GASTROINTESTINAL AND BBB CELL LINES
PS-F-8	WEI YUE	REGULATION OF ORGANIC ANION TRANSPORTING POLYPEPTIDE (OATP) 1B3 FUNCTION BY PROTEIN KINASE C

CLINICAL/ TRANSLATIONAL RESEARCH		
POSTER ID	**PRESENTER**	**TITLE**
PS-F-9	ANTHONY DI PASQUA	SENSITIZATION OF HUMAN NON-SMALL CELL LUNG CANCER CELLS TO CISPLATIN BY NATURALLY OCCURRING ISOTHIOCYANATES
PS-F-10	DANIEL HERTZ	BREAST CANCER PATIENTS CARRYING THE CYP2C8*3 VARIANT ARE MORE LIKELY TO ACHIEVE CLINICAL COMPLETE RESPONSE FROM NEOADJUVANT PACLITAXEL TREATMENT
PS-F-11	HAN HUI CHEONG	CORD LINING PROGENITOR CELLS AS ALTERNATIVE SOURCE OF HEPATOCYTE-LIKE CELLS
PS-F-12	JASMINE TALAMEH	ASSOCIATION OF GENETIC POLYMORPHISMS IN THE SYMPATHETIC ADRENERGIC AND RENIN-ANGIOTENSIN-ALDOSTERONE SYSTEMS WITH CLINICAL OUTCOME IN HEART FAILURE PATIENTS
PS-F-13	LATOYA GRIFFIN	ANTIRETROVIRAL LIVER TOXICITY: UNDERSTANDING THE COMPLEX INTERPLAY BETWEEN TRANSPORTERS, BILE ACIDS AND PROTEASE INHIBITORS

DRUG DESIGN		
POSTER ID	**PRESENTER**	**TITLE**
PS-F-14	LUKE ROODE	DRUGGING THE UNDRUGGABLE TARGET: NON-NUCLEAR RECEPTOR TRANSCRIPTION FACTORS
PS-F-15	MARY CARROLL	STRUCTURALLY RESOLVED DYNAMICS IN MULTI-CONFORMATION RECEPTOR-LIGAND COMPLEXES
PS-F-16	PAVLA SIMERSKA	DESIGN, SYNTHESIS AND BIOLOGICAL EVALUATION OF CARBOHYDRATE-BASED VACCINE CANDIDATES
PS-F-17	SATOMI ARIYOSHI	CUTANEOUS DISPOSITION OF FEXOFENADINE PRODRUG CONTROLLED BY CARBOXYLESTERASE IN RAT
PS-F-18	SEUNGWOO CHUNG	LMWH-TAUROCHOLATE CONJUGATE ACTS AS MOLECULAR TARGETING AGENT AND INHIBITS TUMOR ANGIOGENESIS AND TUMOR GROWTH

FORMULATION		
POSTER ID	**PRESENTER**	**TITLE**
PS-F-19	CHANG-GU KEUM	DOCETAXEL FORMULATION FOR INTRAVENOUS DELIVERY USING A PRODRUG APPROACH
PS-F-20	KASSIBLA DEMPAH	A UNIQUE METHOD FOR EVALUATING PARTICLE SIZE
PS-F-21	LENE JORGENSEN	EFFECT FROM MODIFICATION OF INSULIN STRUCTURE ON PROTEIN ADSORPTION AT SOLID INTERFACES
PS-F-22	PATRICK GULEY	DEVELOPMENT OF NOVEL LIPIDS FOR OPTIMIZED ALBUMIN BINDING
PS-F-23	SARAH PYSZCZYNSKI	TREHALOSE DIHYDRATE: TOWARD A GREATER UNDERSTANDING OF COMPLEX DEHYDRATION BEHAVIOR
PS-F-24	SIRIGUL THONGRANGSALIT	SELF-MICROEMULSION FORMULATION CONTAINING NATURAL OIL
PS-F-25	THOMAS TAUPITZ	IMPROVING THE DISSOLUTION BEHAVIOR OF A FIXED DOSE COMBINATION CONTAINING GLIMEPIRIDE AND PIOGLITAZONE WITH VARIOUS FORMULATION APPROACHES
PS-F-26	THUNJIRADASIREE KOJARUNCHITT	DEVELOPMENT OF SUSTAINED RELEASE VACCINE DELIVERY SYSTEM CONTAINING MODIFIED POLOXAMER 407 LOADED WITH CUBOSOMES
PS-F-27	TOMAS SOU	AN INVESTIGATION ON THE INTERACTION EFFECT OF AMINO ACIDS ON THE PERFORMANCE OF A MANNITOL DRY POWDER FORMULATION USING A DESIGN OF EXPERIMENT APPROACH
PS-F-28	YAJUN LIU	EXAMINATION OF THE INFLUENCE OF WATER-SOLUBLE ACIDS IN CARBOXYLIC ACID-TERMINATED PLGA ON PEPTIDE-PLGA SORPTION

GENE/ PROTEIN DELIVERY		
POSTER ID	**PRESENTER**	**TITLE**
PS-F-29	BEHFAR MOGHADDAM	DNA LIPOPLEX FORMULATION: EFFECT OF SALT ON CHARACTERISTIC PROPERTIES
PS-F-30	DONGYUN LIU	DEVELOPMENT OF W/O MICROEMULSIONS AND HYDROGEL NANOPARTICLES IN W/O MICROEMULSIONS FOR ORAL DELIVERY OF PEPTIDES AND PROTEINS
PS-F-31	JENS SCHAEFER	LIPID COATED POLYETHYLENIMINE COMPLEXES FOR ENHANCED DNA AND SIRNA DELIVERY
PS-F-32	JI-SOOK HWANG	STUDIES FOR THE DEVELOPMENT OF DRUG DELIVERY SYSTEM USING VIRUS-LIKE PARTICLE IN HEPG2 AND CASKI CELLS

PS-F-33	MATTHIAS FUETH	ALPHA-1-ANTITRPSIN PREVENTS DOXORUBICIN-INDUCED CARDIOMYOPATHY

MOLECULAR IMAGING		
POSTER ID	**PRESENTER**	**TITLE**
PS-F-34	CHIA-WEN HSU	SOLVENT-SENSITIVE DYES FOR MULTIPLEXED LIVE CELL IMAGING
PS-F-35	HARUKI HIGASHINO	DETECTION OF COLORECTAL CANCER USING PEANUT AGGLUTININ-IMMOBILIZED FLUORESCENT NANOSPHERES IN THE ORTHOTOPIC ANIMAL MODEL

NANOMEDICINE		
POSTER ID	**PRESENTER**	**TITLE**
PS-F-36	ALBERT DE GRAAF	THERMOSENSITIVE FLOWER-LIKE MICELLES BASED ON PNIPAM-PEG-PNIPAM
PS-F-37	BRITTANY AVARITT	PAMAM DENDRIMERS AS POTENT TIGHT JUNCTIONAL MODULATORS
PS-F-38	JIN-KI KIM	PREPARATION OF HIGH PAYLOAD DEXAMETHASONE PALMITATE NANOPARTICLES AND THE ENHANCEMENT OF TUMOR CELL UPTAKE
PS-F-39	JOSHUA SESTAK	DEVELOPMENT OF NANOMATERIAL IMMUNE CONJUGATES (NICS) TO TREAT MULTIPLE SCLEROSIS
PS-F-40	JUN LI	CALCIUM PHOSPHATE NANOPARTICLES WITH ASYMMETRIC LIPID COATING FOR SIRNA DELIVERY
PS-F-41	KARIM SEMPF	1D GEL ELECTROPHORESIS AS A FIRST STEP FOR ANALYSIS OF THE PLASMA PROTEINS ADSORBED ON NANOPARTICLES
PS-F-42	MARC UEDA	PEPTIDE CONJUGATION WITH AMPHIPHILIC BLOCK COPOLYMERS FOR ENHANCED DELIVERY
PS-F-43	PHILISE WILLIAMS	ENHANCED UPTAKE OF CLASSICAL CLATHRIN MEDIATED ENDOCYTOSIS MARKER (TRANSFERRIN) IN THE PRESENCE OF POLYPLEXES
PS-F-44	TARYN BAGBY	EFFECT OF MOLECULAR WEIGHT AND CHARGE ON LYMPHATIC DRAINAGE PATTERNS AND KINETICS OF LOCALIZED DRUG CARRIERS
PS-F-45	XIULING LU	DUAL THERAPEUTIC-IMAGING NANOVECTORS FOR AUGMENTED DELIVERY OF DEXAMETHASONE TO TUMORS
PS-F-46	YANG LIU	PACLITAXEL NANOCRYSTALS FOR OVERCOMING MULTIDRUG RESISTANCE IN CANCER
PS-F-47	ZHE WANG	NOVEL SYNTHETIC DEXTRAN-OLEATE-CRGDFK CONJUGATE FOR SELF-ASSEMBLED NANOPARTICLE IN TARGETED CHEMOTHERAPEUTIC DELIVERY OF PACLITAXEL
PS-F-48	ZHE WANG	SELF-ASSEMBLED CORE-SHELL NANOPARTICLE DECORATED WITH BOTH HYALURONIC ACID AND RGD PEPTIDE FOR THE TARGETED DELIVERY OF PACLITAXEL TO BREAST CANCER CELLS

PHARMACEUTICAL ANALYSIS		
POSTER ID	**PRESENTER**	**TITLE**
PS-F-49	ANDREA HAWE	FLUORESCENT MOLECULAR ROTORS DCVJ AND CCVJ DETECT PROTEIN AGGREGATION IN POLYSORBATE-CONTAINING MONOCLONAL IGG FORMULATIONS
PS-F-50	BRANDON GUFFORD	PH-DEPENDENT STABILITY OF CREATINE ETHYL ESTER
PS-F-51	SAI PRANEETH R BATHENA	QUANTITATIVE DETERMINATION OF LYSOPHOSPHATIDIC ACID IN HUMAN SALIVA USING LC-MS/MS

PS-F-52	WEI SUN	A FLUORESCENCE POLARIZATION ASSAY FOR IDENTIFICATION OF SMALL-MOLECULE ARFGAP INHIBITORS

PKPD		
POSTER ID	**PRESENTER**	**TITLE**
PS-F-53	ARIK ZUR	COMPARISON BETWEEN THE PHARMACOKINETIC PROPERTIES OF TWO NON METABOLIC LONG CHAIN FATTY ACID ANALOGS FOR THE THERAPY OF METABOLIC SYNDROME
PS-F-54	MARCEL ARNDT	CAN DISSOLUTION RATE CALCULATIONS ESTABLISH THE FORMULATION PARAMETERS NECESSARY TO AVOID FOOD EFFECTS?
PS-F-55	STEFANIE STRAUCH	IS THE BIOWAIVER PROCEDURE APPLICABLE FOR LAMIVUDINE DRUG PRODUCTS?
PS-F-56	TAE EUN KIM	ESTIMATING HIV EVOLUTIONARY PATHWAYS TO RALTEGRAVIR DRUG RESISTANCE

SAFETY		
POSTER ID	**PRESENTER**	**TITLE**
PS-F-57	KRISTINA DESMET	DEVELOPMENT OF A PAFURAMIDINE TREATMENT PROTOCOL THAT ELICITS QUANTIFIABLE LIVER AND KIDNEY TOXICITY

PS-F-1

In vitro models for investigating proton-coupled amino acid transporter 1 (PAT1, SLC36A19) function

A. Jensen, B. Brodin and C. U. Nielsen

Department of Pharmaceutics and Analytical Chemistry, Faculty of Pharmaceutical Sciences, University of Copenhagen, Copenhagen, DK

Purpose: Proton-coupled amino acid and di/tri-peptide carriers, PAT1 and PEPT1, are intestinal drug transporters with shared substrates. The aim of the present study was to construct, characterize and validate *in vitro* cell models for investigating PAT1 function. Two different strategies were employed: a) generation of a cell line stably expressing PAT1 and b) transient down-regulation of PAT1 and PEPT1 protein levels to examine the relative contribution to transport activity.

Methods: a) Epithelial MDCK cells were transfected with the human *PAT1* gene using the mammalian expression vector pcDNA3.1 and Geneporter2 (Genlantis) on 50% confluent serum starved cells. The medium was subsequently supplemented with 0.2 mg/mL geneticin to identify stably transfected cells and select single clones. b) Transient knock down was performed using PAT1 or PEPT1 directed siRNA (Invitrogen) and HiPerFect (Quiagen) in Caco2 cells. Transfections were repeated twice in order to improve protein knock down, and the cells were transferred to transwell filter inserts post transfection. Transfections were performed according to manufactures protocols and protein levels were verified by western blot analysis of total cell lysates using anti-bodies directed against PAT1 (21st Century Biochemicals) and PEPT1 (Santa Cruz).

Results: MDCK cells stably transfected with a *PAT1* containing construct were examined by western blot analysis. Several clones showed induction of a 53 kDa protein, which was recognised by a PAT1 directed anti-body. This is identical to the size of the PAT1 protein and strongly supports that a stable hPAT1 transfection was achieved. Two clones with different PAT1 expression levels were selected for further analyses of PAT1 localisation and function. Further, we transiently transfected Caco2 cells with siRNA directed against PAT1 and PEPT1 leading to approximately 80% and 70% reduction of the protein levels, respectively, as measured by western blotting.

Conclusion: MDCK cells were successfully used to create a cell line continuously expressing PAT1. Likewise, it was possible to down-regulate PAT1 and PEPT1 in Caco2 cells. These *in vitro* models provide a powerful tool for investigating drug transport via PAT1 and for identification of new substrates.

PS-F-2

Absorption of poorly water soluble drugs from self-emulsifying formulations in the Caco-2 cell model using biorelevant media

D. Preisig[1], C. Reppas[2], G. Imanidis[1,3]

[1] Institute of Pharmaceutical Technology, University of Basel, Switzerland
[2] Department of Pharmaceutical Technology, National and Kapodistrian University of Athens, Greece
[3] School of Life Sciences, University of Applied Sciences Northwestern Switzerland

Purpose: The permeation kinetics of model poorly water soluble drug danazol formulated as self-emulsifying drug delivery system through Caco-2 cell monolayers was investigated using biorelevant intestinal media. These formulations are commonly used to improve solubility hence bioavailability of this class of drugs, yet their effect on intestinal permeability and in particular their potential interaction with simulated intestinal media in terms of permeability is currently poorly understood.

Methods: Danazol was formulated as microemulsion, ME, consisting of tri-, di- and monoglyceride and surfactant. Caco-2 cells were cultured on Transwell inserts according to standard protocols. Drug permeation across the cell monolayer was studied with the microemulsion using as media cell-compatible fasted and fed state simulating intestinal fluids, $FaSSIF_{Caco}$ and $FeSSIF_{Caco}$. Control experiments were performed with the unformulated drug using the biorelevant media as well as with the microemulsion and the unformulated drug in purely aqueous transport medium, TM. Transport was measured in both the apical-to-basal and the basal-to-apical direction and data were evaluated with a kinetic model that provided drug permeability coefficients of the apical and the basal plasma membrane and the partition coefficient of drug between the media and the cell compartment.

Results: Permeability coefficient values of the drug with the ME formulation were smaller than of the unformulated drug. This was true when biorelevant media as well as when purely aqueous transport medium were used. $FaSSIF_{Caco}$ and $FeSSIF_{Caco}$ themselves reduced permeability coefficients compared to TM. On the other hand, both the microemulsion and the biorelevant media increased drug solubility in water. The model-deduced media-to-cell partition coefficients varied in accord with the solubility of drug in the media. Apical permeability coefficients were generally 1.5 to 4 times greater than basal values.

Conclusion: These results appear to support the view that incorporation of drug in colloidal structures of the ME formulation and of the biorelevant media diminishes its potential to permeate the cell membrane. Whether, in saturated solutions, this decrease in permeability is counterbalanced or even overpowered by the increased solubility of the drug, yielding potentially higher fluxes is currently under investigation.

PS-F-3

Kinetic analysis of nonlinear oral absorption of three Ca-antagonists in the clinical study with microdose and therapeutic dose

H. Suzuki[1], Y. Masaoka[1], M. Kataoka[1], S.Sakuma[1], Y. Suzaki[2], H. Imai[2], T. Kotegawa[2], T. Morimoto[2], K. Ohashi[2], Y. Sugiyama[3] and S. Yamashita[1]

[1]Faculty of Pharmaceutical Sciences, Setsunan University, Hirakata, Osaka 573-0101, Japan
[2]General Clinical Research Center, Oita University Hospital, Oita, Japan
[3]Graduate School of Pharmaceutical Sciences, The University of Tokyo, Tokyo, Japan

Purpose: Microdose clinical study (MD study) is now attracting a lot of attention as a new strategy for increasing the success probability of drug development. However, the discrepancy in pharmacokinetics and/or bioavailability (BA) between micro- and therapeutic dose is often pointed out as one of the major problems in the MD study. We have conducted MD study with three Ca-antagonists to investigate the dose-linearity in oral BA. Then, in vitro study was performed to elucidate the reason of linear or nonlinear BA of those drugs by measuring their metabolic stability and membrane permeability.

Method: In the MD study, three drugs (nifedipine, nicardipine and diltiazem) were administered orally and intravenously to healthy volunteers (n=8) as a cassette dosing (total dose = 100 μg). After appropriate washout period, these volunteers were also given each drug with therapeutic dose (oral). Drug concentration in blood samples were determined by LC/MS/MS. In the in vitro study, human intestinal and liver microsomes were obtained from XenoTech and were used to assess the metabolic stability of three drugs. Caco-2 cell and MDCK-MDR1 cell monolayers were used to investigate the transport of these drugs by P-glycoprotein (P-gp).

Result: In the MD study, only nifedipine showed the comparable BA with that obtained in the therapeutic dose study, while BA of nicardipine and diltiazem with microdose became significantly lower, indicating the nonlinearity in oral absorption. Since these drugs undergo the extensive first-pass metabolism both in the intestine and liver by CYP3A4, saturation of the enzyme at the therapeutic dose might cause the nonlinear oral BA. In the in vitro study with human intestinal microsomes, nicardipine was most unstable

and the rank order of Km value was nicardipine < diltiazem << nifedipine. In addition, nicardipine and diltiazem were revealed to be transported by P-gp, suggesting the involvement of P-gp mediated transport in the nonlinear absorption of these drugs.

Conclusions: In vitro study for metabolic stability and membrane transport can enhance the usefulness of the MD study by identifying the reason of nonlinear oral BA between MD and therapeutic dose.

PS-F-4

Specific Claudin Family of Proteins Modulate Transport of Small Organic Cations or Anions across Tight Junctions of Epithelial Cell Monolayers.

W. R. Proctor[1], T. Han[1], C. M. Van Itallie[2], J. M. Anderson[2], D. R. Thakker[1]

[1]Eshelman School of Pharmacy, University of North Carolina at Chapel Hill,
[2]School of Medicine, University of North Carolina at Chapel Hill

Purpose: Tight junction protein, claudins, mediate the paracelluar transport of small inorganic ions; however their role in the transport of small organic ions is currently unknown. In our previous study, induction of claudin-2 in Caco-2 cell monolayers by vitamin D_3 increased the paracellular transport of the antidiabetic cationic drug metformin. The aim of this work was to determine the role of cation selective claudins (claudin-2, -15, -10b) and anion-selective claudins (claudin-4 and -10a) in facilitating paracellular transport of small organic cations and anions.

Methods: Claudin-2, 4, 10a, 10b, or 15 was singly expressed in LLC-PK_1 monolayers, and in case of claudin-4 also in MDCK-II cells. The expression of each claudin isoform was controlled through a doxycycline inducible promoter; monolayer integrity was verified by the limited transport of the neutral paracellular probe, [^{14}C]mannitol. Paracellular transport across the cell monolayers of the ionic species [$^{45}Ca^{2+}$], [^{14}C]guanidine, [^{14}C]aminoguanidine, [^{14}C]metformin, [^{14}C]formic acid and [^{14}C]acetic acid was examined. The mass transported for each compound was determined by liquid scintillation spectrometry. Expression of candidate claudins was confirmed by western blotting.

Results: Cation-selective claudins-2, -10b, and -15 increased the transport of organic cations in a size-dependent manner. Only claudin-2 and -15 increased the transport of the metal cation Ca^{2+}. Anion-selective claudin-10a increased paracellular permeability of small organic anions in a size-dependent manner. Claudin-4 had no effect on anions but it inhibited the permeability of cations in MDCK-II cells. The claudin associated pore radius for both cation- and anion-selective isoforms was estimated to be 3.5-4.5 Å by fitting the data to Renkin molecular sieving equation.

Conclusions: This is the first demonstration that cation-selective claudins can facilitate paracellular transport of small organic cations in a size-dependent manner. Claudin expression affects metal cations differently than organic cations. Anion-selective claudin-10a increased the permeability of small organic anions, but anion-selectivity of claudin-4 appeared to be due to inhibiting cation transport. This work represents the first direct evidence demonstrating the role of tight-junction proteins, claudins, in influencing paracellular transport of organic ions. Implications of these findings in relation to intestinal absorption and renal excretion of ionic drugs will be discussed.

PS-F-5

Predicting the Range of Absorption for Compounds that Precipitate in the GI Tract Using a Novel Biopharmaceutical Model

K. Forney, M. Kleppe, R. Bogner

University of Connecticut, Correspondence: robin.bogner@uconn.edu

Purpose: A biopharmaceutical model was developed to predict the range of absorption for compounds that precipitate in the GI tract. The model was utilized to investigate the influence of various factors (i.e., intestinal volume dose) on the extent of oral absorption and to determine the importance of each factor on the fraction absorbed.

Methods: A mathematical model was constructed to relate a typical *in vitro* amorphous drug dissolution-time profile to absorption *in vivo*. The *in vitro* dissolution profile was sparingly parameterized using dissolution volume, plateau concentration, peak concentration and time to peak concentration. Dose, intestinal volume and first order absorption rate constant were also considered in the model. Equations for three *in vivo* cases were derived to consider concentration-dependent and time-dependent precipitation and for permeation-limited and dissolution-limited absorption. The *in vivo* absorption was calculated for several intestinal volumes, doses, first order absorption constants, *in vitro* peak concentrations and times to peak.

Results: The use of the three different cases resulted in determination of an absorption range rather than a single value. As expected, the amount absorbed was influenced greatly by the absorption rate constant and the time at which *in vitro* peak concentration was reached. However, the *in vitro* peak to plateau concentration ratio did not correlated with fraction absorption. Instead, *in vitro* the peak concentration multiplied by time to peak correlated with the extent of absorption. Also, it was shown that the volume available for dissolution in the GI tract dramatically affected the amount absorbed. This is true particularly for low dose drugs in which the majority of the dose can dissolve and be absorbed before precipitation occurs.

Conclusions: A new biopharmaceutical model was used to estimate an absorption range for compounds that precipitation in the GI tract. The model allowed us to find that *in vitro* peak concentration, time to peak, dose and intestinal volume all influence the extent of absorption for amorphous compounds.

PS-F-6

Oligoarginine-linked Polymers as a New Class of Penetration Enhancers

M. Suita[1], S. Sakuma[1], Y. Masaoka[1], M. Kataoka[1], N. Nakajima[2], N. Shinkai[2], H. Yamauchi[2], K-I. Hiwatari[3], H. Tachikawa[3],R. Kimura[3], S. Yamashita[1]

[1]Faculty of Pharmaceutical Sciences, Setsunan University, Hirakata, Osaka 573-0101, Japan
[2]R&D Dpt., NIPROPATCH Co., Ltd., Kasukabe, Saitama 344-0057, Japan
[3]Advanced Materials R&D Lab., ADEKA Co., Arakawa-ku, Tokyo 116-8553, Japan

Purpose: Oligoarginines, which are known as cell-penetrating peptides, enhance the cellular uptake of poorly membrane-permeable bioactive molecules that are chemically conjugated to them. The conjugation of these molecules with arginine-rich cell-penetrating peptides may be a promising strategy that improves their penetrating ability; however, the application of this manner is largely limited because tailor-made synthetic processes should be established for individual molecules. Here, we designed a novel polymer: oligoarginine-linked poly(N-vinylacetamide-co-acrylic acid), with the expectation that the polymers will enhance the cellular uptake of the bioactive molecules that are physically mixed with them.

Methods: Oligoarginines were grafted onto the polymer backbone through the chemical reaction with the carboxyl groups of poly(N-vinylacetamide-co-acrylic acid). The changes in the blood glucose concentration after nasal administration of insulin with and without the polymer were monitored in mice. In vitro internalization of fluorescein isothiocyanate-dextran (FD-4) into Caco-2 cells in the absence and presence of the polymer was also examined.

Results: The oligoarginine unit was successfully introduced onto the polymer backbone. The blood glucose concentration was slightly reduced when insulin was given solely at a dose of 10 IU/kg. A D-octaarginine-linked poly(N-vinylacetamide-co-acrylic acid) with a grafting degree of 2% significantly

enhanced the insulin-induced hypoglycemic effect. The penetration-enhancing function of D-octaarginine-linked poly(N-vinylacetamide-co-acrylic acid) increased dramatically with an increase in the grafting degree of D-octaarginine. Substitution of D-octaarginine with the corresponding optical isomer and an increase in the number of arginine residues rather reduced the penetration-enhancing function. In vitro cell studies also indicated that a D-octaarginine-linked poly(N-vinylacetamide-co-acrylic acid) with a grafting degree of 17% enabled FD-4 to effectively penetrate the cell membrane. To the contrary, intact oligoarginines that were physically mixed with insulin and FD-4 did not have a significant influence on the membrane penetration of both compounds.

Conclusion: Data demonstrated that our oligoarginine-linked polymer has a potential to provide a new class of penetration enhancers.

PS-F-7

Membrane Expression, Localization, and Functional Analysis of Human Peptide/Histidine Transporter 1 in Gastrointestinal and BBB Cell Lines

S. A. Mowery[1], S. M. Carl[1, 2], D. J. Lindley[1, 3], and G. T. Knipp[1]

[1]Purdue University, West Lafayette, Indiana
[2]Unigene Laboratories, Inc., Fairfield, NJ
[3]Abbott Laboratories, Abbot Park, IL

Purpose: Proton-Coupled Oligopeptide Transporter (POT) isoforms play an important role in the di- and tri-peptide nutrient uptake, and have been established as potential transportophoric targets for increasing the bioavailability of peptide-based pharmaceuticals. Of particular interest to our laboratory is the human Peptide/Histidine transporter 1 (hPHT1), which has demonstrated substrate affinity of histidine, di-, and tri-peptides and pharmaceutical compounds. Conservation and expression throughout multiple human tissue types suggests high functional importance of hPHT1. Furthermore, our transport data in human polarized cell lines infers that hPHT1 transports substrates from the cytoplasm into the blood across the basolateral membrane, and has led our laboratory to hypothesize that hPHT1 is expressed on the basolateral membrane.

Methods: The clonal human cell line HT29.Cl19A and the human blood brain barrier cell line hCMEC/D3 were grown to approximately 80-90% confluence. The cells were lysed with a lysis buffer containing protease inhibitors. The resulting lysate was centrifuged in order to separate the apical fractions (pellet) from the basolateral fractions (supernatant). Ultracentrifugation was utilized to further separate the basolateral fractions on a sorbital density gradient. Once the fractionation was complete, Western blotting was employed in order to identify the presence of hPHT1. Alkaline phosphatase and sodium-potassium-ATPase antibodies were used as apical and basolateral controls respectively.

Results: Detection of hPHT1 was observed in fractions collected from the density gradient. Sodium-potassium-ATPase was observed in the hPHT1 positive fractions after stripping and reprobing using the basolateral control antibody. Additionally, no detectable hPHT1 expression was observed in the apical fraction isolates.

Conclusions: Understanding the localization of this transporter is essential to elucidating hPHT1's function. While it has been established that hPepT1 and other transporters mediate absorptive epithelial influx of their substrates from the intestinal lumen, basolateral localization of hPHT1 suggests a role in mediating the vectorial flux of POT substrates across biological membranes. Validation of the basolateral localization of hPHT1 may enable the transportophoric design of peptide-based therapeutic agents that possess molecular signatures required for enhanced permeability across the GI epithelium, and potentially an increased concerted bioavailability.

PS-F-8

Regulation of Organic Anion Transporting Polypeptide (OATP) 1B3 Function by Protein Kinase C

Wei Yue, Kathleen Köck and Kim L.R. Brouwer

Eshelman School of Pharmacy, University of North Carolina at Chapel Hill,

Purpose: The organic anion transporting polypeptide (OATP) 1B3 is a liver-specific protein that transports many clinically important drugs and endogenous compounds including statins, digoxin and cholecystokinin-8 (CCK8); CCK8 is a selective OATP1B3 substrate. To date, little is known about OATP1B3 regulation. OATP1B3 is a putative phosphoprotein with consensus phosphorylation sites for protein kinase C (PKC), a serine/threonine kinase (Scansite 2.0). PKC may be activated by bile acids [e.g. chenodeoxycholic acid (CDCA)], disease states, or drugs that are PKC activators. Studies were designed to investigate the OATP1B3 phosphorylation status, and the role of PKC activation in regulating OATP1B3 function using CCK8 and digoxin as probe substrates.

Methods: OATP1B3 was immunoprecipitated from human sandwich-cultured hepatocytes (SCH). The immunocomplexes were blotted and probed with OATP1B3 or phosphoserine antibody to determine the OATP1B3 phosphorylation status. To examine the effect of PKC activation on OATP1B3 function, initial uptake of [^{3}H]CCK8 (1μM, 3min) and [^{3}H]digoxin (1μM, 2min) into SCH was compared after a 10-min pretreatment with vehicle control, the PKC activator phorbol-12-myristate-13-acetate (PMA; 0.01-10μM), or the inactive PMA analog 4αPDD (0.01-10μM). Furthermore, the effect of CDCA (1-100μM, 30min pretreatment), an endogenous PKC activator, on CCK8 uptake was evaluated in SCH.

Results: OATP1B3 is a serine-phosphorylated protein. Initial CCK8 and digoxin uptake into SCH was 2.42±0.21 and 5.5±1.4 pmol/mg protein, respectively. PMA suppressed hepatic uptake of both CCK8 and digoxin in a concentration-dependent manner with maximal inhibition of ~40% and ~44%, respectively; 4αPDD had no effect on CCK8 or digoxin uptake. CDCA pretreatment (50 or 100μM) significantly suppressed CCK8 uptake in SCH to ~60% and ~36% of control, respectively.

Conclusions: OATP1B3 function was rapidly down-regulated by PKC activation in human hepatocytes. These studies provide a novel mechanism for impaired hepatic uptake of OATP1B3 substrates, and emphasize the utility of SCH to identify potential hepatic transport interactions by PKC activators.

Supported by a UNC University Research Council Grant and NIH GM41935.

PS-F-9

Sensitization of human non-small cell lung cancer cells to cisplatin by naturally occurring isothiocyanates

A. J. Di Pasqua[1, 2], C. Hong[1], M. Y Wu[1], E. McCracken[1], X. Wang[1], L. Mi[1] and F-L. Chung[1]

[1]Department of Oncology, Lombardi Comprehensive Cancer Center, Georgetown University, Washington, DC
[2]Now in the laboratory of Dr. Michael Jay, Division of Molecular Pharmaceutics, Eshelman School of Pharmacy, University of North Carolina, Chapel Hill, NC

Purpose: Non-small cell lung cancer accounts for ~85% of all lung cancers and is the leading cause of cancer-related death in the US. Using naturally occurring isothiocyanates (ITCs) with the platinum anticancer drug cisplatin could be a new strategy for the treatment of non-small cell lung cancer. ITCs may be a safer alternative to the agents currently used in combination with cisplatin in the clinic, such as taxol and vincristine; peripheral neuropathy is a dose-limiting and disabling side effect of both.

Methods: Cytotoxicity toward human NCI-H596 and NCI-H1299 (with tetracycline inducible wild-type p53) non-small cell lung cancer cells was measured using the MTS tetrazolium salt viability assay. Glutathione levels in NCI-H596 cells were measured using Ellman's reagent, cellular platinum accumulation and DNA-platination were determined using inductively coupled plasma mass spectrometry (ICP-MS), and depletion of b-tubulin was determined using Western blot.

Results: Naturally occurring ITCs sensitize human non-small cell lung cancer cells to cisplatin. Moreover, the structure of the ITC side chain moiety is important for sensitization. p53 status is not important for sensitization; cells with wild-type and mutant p53 status respond similarly. Depletion of glutathione by ITCs is not an important event for sensitization, neither is cellular platinum accumulation nor is DNA-platination. Benzyl ITC (BITC) and phenethyl ITC (PEITC) deplete b-tubulin but sulforaphane (SFN) does not; this correlates with and may be important for sensitization.

Conclusions: We conclude that naturally occurring ITCs can sensitize human non-small cell lung cancer cells to cisplatin and that this may be an exciting new strategy for treating lung cancer in the clinic. BITC and PEITC are contained in foodstuffs (i.e., cruciferous vegetables) and thus may be a safer alternative to the agents currently used in combination with cisplatin, such as taxol and vincristine, which are also tubulin binding agents.

PS-F-10

Breast cancer patients carrying the CYP2C8*3 variant are more likely to achieve clinical complete response from neoadjuvant paclitaxel treatment.

Daniel L Hertz[1], E. Claire Dees[2], Alison A Motsinger-Reif[3], Amy Drobish[2], Stacey Winham[3], Howard L McLeod[1,2], Lisa A Carey[2]

[1]UNC Eshelman School of Pharmacy, University of North Carolina, Chapel Hill, NC
[2]Lineberger Comprehensive Cancer Center, University of North Carolina, Chapel Hill, NC
[3]Department of Biostatistics, North Carolina State University, Raleigh, NC.

Purpose: Paclitaxel is one of the most frequently used chemotherapeutic agents in pre-surgical breast cancer treatment. The purpose of this study was to investigate whether patients who carried common single nucleotide polymorphisms (SNPs) in genes relevant to paclitaxel pharmacokinetics were more likely to respond to, or experience toxicity from, paclitaxel therapy.

Methods: Subjects included in this study were treated with paclitaxel-containing regimens in the neoadjuvant setting. Most received sequential anthracycline- and taxane-based therapy in which clinical

response to each phase was collected separately. Treatment response was measured before and after each phase of treatment by clinical tumor measurement and categorized according to RECIST criteria while toxicity data was collected from physician notes. The primary endpoint of this study was achievement of clinical complete response (cCR) during taxane treatment. Secondary endpoints included clinical response rate (cRR, complete response + partial response, cPR), any grade 3 or higher toxicity, and grade 3 or higher neuropathy from paclitaxel treatment. Blood was collected at diagnosis and genotyped using pyrosequencing. The genotypes assessed were CYP1B1*3, CYP2C8*3, CYP3A4*1b, CYP3A5*3C, ABCB1 1236, ABCB1 2677, and ABCB1 3435.

Results: 112 breast cancer patients treated with neoadjuvant paclitaxel were included in this analysis. The median age was 50, tumor stage included II (42 patients), III (60 patients), and presenting stage IV (10 patients), 60 were grade 3, 57 were ER+, and 32 were HER2 positive. Response rate was 27.7% cCR, 31.3% cPR to the paclitaxel component. CYP2C8*3 carriers (23/112, 20.5%) had higher rates of clinical complete response to neoadjuvant paclitaxel treatment (55% versus 22%; OR=3.98 [CI 1.5-10.6], p=0.006). This association remained significant after adjustment for race, tumor grade, ER status, and whether paclitaxel treatment was preceded by another phase of chemotherapy. There were trends for increased clinical response rate (cRR; 82% vs 59%, OR=3.09 [CI 1.0-10.0], p=0.059) and greater risk of grade 3 or higher peripheral neuropathy (22% vs 8%; OR=3.17 [CI 0.9-11.2], p=0.072) in subjects carrying the CYP2C8*3 variant. On multivariate analysis, other paclitaxel drug-metabolizing enzyme polymorphisms did not appear related to either response or toxicity.

Conclusions: CYP2C8 is the primary enzyme responsible for paclitaxel metabolism, and the *3 variant has demonstrated decreased catalytic activity toward paclitaxel in vivo, leading to increased exposure of the patient to the active parent compound. Our results demonstrate that patients carrying CYP2C8*3 are more likely to achieve clinical complete response from neoadjuvant paclitaxel treatment, but may also be at increased risk of experiencing severe peripheral neurotoxicity.

PS-F-11

Cord Lining Progenitor Cells as Alternative Source of Hepatocyte-like Cells

H.H.Cheong[1], F.W. Wong[2], J. Masilamani[3], T. T. Phan[3, 4], C. Y. E.Chan[1], S. Y. Chan[1]

[1]Department of Pharmacy, Faculty of Science, National University of Singapore
[2]Division of Bioengineering, Faculty of Engineering, National University of Singapore
[3]Department of Surgery, Yong Loo Lin School of Medicine, National University of Singapore
[4]CellResearch Corporation, Singapore

Purpose: The aim is to direct umbilical cord lining progenitor cells (UCPCs) to differentiate into hepatocyte-like cells (HLCs), and to compare its drug metabolism abilities against established hepatic cell lines for *in vitro* drug testing and toxicology study model.

Methods: Cord lining epithelial cells (CLECs) isolated from umbilical cord lining were induced to differentiate over 28 days, whereby cells were cultured in hepatic culture medium for 14 days, followed by hepatic maintenance medium for another 14 days. Cryopreserved primary human hepatocytes and the hepatocellular carcinoma cell line, HepG2 were used as control. Immunofluorescence staining for hepatic markers such as albumin and cytokeratin 18 (CK18) were carried out on days 7, 14, 21 and 28. Glycogen storage ability was assessed through Periodic acid-Schiff Stain (PAS). At day 28, reverse transcription polymerase chain reaction (RT-PCR) was performed for gene expression of hepatic nuclear factor 4A and major metabolism cytochrome P450 enzymes (CYP450). Further assay of functional activity of the CYP450 enzymes was validated by incubating the CLEC-derived HLCs for 4 hours with FDA-approved drug substrates, followed by detection of biotransformation of the drug substrates to respective key metabolites using LC/MS/MS.

Results: After differentiation, the CLECs changed from fibroblastic to polygonal cells resembling hepatocytes. Immunofluorescence stain illustrated increasing amount of albumin and CK 18. PAS showed positive glycogen stain, while RT-PCR showed gene expression of hepatic markers. The LC/MS/MS was able to detect metabolite of drug substrate for CYP3A4 enzyme.

Conclusions: The results illustrated that the CLECs-derived HLCs closely resemble hepatocytes. Due to the ease of obtaining UCPCs, it is a promising alternative source of HLCs for high throughput *in vitro* drug testing and toxicology studies, and has the potential for use in bioartificial liver devices.

PS-F-12

Association of Genetic Polymorphisms in the Sympathetic Adrenergic and Renin-Angiotensin-Aldosterone Systems with Clinical Outcome in Heart Failure Patients

J. Talameh[1], J.H. Patterson[1,2], H. McLeod[1,2], J. Hoskins[1], T. Schwartz[3], K.F. Adams[2]

[1] Eshelman School of Pharmacy, University of North Carolina, Chapel Hill, NC
[2] School of Medicine, University of North Carolina, Chapel Hill, NC
[3] Gillings School of Public Health, University of North Carolina, Chapel Hill, NC

Purpose: Heart failure (HF) is a major public health problem in which morbidity and mortality remain high. The sympathetic adrenergic (SAS) and renin-angiotensin-aldosterone (RAAS) systems dually contribute to the progression of HF and are targets for HF pharmacotherapy. We hypothesize that individual and also combinations of genetic polymorphisms in these two systems will be associated with clinical outcome in patients with HF.

Methods: Fourteen polymorphisms in 11 genes of the SAS and RAAS will be analyzed using samples from UNITE-HF; a prospective, multicenter DNA repository of 815 HF patients complemented by a comprehensive clinical database. Genotyping will be accomplished using TaqMan®, QIAxcel®, and Sequenom® methods. Potential associations of genotypes with clinical outcome (death or heart transplant) will be tested using proportional hazards methods. For polymorphisms found to be individually associated with clinical outcome, a genetic risk score (GRS) will be calculated for each UNITE-HF patient based on their number of risk alleles. The GRS will be evaluated as a univariate predictor of outcome and in a multivariable model.

Results: At baseline, UNITE-HF patients are 38% female, 29% African-American, 64% receiving beta-blocker, and the mean age 57 years old. The average follow-up is 8 years, and the mortality rate is 38%. Currently, 173 patients have been genotyped for 13/14 polymorphisms. The concordance, minor allele frequencies (MAF), and Hardy Weinburg Equilibrium (HWE) results are presented in Table 1.

Conclusions: This is a large, long-term genetic association study with accurate genotyping methods, and it will be the first to analyze the additive effect of polymorphism combinations in patients with HF.

Table 1:

Gene	rsID	Concordance	Literature MAF	UNITE-HF MAF	HWE p-value
ADRB1	rs1801252	100%	14%	19%	0.051
	rs1801253	100%	30%	21%	0.439
ADRB2	rs1042713	100%	39%	36%	0.061
	rs1042714	100%	42%	42%	0.814
ACE	rs1799752	100%	44%		
ADRA2C	rs61767072	100%	6%	6.8%	0.937
GRK5	rs17098707	100%	2.6%	1.3%	0.871
AGT	rs5051	100%	40%	40%	0.395
	rs699	100%	57%	62%	0.923
AGTR1	rs5186	100%	35%	28%	0.082

CYP11B2	rs1799998	100%	55%	51%	0.655
SLC6A2	rs2242446	100%	27%	28%	0.287
BDKRB2	exon 1 indel	100%	50%	52%	0.298
ADRA1D	rs2236554	100%	47%	43%	0.483

PS-F-13

Association of Impaired Hepatic Bile Acid Transport with the Hepatotoxicity of Individual and Combination Antiretroviral Protease Inhibitors

LaToya M. Griffin and Kim L. R. Brouwer

[1]University of North Carolina at Chapel Hill, Division of Pharmacotherapy and Experimental Therapeutics

Purpose. The goal of this research project is to elucidate the mechanisms of hepatotoxicity associated with the concomitant use of antiretroviral protease inhibitors. Clarifying the mechanisms of hepatic injury caused by protease inhibitors is critical in helping predict hepatotoxic events. Three frequently used protease inhibitors were selected for investigation: darunavir (DRV), lopinavir (LPV) and ritonavir (RTV). Previous studies demonstrated that individually, these antiretrovirals interact with multiple transport proteins including Mrp2 (Abcc2), Bsep (Abcb11) and Ntcp (Slc10a1).

Methods. Rat sandwich cultured hepatocytes (SCH) were employed to characterize the extent of hepatotoxicity (measured by ATP depletion and LDH release) and inhibition of bile acid (taurocholate; [3H]TC) transport caused by individual and combinations of protease inhibitors. Following 24-hour exposure to LPV and DRV with and without RTV, LDH leakage into SCH medium was determined using the Cytotoxicity Detection Kit. Intracellular ATP levels were measured using the CellTiter-Glo® Luminescent Cell Viability Assay according to manufacturer's protocol. For TC transport studies, day 3 rat SCH were preincubated for 24 hours with LPV (10 or 50 μM) or DRV (10 or 50 μM) with or without RTV (5 μM) and coincubated for 10 minutes with calcium-containing or calcium-free standard HBSS buffer. Hepatocytes were incubated for 10 minutes with 1 μM [3H]-TC in standard HBSS. Cells were rinsed with ice cold standard calcium-containing HBSS buffer and lysed with 0.1% triton-X 100 in PBS and placed on an orbital shaker for at least 20 minutes before collection for drug accumulation and protein content.

Results. Based on the ATP depletion assay, LPV or DRV combined with RTV was more hepatotoxic than LPV or DRV alone. LPV hepatotoxicity appeared to be concentration dependent. DRV hepatotoxicity was modest over the range of concentrations examined. LPV and RTV markedly inhibited both TC uptake and biliary excretion at the concentrations examined. In contrast, DRV partially inhibited TC biliary excretion, with minimal effects on TC uptake.

Conclusion. Inhibition of bile acid transport may be a major contributing factor to the hepatotoxicity experienced by many patients receiving antiretroviral therapy containing multiple protease inhibitors.

PS-F-14

Drugging the undruggable target: non-nuclear receptor transcription factors

L. Roode[1], W. Hasan[1], C. Luft[1], J. DeSimone[1], I. Davis[2]

[1] Eshelman School of Pharmacy, University of North Carolina, Chapel Hill, NC
[2] Department of Genetics, School of Medicine, University of North Carolina, Chapel Hill, NC

Purpose: Transcription factors represent a class of important oncogenic targets that are not amenable to the traditional small molecule-based approach of most therapeutics. The reason for this is, in large part due to the large protein-protein interaction domains and a lack of hydrophobic pockets. Thus, alternative methods for interfering with these targets are needed. Nanoparticles offer the possibility of delivering biologics to interfere with this class of drug targets.

Methods: The Particle Replication in Non-Wetting Templates (PRINT) nanofabrication process can uniquely control the size and shape of fabricated nanoparticles, yet has not been tested for its compatibility with delivery of biologics. Thus, PRINT will be evaluated for its ability to encapsulate biologic agents (i.e. DNA or protein) that are potentially efficacious against Ewings Sarcoma, a soft tissue sarcoma that is dependent upon a tumor-specific transcription factor for growth.

Results: Our results will demonstrate that PRINT particles can be loaded and deliver active biologic agents. Moreover, novel macromolecular/biologic therapies for Ewings Sarcoma will be demonstrated to be efficacious against a Ewings Sarcoma cell line *in vitro*.

Conclusion: Our results may demonstrate a proof-of-concept approach regarding drug strategies for aberrant transcription factors.

PS-F-15

Structurally resolved dynamics in multi-conformation receptor-ligand complexes

M. J. Carroll[1], A. V. Gromova[1], K. R. Miller[2], H. Tang[2], X. S. Wang[1], A. Tripathy[3], S. F. Singleton[1], Edward J. Collins[2,4], and Andrew L. Lee[1,2]

[1]Division of Medicinal Chemistry and Natural Products, Eshelman School of Pharmacy
[2]Department of Biochemistry and Biophysics
[3]UNC Macromolecular Interactions Facility
[4]Department of Microbiology and Immunology, School of Medicine, University of North Carolina at Chapel Hill, Chapel Hill, NC

Purpose: Structure-based drug design relies on static protein crystal structures despite significant evidence for the need to include protein dynamics as a serious consideration. Dynamic motions are ignored because they are not understood well enough to model – a situation resulting from a lack of explicit experimental examples of dynamic receptor-ligand complexes.

Methods: We have examined the details of μs-ms timescale motions in a series of receptor-small molecule complexes using a combination of NMR spectroscopy and X-ray crystallography.

Results: *Escherichia coli* dihydrofolate reductase (DHFR) conformational dynamics differ depending on the chemical structure and binding affinity of small molecule inhibitors bound to the holoenzyme. For one drug-like, nanomolar-affinity inhibitor, dynamics in DHFR are driven by internal switching motions of the small molecule while it is bound. Carr-Purcell-Meiboom-Gill relaxation dispersion experiments and NOEs revealed the crystal structure to be a snapshot of the high-energy ligand conformation. For the remaining inhibitors of the series with more reduced binding affinities (μM), the number of sites experiencing conformational exchange and the rates of exchange correlate well with binding affinity.

Conclusions: The availability of accurate, structurally resolved dynamics in protein-ligand complexes should serve as valuable benchmarks for modeling dynamics in other receptor-ligand complexes and prediction of binding affinities.

PS-F-16

Design, Synthesis and Biological Evaluation of Carbohydrate-based Vaccine Candidates

P. Simerska[1], I. Toth[1]

[1] The University of Queensland, School of Chemistry and Molecular Biosciences, Brisbane, QLD 4072, Australia

Purpose: The aim of this study is to develop a universal self-adjuvanting carbohydrate-based vaccine template which would be applicable against variety of diseases.

Methods: Carbohydrate carriers were synthesized starting from glucose, galactose and mannose bearing four Boc-protected propylamines and adipic linker attached to amine at anomeric C-1. The lipid moiety consisting of three lipoamino acids and two glycine spacers was synthesized by stepwise solid-phase peptide synthesis on *p*MBHA resin. Lipid moieties were coupled to terminal carboxylic acids of carbohydrate cores to form liposaccharides which were used for attachment of four copies of peptide epitopes. Microwave-assisted solid phase synthesis was optimized for lipid and carbohydrate coupling. Library of carbohydrate-based lipopetide vaccine candidates was synthesized by combination of different liposaccharide cores and peptide epitopes from N- and C-terminus of group A streptococcal (GAS) surface M protein. The synthesized vaccine candidates (Fig.1) were purified by HPLC, characterized by MS and tested *in vivo* (subcutaneous immunization of B10.BR mice).

Results: Carbohydrate-based lipopetide vaccines against GAS were designed to incorporate the immunostimulant lipid moiety and four copies of peptide epitopes. The lipid adjuvant was synthesized using lipoamino acids and attached to carbohydrate cores. Synthetic peptide sequences (J8, J14, PL1 or 8830) were coupled to this constructs by stepwise solid-phase peptide synthesis. The potential of carbohydrate carrier-based vaccines was shown by high levels of specific serum IgG antibodies, which were elicited after subcutaneous immunization of mice with these vaccine candidates. The results were comparable to positive controls including peptide epitope administered with CFA and poly-lysine analogue. Moreover, non-a-helical carbohydrate templates were shown to promote a-helix bundles of the covalently attached peptides.

Figure 1: Carbohydrate-based self-adjuvanting vaccine.

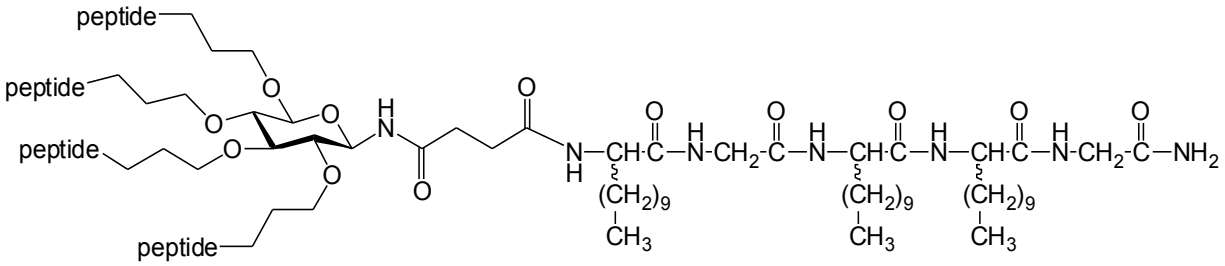

Conclusion: Our vaccine delivery system employs a glycolipid core acting as an adjuvant and a carrier coupled to multiple copies of immunogenic peptides to induce antibody responses without the co-administration of additional potentially toxic adjuvants. Carbohydrates, as carriers, providing numerous attachment points for the conjugation of peptide antigens and their optimal orientation for the recognition by cells of the immune system, reducing degradation of the attached peptide antigens and many other advantages, make carbohydrate-based vaccine highly promising approach.

PS-F-17

Cutaneous disposition of fexofenadine prodrug controlled by carboxylesterase in rat

S. Ariyoshi[1], K. Tasaka[1], K. Ohura[1], T. Imai[1]

[1]Kumamoto University

Purpose: This research is studied for evaluating the fexofenadine prodrug as a percutaneous antiallergic agent. It is known that esterase presents in the skin and plays a major role in prodrug activation. Ethyl-fexofenadine has been designed as a prodrug that accumulates in the stratum corneum (SC) and sustainedly releases fexofenadine in the viable skin. We studied cutaneous permeability, cumulation and hydrolysis of ethyl-fexofenadine in rat skin. Besides, we examined the cutaneous level of esterase in several aged rat.

Methods: Rat skin permeation study was performed by using flow-through diffusion cell. Used skins are followed: 1) intact skin, 2) stripped skin obtained by adhesive tape stripping for 15 times, 3) carboxylesterase inhibited skin by treatment with bis-*p*-nitrophenyl phosphate (BNPP). At the end of permeation study, the amount of drug in the skin and SC was determined. Rat skin in age of 8, 46 and 90 weeks was freshly obtained and their hydrolase activity was determined. The mRNA level of several carboxylesterase isozymes was measured by real-time PCR.

Results: In rat skin permeation study, the partition of ethyl-fexofenadine into SC was greater than fexofenadine due to the increase of hydrophobicity by esterification, resulted in about 85 times greater permeability coefficient. Only fexofenadine was detected in receptor solution, because ethyl-fexofenadine interacted with skin components. In stripped skin, permeation of fexofenadine is greatly increased, suggesting that the cutaneous permeation of fexofenadine is limited by SC. In the skin treated with BNPP, hydrolysis of ethy-fexofenadine was inhibited and permeation of fexofenadine was decreased, although permeation and cutaneous accumulation of ethyl-fexofenadine in rat skin was not affected by treatment of BNPP. From the real-time PCR, it was observed that HydrolaseA, CES1 isozyme, was highly expressed in rat skin. Interestingly, we found mRNA expression level of HydrolaseA was increased with aging in order of 8 < 46 < 90 weeks. The hydrolysis activity of *p*-nitrophenyl acetate was also increased due to elevation of Vmax, related with the expression of HydrolaseA.

Conclusions: We conclude that the ethyl-fexofenadine is a good candidate of prodrug that is locked in SC and sustainedly releases the active drug in the skin.

PS-F-18

LMWH-Taurocholate conjugate acts as molecular targeting agent and inhibits tumor angiogenesis and tumor growth

S. Chung[1], S. M. Bae[2], M. Lee[3], R-W. Park[2], S. Y. Kim[3] and Y. Byun[1]

[1] College of Pharmacy, Seoul National University, Seoul, South Korea
[2] Department of Biochemistry, School of Medicine, Kyungpook National University, Daegu, South Korea
[3] Department of Otolaryngology, College of Medicine, University of Ulsan, Seoul, South Korea

Purpose: Recently, anti-angiogenesis therapy has been established as an attractive approach for cancer therapeutics. Targeting angiogenesis in tumor rather than cancer cell itself has shown advantages over conventional chemotherapy, showing significant tumor inhibition effect with having lower toxicity. Heparin is known to interact with various angiogenic molecules, thus inhibiting angiogenesis. In spite of its ability to inhibit angiogenesis, heparin is inappropriate for clinical use to treat cancer due to its strong anticoagulant activity that can induce severe bleeding in high dose. Herein, we have developed a new angiogenesis inhibitor, LHT7, by chemically modifying low-molecular weight heparin that has almost no anticoagulant activity and furthermore, having enhanced anti-angiogenesis effect.

Methods: LHT7 was synthesized by conjugating average 7 molecules of sodium taurocholic acid to a low-molecular weight heparin molecule. The anticoagulant activity was measured by chromogenic factor Xa assay. Angiogenesis inhibition was evaluated through *in vitro* HUVECs tubular formation assay and *in vivo* matrigel plug assay and intra-tumor angiography. Tumor growth suppression by LHT7 was observed in various cancer cell lines including SCC7, MDA-MB231 and A549. Binding affinity of LHT7 towards $VEGF_{165}$ was measured by using both ITC and SPR. Suppression of VEGF signaling was observed by western blot KDR phosphorylation assay. Finally, binding mechanism of LHT7 on $VEGF_{165}$ was revealed by comparing LHT7 and LHT7 analogs and by *in silico* binding analysis with VEGF-HBD.

Results: LHT7 showed almost no anticoagulant activity but high antiangiogenic activity. It successfully inhibited the vascular formation both *in vitro* and *in vivo* leading to significant inhibition in tumor growth *in vivo*. LHT7 showed strong binding affinity to $VEGF_{165}$ and blocked VEGF signaling through KDR indicating that inhibition of $VEGF_{165}$ by LHT7 would be the major reason of antiangiogenic effect of LHT7. Further experiments showed terminal sulfate groups of taurocholic moiety of LHT7 is the major factor of enhanced binding ability to $VEGF_{165}$ when compared to LMWH.

Conclusion: LHT7 can effectively inhibit angiogenesis in tumor thus suppressing tumor growth by binding strongly with $VEGF_{165}$ through strong electrostatic interaction between sulfate groups on LHT7 and basic amino acids on $VEGF_{165}$.

PS-F-19

Docetaxel formulation for intravenous delivery using a prodrug approach

C-G. Keum[1], C-W Cho[1]

[1]College of Pharmacy, Chungnam National University, Daejeon 305-764, South Korea.

Purpose: Docetaxel(DTX) is an antineoplastic agent belonging to the second generation of the taxoid family. Yet, the only licensed indication for docetaxel is in the treatment of locally advanced or metastatic breast cancer with a first-line chemotherapy regimen. Currently, parenteral formulations are available for its clinical use while oral administration is still limited because of its low oral bioavailability (<5% in mice), which is in part due to its practically insoluble property (4.93 μg/mL in water). Docetaxel is dissolved in 100% (w/v) polysorbate 80 (Tween-80) which results in severe side effects. Severe hypersensitivity reactions characterized by generalized rash/erythema, hypotension and/or bronchospasm, or very rarely fatal anaphylaxis, have been reported in patients. Hypersensitivity reactions require immediate discontinuation of the Taxotere® infusion and administration of appropriate therapy. All the hypersensitive reactions mentioned above are primarily caused by and due to the presence of polysorbate 80 in the formulation. Other solubilizing agents such as cremophor EL having similar allergic reactions should be avoided.

Methods: This study explores the use of prodrugs to affect improved parenteral delivery of poorly water-soluble problematic drugs, using both docetaxel as well as investigational prodrugs as examples. To improve the aqueous solubility of docetaxel for parenteral administration, prodrugs of the disaccharides D-lactose (DTX-L), monosaccharides D-glucose (DTX-G) and the amino carbohydrates sialic acid (DTX-S) were prepared and evaluated for solubility.

Results: Improved solubility at physiologic pH values, combination cosolvents and combination surfactants was observed for prodrugs. The solubility of DTX-G is 853.7, 898.3 and 898.1ug/ml in 20% ethanol-water solution, 20% PEG400-pH6 buffer solution and 20% DMSO-pH6 buffer solution. The solubility of DTX-G is 805.8 and 821.8ug/ml in 2.5% Tween80-water solution and 2.5% Cremophor EL-water solution. A pH-solubility profile of drugs was obtained in the pH range 1.0 to 13.0. The highest solubility (60.1ug/ml) of DTX-G is observed at pH6 buffer.

Conclusions: The aim of this study is to find out the parenteral formulation of prodrug of docetaxel with less surfactant as possible.

PS-F-20

A UNIQUE METHOD FOR EVALUATING PARTICLE SIZE

K. E. Dempah[1], C. J. Berkland[1], E. J. Munson[2]

[1]Department of Pharmaceutical Chemistry, School of Pharmacy, University of Kansas, Lawrence, KS
[2]Department of Pharmaceutical Sciences, College of Pharmacy, University of Kentucky, Lexington, KY

Purpose: To correlate particle size with solid-state nuclear magnetic resonance (SSNMR) parameters such as relaxation times and line widths.

Methods: Salicylic acid (as-received) was sieved to produce different ranges of particle sizes. Micro- and nano-sized particles of salicylic acid were generated by media-milling of the drug in water, followed by freeze drying of the collected suspensions. Grinding with mortar and pestle for 10min or less was also used to reduce the particle size of the as-received material. All of the samples, including the as-received material, were characterized by differential scanning calorimetry (DSC), polarized light microscopy (PLM) and scanning electron microscopy (SEM). In addition, the samples were analyzed using SSNMR, including proton spin-lattice relaxation times (^{1}H T_1).

Results: The PLM micrographs of the sieved fractions showed an increase in primary color, associated with an increase in single crystals, when going down in size. The ^{1}H T_1 value of the as-received material was approximately 4100s. Most of the sieved material was in the 180-425µm size range. The measured ^{1}H T_1 value of that fraction was 3900s. The largest size collected, greater than 850µm, had a ^{1}H T_1 value of 5600s. The ^{1}H T_1 of the material ground for ten minutes was 1300s. The ^{1}H T_1 for the media-milled material was measured to be about 5s. SEM micrographs of this material showed aggregates of particles.

Conclusions: ^{1}H relaxation time is shown to decrease with particle size. Grinding and milling introduce stress to the material and likely contribute to some of the observed decrease in relaxation time. However, in the case of the sieved material, any change in relaxation time can be fully attributed to differences in particle size, where the decreased particle size results in faster spin lattice relaxation. Molecules at the surface of the particles have greater mobility than the ones inside and are expected to be faster relaxers. It is hypothesized that smaller particles allow faster transfer of the magnetization from inner molecules to the exterior surface molecules, which gives rise to decreased ^{1}H spin-lattice relaxation times. Future studies will focus on further correlating particle size and NMR relaxation.

PS-F-21

Effect from modification of insulin structure on protein adsorption at solid interfaces

C. Pinholt[1], S. Hostrup[2], J. T. Bukrinsky[2], S. Frokjaer[1], L. Jorgensen[1]

[1]Department of Pharmaceutics and Analytical Chemistry, Faculty of Pharmaceutical Sciences, University of Copenhagen, Denmark
[2]Novo Nordisk A/S, Denmark

Purpose: To study the effect of acylation on the adsorption of insulin to a hydrophobic surface.

Methods: Adsorption isotherms were established and isothermal titration calorimetry and surface plasmon resonance were used to compare the adsorption of insulin and acylated insulin. Secondary structure and association behavior of the two proteins were studied with circular dichroism.

Results: Circular dichroism showed that the secondary structures of insulin and acylated insulin were dominated by α-helix, and that the association behavior of insulin was affected by acylation. Adsorption isotherms for both insulin and acylated insulin in monomer-dimer mixtures showed high-affinity adsorption to polystyrene, with a lower adsorption plateau for insulin than for acylated insulin. In contrast, equal adsorption plateau values were observed with isothermal titration calorimetry and surface plasmon resonance when adsorption from monomer-dimer-hexamer mixtures was studied. Finally, surface plasmon resonance showed that acylation of insulin decreases the adsorption rate of insulin.

Conclusions: Acylation was observed to decreases the initial adsorption rate of monomeric insulin to a hydrophobic gold surface and the effect of acylation on the amount of insulin molecules adsorbing per unit surface area were found to depend on the association degree of insulin.

PS-F-22

ABSTRACT NOT AVAILABLE

PS-F-23

Trehalose Dihydrate: Toward a Greater Understanding of Complex Dehydration Behavior

S. J. Pyszczynski[1], E. J. Munson[2]

[1]Department of Pharmaceutical Chemistry, University of Kansas, Lawrence, KS
[2]Department of Pharmaceutical Sciences, College of Pharmacy, University of Kentucky, Lexington, KY

Purpose: To investigate the factors that influence the forms of anhydrous trehalose generated upon dehydration of trehalose dihydrate.

Methods: α,α-Trehalose dihydrate was obtained from several manufacturers. Samples of the bulk materials were sieved to obtain particle size fractions of <75 μm, 75-125 μm, 125-180 μm, 180-425 μm, 425-850 μm, and >850 μm. As-received and sieved samples were dehydrated at 125 °C for one hour under vacuum. Techniques used to characterize the as-received, sieved, and dehydrated samples include: differential scanning calorimetry (DSC), thermogravimetric analysis (TGA), hot-stage polarized light microscopy (HSM), and ^{13}C solid-state nuclear magnetic resonance spectroscopy (SSNMR). A heating rate of 10 °C/minute was used for DSC, TGA, and HSM analyses. Open pans were used for DSC analyses.

Results: DSC thermograms showed that a decrease in the particle size of the dihydrates was accompanied by either a significant decrease in the temperature at the peak of the dehydration endotherm or a slight decrease followed by an increase. For samples exhibiting the first behavior, a large amount of the β-anhydrate was formed upon dehydration (all particle size fractions). For samples exhibiting the second behavior, the decrease in particle size was accompanied by a large decrease in the amount of β-anhydrate formed upon dehydration. TGA thermograms showed that dehydration of larger particles was not a single-step process. When examined using HSM, different behaviors were observed for dihydrates from different manufacturers. Some became amorphous upon dehydration, and others transitioned directly to the β-anhydrate. Different degrees of crystallization were observed for the different amorphous samples. Dehydration at 125 °C led to complete amorphization or mixtures of anhydrous forms.

Conclusion: One single factor does not govern the forms of anhydrous trehalose that are generated upon dehydration of the dihydrate. Particle size and morphology influence the dehydration behavior by affecting the rate at which water leaves the crystal structure. Regardless of the particle size, certain samples have a higher propensity to form the β-anhydrate, and other samples tend to form amorphous trehalose.

PS-F-24

Self-microemulsion formulation containing natural oil

S. Thongrangsalit[1], G.C. Ritthidej[1]

[1] Department of Pharmaceutics and Industrial Pharmacy, Faculty of Pharmaceutical Sciences, Chulalongkorn University, Bangkok, Thailand

Purpose: Self-microemulsion formulations which main components are oil and surfactant(s) have been reported to improve drug dissolution and bioavailability of poorly water soluble drugs. Various oils are used including synthetic and modified oils due to ease to obtain self-microemulsion formulations. However, the cost of such oils is quite high. Natural oils are much cheaper, versatile and accepted for human consumption. Therefore, the purpose of this study was to evaluate the feasibility of self-microemulsion formulation containing natural oils.

Methods: Four compendial accepted natural oils were selected: corn oil, sunflower oil, olive oil and castor oil. Tween80 was used as surfactant, Span20, Span80, CremophorEL as cosurfactant. Cosolvents were polyethylene glycol400, propylene glycol, glycerine and ethanol. Pseudo-ternary phase diagrams were constructed using titration method by varying oil to surfactant (O:S) and surfactant to cosolvent (S:Co) ratios. The formulations in microemulsion area on phase diagrams were chosen and then diluted with 100 folds of DI water. Physical appearance was visually observed. Droplet size and morphology before and

after 5% w/w drug loaded (bromocriptine mesylate) were measured by Zetasizer® and TEM, respectively. Physical and chemical stability were conducted for 3 months at room temperature.

Results: Only formulations of castor oil could form microemulsion after dilution with DI water possibly due to more purified fatty acid of less double bond and containing hydroxyl group in triglyceride chain. Castor oil with Tween80:CremophorEL (1:1) at O:S ratios ≤ 2:8 showed clear and transparent emulsion with droplet size <50nm. Drug loading and storage of selected formulations had no effect on size (nm) and size distribution (PdI) (28.47,0.33; 29.64,0.47; 27.47,0.37 and 27.00,0.30 for unloaded and drug loaded microemulsion at time 0 and 3 months, respectively). All droplets were spherical with smooth surface which droplet size was correlated with size analysis. Moreover, drug content was not changed after storage.

Conclusions: Castor oil was the only investigated natural oil that obtained self-microemulsion preparations. Sizes of microemulsion droplets from selected formulations both before and after drug loaded were maintained at <50 nm. Moreover, physical and chemical stability were maintained after 3 months at room temperature.

PS-F-25

Improving the Dissolution Behavior of a Fixed Dose Combination Containing Glimepiride and Pioglitazone with Various Formulation Approaches

T. Taupitz[1], S. Klein[2]

[1]Institute of Pharmaceutical Technology, Johann Wolfgang Goethe University, 9 Max-von-Laue Street, Frankfurt / Main 60439, Germany
[2]Institute of Pharmacy, Biopharmacy and Pharmaceutical Technology, Ernst Moritz Arndt University, 17 Friedrich Ludwig Jahn Street, Greifswald 17489, Germany

Purpose: In the present study we wanted to improve the dissolution behavior of two BCS class II compounds, glimepiride, a weakly acidic drug and pioglitazone, a weak base, in a fixed dose combination product. Two different formulation approaches were used for this purpose. The first approach was an inclusion complex of each of the drugs with hydroxypropyl-ß-cyclodextrin (HP-ß-CD) and the other one was a mixture of solid dispersions of each compound with Soluplus®, a recently marketed copolymer. The main objective was to obtain formulations that show a dissolution behavior superior to that of each of the pure drugs and also to a marketed fixed dose combination named Tandemact®.

Methods: A freeze drying procedure was used to prepare the inclusion complexes of both compounds and HP-ß-CD (each in a molar ratio of 1:2) as well as the solid dispersions with Soluplus® (10% drug load). Formulations were then subject to thermal analysis, solubility and dissolution tests. To elucidate if the dissolution performance of both drugs in the complex and/or the solid dispersion formulation outreaches that of the marketed product, solubility- and dissolution tests were performed in two test fluids simulating conditions in the stomach and the upper small intestine.

Results: DSC spectra of the complex formulations and the solid dispersions revealed the absence of a melting endotherm, indicating that true inclusion complexes and amorphous solid dispersions were obtained. Results of the solubility experiments showed a significant increase of glimepiride and pioglitazone aqueous solubility. Dissolution performance of both fixed dose combination formulations was superior to that of the pure drugs and the marketed formulation under gastric and small intestinal conditions.

Conclusions: Results from the present study indicate that both formulation approaches were successful in terms of improving solubility and dissolution performance of a fixed dose combination product containing glimepiride and pioglitazone. We thus assume that the *in vivo* behavior of our formulations might be superior to that of the marketed formulation. However, this assumption and the applicability of

these formulation approaches to other combinations of weakly basic and a weakly acidic BCS class II drugs needs to be proved.

PS-F-26

Development of sustained release vaccine delivery system containing modified poloxamer 407 loaded with cubosomes

T. Kojarunchitt[1], S. Hook[1], S. Rizwan[1], T. Rades[1], S. Baldursdottir[2]

[1]School of Pharmacy, University of Otago, Dunedin, New Zealand
[2]Faculty of Pharmaceutical Sciences, University of Copenhagen, Denmark

Purpose: To develop a sustained release vaccine delivery system for cubosomes loaded within a modified thermoresponsive gel, poloxamer 407 (P407).

Methods: Three different concentrations of P407 (12%, 15% and 17% w/v) were formulated with various additives (methyl cellulose (MC), dextran, carrageenan and reversed poloxamer (25R4)), with or without cubosomes (20mg/mL). Cubosomes consisted of phytantriol: pluronic and 70% w/w propylene glycol at a lipid: polymer ratio of 6.7:1 w/w. The rheological characteristics of the systems were investigated by oscillatory shear measurements on a TA AR-G2 rheometer using a cone-and-plate geometry. *In vitro* gel stability was investigated by determining gel weight loss over time.

Results: Formulations containing 15% and 17% (w/v) P407 were free-flowing liquids at working temperature (<25°C) and became solid at 37°C while 12% (w/v) formulations did not gel upon heating to 37°C. However, with the addition of cubosomes an increase in complex viscosity and a decrease in sol-gel transition temperature for all three concentrations of P407 was observed, with the 12% formulation now forming a soft gel at 37°C. The physical stability of 12% (w/v) P407 was enhanced by the addition of 0.3% MC, 0.5% dextran and 25R4 (at the molar ratio of 25R4/P407 = 1:1) compared to P407 alone however the addition of 0.2% carrageenan decreased gel stability. Stability was found to be further enhanced by increasing the P407 concentration to 15% and 17%. Additionally, the 25R4 was found to increase the sol-gel transition temperature giving a more suitable viscosity to the systems at working temperatures. The 17% gels containing the copolymer 25R4 in the presence of cubosomes were found to have significantly enhanced stability as compared to all other formulations except for 15% gels containing 25R4 ($p<0.05$).

Conclusion: The addition of 25R4 to P407 allows for the development of formulations that were free flowing liquids at working temperature, had a fast sol-gel transition at 37°C and had improved stability in an aqueous environment. These results indicate that cubosomes loaded 17% P407 with 25R4 in 1:1 molar ratio may have potential applications for sustained release vaccine delivery however the effect of the addition of 25R4 on release of antigen *in vivo* must be determined.

PS-F-27

An Investigation on the Interaction Effect of Amino Acids on the Performance of a Mannitol Dry Powder Formulation using a Design of Experiment Approach

T. Sou[1], L. M. Kaminskas[1], M. P. McIntosh[1], L. Orlando[1], D. A. V. Morton[1]

[1]Drug Delivery, Disposition and Dynamics, Monash Institute of Pharmaceutical Sciences, Monash University, Melbourne, Australia

Purpose: To determine the impact of adding amino acids (leucine, glycine and alanine) on the dispersibility and morphology of a mannitol-based spray-dried powder formulation.

Methods: This study utilised a 2^3 factorial design in which 3 amino acids selected for varying hydrocarbon chain length were added to control specific properties of the formulations. Two levels of 0% and 30% molar concentration of the amino acids were selected. The mid-point concentration, 15% of each of the amino acids, was used to formulate a central point composition. A Spraytec (Malvern Instruments Limited, UK) laser diffraction system was used to measure the aerosolisation efficiency of the dry powder formulations. The median particle size (Dv50) was measured at a flow rate of 60 L/min using the Monodose Inhaler (Miat, Italy) as the dispersion device. Size 3 HPMC capsules were filled with 20 mg of powder for the tests which were performed under controlled temperature (18-25°C) and relative humidity (40-60% RH). The surface morphology of the particles was examined under JOEL JSM 6000F scanning electron microscope (SEM) at 15 kV (JOEL, Tokyo, Japan).

Results: With the exception of mannitol alone as the foundation material, all other formulations without leucine had a Dv50 greater than 5 μm. The mannitol alone had a mean Dv50 of 2.83 (±0.10) μm while the formulations containing 30% glycine and 30% alanine, 30% alanine alone, and 30% glycine alone had mean Dv50s of 28.55 (±5.45) μm, 12.02 (±3.15) μm and 5.52 (±0.75) μm, respectively. In addition, the central point formulations containing 15% leucine, glycine and alanine as additives demonstrated the smallest Dv50 with the mean being 2.43 (±0.29) μm. SEM images revealed distinctive morphological features of the formulations containing leucine.

Conclusion: This study clearly demonstrates the impact achieved by inclusion of leucine on the aerosol performance and morphology of mannitol dry powder formulations. Further investigation is proposed to understand any interaction effect produced from the amino acids, and will be applied in the design of a novel baseline carrier for inhalable dry powder pharmaceuticals.

PS-F-28

Examination of the Influence of Water-soluble Acids in Carboxylic Acid-terminated PLGA on Peptide-PLGA Sorption

Y.Liu[1], Y. Zhang[2], S. P. Schwendeman[1]

[1]Department of Pharmaceutical Science, College of Pharmacy, The University of Michigan, Ann Arbor, MI
[2]Division of Drug Delivery Systems, 3M, St. Paul, MN

Purpose: To investigate the effect of the water-soluble acids released from free acid-terminated poly(lactide-co-glycolic acid) (PLGA) on peptide sorption.

Methods: Free-acid terminated PLGA (RESOMER® RG502H, Boehringer-Ingelheim) was incubated as received at 37 °C in PBS or 0.1 M HEPES buffer, pH = 7.4 for 1, 3, and 24 h in the presence or absence of 1 mg/ml octreotide or leuprolide acetate salts. The kinetics and distribution of water-soluble acids in incubation medium was analyzed by a pre-derivatization HPLC method and PLGA acid number was determined by potentiometric titration with phenolphthalein indicator. Peptide sorption was determined by loss of peptide from solution, monitored by HPLC. The effect of water-soluble acids was determined by peptide sorption after 1 h with and without prior removal of free acids liberated by PLGA.

Results: In the absence of peptide, the PLGA acid number (11.7 ± 0.1, mean ± SD, n=3) rapidly decreased after 1 h reaching a quasi-equilibrium (~50% of the initial value) by 3 h irrespective of the buffer used. Over the same interval, lactic and lactoyllactic acids accumulated in the PBS with no detectable glycolic acid, accounting for the acids lost by the polymer (e.g., 107.1% and 107.2% mass balance at 1 and 3 h). However, significant glycolic acid appeared after 24 h, helping to increase the total number of acids from the polymer and release media by ~ 68% of original. Both peptides sorbed substantially to the 502H with 25% and 10% loss from octreotide and leuprolide solutions at 1 h, respectively. Interestingly, removal of acids after pre-incubation of PLGA led to either strong or weak inhibition of peptide sorption. For example, octreotide removal from solution was strongly inhibited, e.g.,

7.8%±1.8% and 6.2%±0.3% loss vs. 25.0%±2.3% control and that for leuprolide was not, e.g., 8.8%±0.6% and 7.4%±0.1% loss vs. 10.0%±0.8% control after 1 and 3 h pre-incubation, respectively.

Conclusions: The principal water-soluble acids released initially from 502H are lactic and lactoyllactic acids, which can have strong or weak effects on peptide sorption. These data may provide further insight into the mechanism of peptide sorption and acylation in carboxylic acid-terminated PLGAs.

PS-F-29

DNA lipoplex formulation: Effect of salt on characteristic properties

B. Moghaddam, D. Kirby, Q. Zheng and Y. Perrie

School of Life and Health Sciences, Aston University, Birmingham, UK.

Purpose: Previous research has shown cationic liposomes to be useful in delivery of nucleic acids both *in vitro* and *in vivo*. However liposomes prepared from cationic lipids have been shown to be influenced by salt concentrations as according to polyelectrolyte theory salt affects conformational properties as well as stability of polyelectrolytes. Previous studies have shown that low concentration of salt in lipoplex formulation will not affect stability of the formulation. Indeed recent studies have shown that the addition of low concentration of salt to cationic liposomes during complex formation could lead to an improved vaccine adjuvant action. The aim of the current research was to investigate the effect of salts on lipoplexes.

Methods: MLV and SUV liposomes composed of range of different lipids were prepared by hydration in dH_2O or PBS. In all cases, DNA complexes were formed by mixing the cationic liposomes with DNA at various concentrations. Their characteristics in terms of size and zeta potential were measured as well as DNA complexation.

Results: For all formulations tested the rehydration media was shown to influence both the size and zeta potential. Most notable was the inability to prepare DSPE:DOTAP liposomes in PBS. Additionally, rehydration of other formulations in PBS resulted in a decreased zeta potential compared to those prepared in dH_2O. In terms of the size, whilst no significant difference was measured for DOPE:DSTAP liposomes, prepared in either of the two aqueous media, DOPE:DOTAP vesicle size was increased by hydration in PBS compared to dH_2O. In terms of DNA adsorption, DOPE:DOTAP lipoplexes showed high association of DNA irrespective of the hydration media used.

Conclusion: Characterisation studies demonstrated that rehydration medium has a notable influence on the physiochemical characteristics lipoplexes: depending on the lipid structure, not all cationic lipids can support liposome formation in the presence of salts. The presence of salts within aqueous media influences both the vesicle size of the liposomes and their zeta potential; however did not adversely influence their ability to complex DNA.

PS-F-30

Development of w/o Microemulsions and Hydrogel Nanoparticles in w/o Microemulsions for Oral Delivery of Peptides and Proteins

D. Liu[1], S. E. Plevy[2, 3], R. J. Mumper[1, 3]

[1] Division of Molecular Pharmaceutics, Center for Nanotechnology in Drug Delivery, UNC Eshelman School of Pharmacy, University of North Carolina at Chapel Hill, Chapel Hill, NC 27599, USA
[2] Department of Medicine, Division of Gastroenterology and Hepatology, School of Medicine, University of North Carolina at Chapel Hill, Chapel Hill, NC 27599, USA
[3] UNC Lineberger Comprehensive Cancer Center, University of North Carolina at Chapel Hill, NC 27599, USA

Purpose: The purpose of these studies was to i) develop water-in-oil (w/o) microemulsions (MEs) and hydrogel nanoparticles (NPs) in w/o MEs for improved oral delivery of peptides and proteins, and ii) evaluate the delivery system *in vitro* and *in vivo*.

Methods: A w/o microemulsion system and hydrogel nanoparticles (NPs) in w/o MEs were developed according to the corresponding partial pseudo-ternary phase diagrams, and characterized in terms of viscosity, particle size, freeze fracture transmission electron microscopy (FFTEM) imaging, etc. A

lipophilic fluorescent marker, DiOC18(3), was applied to investigate the phase inversion behaviors of the w/o ME system. The system advantage of w/o MEs was evaluated *in vitro* using a marker molecule thrombin. An *in vivo* proof-of-concept study for intestinal delivery of cell penetrating peptides was evaluated using TAMRA-TAT in w/o MEs. TAMRA-TAT in water and TAMRA-control peptide in water served as controls. Fluorescent staining of gut tissue was examined using confocal microscopy.

Results: Both w/o MEs and hydrogel NPs in w/o MEs were formed spontaneously without the application of heating or high shear stress and stayed stable at room temperature. The phase inversion studies showed some evidence of w/o MEs inverted into o/w emulsions upon dilution into aqueous phase. *In vitro* studies indicated a potential better protection effect provided by w/o MEs compared to aqueous solutions alone. *In vivo* studies showed that TAMRA-TAT incorporated into w/o MEs resulted in much greater frequency of colonic cell staining compared to the controls. Further characterization and *in vitro* and *in vivo* evaluation of hydrogel NPs in w/o MEs are on-going.

Conclusion: The w/o ME system developed was a thermodynamically favored stable system, which could serve as a platform for oral delivery of water soluble drugs, especially heat-labile peptides or proteins.

PS-F-31

Lipid coated polyethylenimine complexes for enhanced DNA and siRNA delivery

J. Schäfer[1], S. Höbel[2], U. Bakowsky[1], A. Aigner[2]

[1] Department of Pharm. Technology and Biopharm., Philipps-University Marburg, Germany
[2] Department of Pharmacology, Philipps-University Marburg, Germany

Purpose: Positively charged polyethylenimines (PEI) are well known for efficient delivery of DNA for gene transfection and small interfering RNAs (siRNAs) for the induction of RNA interference (RNAi). Certain liposome formulations can act as transfection reagents and show increased endocytosis and influence endosomal escape. In this study we combine the favourable properties of both polyplexes and lipids resulting in a new formulation, the liposome-PEI complexes.

Methods: By adding freshly prepared liposomes to pre-formed polyplexes, we receive liposome-PEI complexes (lipopolyplexes). The lipopolyplexes are characterised regarding size, shape and zeta-potential and results are compared to their 'parent' polyplexes and liposomes. Furthermore, we investigate the influence of the lipidation of polyplexes on their toxicity, DNA transfection, siRNA mediated knockdown efficiency and their mechanism and kinetics of cellular uptake.

Results: The new liposome-polyethylenimine complexes form stable lipopolyplexes as optimal transfection reagents for DNA and siRNA and the lipidation of polyplexes generally decreases their toxicity. Our studies on DNA transfection and siRNA mediated knockdown show that certain lipopolyplexes based on rigid, negatively charged lipids are suitable as particularly efficient vehicles for nucleic acid delivery and are further improving DNA transfection. Analysing their mechanism and kinetics of cellular uptake confirms that the biological properties of lipopolyplexes are mainly determined by the liposome shell rather than the polyplex core.

Conclusion: Certain lipopolyplexes show improved biological properties over PEI complexes, thus representing potentially attractive non-viral vectors for gene therapy and RNAi.

PS-F-32

Studies for the development of drug delivery system using virus-like particle in HepG2 and CaSki cells

J-S. Hwang[1], H-J. Kim[2], C-W. Cho[1]

[1]College of Pharmacy, Chungnam National University, Daejeon 305-764, Republic of Korea
[2]College of Pharmacy, Chung-Ang National University, Seoul 156-756, Republic of Korea

Purpose: The human papillomavirus (HPV) virus-like particles (VLPs) possess a typical icosahedral lattice structure about 60nm in size and each VLP is formed by assembly of 72 L1 protein pentamers. It has been known that the VLP has a well-defined quaternary structure, and is capable of internalizing not only genes but also proteins, small molecules, and peptides. In addition, the L1 protein, one of the major capsid proteins of HPV virion, is able to self-assemble into VLPs when expressed in eukaryotic expression system. To initiate infection, papillomaviruses are presumed to attach to cells through interaction between the viral capsid and cell membrane components, i.e. the papillomavirus receptor. Based on the fact that virus can penetrate the cell, we studied whether the VLP originated from HPV 16 L1 (HPV 16L1 VLP) can enter into HepG2 cells, the human cancer cell lines, and CaSki cells, which is one of the human female cervical cancer cell lines and has HPV receptor.

Methods: After incubation of cells with the purified VLPs at amounts of 0.02nM to 0.3nM and several incubation times, the VLPs in HepG2 and CaSki cells were detected by western blot analysis (WB) using anti-HPV16 L1 monoclonal antibody. Simultaneously, Immunofluorescence staining to localize the VLP in cells was conducted using FITC-conjugated secondary antibody and mounting solution with DAPI.

Results: In WB analysis, VLP was detected in both of HepG2 and CaSki cells and increased according to the incubation time and amounts of VLP. Whereas somewhat degradants which may be deduced from VLPs were detected in the cells, which incubated with VLP longer than 3 hours. Moreover, the existence of VLP was observed in the cytosol of the HepG2 and CaSki cells using confocal microscopy.

Conclusions: From these data, we identified entrance of VLP to the cells and supposed that VLP can be used as a drug delivery system.

PS-F-33

Alpha-1-antitrpsin prevents doxorubicin-induced cardiomyopathy

M. Fueth[1], W. Li[1], S. Song[1]

[1]Department of Pharmaceutics, College of Pharmacy, University of Florida, Gainesville Florida.

Objective: The use of the antineoplastic drug doxorubicin is limited by its cumulative dose-dependent cardiotoxicity, which may involve in intense cardiac oxidative stress and inflammation. Development of a therapeutic strategy to prevent or treat doxorubicin-induced cardiomyopathy is desired. We and others have previously shown human alpha-1-antitrypsin (hAAT) has anti-inflammatory and antioxidative properties, and protects pancreatic beta cell from cytokine-induced apoptosis. In the present study, we investigated the feasibility of using hAAT to protect heart from doxorubicin-induce cardiotoxicity.

Methods: *Two different mouse models,* C57BL/6J mice receiving hAAT (2mg/3days) and hAAT transgenic NOD mice were used. After an *intraperitoneal (IP) injection* of doxorubicin (15mg/kg)*, heart function were monitored by* electrocardiography (ECG) and serum troponin I levels. Body weight was evaluated. Pathological examinations in heart tissue were also performed. In addition, we investigated the effect of hAAT on doxorubicin-induced apoptosis *in vitro* in C2C12 cells using MTT assay.

Results: In C57BL/6 mice, hAAT treatment significantly inhibited doxorubicin-induced body weight loss, serum troponin I elevation and alternations of QT- and QRS-interval in ECG. Similarly, hAAT transgenic mice showed significant reduction of doxorubicin-induced toxic effects than control mice (without hAAT). *In vitro* studies showed that hAAT significantly reduced doxorubicin-induced apoptosis and cell death.

Conclusion: Our results suggest that hAAT may potentially serve as a novel cardioprotective agent against doxorubicin-induced cardiac injury.

PS-F-34

Solvent-sensitive Dyes for Multiplexed Live Cell Imaging

C-W. Hsu[1], D. Gremyachinskiy[2], A. Toutchkine[2], K. Hahn[1, 2, 3]

[1]Division of Medicinal Chemistry and Natural Products, Eshelman School of Pharmacy, University of North Carolina at Chapel Hill, Chapel Hill, NC
[2]Department of Pharmacology, School of Medicine, University of North Carolina at Chapel Hill, Chapel Hill, NC
[3]Lineberger Comprehensive Cancer Center, University of North Carolina at Chapel Hill, Chapel Hill, NC

Purpose: Many cell behaviors are mediated by transient signaling at specific locations, with subseconds and submicron coordination. Live cell imaging enables the study of such dynamic processes. It has been challenging to monitor multiple cellular events simultaneously due to the overlapping excitation/emission spectra of current biosensors. In addition, introducing two or more biosensors in the same cell tends to disrupt normal cell function. The merocyanine dyes used in our dye-based biosensors are brighter than fluorescent proteins and are highly sensitive to local changes in polarity and viscosity. Therefore smaller amount of biosensors are required, causing less biological perturbation. In this study, we aim to develop red-shifted solvent-sensitive dyes and visualize multiple protein activities in a single living cell.

Methods: Here we describe strategies to generate new merocyanines for multiplexed live cell imaging. This work includes two parts: 1) red-shifting the wavelengths of merocyanines and 2) developing novel ratiometric merocyanines.

Results: The red-shifted merocyanines are excited at near infrared regions where background autofluorescence is greatly reduced. The ratiomeric response of this type of dye-based biosensor is obtained by combining a merocyanine molecule and a nonresponsive fluorophore. To accommodate multiple biosensors in the same cell, we also developed new merocyanines exhibiting intrinsic ratiometric response. The intrinsic ratiometric response utilizes changes in both intensity and wavelength in excitation spectra. Thus no second fluorophores are required for this type of dye-based biosensor.

Conclusion: The wavelengths of new merocyanines are complementary to the existing FRET biosensors, enabling the use of multiple biosensors in a single cell. These multiplexing tools will be very useful for studying complex parallel pathways such as the mitogen-activated protein kinase (MAPK) signaling network or sequential regulation cascades such as the Src-RhoGDI-Cdc42 pathway.

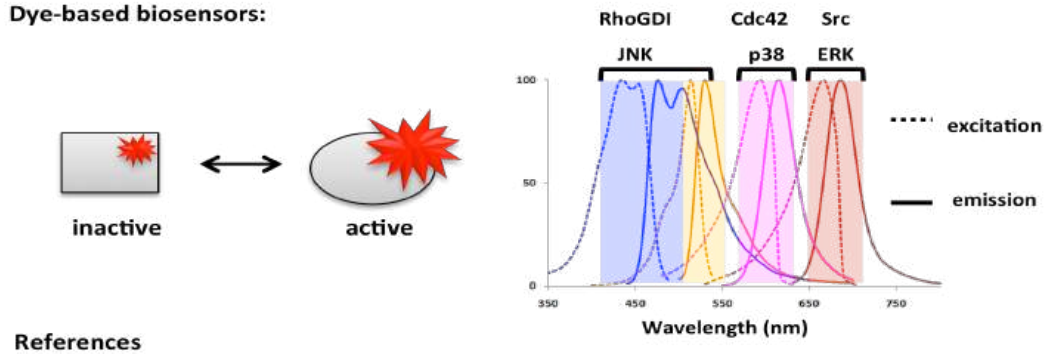

References
1. Nalbant P *et al* *Science* 305: 1615-1619 (**2004**)
2. Machacek M *et al* *Nature* 461: 99-103 (**2009**)

GPEN.2010
University of North Carolina at Chapel Hill

PS-F-35

Detection of Colorectal Cancer Using Peanut Agglutinin-immobilized Fluorescent Nanospheres in the Orthotopic Animal Model

H. Higashino[1], S. Sakuma[1], Y. Masaoka[1], M. Kataoka[1], K. Hiwatari[2], H. Tachikawa[2], Y. Shoji[2], R. Kimura[2], K. Nakamura[2], H. Ma[3], Z. Yang[3], L. Tang[3], R. M. Hoffman[3,4], S. Yamashita[1]

[1] Setsunan University
[2] ADEKA Co.
[3] AntiCancer Inc.
[4] University of California at San Diego

Purpose: We are investigating a novel colonoscopic imaging agent that can recognize tumor-derived changes in the large intestinal mucosa. The imaging agent is peanut agglutinin (PNA)-immobilized fluorescent nanospheres. PNA is a targeting moiety that binds to β-D-galactosyl-(1-3)-N-acetyl-D-galactosamine, which is the terminal sugar of the Thomsen-Friedenreich (TF) antigen that is specifically expressed on the mucosal side of colorectal cancer cells. Our previous study using a loop of the tumor-bearing cecum showed that the imaging agent recognized millimeter-sized tumors on the cecal mucosa with high affinity and specificity. This paper reports in vivo real-time imaging of HT-29 cells, TF antigen-positive human colorectal cancer cells, that were orthotopically implanted on the colon of nude mice.

Methods: Vinylbenzyl group-terminated poly(N-vinylacetamide) and vinylbenzyl group-terminated poly(methacrylic acid) were copolymerized with styrene in an ethanol/water mixture containing coumarin 6. PNA was subsequently immobilized on the surface of fluorescent nanospheres by coupling the amino groups of PNA with the carboxyl groups of poly(methacrylic acid). HT-29 cells were implanted orthotopically on the serosal side of the descending colon of nude mice, and the mice were maintained for several weeks. After enema administration of the imaging agent suspension to overnight-fasted mice, the colon was washed with PBS. During the washing, the fluorescence in the abdomen was monitored with an in vivo imaging apparatus.

Results: Imaging agent-derived fluorescence was observed throughout the colon after the luminal side was filled with the imaging agent. Most of the imaging agent was washed out with PBS; however, there was still fluorescence in the position on which HT-29 cells were implanted. The histological evaluation revealed that the cancer cells invaded the mucosal side in this position. On the contrary, when nude mice that did not undergo cancer cell implantation were used, no fluorescence was observed after washing the luminal side of the colon with PBS.

Conclusion: It is anticipated that real-time diagnosis of small-sized colorectal cancer is achieved through observations of a clear fluorescence contrast between the normal and tumor tissues because PNA-immobilized fluorescent nanospheres (the imaging agent) can recognize tumors specifically.

PS-F-36

Thermosensitive flower-like micelles based on pNIPAM-PEG-pNIPAM

A.J. de Graaf[1], K.W.M. Boere[1], J. Kemmink[2], S.H.E. Gradmann[3], T. Vermonden[1], C.F. van Nostrum[1], D.T.S. Rijkers[2], M. Baldus[3], E. Mastrobattista[1], W.E. Hennink[1]

[1] Department of Pharmaceutics, University of Utrecht, the Netherlands
[2] Department of Medicinal Chemistry & Chemical Biology, University of Utrecht, the Netherlands
[3] NMR spectroscopy Research Group, University of Utrecht, the Netherlands

Purpose: Polymeric micelles are widely studied as delivery vehicles for hydrophobic, low molecular weight drugs. Two important features are their generally low critical micelle concentration and small size (several tens of nanometers) which renders them suitable for passive targeting using the enhanced permeability and retention effect.[1]
Micelles with a hydrophobic core and a hydrophilic shell are obtained by dispersing amphiphilic AB blockcopolymers in water. ABA triblock copolymers with a hydrophilic midblock flanked by two hydrophobic blocks have been hypothesized to self-assemble into so-called 'flower-like micelles'.[2] Evidence that such structures are formed is, however, only indirect. Because of their small size a anticipated higher stability, flower like micelles might have potential advantages over classical micelles based on AB blockcopolymers for drug delivery applications.
In the present study we compare micelles of AB and ABA block copolymers of the thermosensitive poly(*N*-isopropylacrylamide) (pNIPAm), block A, and poly(ethylene glycol) (PEG), block B. Using NMR relaxometry we aim to prove that the hydrophilic block of the copolymer micelles is less flexible in the ABA block copolymer compared to the AB block copolymer due to adoption of a looped conformation in flower-like micelles. Such decreased flexibility may e.g. aid in forcing a coupled active targeting ligand to position itself on the outside of a micelle's corona.

Methods: mPEG-pNIPAM and pNIPAM-PEG-pNIPAM block copolymers were synthesized by atom transfer radical polymerization of pNIPAm blocks from functionalized $mPEG_{2000}$ and PEG_{4000} macroinitiators, respectively. The pNIPAM block length was varied from 4 kDa to 16 kDa. Micelles were formed by heat-shocking aqueous polymer solutions to 50°C and equilibrating at 40°C. The resulting micelles were characterized by Dynamic Light Scattering (DLS). ^{1}H NMR relaxometry of the polymers dissolved in water having 16kDa pNIPAM blocks was performed at 500 MHz as a function of temperature. T_1 relaxation was studied using the inversion recovery method and T_2 relaxation using the Carr-Purcell-Meiboom-Gill sequence. In both cases, relaxation times were obtained by nonlinear least squares fitting of a bi-exponential function.

Results: The diblock and triblock copolymers were prepared in good yield with polydispersities of 1.4 (diblock) and 1.5-1.9 (triblock). Cloud points were similar for diblock and triblock copolymers and decreased with pNIPAM block length to 36.5 °C for the 16 kDa pNIPAM. The hydrodynamic radius and polydispersity of the resulting micelles also decreased with increasing pNIPAM block length, to 32 nm (PDI 0.05) and 24 nm (PDI 0.09) for di- and triblock copolymer with 16 kDa pNIPAM, respectively. T_1 values of the PEG blocks increased linearly with temperature for both polymers, however for the triblock copolymer the slope became markedly smaller above the cloud point. The curve of T_2 vs. temperature was almost linear for the diblock copolymer, whereas the T_2 of the triblock copolymer showed a large drop at the cloud point. This demonstrates a dramatically lower PEG chain mobility in micelles of the triblock copolymer

Conclusion: AB and ABA amphiphilic thermosensitive block copolymers have been prepared from PEG and pNIPAM. They self-assemble into very similar structures, however the mobility of the hydrophilic A block in micelles of a BAB copolymer is highly reduced. This indicates a looped conformation, consistent with the formation of flower-like micelles.

[1] For a review, see e.g. V.P. Torchilin, Pharm. Res. 2007;24(1), p1-16
[2] Z. Zhou and B. Chu, Macromolecules 1994;28, p2025-2033

PS-F-37

PAMAM Dendrimers as Potent Tight Junctional Modulators

B. Avaritt[1], D. Goldberg[1,2], H. Ghandehari[3], P. Swaan[1]

[1] Department of Pharmaceutical Sciences, Center for Nanomedicine and Cellular Delivery, University of Maryland, Baltimore, MD
[2] Fischell Department of Bioengineering, University of Maryland, College Park, MD
[3] Departments of Pharmaceutics and Pharmaceutical Chemistry & Bioengineering, Center for Nanomedicine, Nano Institute of Utah, University of Utah, Salt Lake City, UT

Purpose: Poly (amidoamine) (PAMAM) dendrimers show promise in oral drug delivery due to their ability to translocate across the epithelial layer of the gut. It has been established that dendrimers are partially transported by the paracellular route; however, the mechanisms of tight junctional modulation and the size of the openings created are still unknown.

Methods: The mechanisms of tight junctional opening by anionic G3.5 and cationic G4 PAMAM dendrimers in Caco-2 cell monolayers were investigated. Permeability of lucifer yellow and FITC-dextran (4 kD), differentially-sized paracellular permeability markers, was measured in the presence and absence of dendrimers. Monolayers were also treated with known permeation enhancers including ethylene glycol tetraacetic acid (EGTA) with calcium free buffer and sodium caprate, for comparison. Accessibility of tight junctional proteins occludin, ZO-1, and actin after dendrimer treatment was investigated using confocal laser scanning microscopy.

Results: Treatment of monolayers with G3.5 and G4 dendrimers caused a two- to six-fold increase in lucifer yellow and FITC-dextran permeability compared to the untreated control, indicating that dendrimers open tight junctions. Sodium caprate and G4 dendrimers caused a similar increase in marker permeability, while EGTA created a 500-fold increase in marker permeability. Permeability of lucifer yellow and FITC-dextran measured 48 hours after treatment removal returned to pre-treatment levels, illustrating that tight junction opening by dendrimers is reversible. Dendrimer treatment produced a two-fold increase in occludin and ZO-1 accessibility in cell monolayers as compared to untreated monolayers. Treated monolayers also exhibited a four-fold increase in actin accessibility.

Conclusion: PAMAM dendrimers are capable of opening the tight junctions of epithelial monolayers to allow the paracellular transport of molecules with a molecular weight of at least 4 kD, the highest molecular weight tested in this study. Dendrimers cause marker permeability increases comparable to sodium caprate, but far less than EGTA; suggesting that dendrimers do not open tight junctions by extracellular calcium chelation, but instead may initiate an intracellular signaling cascade similar to sodium caprate. The increased tight junctional protein accessibility confirms tight junctional modulation and indicates that multiple proteins are involved. These findings will guide the design of oral drug delivery systems utilizing dendrimers.

PS-F-38

Preparation of High Payload Dexamethasone Palmitate Nanoparticles and the Enhancement of Tumor Cell Uptake

J.K. Kim, X. Lu, M. Jay

Division of Molecular Pharmaceutics, Eshelman School of Pharmacy, University of North Carolina, Chapel Hill, NC

Purpose: To engineer and characterize dexamethasone palmitate (DEX-P)-loaded nanoparticles (NPs) for enhancing the delivery of DEX to tumors in order to reduce the elevated tumor interstitial fluid pressure.

Methods: DEX-P was incorporated into solid lipid NPs using the nanotemplate engineering technology. The preparation process was optimized for maximum drug entrapment and drug loading by using radiolabeled lipid and drug, [^{14}C]-stearyl alcohol and [^{3}H]-DEX-P, respectively. The entrapment efficiency of DEX-P in NPs was determined by ultrafiltration and gel permeation chromatography (GPC). The amount of drug and lipid was calculated according to the specific radioactivity. The stability of the drug association with NPs in human plasma was studied by incubating the NPs with 50% human plasma at 37°C for 24 h. The uptake of DEX-P and DEX-P NPs into human lung epithelial carcinoma A549 cells was compared at a concentration lower than the IC_{50}.

Results: DEX-P-loaded NPs with a drug-to-lipid mass ratio of 1:1 showed uniform particle size below 150 nm. This optimized formulation exhibited better drug distributions based on the GPC profile compared to the previous formulation with low drug-to-lipid ratio. In the previous formulation, the drug deposited in the two populations containing high or low amount of lipids although the particle size exhibited narrow distribution. For both formulations the entrapment efficiency of DEX-P as determined by ultrafiltration was > 93%. After incubating the NPs with human plasma at 37°C for 24 h, <10% of the drug formed aggregates which were not able to pass through a 0.2 μm filter and <4% of the drug was released from the NPs. Tumor cell uptake of DEX-P achieved a 10-fold increase by incorporation into the NPs.

Conclusion: The high DEX-P payload in NPs might make this formulation amenable to FDA approval for ultimate use in human clinical trials. Moreover, the incorporated DEX-P was associated with NPs after a 24 h-incubation in human plasma. The incorporation of DEX-P into NPs dramatically increased the tumor cell uptake of DEX-P, suggesting the potential application for enhancement of tumor delivery of DEX and improving the efficacy of chemotherapeutic agents.

PS-F-39

Development of Nanomaterial Immune Conjugates (NICs) to treat Multiple Sclerosis

Joshua Sestak[1] and Cory Berkland[1,2]

[1]Pharmaceutical Chemistry Dept, The University of Kansas
[2]Chemical and Petroleum Engineering Dept, The University of Kansas

Purpose: To develop a multivalent peptide-polymer complex (NIC) displaying signal-1 (antigen), signal-2 (targeting), or combination of both signal-1 and signal-2 peptides using facile chemistry and simplified purification methods. After manufacture the *in vivo* lymphatic drainage characteristics and therapeutic efficacy to treat Multiple Sclerosis was evaluated.

Methods: This project utilized 9-fluorenylmethyloxycarbonyl-protected amino acid chemistry on polyethylene glycol-polystyrene resins to manufacture peptide haptens. Peptides were purified by Prep HPLC using a C18 column. Purified peptides were conjugated to polymer back bones using oxime chemistry to manufacture NICs. NICs were purified by dialysis and dialyzed product was lyophilized. NICs were evaluated by gel permeation chromatography and mass spec to determine conjugate size and RP-HPLC to determine the concentration and ratio of conjugated peptides on the polymer. *In vivo* lymphatic drainage characteristics were determined by using a CRI Maestro imaging system and fluorescently tagged NICs. Therapeutic efficacy of the purified NIC products was evaluated in the mouse experimental autoimmune encephalomyelitis MS model, (EAE), by tracking animal weight and clinical score.

Results: The NIC products could be easily synthesized and characterized. The characterization results showed the expected increase in molecular weight as well as verified concentration of peptides conjugated to the polymer. Additionally, it was demonstrated peptides could be conjugated in expected ratios with minimal variation from batch to batch. Dose ranging studies in the EAE model were established the optimum dose to achieve significant disease suppression compared to controls. Additionally, *in vivo* studies have been completed to evaluate the effect of size, signaling peptide array, long term effectiveness, and suppression of side effects such as anaphylaxis upon chronic dosing. By

utilizing *in vivo* imaging we are able to track the NIC conjugates after injection and optimize injection schedule and site to achieve the desired delivery profile.

Conclusion: A multivalent, poly-haptenated, nanomaterial conjugate was developed and successfully characterized. When evaluated in the EAE model the NICs provided significant suppression of disease and relapses compared to controls. Additionally, with the use of *in vivo* imaging it has been seen that injection site plays a critical role in the drainage of the NIC post injection.

PS-F-40

ABSTRACT NOT AVAILABLE

PS-F-41

1D Gel Electrophoresis as a first step for analysis of the plasma proteins adsorbed on nanoparticles

Karim Sempf, Jörg Kreuter

Institute of Pharmaceutical Technology, Goethe University Frankfurt/Main, Germany

Purpose: Plasma proteins play a very important role in the biodistribution of nanoparticles. In order to optimise the delivery of drugs across the blood-brain barrier using these colloidal carriers, the protein adsorption profile of nanoparticles after their incubation in plasma was studied. A combination of 1D gel Electrophoresis and nLC-MALDI-MS/MS was employed to investigate the nature and the quantity of the proteins absorbed on the surface of the nanoparticles.

Methods: Three human plasma batches provided by the DRK Blutspendedienste Frankfurt am Main, Germany, served as plasma samples. For the preparation of the 1D Gels the MiniProtean Tetra cell from Biorad was used. The PLGA and PLGA-PEG Nanoparticles were synthesised using the double-emulsion/evaporation method.
The nanoparticles were incubated with the plasma for 30 min at 37 °C followed by centrifugation of the nanoparticle for 30 min at 20000 rpm. Thereafter the particles were washed twice with water and again centrifuged. Desorption of the adsorbed plasma proteins was achieved with 2.5 % SDS and 30 mM DTE or 8 % urea after resuspension. These samples were then analysed by 1D GEL electrophoresis.

Results: The analysis of the 1D gels showed that urea can replace SDS which is problematic for nLC-MALDI-MS/MS analysis. Both showed similar protein patterns although the desorbed quantities were lower with urea. With the exception of apolipoprotein E the amount of plasma proteins was lower with PLGA-PEG nanoparticles than with PLGA nanoparticles.

Conclusions: Plasma protein desorption procedure can be carried out with urea instead of SDS/DTE, the amount of protein desorbed is lower but detectable. In contrast to PLGA nanoparticles PLGA-PEG nanoparticles appear to adsorb apolipoprotein E which is a lipoprotein that enables interaction of the nanoparticles with the respective receptors on the blood-brain barrier and the drug delivery to the brain by these particles.

PS-F-42

Peptide Conjugation with Amphiphilic Block Copolymers for Enhanced Delivery

M. Ueda, X. Yi, A. Kabanov

Department of Pharmaceutical Sciences, College of Pharmacy, and the Center for Drug Delivery and Nanomedicine, University of Nebraska Medical Center, Omaha, NE.

Purpose: Conjugation of amphiphilic block copolymers to protein has previously been shown to enhance cellular uptake and some copolymers have resulted in beneficial biological effects not seen in polymer naive protein. We investigated further the potential of conjugating an amphiphilic block copolymer to a smaller molecular weight peptide species using degradable linkers.

Methods: Peptides were synthesized with the addition of an N-terminus protection group to allow for isolated C-terminus reactions. Conversely, protection groups were added to the C-terminus with an exposed N-terminus for amine linkage. The peptide was allowed to react with an excess of the linker to achieve the maximum yield of "activated peptide." Various amphiphilic block copolymers were used in reactions with the activated peptide. Peptide-copolymer conjugates were purified by Fast Protein Liquid Chromatography and fractions were collected. Fractions were concentrated and evaluated by mass spectrometry to detect the addition of the block copolymer as compared to native peptide and unmodified block copolymer. The peptide-copolymer conjugates were evaluated against each other (with native peptide and unmodified block copolymer controls) for yield, activity, and cellular uptake.

Results: Degree of modification of the peptide is low; analysis by mass spectrometry shows the conjugation of peptide with amphiphilic block copolymers is successful; however, there is still a high percentage of native peptide that does not react with the copolymer species. The conjugation reaction is being optimized to increase reaction success.

Conclusion: Conjugation of amphiphilic block copolymers to peptide species is achievable; however, we need to increase yield to continue further with characterization and move into *in vitro* and *in vivo* experiments.

PS-F-43

Enhanced Uptake of Classical Clathrin Mediated Endocytosis Marker (Transferrin) in the Presence of Polyplexes

P. N. Williams[1], G. Sahay [2], J. Kim[1], H. Vishwarao[1], P. Sorgen[1], T. K. Bronich[1], A. V. Kabanov[1,3]

[1] Department of Pharmaceutical Sciences and Center for Drug Delivery and Nanomedicine, College of Pharmacy, University of Nebraska Medical Center, Omaha, NE 68198-5830
[2] David H. Koch Institute for Integrative Cancer Research Massachusetts Institute of Technology, Boston, MA 02139
[3] Faculty of Chemistry, M.V. Lomonosov Moscow State University, 119899 Moscow, Russia

Purpose: Our study evaluates the effects of DNA/polycation complexes (polyplexes) on clathrin-mediated endocytosis in breast cancer cell lines. Breast cancers are known to have many different subtypes including Estrogen Receptor/ Progesterone Receptor Positive (ER/PR+), Human Epidermal Growth Factor Receptor 2 (HER/neu), and Triple Negative which lead to different treatment plans.

Methods: In this study, polyplex were prepared using plasmid DNA and polyethyleneimine (PEI). Tranferrin (Tf) was used as a marker for clathrin mediated endocytosis and was administered alone and in the presence of polyplexes. Dynamic light scattering, quantitative flow cytometry, and laser scanning live cell confocal microscopy were used.

Results: Polyplexes were shown to induce significant increases in the uptake of Tf but showed no effect on the uptake of cholera toxin B (CTB), a marker for caveolae-mediated endocytosis. The increase in uptake of tranferrin was not breast cancer subtype specific. This increase was also seen in mouse fibroblasts, MDR phenotype expressing cells, and human ovarian carcinoma cells devoid of CTB. This increase in uptake was not seen with both DNA alone and polycation alone.

Conclusion: Polyplexes increase uptake of Transferrin, a classical marker for clathrin-mediated endocytosis with no regard for clinically relevant differences in cells. In future work, polyplexes could be used to enhance clathrin mediated endocytosis of nanomedicines.

PS-F-44

Effect of Molecular Weight and Charge on Lymphatic Drainage Patterns and Kinetics of Localized Drug Carriers

Taryn R. Bagby[1], Sharadvi Thati[1], Shaofeng Duan[1], Shuang Cai[1], M. Laird Forrest[1]

[1]Department of Pharmaceutical Chemistry, University of Kansas, Lawrence, KS

Purpose: To determine the effect of molecular weight and surface charge on the disposition, extent and kinetics, of lymphatic drainage of polymer-dye conjugates after subcutaneous injection using in vivo imaging.

Methods: A near IR dye, IR820, was conjugated to six different molecular weights (MW) of hyaluronan (HA), and multi-arm polyester/polysaccharide star polymers with various anionic surface charge densities and molecular weights. Size exclusion chromatography and dynamic light scattering were conducted to correlate molecular weight and size. Mice were injected subcutaneously in the right hind footpad or right front forearm with 10 µL of a 1-mg/mL (dye conc.) solution of polymer-dye conjugates of various molecular weights (6.4kD - 697kD) and surface charges. Whole animal fluorescent imaging was used to track the kinetics and disposition of the polymer-dye conjugates after injection. The animals were imaged at pre-determined intervals using a Maestro Flex imager (ex 730 nm, em 800-950 nm).

Results: For the hind footpad injections**,** as the molecular weight increases, the lymphatic uptake and distribution decrease; except for 357kDa HA, which exhibits rapid lymphatic uptake and slowly clears from the lymph nodes. Low to mid-ranged molecular weights (6.4 - 74 kDa) drained from the injection site and accumulated in the inguinal and iliac nodes, subsequently cleared from the lymphatics into systemic circulation. Larger MWs (≥132 kDa, except 357 kDa) exhibited slow injection site drainage and were highly retained by the inguinal node. Similar distribution and drainage patterns into the axillary lymph node package were observed for the front forearm injections for all molecular weights except 357 kDa, which drained rapidly and was highly retained by the axillary lymph node. The AUC for 357 kDa HA-IR820 is 2.5 - 3 times higher than that for the other molecular weights.

Conclusions: There is an optimum range for lymphatic uptake of subcutaneously injected particles: larger particles will remain largely confined to injection site, particles 10-80 nm are preferentially taken up by the lymphatics, and smaller particles will be quickly absorbed and cleared by systemic circulation. Therefore, appropriate size and charge density can be specifically tailored to the unique release characteristics of each drug carrier and disease model.

PS-F-45

Dual Therapeutic-Imaging Nanovectors for Augmented Delivery of Dexamethasone to Tumors

X. Lu, J.K. Kim, M. Jay

Eshelman School of Pharmacy, University of North Carolina, Chapel Hill, NC

Purpose: To deliver dexamethasone (DEX) to tumors via solid lipid nanoparticles (NPs) to enhance uptake of chemotherapy while minimizing systemic toxicities, and to simultaneously assess tumor uptake by magnetic resonance imaging (MRI) or single photon emission computed tomography (SPECT).

Methods: Dexamethasone palmitate (DEX-P) was synthesized and incorporated into NPs using the nanotemplate engineering method. Pegylation of the NPs as a means to enhance their stealth properties

was evaluated by measuring the adsorption of [^{125}I]-IgG onto the surface of the NPs and by quantifying the uptake of ^{14}C-labeled NPs by murine macrophages. The stability of the solid lipid NPs containing [^{3}H]-DEX-P in plasma from various sources was assessed by measuring the release of tritium from the NPs. DMPE-DTPA was added to the formulation to prepare DEX-P NPs with Gd or ^{111}In atoms bound to their surface to produce dual imaging-therapeutic nanovectors. The biodistribution profiles, pharmacokinetics and the enhancement in the tumor region were studied following administration of Gd-NPs or ^{111}In-NP to nude mice bearing A549 lung carcinoma xenografts.

Results: Pegylated DEX-P nanoparticles of uniform particle size (120 nm) were prepared with >90% entrapment efficiency. Improved stealth properties were demonstrated *in vitro* by a 27-fold lower adsorption of IgG compared to control latex particles and reduced uptake of ^{14}C-labeled NPs by macrophages. Extensive release of radioactivity was observed from [^{3}H]-DEX-P NPs following a 24-hour incubation in mouse plasma and tumor homogenate, while only a small amount was released in human plasma. The amount of the radioactivity released in plasma obtained from carboxylesterase-deficient mice (Es1e(-/-)/SCID) was significantly reduced. MR and SPECT imaging demonstrated the significantly enhanced tumor uptake of Gd-NPs or ^{111}In-NP.

Conclusion: In humans, pegylated DEX palmitate NPs are expected to augment the delivery of the prodrug to tumors and bioresponsively release DEX to improve the efficacy of chemotherapeutic agents. Tumor uptake of the nanovectors can be assessed by MRI and SPECT.

PS-F-46

Paclitaxel Nanocrystals for Overcoming Multidrug Resistance in Cancer

Yang Liu, Leaf Huang, and Feng Liu

Division of Molecular Pharmaceutics, Eshelman School of Pharmacy, University of North Carolina at Chapel Hill, Chapel Hill, North Carolina 27599-7360

Purpose: Multidrug resistance (MDR) represents a major challenge in the clinical cure of cancer. Elevated expression of P-glycoprotein (P-gp) plays a key role in mediating the resistance to bulky anticancer agents such as paclitaxel (PTX). Here we developed a PTX nanocrystal formulation using D-R-tocopheryl polyethylene glycol 1000 succinate (TPGS) as the sole excipient. TPGS serves as a surfactant to stabilize the nanocrystals and a P-gp inhibitor to reverse MDR.

Methods: The nanocrystals were prepared by the method of the stabilization of nanocrystal. The size and morphology of the nanocrystals were studied by transmission electron microscopy, and the crystalline structure was determined by powder X-ray diffraction. Particle size of nanocrystals was measured to evaluate the stability. The release kinetics was assessed *in vitro* by dialysis. Cytotoxicity of PTX/TPGS nanocrystals was evaluated in NCI/ADR-RES, KB and H460 cells. Cellular apoptosis was assessed using flow cytometry by Annexin-V/PI staining in NCI/ADR-RES cells. *In vivo* anticancer effects were investigated in the xenograft model established in mice using NCI/ADR-RES cells.

Results: PTX/TPGS nanocrystals are rod shape with moderate uniform particle size. The average width is about 40nm and the length is around 150nm. The size of nanocrystals remained stable at room temperature for more than two weeks. The *in vitro* drug release profile showed that the nanocrystals exhibited sustained release kinetics compared to Taxol, which is the clinical paclitaxel formulation. PTX/TPGS nanocrystals and other formulations greatly inhibited cell proliferation in KB and H460 cells. However, in NCI/ADR-RES cells, which overexpress P-gp and are resistance to PTX, PTX/TPGS nanocrystals exhibited significantly enhanced anti-proliferation effect cells over other formulations. PTX/TPGS nanocrystals also showed potent apoptosis-inducing effect (>95%) in NCI/ADR-RES cells. In the *in vivo* study, Taxol given at a dose of 10 mg/kg was generally ineffective in inhibiting tumor growth. An obvious tumor regression was observed in animals treated with10 mg/kg of PTX/TPGS nanocrystals, indicating a significantly enhanced tumor inhibition effect over Taxol ($p < 0.01$).

Conclusion: We have demonstrated that PTX/TPGS nanocrystals can provide a variety of benefits including high drug loading capacity, high stability, sustained release, and most importantly, the ability to overcome MDR both *in vitro* and *in vivo*. This nano-scaled formulation may provide a novel strategy for overcoming multidrug resistance in cancer therapy.

PS-F-47

Novel synthetic dextran-oleate-cRGDfK conjugate for self-assembled nanoparticle in targeted chemotherapeutic delivery of paclitaxel

Zhe Wang, Ting Yee Lee, Felicia Liew, Paul Ho

Laboratory for Experimental and Applied Pharmacokinetics and Pharmacodynamics (LEAP),Department of Pharmacy, National University of Singapore

Purpose: Nanomedicine holds great potential to delivery chemotherapeutic drugs for fighting against cancers. Nowadays, there are numerous drug delivery systems available for effective anticancer drug delivery. Herein, we reported a novel synthetic biocompatible amphiphilic material used as the surfactant for nanoparticle preparation via nanoprecipitation method to deliver paclitaxel for anticancer therapy.

Methods: To prepare the amphiphilic materials, fatty acid was conjugated with dextran which was further decorated with cRGDfK peptide for active targeting purpose. This new material was further used as the surfactant to form nanoparticle with PLGA via a new self-assembled nanoprecipitation method. A prototype anticancer drug, paclitaxel, was encapsulated in this novel nanoparticle.

Results: The NMR and FTIR confirmed the successful conjugation of oleic acid to dextran, and CMC of the amphiphilic conjugate was determined to be 0.5mg/ml. The resultant nanoparticle had a high drug loading efficiency at 47.1%. And the release of paclitaxel from the nanoparticle presented sustained release manner. In cultured assays, The RGD directed active ability could be reversed by adding free RGD ligand in the culture medium. What is more, the resultant drug loaded targeting nanoparticle showed high therapeutic efficacy to induce DAN fragmentation demonstrated by TUNEL assay, and Caspase 3/7 activation as determined by flow cytometry in αvβ3 integrin overexpressed breast cancer cells.

Conclusion: These results suggest that our novel drug loaded targeting nanoparticle could more effectively induce apoptosis in tested cancer cells than that of Taxol®. Thus, our novel drug delivery strategy may open another window in cancer therapy.

PS-F-48

Self-assembled core-shell nanoparticle decorated with both hyaluronic acid and RGD peptide for the targeted delivery of paclitaxel to breast cancer cells

Z. Wang[1], F. G. Liew[1], P.C. Ho[1]

[1] Laboratory for Experimental and Applied Pharmacokinetics and Pharmacodynamics (LEAP[2])
[2] Department of Pharmacy, National University of Singapore

Purpose: Targeted therapeutic nanoparticles have been substantially explored for chemotherapeutic drugs delivery. In particular human mammary carcinoma cells, there is a simultaneous overexpression of CD44 and integrins receptors. These receptors bind to hyaluronic acid (HA) and arginine-glycine-aspartic acid (RGD) mimic peptides, respectively. In this study, we proposed that HA and RGD surface-modified nanoparticles would enhance uptake of paclitaxel to cancer cells, hence, effectively induce apoptosis in cancer cells for anticancer therapy.

Methods: Distearoylphosphatidylethanolamine (DSPE)-HA-cRGD conjugate was first yielded with EDC chemistry through amide bond between HA and DSPE, followed by conjugation of RGD on HA. Functional nanoparticles loaded with paclitaxel were prepared through nanoprecipitation method using the as-synthetic conjugate and poly(lactide-co-glycotic acid) (PLGA) as building-up matrix.

Results: The NMR and FTIR results confirmed the conjugation formation. And the resultant nanoparticle had an average size of about 170nm with narrow size distribution. TEM picture showed that the nanoparticles were spherical and well-dispersed. *In vitro* cytotoxicity effects of the cRGD-HA-DSPE-PLGA-Paclitxel nanoparticles were evaluated using MDA-MD-231 human mammary carcinoma cells via MTT assay. These two ligands targeting nanoparticles proved to enhance cellular uptake due to high affinity to CD44 and αvβ3 integrin receptors on cancer cells. In addition, paclitaxel in nanoparticles were found to retain and exhibit high efficacy in inducing apoptosis via terminal deoxynucleotidyl transferase dUTP nick end labelling (TUNEL) and caspase 3/7 activation assays compared those of Taxol®.

Conclusion: These results suggest that two ligands targeting cRGD-HA-DSPE-PLGA-Paclitaxel nanoparticles could be potentially an effective drug delivery vehicle for chemotherapy.

PS-F-49

Fluorescent molecular rotors DCVJ and CCVJ detect protein aggregation in polysorbate-containing monoclonal IgG formulations

Andrea Hawe, Vasco Filipe, Wim Jiskoot

Leiden University, Leiden/Amsterdam Center for Drug Research

Purpose: The aim was to evaluate fluorescent molecular rotors (DCVJ and CCVJ), which are mainly sensitive to viscosity, for the characterization of polysorbate-containing monoclonal IgG formulations and compare them to the polarity sensitive dyes ANS, Bis-ANS and Nile Red.

Methods: Monoclonal IgG formulations with polysorbate 20 or 80 were stressed below the aggregation temperature and analyzed by steady state fluorescence, time-resolved fluorescence, and HP-SEC with UV and fluorescent dye detection (Bis-ANS and CCVJ). Furthermore, commercial protein preparations of therapeutic proteins (Enbrel®50 mg, Humira®40 mg and MabThera®100 mg) were aggregated accordingly and analyzed with CCVJ fluorescence and HP-SEC with UV and CCVJ fluorescence detection.

Results: Contrarily to ANS, Bis-ANS and Nile Red, the molecular rotors DCVJ and CCVJ showed low background fluorescence in polysorbate-containing buffers. Both DCVJ and CCVJ showed enhanced fluorescence intensity for aggregated IgG formulations and were suitable for the detection of aggregation in polysorbate-containing IgG formulations by steady state fluorescence and HP-SEC with dye detection (CCVJ). Time-resolved fluorescence experiments confirmed the steady state fluorescence data, and additionally allowed to distinguish between Bis-ANS interacting with polysorbate (5.5 ns lifetime component) and with heat-induced IgG aggregates (10 ns lifetime component). CCVJ was capable to detect thermally induced aggregation in the commercial polysorbate-containing products Enbrel®50 mg, Humira®40 mg and MabThera®100 mg in steady state fluorescence and HP-SEC with fluorescence detection.

Conclusions: Fluorescent molecular rotors are suitable probes to detect aggregation in polysorbate-containing monoclonal IgG formulations and can be used for highly concentrated commercial preparations, as shown for Enbrel®50 mg, Humira®40 mg and MabThera®100 mg. Moreover, CCVJ can be used within the mobile phase of the HP-SEC for the analysis of polysorbate-containing samples using online fluorescence detection.

PS-F-50

pH-Dependent Stability of Creatine Ethyl Ester

Brandon T. Gufford[1], Edward L. Ezell[2], Jonathan L. Vennerstrom[1], and Dennis H. Robinson[1]

[1]Department of Pharmaceutical Sciences, College of Pharmacy, University of Nebraska Medical Center, Omaha, NE
[2]Eppley Institute for Research in Cancer, University of Nebraska Medical Center, Omaha, NE

Purpose: The purpose of these experiments was to study the pH-dependent stability of creatine ethyl ester (CEE) in aqueous solutions and simulated biological media using both HPLC and NMR.

Methods: CEE, creatine, and creatinine concentrations were simultaneously quantified by HPLC using an isocratic mobile phase of 20 % v/v acetonitrile, 5 mM formic acid, and 5 mM 1-octanesulfonic acid sodium at a flow rate of 1.5 mL/min and a Waters Atlantis® T3 C18 column maintained at 30 °C. HPLC analysis was used to measure the stability at pH 1.0, 2.5, 4.0, and 4.6 by monitoring the UV absorbance at 210 nm and 235 nm. Because the degradation was too rapid at more neutral pH, NMR was used to measure the concentration of these compounds at pH 4.6, 7.4, 8.0, 9.5, and 10.5 as well as in cell culture media, human plasma, simulated intestinal fluid, and soy lecithin solutions. The degradation of CEE was

quantified by measuring the ^{1}H NMR spectra over time on a 400 MHz Bruker Avance III spectrometer as pseudo-2D data sets using presaturation with a spoil gradient for water suppression.

Results: The cyclization of CEE to form creatinine and ethanol was linear over the pH range of 2.5 - 8.0 ($y = 0.8263x - 8.1781$, $R^2 = 0.997$). CEE is most stable at pH 1 ($t_{1/2}$ = 570 hr) compared to physiological pH 7.4 ($t_{1/2}$ = 76 s). A relatively slow hydrolytic degradation of CEE to free creatine occurred at pH ≤ 1.0 only, suggesting oral absorption of the ester is possible. The addition of creatinine did not decrease the rate of degradation of CEE as this is not an equilibrium reaction. The rate of CEE degradation in cell culture media, human plasma, and SIF was also pH dependent although high concentration of soy lecithin slowed the decomposition.

Conclusions: This study confirms the pH-dependent, non-enzymatic degradation of CEE is a cyclization reaction to creatinine and ethanol in the pH range 2 to 8. CEE is most stable at pH 1 where degradation occurs via slow hydrolysis.

PS-F-51

Quantitative determination of lysophosphatidic acid in human saliva using LC-MS/MS

Sai Praneeth R Bathena[1], Jiangeng Huang[1], D Roselyn Cerutis[2], Yazen Alnouti[1]

[1]Department of Pharmaceutical Sciences, College of Pharmacy, University of Nebraska Medical Center, Omaha, NE
[2]Department of Oral Biology, Creighton University Dental School, Omaha, NE

Purpose: Lysophosphatidic acids (LPAs) in saliva play important physiological and pathophysiological roles in periodontal wound healing. LPAs exhibit multiple cellular responses by acting through specific G protein-coupled LPA receptors. These receptors are highly expressed in oral fibroblasts and LPAs were shown to play a role in fibroblast stimulation, migration, and proliferation. LPAs are known to be key mediators in inflammation and recent evidence suggests they play a role in inflammatory periodontal diseases. Therefore, the aim of this study was to develop and validate a LC-MS/MS method to quantify LPAs in human saliva to be used to understand the role of LPA in periodontal diseases.
Methods: The LPA species (LPA 18:0, LPA 16:0, LPA 18:1 and LPA 20:4) were extracted from saliva by liquid-liquid extraction with acidified butanol. The chromatographic separation was carried out on a Macherey-Nagel NUCLEODUR® C8 Gravity Column (125mm × 2.0mm ID) with 75% methanol in water, 0.5% formic acid, 5mM ammonium formate (mobile Phase A) and 99% methanol in water, 0.5% formic acid, 5mM ammonium formate (mobile phase B) at a flow rate of 0.5 mL/min. LPA 17:0 was used as an internal standard. The MS/MS analysis were performed in negative mode on Applied Biosystems/MDS SCIEX 4000 Q TRAP® quadrupole linear ion trap mass spectrometer with an electrospray ionization (ESI) source.
Results: The limit of quantification was 3ng/ml for all LPA species and the method was linear over the range of 1-200 ng/ml. Inter-day and intra-day accuracy and precision was <20% at the lower limit of quantification (3ng/ml) and <15% for the other 3 QC points (20ng/ml, 150ng/ml and 200ng/ml). The slopes, intercepts, and R^2 values (>0.99) were consistent for the three validation runs. The extraction recoveries were >70% in human saliva. LPAs were stable for at least 2 days, 1 week and 2 weeks in autosampler, bench, and -20 °C freezer respectively.
Conclusions: A specific, sensitive, accurate, and reliable LC-MS/MS method was developed and validated for the quantification of four LPA species in saliva. This LC-MS/MS assay was successfully applied to study the physiological roles of LPA in periodontal diseases.

PS-F-52

A Fluorescence Polarization Assay for Identification of Small-Molecule ArfGAP Inhibitors

W.Sun[1], Q. Zhang[1]

[1] Eshelman School of Pharmacy, University of North Carolina, Chapel Hill, NC

Purpose: GTPase-activating proteins of ADP-ribosylation factors (ArfGAPs) represent a family of proteins that play key roles in membrane traffic and cytoskeleton reorganization. Increasing evidence also indicate that ArfGAPs are involved in various diseases, including cancer, Alzheimer's disease, and autism. There are no small molecules that directly inhibit ArfGAPs, despite their potential use as therapeutic targets. We are seeking to develop small molecule inhibitors that regulate ArfGAP proteins.

Methods: An ArfGAP enzymatic assay which is amenable to high-throughput (HTS) screening will be developed. To carry out the HTS, highly pure Arf1, ArfGAP1 and ASAP1 for HTS will be prepared according to literature protocols. The standard Z factor and DMSO tolerance will be tested. A pilot screening will be operated to demonstrate the feasibility of future screen in larger scale.

Results: We have successfully developed a novel fluorescence polarization (FP) assay. We have applied this assay into other several GAP proteins and demonstrated that this novel assay could be used as a generic GAP enzymatic assay. After optimizing it into a HTS screening assay, we have screened up to 1000 small molecule compounds. And found some promising small molecules regulators.

Conclusion: With this HST assay, the first set of ArfGAP inhibitors will be discovered soon. With the help of ArfGAP regulators, we will have a better understanding of ArfGAP functions in the whole signaling pathway and related diseases.

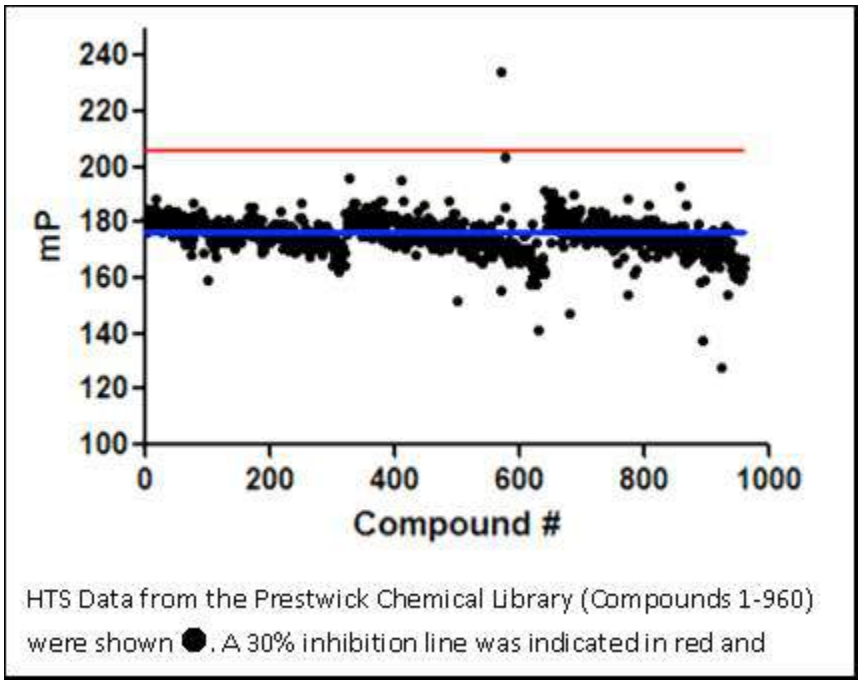

HTS Data from the Prestwick Chemical Library (Compounds 1-960) were shown ●. A 30% inhibition line was indicated in red and

PS-F-53

Comparison between the pharmacokinetic properties of two non metabolic long chain fatty acid analogs for the therapy of metabolic syndrome

A. A. Zur[1,2], A. Hoffman[1], J. Bar-Tana[2]

[1]Institute for Drug Research, [2]Department of Metabolism & Human nutrition,
Faculty of Medicine, The Hebrew University of Jerusalem, Jerusalem, Israel

Purpose: Free fatty acids (FFA) are a major energy source in human nutrition as well as potent regulators of physiological metabolic signaling. Various non metabolic analogs of FFA have been developed as potent therapeutics mimicking the features of native FFA with increased pharmacodynamic efficacy and altered pharmacokinetic properties. Mαα and Mββ, two non metabolic analogs that differ in the location of their methyl group, exhibited marked hypolipidemic and insulin sensitizing effects in preclinical studies. Considering the high therapeutic potential as a treatment for the Metabolic Syndrome, the aim of this work was to compare these compounds in terms of pharmacokinetic parameters including metabolic pathways, tissue distribution and oral bioavailability.

Methods: Pharmacokinetics and oral bioavailability of Mαα and Mββ was assessed in male Wistar rats following single IV and PO administration. LC-MS analysis was used for compounds quantification. Intestinal permeability properties of Mαα and Mββ were measured in Caco-2 cells and permeation flux ratio was evaluated. In-vitro enzymatic metabolism was assessed using rat pooled liver microsomes. Tissue distribution was examined using radio-labeled compounds. Pharmacokinetic parameters were determined using compartmental analysis.

Results: A two-compartment model with an elimination half-life of approximately 3 hours describes the pharmacokinetics of both analogs following intravenous administration. Plasma concentrations following oral doses are higher for Mαα in comparison to Mββ with peak concentrations of 77±40 and 39±5 g/ml respectively, and similar absolute oral bioavailability of 55%. Both compounds exhibit high permeability through CaCo2 monolayer with influx ratios of 5 and 1 for Mαα and Mββ respectively. Systemic clearance and volume of distribution at steady state of Mββ were higher than Mαα (39±2 and 20±3 ml/kg/hour, 140±20, 57±6 ml/kg respectively). Mββ was more extensively metabolized by rat liver microsomes and was distributed to liver, fat and muscle tissues while Mαα was found mainly in the liver.

Conclusion: Mαα lower clearance and diminished susceptibility to oxidative enzymatic metabolism as well as protein mediated intestinal influx are ascribed to methyl substitution on α to carboxyl position. These relatively minor structural changes also alter tissue distribution and play a role in fatty acid analogs pharmacokinetics.

PS-F-54

Can dissolution rate calculations establish the formulation parameters necessary to avoid food effects?

M. Arndt, D. Jünemann, E. Kostewicz, J. Dressman

Department of Pharmaceutical Technology, Johann Wolfgang Goethe University, Frankfurt am Main, Germany

Purpose: Reducing the particle size of the API is a strategy used often to help eliminate food effects of poorly soluble drugs. To avoid unnecessary formulation effort, it would be helpful to understand the relationship between PK parameters like Cmax and the *in vitro* dissolution rate. In this study, the critical particle size of fenofibrate needed to eliminate the food effect was identified using experimental dissolution rates in biorelevant media coupled with a STELLA® model for the PK.

Methods: Dissolution rates of fenofibrate from micronized (Lipidil-Ter®) and nanosized (Lipidil-ONE®) products were measured in the biorelevant medium FaSSIF-V2 in the USP 2 apparatus at 37°C and 75 rpm. The dissolution rates (z-values) were calculated from the dissolution profiles. Sensitivity of the plasma profile to values of z was determined using a range of simulated values for the gastric ($z_{gastric}$) and intestinal ($z_{intestinal}$) by applying a STELLA® model for fenofibrate dissolution and absorption. Critical values of $z_{intestinal}$ for avoiding food effects were then identified for fenofibrate.

Results: Simulated plasma profiles for fenofibrate proved to be sensitive to $z_{intestinal}$ but not $z_{gastric.}$ In FaSSIF-V2 the $z_{intestinal}$ was 0.34 for Lipidil-Ter® but 2.29 for Lipidil-ONE® i.e. notably higher for the nanosized product. By varying the value of $z_{intestinal}$ in the simulation, a relationship was established between the z value and the expected Cmax value. A critical value of z=0.6 was identified, above which the formulation would be expected to behave like Lipidil-ONE® i.e. be bioequivalent to Lipidil ONE® and, like Lipidil ONE®, exhibit no food effect. Since this critical value is far lower than the observed z value for Lipidil ONE®, it suggests that the particle size of fenofibrate in Lipidil One® is perhaps smaller than necessary to eliminate the food effect.

Conclusion: Dissolution testing in biorelevant media to generate z values may be a useful tool in identifying an optimum target particle size for formulation of poorly soluble APIs with a view to eliminating the food effect or to formulating a bioequivalent generic version.

PS-F-55

Is the Biowaiver Procedure Applicable for Lamivudine Drug Products?

Stefanie Strauch,[1] Ekarat Jantratid,[2] Jennifer B. Dressman[1]

[1]Department of Pharmaceutical Technology, Johann Wolfgang Goethe University, Frankfurt, Germany
[2]Department of Pharmacy, Faculty of Pharmacy, Mahidol University, Bangkok, Thailand

Purpose: The aim of this work was to evaluate whether the Biopharmaceutics Classification System (BCS)-based biowaiver approval process is appropriate for new lamivudine formulations. Therefore, all relevant data needed for a risk-benefit analysis was taken into consideration, appraising the advantages of the biowaiver procedure for lamivudine as well as the risks of an incorrect biowaiver decision for this active pharmaceutical ingredient (API).

Methods: All pertinent data publicly available on solubility of the API, pharmacokinetics and permeability, the therapeutic window, data on excipient interactions and problems with bioavailability and/or bioequivalence (BE) were gathered and critically analyzed. Additionally, the solubility characteristics of the pure drug as well as the dissolution behavior of the drug and a selection of lamivudine drug products were investigated according to the methods given in the WHO Guidelines.

Results: Lamivudine has demonstrated to be highly soluble, but its permeability data in literature is not consistent, the API therefore cannot be classified to the BCS with certainty and thus, to guarantee the patients safety it is conservatively assigned to BCS Class III. However, the API has a wide therapeutic index and to date no studies of excipient interactions or bioavailability problems due to manufacturing variations have been reported in the literature. In addition, no reported cases of either failure to meet BE or of bio*in*equivalence are existent. Furthermore, all tested drug products fulfilled the WHO requirements for “very rapidly dissolving” products and it can be assumed that the patient’s risks associated with bio*in*equivalence are quite marginal as long as the products pass the dissolution criteria for biowaiver-based approval.

Conclusion: Based on the literature and experimental data, it is suggested that the BCS-based biowaiver procedure for simplified approval of new lamivudine multisource products can be applied on the basis of the WHO and the EMEA criteria. However, as a BCS Class III compound, lamivudine is not suitable for the BCS-based biowaiver approval according to the FDA guidance.

PS-F-56

Estimating HIV Evolutionary Pathways to Raltegravir Drug Resistance

Tae Eun Kim[1], Mark Lovern[2]

[1] Eshelman School of Pharmacy, University of North Carolina, Chapel Hill, NC
[2] Clinical Pharmacology and Modeling and Simulation, GlaxoSmithKline, RTP, NC

Purpose: To estimate the genetic pathways to emergence of raltegravir resistance mutations in antiretroviral-experienced patients with virological failure on raltegravir-containing regimens, using a mixture model of mutagenetic trees and publicly-available cross sectional data.

Methods: 148 genotypes from 81 subtype B subjects were obtained from the Stanford HIV Drug Resistance Database. The dataset used for estimating models consisted of binary patterns that describe the occurrence of the following set of integrase amino acid substitutions: Y143R/C/H, Q148H/K/R, G140S/A, N155H, E92Q/A, E138K/A and L74M. The data were then fit by mixture models of mutagenetic trees that are reconstructed from all pairwise joint probability of genetic events [1]. Model selection was performed in 20 runs of random 10-fold cross validation in order to estimate the number of mutagenetic trees (K) in the mixture model. All models with up to $K \leq 10$ were considered. Of these candidates, the most parsimonious model within one standard deviation of the maximum mean log-likelihood was selected as the final model. This model was then statistically validated by comparing its predictive performance of with those of the single-tree and null models in 20 runs of random cross validation. The stability of the final model was evaluated by re-running the analysis on 1000 bootstrap samples of the available data. By assuming Poisson processes for the occurrence of mutations and for the observed sampling times, it was possible to derive a time-scaled mutagenetic tree model, and thereby estimate the expected waiting times for each mutation to occur. Mutagenetic tree modeling was performed using Rtreemix, an R package [2].

Results: The optimal number of mutagenetic trees (K) for the mixture model was estimated to be 2. The first tree modeled the mutations as independent events and explained 8% of the data. The second tree captured 92% of the samples in a tree that consisted of 3 parallel pathways, namely 148H/K/R-G140S/A-138K/A (pattern 148), 155H-92Q/A (pattern 155) and 143R/C/H-74M (pattern 143). The model predicts Y143R/C/H, Q148H/K/R and N144H are the initial mutations to appear, and that a strong association exists between Q148H/K/R and G140S/A. These predictions are in accord with clinical observations [3]. Also, the estimated order for these mutations was highly conserved in the analysis of the bootstrapped data, while the estimated ordering of other mutations were less stable, possibly due to the small number of samples harboring this resistance pattern. The time-scaled mutagenetic tree model estimated that Q148H/K/R appears approximately 25 weeks after the initiation of raltegravir-based therapy, which is more rapid than expected waiting times for Y143R/C/H (71 weeks) and N155 (50 weeks) . Interestingly, the model predicted G140S/A to appear approximately 3 weeks following the emergence of Q148H/K/R.

Conclusion: A mixture model of mutagenetic trees was successfully developed and yielded prediction consistent with experimental observation. In the future, it is planned to this approach with a method of genotype-phenotype prediction in order to predict raltegravir genetic barrier to drug resistance.

1. Beerenwinkel, N., et al., *Learning multiple evolutionary pathways from cross-sectional data.* J Comput Biol, 2005. **12**(6): p. 584-98.
2. Bogojeska, J., et al., *Rtreemix: an R package for estimating evolutionary pathways and genetic progression scores.* Bioinformatics, 2008. **24**(20): p. 2391-2.
3. Sichtig, N., et al., *Evolution of raltegravir resistance during therapy.* J Antimicrob Chemother, 2009. **64**(1): p. 25-32.

GPEN.2010
University of North Carolina at Chapel Hill

PS-F-57

Development of a Pafuramidine Treatment Protocol that Elicits Quantifiable Liver and Kidney Toxicity

K. DeSmet[1], A. Harrill[1], J.E. Hall[2], M. Paine[3], M.Z. Wang[3], R. Tidwell[2], P.B. Watkins[1]

[1]The UNC-Hamner Institute for Drug Safety Sciences, The Hamner Institutes for Health Sciences, Research Triangle Park, NC
[2]Department of Pathology and Lab Medicine, University of North Carolina, Chapel Hill, NC
[3]Eshelman School of Pharmacy, University of North Carolina, Chapel Hill, NC

Purpose: Pafuramidine (DB289) is a prime example of a drug that demonstrated reversible hepatotoxicity and no renal toxicity in traditional preclinical and early clinical programs. Kidney toxicity was not observed until an expanded Phase 1 clinical trial in healthy volunteers was undertaken in South Africa. The objective of this study was to determine optimal dose of pafuramidine, treatment duration and sex in CD-1 mice that elicits quantifiable liver and kidney toxicity. These parameters will be used to design a treatment protocol to evaluate mechanisms of pafuramidine-induced hepatic and renal toxicity utilizing a panel of inbred mouse strains to mimic genetic variation in patient populations.

Methods: Male and female CD-1 mice were treated for 2, 4, or 14 days with 75, 125, or 250 µmol/kg pafuramidine. Animals were euthanized 24 hours post-dosing. Hematoxylin and eosin was used to stain sections of left kidney and left liver lobe for histological analysis. Terminal serum samples were analyzed for blood urea nitrogen, creatinine, and alanine transaminase.

Results: Pafuramidine treatment for 2 days resulted in a dose-dependent decrease in body weight; significant increases in mean serum ALT and AST in females treated with the highest dose; and minimal liver pathology changes in both males and females. Pafuramidine treatment for 4 days with the highest dose (250 µmol/kg) resulted in significant increases in mean serum ALT and AST and treatment-related liver pathology changes. Pafuramidine treatment (75 or 125 µmol/kg) for 14 days resulted in a dose-dependent increase in mean serum ALT and AST in both males and females. Treatment-related liver pathology changes in 14 day treated mice were, overall, more extensive than those observed in 2 and 4 day treatment groups. Mild renal pathology changes were also noted at these doses and treatment duration.

Conclusion: A clear pafuramidine-induced hepatotoxicity phenotype has been characterized. Mild pafuramidine-induced kidney injury has been elicited in CD-1 mice. The next planned study will utilize information obtained from this pilot study in a panel of inbred strains of mice to provide insight into mechanisms underlying pafuramidine-induced liver and kidney injury and explain variation in susceptibility to these toxicities across species.

Short Courses, Thursday, November 11th

Location: The William and Ida Friday Center for Continuing Education

Short Course Title	Course Coordinator	Student Chair	Location
Morning Session (8:30 AM – 12:00 noon) *Course begins at 8:00 AM			
Drug-induced Toxicity: A Major Factor in Clinical Failure of Drug Candidates	Dr. Paul Watkins	LaToya Griffin	Bellflower
Drug Discovery in Academic Institutions: New Opportunities	Dr. Stephen Frye	Mary Carroll	Sunflower
Nanomedicines and Gene Therapy Delivery – Challenges and Opportunities*	Dr. Tom Anchordoquy	Saurabh Wadhwa	Dogwood
Transporters – Implication in the Design, Delivery, and Safety of Medicines	Dr. Kim Brouwer	Nathan Pfeifer	Redbud
Afternoon Session (1:30 – 5:00 PM)			
Emerging Role of Pharmacogenomics in Drug Development and Human Therapeutics	Dr. Howard McLeod	Dan Hertz	Sunflower
De-risking Drug Candidates: Optimizing Solubility, Permeability, and DM-PK	Dr. Ron Borchardt	Yong Zhang	Dogwood
Stability of Proteins and Peptides in Solid Phase Formulations	Dr. Liz Topp	Bob Schuck	Redbud
Computer Assisted Drug Design	Dr. Alex Tropsha	Andy Fant	Bellflower
Banquet at Carolina Inn (6:30 PM Cocktail Hour, 7:30 PM Dinner)			

Drug Discovery in Academic Institutions: New Opportunities

Course Coordinator: Dr. Stephen V. Frye, Director of the Center for Integrative Chemical Biology and Drug Discovery, University of North Carolina at Chapel Hill

There is a clear societal need for enhanced innovation and productivity in drug discovery in order for advances in basic biomedical research to result in new medicines. Drug discovery efforts at academic institutions have grown markedly over the last decade, due to an increased focus on translational research by the National Institutes of Health and a decreased emphasis on early drug discovery by the pharmaceutical industry. Bringing a variety of scientific approaches and sponsors to the early stages of drug discovery will result in greater technological innovation; exploration of higher risk targets; and more balance between the dominant pharmaceutical focus on the diseases of affluent societies and less prevalent diseases and the diseases of the developing world. Given its non-profit service mission and innovative environment, academia is well situated to contribute directly to meeting this challenge. Current academic translational research efforts include the discovery and validation of new pharmaceutically relevant biological targets, screening of compound libraries to generate chemical starting points for drug discovery, design of chemical probes that modulate protein function, and deciphering the biological effects of such probes *in vitro* and *in vivo*.

In this short course, the emerging impact of academic research on drug discovery will be discussed by experts in the field. Instructional examples to be highlighted include public-private partnerships in structural genomics toward chemical probe design and unraveling the mechanisms of action for CNS active drugs.

Stephen Frye, University of North Carolina at Chapel Hill: “Center for Integrative Chemical Biology and Drug Discovery”

Tim Willson, GlaxoSmithKline: “Chemical Biology at GSK”

Helen Ha (student presenter), University of Southern California: “Development of CXCR2 Inhibitors for Lung Cancer Treatment”

Andrew Dixon (student presenter), University of Utah: “Disruption of Bcr-Abl Oligomerization by Design”

Bryan Roth, University of North Carolina at Chapel Hill: “Mining the receptorome for therapeutics: in silico, in vitro, and in vivo”

PD-SC-1

Design and Discovery of Novel CXCR2 Inhibitors for Treatment of Lung Cancer

H. Ha, S. Odde, and N. Neamati

Department of Pharmacology and Pharmaceutical Sciences, School of Pharmacy,
University of Southern California, Los Angeles, CA

Purpose: Chemokine receptor, CXCR2, and its ligand interleukin-8 (IL-8) have been shown to promote tumorigenesis in a number of *in vitro* and *in vivo* studies by facilitating blood vessel formation in the tumor microenvironment, activating cancer cell proliferation pathways (MAPK) and enhancing cancer cell migration and invasion. Recognizing the anticancer potential of CXCR2 inhibition for the treatment of various cancers, we pursued the development of novel CXCR2 small-molecule inhibitors in our current studies.

Methods: We have developed several chemical-based pharmacophore models based on known CXCR2 inhibitors to screen an in-house database of two million compounds. Compounds with >5 fitness value and favorable ADMET properties were selected for *in vitro* screening in CXCR2-specific assays. First, compounds were tested in the CXCR2 Tango™ assay (β-lactamase reporter gene assay). Active compounds were further assessed in ligand-receptor binding and cAMP assay. To assess the anticancer properties of active compounds, cell proliferation (MTT) and cell migration assays were also performed.

Results: Through pharmacophore screening, we have identified ~1000 compounds that show favorable ADMET properties and potential anti-CXCR2 properties. Of these, we identified several classes of inhibitors and two lead compounds (CX25 and CX4338) showing potent anti-CXCR2 and anticancer properties. CX25 potently inhibits IL-8-induced CXCR2 activation (IC_{50} = 0.4μM), cell proliferation and cell migration. CX4338 inhibits IL-8 induced CXCR2 activation (IC_{50} = 5.9μM), cell migration, and synergistically inhibits cell proliferation with known anticancer drugs in lung cancer cell lines.

Conclusion: We have identified several potential classes of compounds that can be further characterized and optimized to yield improved anti-CXCR2 activities. Our lead compounds, CX25 and CX4338 show promising anti-CXCR2 and anticancer activities, which we will further pursue in mouse xenograft models of lung cancer.

PD-SC-2

A Designed Coiled Coil for Improved Disruption of Bcr-Abl Oligomerization

Andrew S. Dixon[1], Benjamin J. Bruno[1], David W. Woessner[2], Carol S. Lim[1]

[1]Department of Pharmaceutics and Pharmaceutical Chemistry, University of Utah, Salt Lake City, UT
[2]Department of Pharmacology and Toxicology, University of Utah, Salt Lake City, UT

Purpose: The oligomerization via a coiled coil is critical to the activity of many proteins such as the oncoprotein Bcr-Abl, the causative agent of chronic myelogenous leukemia (CML). The design of a coiled-coil domain with enhanced ability to oligomerize with the target has therapeutic potential. We designed an oligomeric-disrupting coiled coil with reduced tendency to self-associate and improved binding to Bcr-Abl. Amino acids that would introduce charge-charge repulsions in the self-associating coiled coil and that could form additional intermolecular salt bridges with Bcr-Abl were indentified to improve the efficacy. The ultimate goal is to use this improved coiled coil as a therapeutic agent to block the oncogenic activity of Bcr-Abl.

Methods: Site-directed mutagenesis was performed on a plasmid encoding the wild-type coiled-coil domain to introduce 5 rationally designed amino acid mutations (CCmut: C38A, S41R, E48R, L45D, and Q60E). The nuclear translocation assay (NTA) and 2-hybrid assay were used to study binding. Western blotting with antibodies that recognize phosphorylated Bcr-Abl and two downstream substrates was performed to demonstrate the inhibitory effects of the CCmut. The reduction of cell proliferation after transfection of the CCmut was demonstrated via a colony forming assay and by cell counts. The Enz-Chek Caspase-3 assay (Invitrogen) was used to measure the induction of apoptosis.

Results: Both the NTA and 2-hybrid assays indicated CCmut exhibited greater binding to the wild-type coiled-coil domain and reduced homooligomerization, demonstrating an improvement in binding and specificity. After transfecting the CCmut into K562 cells, the phosphorylation level of Bcr-Abl decreased, indicating the interference with the oligomeric state of Bcr-Abl. Further, the Bcr-Abl substrates STAT5 and CrkL also had decreased phosphorylation levels. The inhibition of Bcr-Abl signaling through addition of the CCmut resulted in decreased proliferation of the cells, as well as apoptosis.

Conclusions: The CCmut exhibited improved binding to Bcr-Abl, including increased specificity. The activity of oncogenic Bcr-Abl was reduced after treatment with the CCmut. This inhibition of the Bcr-Abl activity resulted in decreased proliferation of Bcr-Abl containing cells and induction of apoptosis. The CCmut may be a novel alternative for inhibiting Bcr-Abl with the potential to treat CML including some drug-resistant versions.

Nanomedicines and Gene Therapy Delivery:

Challenges and Opportunities

Course Coordinator: Dr. Tom Anchordoquy, University of Colorado

Dr. Satyanarayana Somavarapu, University of London: "Nanomedicines for the Delivery of Genes"

Dr. Joseph DeSimone, University of North Carolina at Chapel Hill: "Co-opting Moore's Law: Vaccines, Medicines and Biological Particles Made on a Wafer"

Dr. Yoshinobu Takakura, Kyoto University: "Nanotechnology and Delivery Technology for Nucleic Acid Therapeutics"

Dr. Jean-Christophe Leroux, ETH Zürich: "Injectable nanocarriers for the treatment of drug overdose"

Dr. Na Zhang, Shandong University: "Novel Modified Solid Lipid Nanoparticles for Targeted Gene Delivery

Saurabh Wadhwa, University of North Carolina at Chapel Hill: "Anti-cancer Conjugates of Polyglutamic Acid with D-penicillamine Alone or in Combination with Idarubicin"

Abstract

Nanomedicines for the Delivery of Genes

Ijeoma F. Uchegbu and Andreas G. Schätzlein, School of Pharmacy, University of London, 29 – 39 Brunswick Square, London WC1N 1AX

Nanomedicines

Medicines discovery and development is an expensive process involving a number of steps and high failure rates, some of which are associated with an inability to surmount delivery challenges. Nucleic acids pharmacokinetics may be favourably controlled and these actives steered inside the cell and cell nucleus by packaging in nanoparticles, termed nanomedicines. Our laboratory has used these techniques to develop cancer therapeutics.

Gene Therapy of Cancer

Cancer killed 7.9 million people worldwide in 2007[1] and the death toll from this disease is predicted to rise by 45% over the coming two decades[1, 2]. It is clear that new therapies are needed, such as gene therapy[3, 4]; where a gene encoding for a tumouricidal protein is administered and expression of the tumouricidal protein within the tumour cell nucleus leads to tumour cell death. Gene delivery to tumour cell nuclei is however extremely challenging. We have used generation 3 poly(propylenimine) (PPI) dendrimers and 100 – 500 nm PPI dendrimer – gene complexes[5]of PPI as the basis of a cancer gene medicine[6-8]. The intravenous administration of a PPI dendrimer – tumour necrosis factor alpha gene complex results in *complete regression and long term cures in around* 80% of tumours[6]. Furthermore the PPI dendrimer vector system also efficiently delivers RNAi based therapies: shRNA based knock down of an inhibitor of the apoptosis causing gene - p73 results in de-repression of p73 and tumouricidal activity in vivo[7].

Conclusions

Nanomedicines, which significantly improve the pharmacological activity of genes could offer new therapies for the treatment of solid tumours.

References

1. WorldHealthOrganisation. *Are the number of cancer cases increasing or decreasing in the world?* 2008; Available from: http://www.who.int/features/qa/15/en/index.html.
2. Mathers, C.D. and D. Loncar. Plos Medicine, 2006. **3**: p. 2011 - 2030.
3. Schatzlein, A.G. European Journal of Cancer, 2006. **42**(9): p. 1309-1315.
4. Peng, Z. Human Gene Therapy, 2005. **16**: p. 1016-1027.
5. Zinselmeyer, B.H., S.P. Mackay, A.G. Schatzlein, and I.F. Uchegbu. Pharmaceutical Research, 2002. **19**(7): p. 960-967.
6. Dufes, C., W.N. Keith, A. Bilsland, I. Proutski, J.F. Uchegbu, and A.G. Schatzlein. Cancer Research, 2005. **65**(18): p. 8079-8084.
7. Bell, H.S., C. Dufes, J. O'Prey, D. Crighton, D. Bergamaschi, X. Lu, A.G. Schatzlein, K.H. Vousden, and K.M. Ryan. Journal of Clinical Investigation, 2007. **117**(4): p. 1008-1018.
8. Chisholm, E.J., G. Vassaux, P. Martin-Duque, R. Chevre, O. Lambert, B. Pitard, A. Merron, M. Weeks, J. Burnet, I. Peerlinck, M.-S. Dai, G. Alusi, S.J. Mather, K. Bolton, I.F. Uchegbu, A.G. Schatzlein, and P. Baril. Cancer Res., 2009. **69**: p. 2955-2962.

Abstract

Co-opting Moore's Law: Vaccines, Medicines and Biological Particles Made on a Wafer

Joseph M. DeSimone
Departments of Chemistry and Pharmacology
Institute for Advanced Materials
Institute for Nanomedicine
Center for Cancer Nanotechnology Excellence
Lineberger Comprehensive Cancer Center
University of North Carolina at Chapel Hill
and
Department of Chemical and Biomolecular Engineering
North Carolina State University
and
Memorial Sloan-Kettering Institute for Cancer Research
Memorial Sloan-Kettering Cancer Center
and
Liquidia Technologies

In 1965, Gordon Moore, co-founder of Intel, described the trend that the number of components in integrated circuits had doubled every year since 1958. This trend has continued to today, enabled by advances in photolithography which has taken the minimum feature size of transistors down from about 10 microns in 1970 to 0.045 microns (45 nm) today. In biological terms, this corresponds to going from the size of a red blood cell to the size of a single virus particle! As such, this top-down nano-fabrication technology from the semiconductor industry is, for the first time, in the size range to be relevant for the design of medicines, vaccines and interfacially active Janus particles. This lecture will describe the design, synthesis and efficacy of organic nano- and micro-particles using a top-down nano-fabrication technique we developed called PRINT (Particle Replication in Non-wetting Templates). PRINT is a continuous, roll-to-roll, high resolution molding technique that allows the fabrication of precisely defined micro- and nano-particles in a continuous manner with control over chemical composition, size, shape, deformability and surface chemistry. Examples to be described will include the design of PRINT particles useful as vaccines (influenza, H1N1, pneumo), targeted chemotherapy agents, anti-bacterials, inhalation therapeutics and even as an entirely new class of particle-based surfactants.

Abstract

Nanotechnology and Delivery Technology for Nucleic Acid Therapeutics

Yoshinobu Takakura
Graduate School of Pharmaceutical Sciences, Kyoto University, Japan

Success of in vivo gene therapy depends on the development of gene delivery technologies, by which a well-controlled transgene expression is achieved as far as the spatial and temporal profile of the expression is concerned. Plasmid DNA-based nonviral vectors are the more useful gene delivery vectors compared with viral vectors in terms of simplicity and safety. In addition to plasmid DNA, a variety of nucleic acid therapeutics, such as antisense oligonucleotides and siRNAs, have been developed for the treatment of malignant diseases, vital infections and other diseases in the clinical field (1). Typical delivery systems for these nucleic acid therapeutics include lipoplexes and polyplexes in which the polyanionic nucleic acids and cationic liposomes/polymers form complexes via electrostatic interaction. Local or systemic (e.g. hydrodynamic) injection of the solution of a nucleic acid in its naked form is also an option for efficient delivery. Current status of nanotechnology and delivery technology for nucleic acid therapeutics will be overviewed in my talk.

Recent approaches for plasmid DNA delivery for interferon (IFN) gene delivery in our laboratory will be also presented. We have developed a CpG motif reduced plasmid vectors encoding mouse IFN-beta and INF-gamma. Hydrodynamic injection of the CpG-reduced vectors resulted in a sustained transgene expression in mice compared with conventional CpG-replete vectors. The CpG-reduced vectors markedly inhibited the pulmonary metastasis of colon tumor cells, CT-26 cells, and prolonged the survival of mice, indicating that long-term expression of IFN can be achieved by CpG-reduced vectors and sustained IFN gene expression results in enhanced therapeutic effects of IFN gene transfer against tumor metastasis. We have also demonstrated that delivery of the gene encoding IFN-gamma, a Th-1 cytokine, is effective in the treatment of an allergy, atopic dermatitis (Th2-dominant skin disease). A single hydrodynamic injection of another CpG motif reduced vector into NC/Nga mice, a model for human atopic dermatitis, at a low dose resulted in a sustained concentration of IFN-gamma in the serum, and a high concentration was maintained over 80 days. An increase in the serum concentration of IL-12, reduced production of IgE, and inhibition of mRNA expression of Th-2 cytokines were also observed. The mice receiving IFN-gamma gene therapy showed a significant reduction in the severity of skin lesions and in the intensity of their scratching behavior. These results demonstrated that the IFN gene delivery by this technology can be an effective therapeutic approach for various diseases.

References

1. Lares MR, Rossi JJ, Ouellet DL. RNAi and small interfering RNAs in human disease therapeutic applications. ***Trends Biotechnol***. 2010 , in press. PMID: 20833440
2. Kawano H, et al. Improved anti-cancer effect of interferon gene transfer by sustained expression using CpG-reduced plasmid DNA. ***Int J Cancer***. 2007, 121(2):401-6. PMID: 17372909
3. Hattori K, et al. Sustained exogenous expression of therapeutic levels of IFN-gamma ameliorates atopic dermatitis in NC/Nga mice via Th1 polarization. ***J Immunol***. 2010, 184(5):2729-35. PMID: 20107184

Abstract

Injectable nanoccarriers for the treatment of drug overdose

Jean-Christophe Leroux, Institute of Pharmaceutical Sciences,
Department of Chemistry and Applied Biosciences, ETH Zürich, Switzerland

Hospitals are confronted with poisoned patients on a routine basis, with clinical scenarios ranging from drug overdose to illicit drug use, suicide attempts, or accidental toxic exposures. Unfortunately, for many life-threatening intoxications, specific antidotes are not available. One possible strategy for the management of overdose consists in administering systemically particulate carriers which could reduce the bioavailable drug concentration in the body by acting as a sink for the toxin/drug. To be useful in drug detoxification, particulate carriers should exhibit the following properties: physical stability, mean diameter in the 70 - 150 nm size range, long circulation time after intravenous administration, high affinity for the toxic compound, biocompatibility, and biodegradability (or elimination by renal filtration). In this short course, we will review different nanosized systems (nanoparticles, lipid nanocapsules, polymeric binders, liposomes) that are being investigated for drug detoxification purposes and discuss their advantages and limitations. A particular emphasis will be given on transmenbrane pH-gradient vesicles which can capture high amounts of ionizable drugs under physiological conditions. The Swiss National Science Foundation is acknowledged for financial support (ID 31003A_124882).

Abstract

Anti-cancer Conjugates of Polyglutamic Acid with D-penicillamine Alone or in Combination with Idarubicin

Saurabh Wadhwa, Anuraag Sarangi, and Russell J. Mumper
Division of Molecular Pharmaceutics, UNC Eshelman School of Pharmacy,
University of North Carolina at Chapel Hill, Chapel Hill, NC 27599-7362

Cytotoxicity of D-pen, an aminothiol, to cancer cells is mediated via elevation of intracellular reactive oxygen species (ROS) levels[1] and cancer cells have been shown to be 12 to 480-fold more sensitive to D-pen than non-malignant (fibroblasts) cells[2]. However, high hydrophilicity and stereochemistry make D-pen impermeable to the cell membrane[3]. We hypothesized that polymer conjugation will enhance the intracellular permeability of D-pen and result in improved survival in a mouse leukemia model.

PGA-D-pen conjugate with 35 moles of D-pen per mole of PGA was synthesized as determined by HPLC (Fig. 1A). The fluorescently labeled conjugate was taken up by human leukemia (HL-60) cells in a dose and time dependent manner (Fig. 1B). The conjugate resulted in significant elevation of ROS as measured by H_2DCFDA fluorescence and a dose dependent cytotoxicity in several human cancer cell lines. Treatment with the conjugate resulted in significant enhancement in the survival of CD2F1 mice bearing intraperitoneal P388 murine leukemia compared to saline control[9] (Fig. 2).

Idarubicin (Ida), an anthracycline analogue, is a first line chemotherapeutic in the treatment of Acute Myeloid Leukemia (AML). Among several mechanisms of cytotoxicity, damage via generation of ROS has been considered significant[4]. This involves formation of very strong intracellular iron complexes[5]. Thiol

1. A) Structure of the PGA-D-pen conjugate; B) Uptake of PGA-D-pen conjugate by confocal microscopy; C) Apoptosis ction by PGA-D-pen conjugate.

2. A) Intracellular ROS generation by PGA-D-pen conjugate in HL-60 cells; B) *In-vitro* cytotoxicity of PGA-D-pen conjugate hr; C) *In-vivo* survival enhancement by PGA-D-pen conjugate in CD2F1 mice bearing intra-peritoneal leukemia

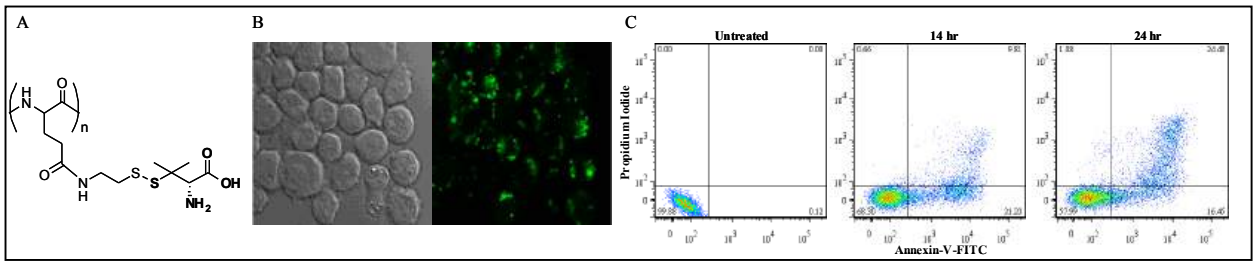

dependent reduction of these complexes leads to the formation of superoxide anion and the reduced complexes can further participate in ROS cascade leading to generation of highly damaging hydroxyl radicals via fenton type reactions[5,6]. We hypothesized that the delivery of D-pen (an aminothiol) and Ida using Dual Drug Conjugates (DDC) to cancer cells will result in enhanced cytotoxicity via intracellular ROS elevation. To investigate the potential of co-delivery of D-pen with Ida, DDC were synthesized having 40 moles of D-pen and 4-6 moles of Ida per mole of PGA respectively. The DDC released both the drugs *in-vitro* in conditions mimicking the endosomal pH and cytosolic glutathione levels respectively and were analyzed by separate HPLC assay methods. The DDC had comparable *in-vitro* cytotoxicity to Ida at 4-fold lower intracellular concentrations as determined by flow cytometry.

Sigma receptors have been shown to be over-expressed in several human and non-human cancer cell lines including breast, lung, prostrate, renal and brain[7] and have been successfully targeted to deliver high concentrations of chemotherapeutics to cancer cells[8]. However, usefulness of Sigma-1 receptors

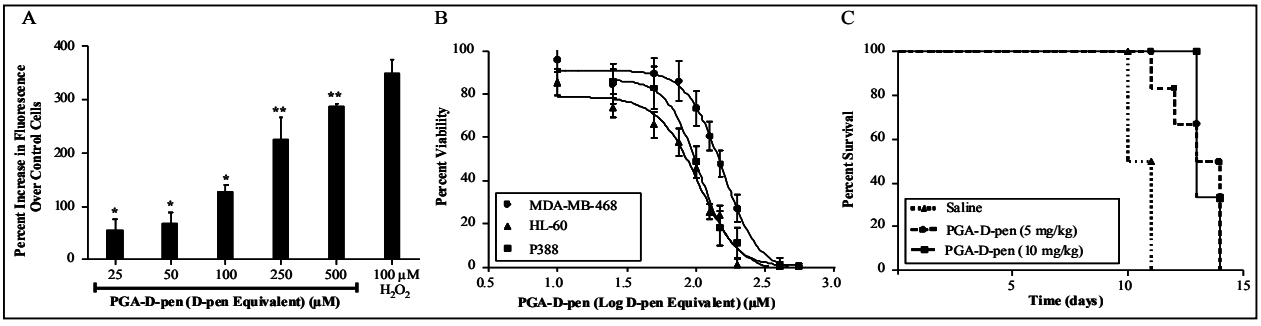

has not been investigated in leukemia for drug targeting. We hypothesized that DDC targeted to Sigma-1 receptor using anisamide will result in enhanced cellular uptake and accumulation. Sigma-1 targeted DDC were synthesized with 4-6 moles of anisamide per mole of DDC. We have shown that several human leukemia cells over-express Sigma-1 receptor and are currently investigating the cellular uptake of targeted DDC as compared to the untargeted DDC.

References:

1. Gupte and Mumper, Free Rad. Biol. Med., 2007, 43 (9), 1271.
2. Havre et al., Cancer Res., 2002, 62 (5), 1443.
3. Lodemann, Biochem. Biophys. Res. Commun., 1981, 102 (2), 775.
4. Minotti et al., Pharmcol. Rev., 2004, 56 (2), 185.
5. Xu et al., Mol. Pharmacol., 2005, 68 (2), 261.
6. Held et al., Radiat. Res., 1996, 145 (5), 542.
7. Vilner et al., Cancer Res., 1995, 55 (2), 408.
8. Banerjee et al., Int. J. Cancer, 2004, 112 (4), 693.
9. Wadhwa and Mumper, Mol. Pharm., 2010, 7 (3), 854.

Transporters – Implication in the Design, Delivery, and Safety of Medicines

Course Coordinator: Prof. Kim R. Brouwer, PharmD PhD,
University of North Carolina at Chapel Hill, USA

Molecular and functional characterization of xenobiotic and nutrient transport proteins is a rapidly-evolving field, with a growing list of drugs and derived metabolites shown to be substrates and/or inhibitors. The role of transport in drug absorption, distribution and elimination and affects on pharmacokinetics and pharmacodynamics may be desirable or deleterious. Information about transport specificity and selectivity can be used to improve drug absorption and bioavailability, target or avoid organs or tissues, help control pathways of elimination, and minimize the risk of unforeseen drug interactions. An expanding arsenal of in vitro tools is available to identify interactions with transport proteins, either individually or in concert, and enable improved drug design and delivery, as well as explain and predict previously unknown transport-mediated limitations to effective therapy, including toxicity and intersubject variability. This short course will include select examples of transport interactions with known in vivo relevance and explore how mechanistic information obtained using in vitro tools can be used to improve drug therapy.

Prof. Peter W. Swaan PhD, University of Maryland, USA: "Application of Computational and Pharmacophore Models to Predict In Vivo Drug Effects in Humans"

Prof. Per Artursson PhD, Uppsala University, Sweden: "Intestinal Absorption and Transport"

Assoc. Prof. Hiroyuki Kusuhara PhD, University of Tokyo, Japan: "Role of Transport in Drug Disposition"

Prof. Ikumi Tamai PhD, Kanazawa University, Japan: "Renal and Intestinal Transport and Interactions"

Nora Lee, University of Washington, USA: "Cloning and Functional Characterization of Rat Plasma Membrane Monoamine Transporter (rPMAT)"

Mari Miyajima, The University of Tokyo, Japan: "Transport Mechanisms of Organic Anions at the Blood-Brain Barrier"

PD-SC-3

Cloning and Functional Characterization of Rat Plasma Membrane Monoamine Transporter (rPMAT)

Nora Lee, Horace Ho, and Joanne Wang

Department of Pharmaceutics, School of Pharmacy, University of Washington, Seattle WA

Purpose: The human Solute Carrier 29 family consists of four members respectively termed human equilibrative nucleoside transporters 1, 2, 3 and 4 (hENT1-4). We previously demonstrated that unlike ENT1-3, which exclusively transport nucleosides and nucleobases, hENT4 functions as a low affinity, high capacity monoamine transporter. Based on its physiological substrate profile, we designated hENT4 as human plasma membrane monoamine transporter (hPMAT). Strongly expressed in the human brain, hPMAT may play a role in maintaining brain homeostasis of monoamines in concert with high affinity monoamine transporters. Rats are widely used as preclinical models for drug discovery and development. The goal of this study is to clone and characterize rat PMAT (rPMAT) to investigate whether there is any functional difference between hPMAT and rPMAT.

Methods: The full length rPMAT cDNA was isolated from rat brain by RT-PCR and subcloned to the yellow fluorescent protein (YFP) tagged vector, pEYFP-C1. rPMAT, hPMAT, and empty pEYFP-C1 vector were stably expressed in Madin-Darby canine kidney (MDCK) cells. Transport studies were carried out using radiotrace assays.

Results: Both rPMAT and hPMAT robustly transported serotonin, dopamine, and MPP+. In contrast, there was no significant interaction of either rPMAT or hPMAT with nucleosides or nucleobases. The apparent binding affinities (Km) of rPMAT towards serotonin (Km = 83 μM), dopamine (Km= 271 μM), and MPP+ (Km = 70 μM) are similar to those of hPMAT. Decynium 22, a potent inhibitor of hPMAT (Ki = 0.12 μM), also potently inhibited rPMAT with a Ki value of 0.4 μM.

Conclusions: Like hPMAT, rPMAT functions as a monoamine, but not a nucleoside, transporter. The transport kinetics and inhibitor sensitivity of rPMAT are similar to those of hPMAT. Thus, rats can be used as a valid animal model for further investigating the *in vivo* function of PMAT.

This work is supported by the National Institutes of Health Grant GM066233.

PD-SC-4

Transport Mechanisms of Organic Anions at the Blood-Brain Barrier

Mari Miyajima, Hiroyuki Kusuhara, Hiroshi Kodaira and Yuichi Sugiyama

Department of Pharmaceutical Sciences, The University of Tokyo, 7-3-1 Hongo, Bunkyo-ku, Tokyo 113-0033, Japan

Purpose: Numerous transporters are expressed at the blood-brain barrier (BBB), thus regulating the blood-to-brain uptake and brain-to-blood efflux of compounds. Because of its broad substrate specificity and high expression, organic anion transporting polypeptide 1a4 (Oatp1a4) and organic anion transporter 3 (Oat3) is considered to be important in the organic anion transport at the BBB. From *in vivo* inhibition studies performed in rats, Oatp1a4 was suggested to mainly contribute to transport of amphipathic organic anions, whereas Oat3 is important in that of hydrophilic compounds. In this study, we examined contribution of these two transporters in organic anion transport across the BBB using knockout mice. We used para-amino hippuric acid (PAH) and benzylpenicillin (PCG) as a probe for hydrophilic organic anions and dehydroepiandrosterone sulfate (DHEAS) for amphipathic organic anions.

Methods: Efflux of organic anions from the brain was investigated in mice using the brain efflux index (BEI) method. A solution containing [^{3}H] labeled compounds and an impermeable reference compound, [^{14}C]inulin, in extracellular fluid buffer was administered in the parietal cortex area 2 region of the brain. After the microinjection, the radioactivity remaining in the cerebrum was determined, yielding the remaining percentage of test compounds in the cerebrum. We obtained the distribution volume of DHEAS in the brain using brain slices *in vitro*.
In vitro uptake studies were performed using mOatp1a4-expressing HEK293 cells and mOat3-expressing oocytes.

Results: In Oatp1a4 knockout mice, efflux of DHEAS was similar to that in wild-type mice, whereas in Oat3 knockout mice, elimination of PAH, PCG and DHEAS was significantly delayed. Efflux transport was partially reduced for these compounds (from 30 to 60%) in these mice. Furthermore, coadministation of probenecid, a xenobiotic that is widely recognized as an inhibitor of organic anion transporters, affected efflux of these compounds differently: PAH efflux was hardly changed, whereas for PCG and DHEAS, efflux from the brain was completely abolished.

Conclusion: Oatp1a4 was suggested to play a minor role in the efflux of DHEAS. On the other hand, Oat3 and other organic anion transporters, both probenecid-sensitive and probenecid-insensitive, are involved in the transport of hydrophilic and amphipathic organic anions at the BBB.

Emerging Role of Pharmacogenomics in Drug Development and Human Therapeutics

Course Coordinator: Howard McLeod PharmD, The University of North Carolina at Chapel Hill

Pharmacogenomic research seeks to investigate the effect of genetic variation on drug response. Changes in genes encoding proteins which are related to drug disposition or drug action can have beneficial or detrimental consequences for the patient. Genetic information gathered from treated patient cohorts is helping explain interpatient differences in therapeutic outcomes. Identification of the underlying genetic determinants of diminished efficacy or enhanced toxicity may enable future clinicians to tailor treatment to patients who are at risk for suboptimal outcomes. Additionally, genomic technology is helping elucidate currently unknown mechanisms of drug action and toxicity. This knowledge could facilitate drug design that maximizes target specificity or eludes unwanted off-target effects. In this short course we will discuss the application of pharmacogenomic research to drug discovery, its role in benefitting patient therapy, and the vast scope of benefit that pharmacogenomics could provide if applied to healthcare internationally.

Venita Gresham Watson, The University of North Carolina at Chapel Hill: “Pharmacogenomic Study of Mechanism Using A Cell-Based Model”

Wayne Anderson, GlaxoSmithKline: “Pharmacogenomics: An Industrial Perspective”

Janine Micheli, University of California, San Francisco: “Genetic Contribution to Variability in Nevirapine Pharmacokinetics: Overall Genetic Contribution and Contribution of Selected Polymorphisms”

Howard L McLeod, The University of North Carolina at Chapel Hill: “Making Pharmacogenomics Practical”

PD-SC-5

Genetic Contribution to Variability in Nevirapine Pharmacokinetics: Overall Genetic Contribution and Contribution of Selected Polymorphisms

Janine Micheli, Leslie Chinn, Ashish Patel, Deanna Kroetz

Department of Bioengineering and Therapeutic Sciences, University of California, San Francisco.

Purpose: Nevirapine (NVP) is an alternative first line non nucleoside reverse transcriptase inhibitor and is commonly used as a component of Highly Active Antiretroviral Therapy (HAART) in resource poor settings and Prevention of Mother to Child Transmission (PMTCT). Increases in NVP plasma levels have been associated with increased efficacy and some toxicities. Variations in NVP plasma levels have been associated with gender, ethnicity, weight and concomitant hepatic disease. Studies have been performed on some genetic polymorphisms that may influence NVP plasma levels, but many have contradicting results. The objective of our study is to increase the knowledge of NVP pharmacogenomics by determining if there is a genetic contribution to the overall variability in NVP pharmacokinetics and if selected genetic polymorphisms are contributing to this variation.

Methods: We performed a repeated-dose administration (RDA) study on a group of low-income HIV+ patients from San Francisco to determine if there was an overall genetic contribution to NVP pharmacokinetics. Subsequently, we obtained plasma samples from 45 HIV+ patients from Uganda on NVP containing treatment regimens. Nevirapine plasma concentrations were determined by LC/MS/MS and the patients were genotyped for three candidate SNPs in two genes. Associations between genotype and NVP plasma levels were then assessed.

Results: A significant overall genetic contribution to the variability in NVP pharmacokinetics was found through the use of an RDA study, with an estimate of 0.9 heritable contribution to variability in NVP plasma levels in African Americans and Caucasian Americans. A polymorphism in *CYP2B6* (983T>C) significantly contributed to variability in NVP C_{min} concentrations in a Ugandan HIV+ population. Patients carrying the variant allele had significantly higher C_{min} NVP concentrations than those with the reference allele. There was no significant effect of *ABCB1* 3435C>T and *CYP2B6* 516G>T on NVP trough levels.

Conclusions: There is a significant genetic contribution to the overall variability in NVP pharmacokinetics. The *CYP2B6* 983T>C polymorphism is associated with higher NVP C_{min} concentrations in a Ugandan population. These results are currently being confirmed in a larger patient population. If replicated, these findings can be used to optimize HAART therapy in HIV+ patients.

De-Risking Drug Candidates: Optimizing Solubility, Permeability, and DM-PK

Course Coordinator: Ronald T. Borchardt PhD, Solon E. Summerfield Distinguished Professor, University of Kansas

Drug discovery and development is a very complex, costly, and time-consuming process. Because of the uncertainties associated with predicting the pharmacological and toxicological effects of new chemical entities (NCEs) in man, the clinical development of NCEs is quite prone to failure. In an attempt to reduce the attrition rate of NCEs in development, many companies have implemented a new drug discovery paradigm that involves optimizing the "pharmacological activity" as well as the "drug like properties" (e.g., solubility, cell permeability, DM-PK) during lead optimization. Traditionally, optimizing "drug-like properties" was not considered by discovery scientists to be their responsibility. Instead, discovery scientists felt that undesirable "drug-like properties" in drug candidates would be "fixed" by preclinical development scientists. However, today most discovery scientists recognize that the "drug-like properties" of NCEs are intrinsic properties of the molecules and that it is their responsibility to optimize both the "pharmacological activity" and the "drug-like properties" of these molecules. During this short course, the instructors will elaborate further on the rational for this paradigm shift in drug discovery and they will describe the strategies and the methodologies used to optimize the solubility, permeability and DM-PK properties of drug candidates.

Prof. Ronald T. Borchardt PhD, University of Kansas, USA: "Rationale for Pharmaceutical Profiling in Lead Optimization"

Prof. Per Artursson PhD, Uppsala University, Sweden: "Permeability and Transport Profiling of Drug Candidates"

H. C. Helms, University of Copenhagen, Denmark: "Claudin-5 mRNA Expression and Transendothelial Electrical Resistance (TEER) Correlate in the BCEC/Astrocyte Blood-Brain Barrier Model"

Prof. Patrick Augustijns PhD, Katholieke Universiteit-Leuven, Belgium: "Solubility Profiling of Structural Leads"

Yvonne E. Arnold, University of Basel, Switzerland: "New Online/Inline Analytical Tools and a Nucleation and Growth Model for Drug Precipitation Upon Transfer from Simulated Gastric to Intestinal Fluid"

Prof. Dhiren Thakker PhD, UNC-Chapel Hill, USA: "Rational Use of In Vitro and In Vivo Studies to Optimize DM-PK Properties of Drug Candidates"

PD-SC-6

Claudin-5 mRNA expression and transendothelial electrical resistance (TEER) correlate in the BCEC/astrocyte blood-brain barrier model

H. C. Helms, H. S. Waagepetersen, C. U. Nielsen, B. Brodin

Faculty of Pharmaceutical Sciences, University of Copenhagen, Denmark

Purpose: The aim of the present study was to characterize an *in vitro* blood-brain barrier model consisting of an astrocyte/endothelial cell co-culture and investigate the tight junction protein expression pattern in the established model.

Methods: Cerebral endothelial cells were isolated from bovine brains and co-cultured with rat astrocytes on permeable supports, as described by Gaillard *et al.* 2001. The resulting co-culture model was characterised using immunocytochemical staining and Confocal Laser Scanning Microscopy (CLSM) of cell-type specific proteins, tight junction proteins and filamenteous actin. Moreover, the expression of various tight junction proteins was examined using conventional PCR. Tight junction functionality was evaluated by transendothelial electrical resistance (TEER) measurements and transcellular transport of radiolabelled mannitol.

Results: Bovine capillary endothelial cells and rat astrocytes were isolated and co-cultured. The endothelial cells expressed Von-Willebrands Factor, spindle-shape morphology and Pgp confirmed by immunostaining and CLSM. The co-culture developed high resistance monolayers with TEER values up to 1638±258 Ω x cm^2 and $Papp_{mannitol}$ as low as 4.83±1.41 x 10^{-7} cm/s at day 6 of co-culture. The expression of the tight junction proteins Claudin-5 (fig 1A), Occludin and ZO-1 were confirmed using CLSM.

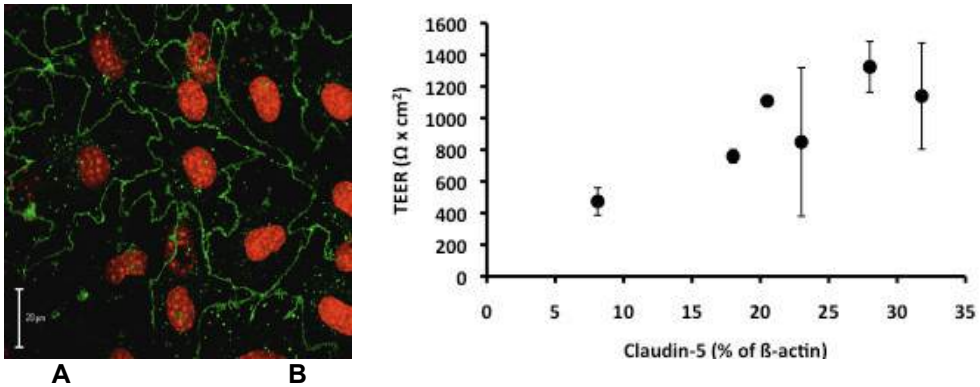

A B

fig 1: (A) Immunocytochemical staining of Claudin-5, nuclei stained with propidium iodide. (B) TEER as a function of Claudin-5 mRNA-expression. Each point is an average of three filter inserts pooled for RNA isolation.

The mRNA-expression of Claudin-1, Claudin 5, ZO-1, JAM-1 and Occludin was confirmed by PCR. The claudin-5 mRNA-transcript expression level was shown to correlate with TEER (fig 1B), whereas the expression levels of the other tight junction proteins remained constant.

Conclusion: A model of the blood-brain barrier was established and mRNA-levels and protein expression of marker proteins were measured. The model expressed functional tightness towards paracellular transport among the highest shown for endothelial derived blood-brain barrier models. Moreover, a correlation between Claudin-5 mRNA-expression and TEER was observed, which indicates that claudin-5 may responsible for the selective tightness towards small molecules.

Acknowledgements: The authors thank Carlsberg foundation, the PDA consortium and Novo Scholarship Programme for financial support. Senior laboratory technician Heidi Nielsen is acknowledged for her support.

PD-SC-7

New online/inline analytical tools and a nucleation and growth model for drug precipitation upon transfer from simulated gastric to intestinal fluid

Yvonne E. Arnold[1,2], Martin T. Kuentz[2], Georgios Imanidis[1,2]

[1] Institute of Pharmaceutical Technology, University of Basel, Switzerland
[2] School of Life Sciences, University of Applied Sciences Northwestern Switzerland

Purpose: Using new analytical tools and a kinetic nucleation and growth model, drug precipitation was investigated in a transfer test with biorelevant media. Poorly water soluble weak bases can precipitate in the intestine, which potentially leads to incomplete absorption. So far, there is no comprehensive understanding of this process with respect to kinetics, crystal form and modification, and final drug mass balance.

Methods: Drug transfer from the stomach to the intestine was simulated in vitro by pumping a solution of the model drug dipyridamole in simulated gastric fluid (FaSSGF) into simulated intestinal fluid (FeSSIF, acceptor medium). Gastric emptying was mimicked at two different transfer rates. Precipitation events in the acceptor medium were monitored using online dynamic image analysis and inline Raman spectroscopy. Drug concentration was obtained by HPLC analysis. A mathematical model based on a power law approach was developed to describe the drug concentration profile.

Results: The dynamic image analysis revealed a complex structure of the precipitated particles having the form of star-like crystals or aggregates of elongated primary particles. The particle size increased as a function of time, whereas at early time points the size distribution was shifted towards a smaller particle size at the low transfer rate compared to the high transfer rate. The onset of drug precipitation detected by Raman spectroscopy agreed with the respective finding of the image analysis. Moreover, the amount of precipitated drug determined by Raman spectroscopy was in agreement with the HPLC measurements. The kinetic model described very well the experimental data yielding consistently a nucleation exponent of 5 and a growth exponent of 1.5.

Conclusions: The analytical methods and the kinetic model proved to be excellent tools for monitoring drug precipitation and provided new insights into nucleation and particle growth. Results could be used for physiologically-based absorption modelling, which facilitates correlations with in vivo findings. This is the key to better optimize pharmaceutical formulations based on in vitro tests.

Stability of Proteins and Peptides in Solid Phase Formulations

Coordinator: Elizabeth M. Topp, Purdue University

Protein and peptide based drugs are among the fastest growing sectors of the biopharmaceutical industry. More than 40% of current protein drug products are marketed as solid forms, and protein APIs are often stored as dry powders prior to fill-finish operations. Though solid forms are often chosen in an attempt to preserve stability, peptides and proteins undergo a variety of chemical and physical degradation processes in the solid state that can alter their safety and efficacy. The rational development of solid formulations of peptides and proteins requires an understanding of the factors influencing their stability in solids. This short course presents mechanistic approaches to understanding the chemical reactivity of proteins and peptides in amorphous solids, the stability of proteins and peptides in Poly(lactic-co-glycolic acid) (PLGA) , the use of adjuvants in vaccine formulation, and immunological concerns and analytical challenges associated with protein aggregation.

Brad Anderson, University of Kentucky: “Understanding Chemical Reactivity of Peptides/Proteins in Amorphous Solids - Applicability of Solution-Based Mechanistic Information”

Steven P. Schwendeman, University of Michigan: “Stability of peptides and proteins in PLGA delivery systems”

LaToya Jones Braun, University of Colorado: “Stability of proteins at solid surfaces - From Aluminum-containing adjuvants to Zirconia crystals”

Wim Jiskoot, Leiden University: “Protein Aggregation - Immunological Concerns and Analytical Challenges”

Computer-Aided Drug Design

Course Coordinator: Alexander Tropsha, Ph.D., UNC-Chapel Hill

Recent advances in high-throughput technologies for both chemical synthesis and biological testing of chemicals have led to the rapid growth of databases containing information about chemical structures and the results of their experimental studies. The computational exploration and exploitation of these databases can afford a predictive knowledge about the relationship between the structures and their biological effects. Cheminformatics is defined as the study of molecules represented by *chemical descriptors* in relation to observed physical, chemical, and biological properties. Quantitative Structure-Activity Relationships (QSAR) modeling is one of the key cheminformatics approaches to the analysis of datasets of molecules with empirically studied properties. QSAR models are widely used to predict the physical properties (e.g., aqueous solubility, melting point) and biological activities (e.g., receptor binding affinity) of chemicals from their structure. These models are also actively used as virtual screening tools to select compounds with the desired biological activity from large chemical databases or virtual chemical libraries. Similar approaches are also used to optimize various "drug-like" properties, such as Adsorption, Distribution, Metabolism, Excretion, and Toxicity (ADMET), and assist in selecting drug candidates with better biological activity as well as safety profiles.

Alexander Tropsha. Ph.D., UNC-Chapel Hill: "Introduction to Cheminformatics"

Denis Fourches, Ph.D., UNC-Chapel Hill: "QSAR Model Development and Validation"

Diane Pozefsky, Ph.D., UNC-Chapel Hill: "CHEMBENCH: A Web Portal for QSAR Modeling"

University Participants

Aston University	
Professor Daniel J Kirby	d.j.kirby1@aston.ac.uk
Mr. Behfar Moghaddam	moghadb1@aston.ac.uk
Campbell University	
Professor Timothy J Marks	markst@campbell.edu
Chulalongkorn University	
Professor Garnpimol C Ritthidej	garnpimol.r@chula.ac.th
Ms. Sirigul Thongrangsalit	sirigul_t@hotmail.com
Ms. Amolnat Tunsirikongkon	sriopa@yahoo.com
Chungnam National University	
Professor Cheong-Weon Cho	chocw@cnu.ac.kr
Dr. Ji-Sook Hwang	hjs1016@hanmail.net
Mr. Chang-gu Keum	kcg1986@naver.com
ETH-Zurich	
Professor Marc A Gauthier	marc.gauthier@pharme.ethz.ch
Ms. Elisabeth V. Giger	elisabeth.giger@pharma.ethz.ch
Professor Jean-Christophe Leroux	jleroux@ethz.ch
Dr. Paola Luciani	paola.luciani@pharma.ethz.ch
Hacettepe University	
Ms. Ozge Cevik	ozgec04@hacettepe.edu.tr
Mrs. Tugba Gulsun Inal	tgulsun@hacettepe.edu.tr
Professor Neslihan R. Gürsoy	ngursoy@hacettepe.edu.tr
Mr. Firat Yerlikaya	firat01@hacettepe.edu.tr
Hebrew University of Jersalem	
Ms. Anna Elgart	anna.elgart@mail.huji.ac.il
Ms. Efrat Harel	efrat.abutbul@mail.huji.ac.il
Mr. Arik A Zur	arikz@ekmd.huji.ac.il
Kanazawa University	
Dr. Yoshiyuki Shirasaka	shira@p.kanazawa-u.ac.jp
Professor Ikumi Tamai	tamai@p.kanazawa-u.ac.jp
Ms. Mayuko Yoshifuji	mayuko-y@stu.kanazawa-u.ac.jp
Katholieke Universiteit Leuven	
Professor Patrick Augustijns	Patrick.Augustijns@pharm.kuleuven.be
Mr. Jan Bevernage	jan.bevernage@pharm.kuleuven.be
Mr. Michiel Van Speybroeck	michiel.vanspeybroeck@pharm.kuleuven.be
Kumamoto University	
Ms. Satomi Ariyoshi	097y8137@st.kumamoto-u.ac.jp
Professor Teruko Imai	iteruko@gpo.kumamoto-u.ac.jp
Mr. Yoshiaki Suwa	ysuwa@gpo.kumamoto-u.ac.jp
Kyoto University	
Mr. Kosuke Kusamori	K.Kusamori@ks4.ecs.kyoto-u.ac.jp
Mr. Kohta Mohri	k.mohri@ky8.ecs.kyoto-u.ac.jp
Professor Yoshinobu Takakura	takakura@pharm.kyoto-u.ac.jp

University Participants

Leiden University	
Mr. Vasco Filipe	v.filipe@lacDr. leidenuniv.nl
Dr. Andrea Hawe	ahawe@chem.leidenuniv.nl
Professor Wim Jiskoot	w.jiskoot@lacDr. leidenuniv.nl
Mr. Koen van der Maaden	k.van.der.maaden@lacDr. leidenuniv.nl
Monash University	
Ms. Annette Marie Dahlberg	gnetts@hotmail.com
Mr. Sifei Han	sifei.han@monash.edu
Mr. Liang Jin	liang.jin@pharm.monash.edu.au
Professor Michelle P McIntosh	michelle.mcintosh@monash.edu
Professor Joseph A Nicolazzo	joseph.nicolazzo@monash.edu
Mr. Tomas Sou	tomas.sou@pharm.monash.edu.au
NIPER	
Mr. Amit Kumar Jain	amit81jainster@gmail.com
Mr. Lokesh Kumar	lokesh.niper@gmail.com
Paris-Sud	
Ms. Perrine Pivette	perrine.pivette@u-psud.fr
Philipps University	
Dr. Marcus T. Kehrel	marcus.kehrel@staff.uni-marburg.de
Professor Michael Keusgen	dekanat.pharmazie@staff.uni-marburg.de
Mr. Jens Schäfer	j.schaefer@staff.uni-marburg.de
Purdue University	
Ms. Stephanie Anne Mowery	smowery@purdue.edu
Ms. Li Pan	lfpan@purdue.edu
Professor Elizabeth M. Topp	topp@purdue.edu
Saarland University	
Professor Eva-Maria Collnot	e.collnot@mx.uni-saarland.de
Ms. Claudia Henn	c.henn@mx.uni-saarland.de
Dr. Qingzhong Hu	q.hu@mx.uni-saarland.de
Ms. Fransisca Leonard	f.leonard@mx.uni-saarland.de
Mr. Christian A. Ruge	c.ruge@mx.uni-saarland.de
Seoul National University	
Professor Youngro Byun	yrbyun@me.com
Mr. Seungwoo Chung	swchung@me.com
Mr. Jee Heon Jeong	ilikemil@snu.ac.kr
Setsunan University	
Mr. Haruki Higashino	09m114hh@edu.setsunan.ac.jp
Professor Yoshie Masaoka	yokko@pharm.setsunan.ac.jp
Mr. Masaya Suita	09m117mm@edu.setsunan.ac.jp
Mr. Hidenori Suzuki	09m108sh@edu.setsunan.ac.jp
Dr. Ryusuke Takano	takanorus@chugai-pharm.co.jp
Mr. Yuki Terashima	09m111ty@edu.setsunan.ac.jp
Shandong University	

Professor Fengshan Wang	fswang@sdu.edu.cn
Ms. Mingyan Yu	mingyany@yahoo.cn
Professor Na Zhang	zhangnancy9@sdu.edu.cn
Ms. Ting Zhao	zhaoting2110000@yahoo.com.cn
The Hamner Institute	
Dr. Kristina DeSmet	kdesmet@thehamner.org
The National University of Singapore	
Professor Sui Yung Chan	phahead@nus.edu.sg
Ms. Han Hui Cheong	g0600606@nus.edu.sg
Professor Rachel Ee	phaeplr@nus.edu.sg
Professor Paul Ho	phahocl@nus.edu.sg
Mr. Tarang Nema	tarang.n@nus.edu.sg
Mr. Zhe Wang	g0600614@nus.edu.sg
The University of California at San Francisco	
Professor Nadav Ahituv	nadav.ahituv@ucsf.edu
Mr. Ethan G Geier	Ethan.Geier@ucsf.edu
Ms. Janine Micheli	Janine.Micheli@ucsf.edu
The University of Colorado	
Professor Tom Anchordoquy	tom.anchordoquy@ucdenver.edu
Professor LaToya Jones Braun	latoya.jonesbraun@ucdenver.edu
Ms. Tanya Clapp	tanya.clapp@ucdenver.edu
Ms. Regina L Hutchings	regina.hutchings@ucdenver.edu
Mr. Tyson J Smyth	Tyson.Smyth@ucdenver.edu
The University of Connecticut	
Professor Bodhisattwa Chaudhuri	bodhi.chaudhuri@uconn.edu
Ms. Mary Kleppe	mary.kleppe@uconn.edu
Mr. Xiaoming Xu	xuxiaoming.nj@gmail.com
The University of Florida	
Mr. Matthias Fueth	m.fueth@ufl.edu
Professor Anthony Palmieri	palmieri@cop.ufl.edu
Mr. Benjamin Weber	benjaminweber@ufl.edu
The University of Frankfurt	
Mr. Marcel Arndt	m.arndt@em.uni-frankfurt.de
Professor Edmund S Kostewicz	kostewicz@em.uni-frankfurt.de
Mr. Karim Sempf	sempf@em.uni-frankfurt.de
Ms. Stefanie Strauch	strauch@em.uni-frankfurt.de
Mr. Thomas Taupitz	taupitz@em.uni-frankfurt.de
Mr. Matthias Wacker	wacker@em.uni-frankfurt.de
Mr. Christian Wagner	christian.wagner@em.uni-frankfurt.de
Ms. Stefanie Wohlfart	wohlfart@em.uni-frankfurt.de
The University of Geneva	
Ms. Surekha Pimple	Surekha.Pimple@hcuge.ch
Professor Leonardo Scapozza	leonardo.scapozza@unige.ch

University Participants

The University of Helsinki	
Mrs. Polina Ilina	polina.ilina@helsinki.fi
Dr. Yanru Lou	yan-ru.lou@helsinki.fi
Ms. Melina M Malinen	melina.malinen@helsinki.fi
Professor Arto Urtti	arto.urtti@helsinki.fi
The University of Kansas	
Professor Kenneth L. Audus	audus@ku.edu
Mr. Ahmed H Badawi	abadawi@ku.edu
Ms. Taryn R Bagby	tmeyer@ku.edu
Professor Ronald T. Borchardt	RBorchardt@ku.edu
Ms. Shuang Cai	scai@ku.edu
Ms. Jessica S Creamer	jessica.s.creamer@gmail.com
Ms. Kassibla E Dempah	kedempah@ku.edu
Mr. Ryan Sol Funk	ryanfunk@ku.edu
Mr. Lei Hu	leihu@ku.edu
Professor Jeff Krise	krise@ku.edu
Professor Jennifer Laurence	laurencj@ku.edu
Ms. Sarah Pyszczynski	sjpysz@ku.edu
Professor Christian Schoneich	schoneic@ku.edu
Mr. Joshua O Sestak	jsestak@ku.edu
Professor Teruna J. Siahaan	siahaan@ku.edu
Professor Valentino J Stella	stella@ku.edu
The University of Kentucky	
Professor Bradley D Anderson	bande2@email.uky.edu
Mr. Mikolaj Milewski	mmile2@email.uky.edu
Professor Eric Munson	eric.munson@email.uky.edu
Mr. Dhaval D Patel	dhaval.d.patel@uky.edu
The University of London	
Ms. Abeer Ahmed	abeer.hashim@live.pharmacy.ac.uk
Dr. AikateriniLalatsa	aikaterini.lalatsa@pharmacy.ac.uk
Professor Satyanarayana Somavarapu	soma@pharmacy.ac.uk
The University of Manitoba	
Professor Donald Miller	miller5@cc.umanitoba.ca
Ms. Ngoc H On	ngocwpg@hotmail.com
Mr. Vinith Yathindranath	umvinith@cc.umanitoba.ca
The University of Maryland	
Ms. Brittany Avaritt	bavar001@umaryland.edu
Ms. Tatiana Claro da Silva	tsilv003@umaryland.edu
Mr. Lei Diao	ldiao001@umaryland.edu
Ms. Deborah S Goldberg	dsweet3@umd.edu
Professor Peter W. Swaan	pswaan@rx.umaryland.edu
Mr. Duan Wang	dwang003@umaryland.edu
The University of Michigan	

University Participants

Dr. Kashappa-Goud H. Desai	kgdesai@umich.edu
Ms. Yajun Liu	yajunl@umich.edu
Professor Steven P. Schwendeman	schwende@umich.edu
The University of Minnesota	
Mr. Tanmoy Sadhukha	sadhu001@umn.edu
Mr. Jing Wang	wangx976@umn.edu
Professor Cheryl L Zimmerman	zimme005@umn.edu
The University of Montana	
Professor Erica L Woodahl	erica.woodahl@umontana.edu
The University of Nebraska	
Ms. Daria Y Alakhova	dalakhova@unmc.edu
Mr. Sai Praneeth Reddy Bathena	sbathena@unmc.edu
Mr. Brandon T Gufford	btguffor@unmc.edu
Mr. Hardeep S Oberoi	hoberoi@unmc.edu
Professor Dennis H Robinson	dhrobins@unmc.edu
Mr. Marc Ueda	mueda@unmc.ecu
Miss Philise Nicole Williams	pnwilliams@unmc.edu
The University of North Carolina	
Ms. Amber M Allen	amber_allen@unc.edu
Mr. Scott J. Brantley	scottbrantley@unc.edu
Professor Kim Brouwer	kbrouwer@unc.edu
Mr. Justin Brown	justin_brown@med.unc.edu
Ms. Mary J Carroll	carroll4@email.unc.edu
Mr. Chester Lee Costales	chester.costales@unc.edu
Dr. Anthony J. Di Pasqua	dipasqua@gmail.com
Mr. Matthew B Dufek	mdufek@unc.edu
Mr. Andrew D Fant	andrew.fant@unc.edu
Ms. LaToya Griffin	poolelm@email.unc.edu
Mr. Patrick C Guley	pguley@gmail.com
Dr. Rima M. Hajjo	hajjo@email.unc.edu
Mr. Tianxiang Han	hant@email.unc.edu
Dr. Martin Herold	martin.herold@unc.edu
Dr. Daniel L Hertz	danhertz@email.unc.edu
Ms. Chia-Wen Hsu	hsuc@email.unc.edu
Dr. Wujian Ju	wju@email.unc.edu
Dr. Jin-Ki Kim	jkkim@unc.edu
Ms. Tae Eun Kim	taeeun.grace@gmail.com
Mr. Sang Kyoon Kim	kimsk@email.unc.edu
Ms. Kayla Knilans	knilans@email.unc.edu
Mr. Jun Li	lijun08@email.unc.edu
Ms. Dongyun Liu	dongyun@email.unc.edu
Ms. Yang Liu	liu0702@email.unc.edu
Dr. Xiuling Lu	xiuling.lu@unc.edu

University Participants

Ms. Man Luo	mluo@email.unc.edu
Mr. PingMa	PINGMA@EMAIL.UNC.EDU
Ms. Lei Peng	leipeng@email.unc.edu
Dr. Nathan D Pfeifer	npfeifer@email.unc.edu
Mr. Luke E Roode	lroode@unc.edu
Dr. Cristina Santos	santosc@email.unc.edu
Dr. Robert N Schuck	schuck@unc.edu
Mr. Wei Sun	sunw@unc.edu
Dr. Jasmine Talameh	jtalameh@email.unc.edu
Professor Dhiren R Thakker	dhiren_thakker@unc.edu
Dr. Katherine Theken	ktheken@unc.edu
Mr. Saurabh Wadhwa	saurabhwadhwa@unc.edu
Dr. Christina Won	cwon@email.unc.edu
Dr. Julianne M Yost	Jyost@unc.edu
Dr. Wei Yue	wei_yue@med.unc.edu
Mr. Yong Zhang	yongzhang@unc.edu
The University of Otago	
Ms. Thunjiradasiree Kojarunchitt	sriva214@student.otago.ac.nz
Professor Arlene McDowell	arlene.mcdowell@otago.ac.nz
Professor Natalie J Medlicott	natalie.medlicott@otago.ac.nz
Professor Thomas Rades	thomas.rades@otago.ac.nz
Mr. Nicky Thomas	nicky.thomas@otago.ac.nz
The University of Queensland	
Mr. Daryn Goodwin	daryn.goodwin@uqconnect.edu.au
Dr. Pavla Simerska	p.simerska@uq.edu.au
Professor Istvan Toth	i.toth@uq.edu.au
The University of Sao Paulo	
Professor Silvia Berlanga Moraes Barros	smbarros@usp.br
Mr. Diogo Pineda Rivelli	diogopineda@usp.br
Dr. Fabiana TMC Vicentini	fabtesta@fcfrp.usp.br
The University of Southern California	
Ms. Helen Ha	helenha@usc.edu
Professor Bogdan Z Olenyuk	bogdan@usc.edu
Ms. Kavya Ramkumar	ramkumar@usc.edu
The University of Utah	
Ms. Anna Astashkina	anna.astashkina@utah.edu
Mr. Andrew S Dixon	andy.dixon@utah.edu
Professor Carol S. Lim	carol.lim@pharm.utah.edu
The University of Washington	
Professor Nina Isoherranen	ni2@uw.edu
Ms. Nora Lee	noralee@uw.edu
Dr. Jakob Shimshoni	jakobs3@u.washington.edu
The University of Wisconsin	

University Participants

Mr. Tsz Chung Lai	tlai@wisc.edu
Professor May Xiong	mpxiong@wisc.edu
University of Basel	
Ms. Yvonne E Arnold	yvonne.arnold@unibas.ch
Professor Georgios Imanidis	georgios.imanidis@unibas.ch
Mr. Daniel Preisig	daniel.preisig@stud.unibas.ch
University of Copenhagen	
Professor Birger Brodin	bbr@farma.ku.dk
Ms. Anne Sophie Grandvuinet	asg@farma.ku.dk
Mr. Hans Christian Christian Helms	hch@farma.ku.dk
Dr. Anne Jensen	aj@farma.ku.dk
Professor Lene Jorgensen	lej@farma.ku.dk
Ms. Anne Larsen	al@farma.ku.dk
Professor Anette Müllertz	amu@farma.ku.dk
University of Eastern Finland	
Professor PaavoHonkakoski	paavo.honkakoski@uef.fi
Ms. Johanna Maria Räikkönen	johanna.raikkonen@uef.fi
Professor Jarkko Rautio	jarkko.t.rautio@uef.fi
Mr. Mika Reinisalo	mika.reinisalo@uef.fi
Mr. Pyry Antti Valitalo	pyry.valitalo@uef.fi
University of Tokyo	
Mr. Sumito Ito	ff107202@mail.ecc.u-tokyo.ac.jp
Professor Hiroyuki Kusuhara	kusuhara@mol.f.u-tokyo.ac.jp
Ms. Mari Miyajima	ff097211@mail.ecc.u-tokyo.ac.jp
Uppsala University	
Professor Per Artursson	per.artursson@farmaci.uu.se
Ms. Ge Gao	ge.gao@farmaci.uu.se
Ms. Anna Vildhede	anna.vildhede@farmaci.uu.se
Utrecht University	
Dr. Maria E Dolman	m.e.m.dolman@uu.nl
Mr. Albert J. de Graaf	a.j.degraaf1@uu.nl
Professor Wim Hennink	w.e.hennink@uu.nl
Professor Robbert J Kok	r.j.kok@uu.nl

Industrial Participants

AAPS
Maggie Motley

Abbott
Todd McDermott
Dennis Stephens

Allergan
Kevin Warner

American Chemical Society
Andrew Clinton

Amgen
Janan Jona

Amylin
Robert N. Jennings

AstraZeneca
Tommy B. Andersson
Martin DeBeradinis
Simon Roberts
Weijia Zheng

Boehringer-Ingelheim
Chen-Ming Lee

Bristol-Myers Squibb
Neil Mathias
Lian Zhou

Cephalon
Kevin J. Wells-Knecht

Eisai
Geoffrey Hird

Genentech
Paroma Chakravarty
Richard Graham
Bianca M. Liederer
Kai Zheng

GlaxoSmithKline
Giselle Limentani

HO West Foundation
Vinod Vilivalam

Human Genome Sciences
Kristin Auge

Johnson and Johnson
Weiguo Dai
Shannon Dallas
Ivo Van Assche

Merck
Peter Wuelfing

Novartis
Andrew Snoddy

Patheon
Edgar N Jaynes

Pfizer
Amy S Antipas
Ayman F El-Kattan
Gold Kaul

Warner Chilcott
Mahdi Fawzi

UNC-Chapel Hill Campus Map

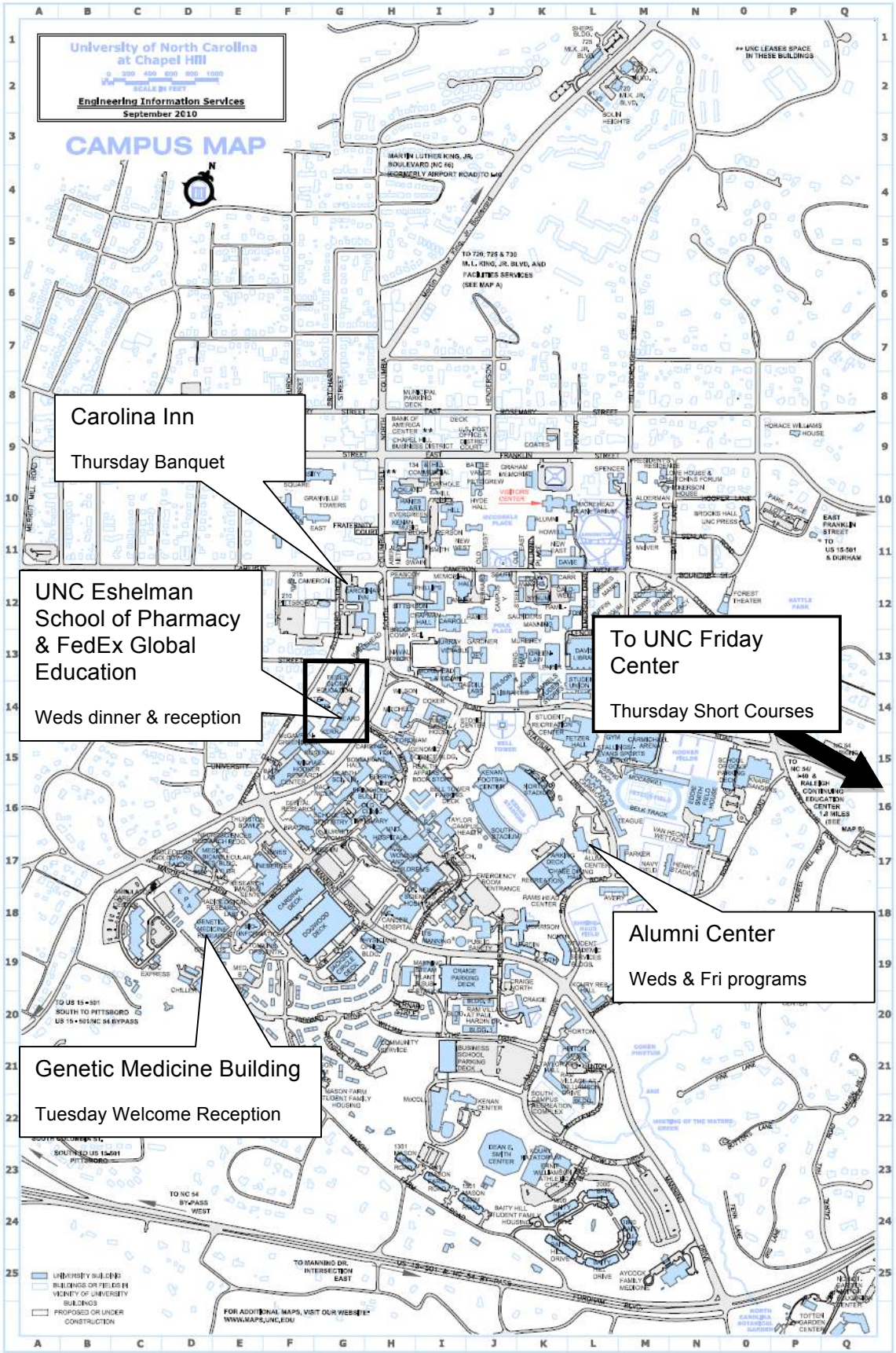

Short Course Venue Floor Plan:

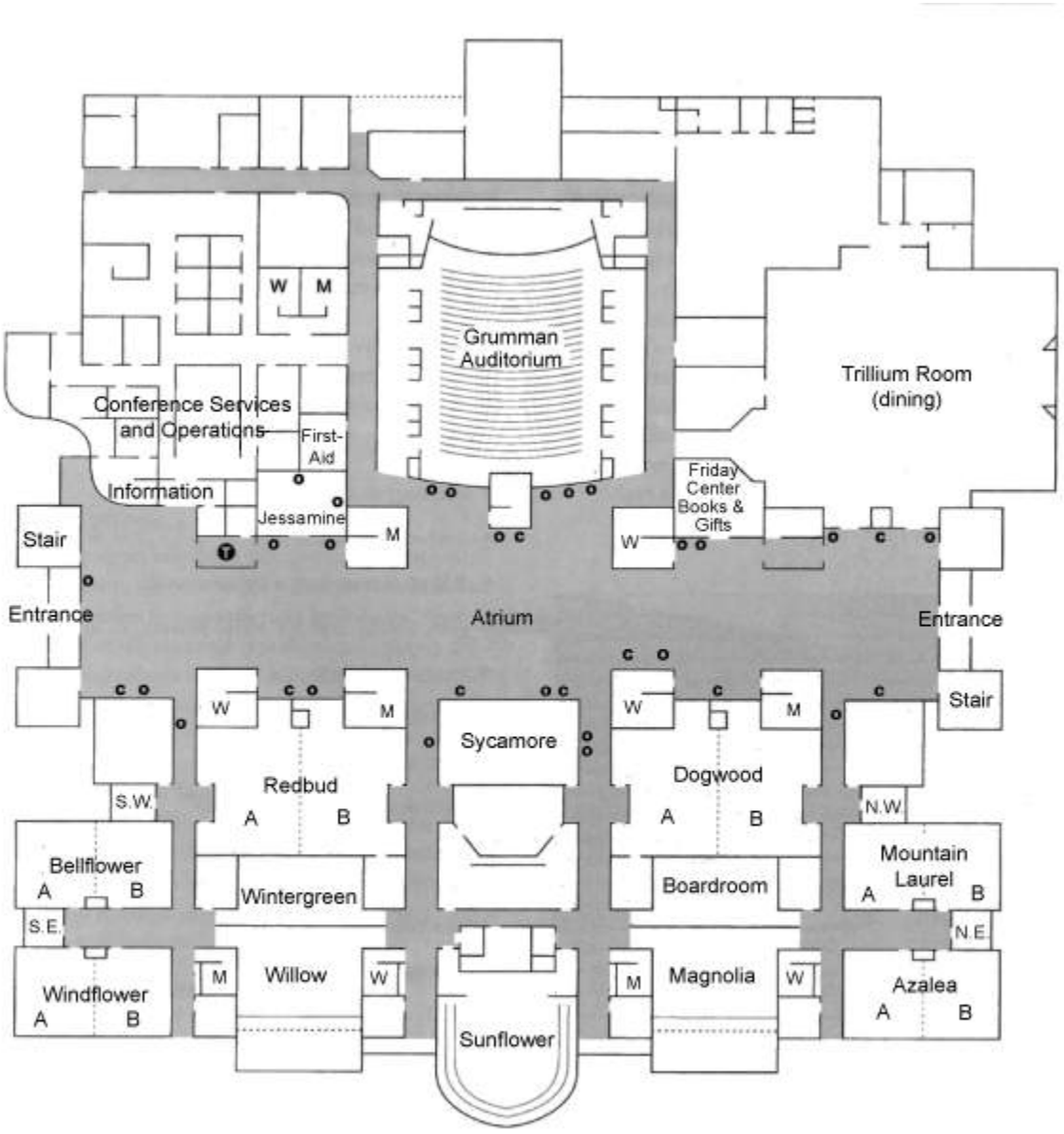

Floor Plan
The William and Ida Friday Center for Continuing Education

Registration and Welcome Desk

A Registration and Welcome Desk will be available and attended by GPEN 2010 Planning Committee members each day at the conference venue. GPEN-sponsored participants will find their meeting materials (badge and program binder) waiting for them upon check-in at the hotels. All other participants can collect their materials at the Registration and Welcome Desk. Assistance and general information can also be obtained at this desk.

Smoking

Smoking is NOT ALLOWED in or on campus buildings and property. You must be 100 yards from any University building in order to smoke.

Meals

Light, continental breakfast fare will be available to registered attendees at the conference venues each morning. Snacks and beverages (coffee, tea, soft drinks) are available during morning and afternoon breaks. Lunch is provided throughout the program for registered conference attendees. Dinner is offered Tuesday, Wednesday and Thursday evening as part of the conference program.

Restaurants and Bars

Franklin Street is the heart of downtown Chapel Hill, divided at the intersection with Columbia Street into East and West Franklin. On Franklin Street you will find a wide variety of bars and restaurants for every budget. Some local favorites include:

- Top of the Hill, 100 East Franklin St (at Columbia): a Chapel Hill landmark, restaurant and brewery. Try some local specialties like fried chicken or pulled pork.
- Mediterranean Deli, 410 West Franklin Street: fresh, authentic Mediterranean and Greek food
- Carolina Brewery, 460 West Franklin Street: restaurant and brewpub for a casual meal or pint
- West End Wine Bar, 450 West Franklin Street: three floors including an upscale wine bar and The Cellar, a local “dive” bar in the basement
- Kildare’s Irish Pub, 206 West Franklin Street: the name says it all, also one of the better places to catch your favorite sports team on the flat screen TVs in the back

Transportation in Chapel Hill

Bus Transportation Provided by GPEN

Shuttle buses will be available to bring participants from their hotels to the various meeting locations beginning at 7 am. Bus service will also bring participants from conference venues back to hotels after the daily presentations, from hotels to evening dinner events, and again from dinner to hotels at the conclusion of the day's scheduled activities. Public transportation within the town of Chapel Hill is also free of charge (see below).

On Friday, November 12th, shuttles from the hotels to RDU airport will run once an hour between 12 noon and 7:30 pm. If you need to arrange transportation outside of this time interval, there are several other transportation options between RDU and Chapel Hill (see below).

Chapel Hill Transit Public Bus System

Free local bus system serving Chapel Hill and surrounding areas, mostly designed around day time commuting to & from UNC campus and hospitals. Some routes run in to the night. Maps and schedules can be found here: http://www.townofchapelhill.org/index.aspx?page=1176

Taxi & Transportation Companies Serving Chapel Hill

Tar Heel Taxi	919-933-1255
Chapel Hill Taxi & Transportation shuttle	919-417-8294
Trust Taxis Service	919-357-1085
On Time Taxi	919-493-5050
Airport and Intown Taxi of Chapel Hill	919-942-4492
IKE Transportation Service	919-961-2477

Conference Hotel Information

Siena Hotel
1505 East Franklin Street
Chapel Hill, NC 27514
(800) 223-7379

Courtyard Marriott Hotel
100 Marriott Way
Chapel Hill, NC 27517
(919) 883-0700

Hampton Inn
1740 North Fordham Boulevard
Chapel Hill, NC 27514
(919) 968-3000

UNC-Chapel Hill GPEN 2010 Conference Personnel Contact Information:

Katie Theken, GPEN 2010 Co-Chair
Cell: (412) 638-2841
Email: ktheken@unc.edu

Cristina Santos, GPEN 2010 Co-Chair
Cell: (919) 636-8059
Email: santosc@email.unc.edu

Ms. Amber Allen, GPEN Organizing Committee Staff Liason
Cell: (336) 214-0283
Email: amber_allen@unc.edu

Dr. Dhiren Thakker, GPEN 2010 Faculty Advisor
Cell: (919) 606-6688
Email: dhiren_thakker@unc.edu

Map of UNC-Chapel Hill Campus and Surrounding Area: